



**HAL**  
open science

# Importance of glucocorticoid receptors in the physiopathology of Alzheimer's disease

Scherazad Kootar

► **To cite this version:**

Scherazad Kootar. Importance of glucocorticoid receptors in the physiopathology of Alzheimer's disease. Agricultural sciences. Université Côte d'Azur, 2017. English. NNT: 2017AZUR4015 . tel-01547457

**HAL Id: tel-01547457**

**<https://theses.hal.science/tel-01547457>**

Submitted on 26 Jun 2017

**HAL** is a multi-disciplinary open access archive for the deposit and dissemination of scientific research documents, whether they are published or not. The documents may come from teaching and research institutions in France or abroad, or from public or private research centers.

L'archive ouverte pluridisciplinaire **HAL**, est destinée au dépôt et à la diffusion de documents scientifiques de niveau recherche, publiés ou non, émanant des établissements d'enseignement et de recherche français ou étrangers, des laboratoires publics ou privés.

Université Côte d'Azur, École doctorale 85 Sciences de la Vie et de la Santé

Institut de Pharmacologie Moléculaire et Cellulaire, UMR 7275, CNRS/UCA

# Thèse de doctorat

Présentée en vue de l'obtention du grade de

Docteur en Sciences

Mention Interactions Moléculaires et Cellulaires

de l'Université Côte d'Azur

Par :

**SCHERAZAD KOOTAR**

## **L'importance des récepteurs aux glucocorticoïdes dans la physiopathologie de la maladie d'Alzheimer**

“Importance of glucocorticoid receptors in the physiopathology of Alzheimer's disease”

Thèse dirigée par Dr Hélène MARIE

Soutenue le 24 Mars 2017

Devant le jury composé de :

Dr Alain  
Dr Hélène  
Dr Stéphane  
Dr Ioannis

Buisson  
Marie  
Martin  
Sotiropoulos

Professeur, Université de Grenoble  
CR1 CNRS/HDR, IPMC  
DR2 INSERM, IPMC  
Group leader/eq. HDR, University of Minho

Rapporteur  
Directrice de thèse  
Président de Jury  
Rapporteur



Université Côte d'Azur, École doctorale 85 Sciences de la Vie et de la Santé

Institut de Pharmacologie Moléculaire et Cellulaire, UMR 7275, CNRS/UCA

# Thèse de doctorat

Présentée en vue de l'obtention du grade de

Docteur en Sciences

Mention Interactions Moléculaires et Cellulaires

de l'Université Côte d'Azur

Par :

**SCHERAZAD KOOTAR**

## **L'importance des récepteurs aux glucocorticoïdes dans la physiopathologie de la maladie d'Alzheimer**

“Importance of glucocorticoid receptors in the physiopathology of Alzheimer's disease”

Thèse dirigée par Dr Hélène MARIE

Soutenue le 24 Mars 2017

Devant le jury composé de :

Dr Alain  
Dr Hélène  
Dr Stéphane  
Dr Ioannis

Buisson  
Marie  
Martin  
Sotiropoulos

Professeur, Université de Grenoble  
CR1 CNRS/HDR, IPMC  
DR2 INSERM, IPMC  
Group leader/eq. HDR, University of Minho

Rapporteur  
Directrice de thèse  
Président de Jury  
Rapporteur

## Acknowledgments

It gives me great pleasure to express my gratitude to my PhD supervisor **Dr. Hélène Marie**. Her expertise in electrophysiology, meticulous scientific approach, timely advice, and excellent organizational skills have helped me throughout. I would like to thank her for her patience and ultimate confidence in me. I would like to thank **Dr. Jacques Barik** for the GR<sup>lox/lox</sup> mice he introduced to the lab, this taught me much about how to breed mice and systematically record them. His experience in the field of stress, his enthusiasm and forward thinking have been helpful during the thesis. I would also like to convey my thanks to **Dr. Ingrid Bethus** who has played an important role in my PhD. She taught me various techniques like stereotaxic injections, behavioural paradigms and surgery for cannula implantations. Her enthusiasm for neurobiology has been outstanding as are her teaching methods. A big thank you to **Dr. Sebastian Fernandez**, who has helped me enormously throughout my project. His experience and vast knowledge in the field of neurobiology has helped me with quick solutions hence saving valuable time. Apart from being a good researcher, his fantastic sense of humour has helped us pass some not so easy days with a smile. I would also like to thank **Dr. Paula Pousinha**, for all the discussions we have had and the critical analysis of data that helped me to understand things better. I have been captivated by her amazing teaching skills. Her smiles and laughs will be always be remembered. My sincere thanks to **Ana Rita Salgueiro Pereira** for all the help over the years. We have had some memorable times working together and these will always be cherished. A very big thank you to **Dr. Marie-Lise Frandemiche**. Her participation in my project has been highly appreciated. She has been very helpful and patient in providing input throughout my project. Another big thanks to **Xavier Mouska**, who has been so kind and patient and helped me in troubleshooting with different techniques and most importantly with his good lab practices. I extend my gratitude to **Précillia Rodrigues**. She was the first member in the lab with whom I worked. I do remember those long nights doing dissections and blood collection! I would also like to thank **Loic Broussot** and **Maria Mensch** who have been supportive and kind especially during the last few months of my PhD. I am sure they will both do well in their projects. Overall, the lab members have been a most wonderful team. What was amazing is that we are all from different countries, backgrounds and cultures and yet we made an amazing team. It all shows that “Variety is the *Spice* of Life”. I cannot forget to thank **Dr. Konstanze Beck**, who has been extremely supportive and has helped all of us, the Labex SIGNALIFE students from day one of our stay in France. She has executed all her administrative and bureaucratic work patiently and to perfection. I would also like to thank all the members of the animal facility - Anipro and Animex especially **Benjamin, Lucien, Véronique, and Thomas** who have taken care of the animal facility throughout the years. The guidance of **Dr. Férédic Brau** has provided me authorisation to use confocal and other microscopic instruments. **Dr. Thomas Lorivel** has helped me out in the statistical analysis. A big thank you to both of you. I would also like to appreciate the good moments I spent with my friends apart from the lab, **Rohan, Nikita, Magda, Anida, Sochea**. Last but not the least I would like to thank my family for their unconditional love and support which has been invaluable.

## SUMMARY

Alzheimer's disease (AD) is a neurodegenerative disorder characterized by an irreversible loss of cognitive functions. In the early phase of the disease, there is evidence that synapse dysfunction promotes loss of hippocampus-dependent episodic memories. Strong evidence suggests that the oligomeric forms of the amyloid- $\beta$  peptide (oA $\beta$ ) are responsible for these synapse dysfunctions. Concomitantly, AD is associated to dysregulation of the Hypothalamus-Pituitary-Adrenal (HPA) axis as observed in human and mouse models. HPA axis dysregulation in AD produces an increase in glucocorticoids (GCs), which bind to glucocorticoid receptors (GRs). We recently showed that inhibiting these receptors in an AD transgenic mouse model, the Tg2576 (Tg<sup>+</sup>) mouse, prevented early episodic memory and synaptic plasticity deficits (Lanté et al, 2015 Neuropsychopharmacology).

In this context, we further assessed the extent of the contribution of GRs to AD physiopathology. First, we focussed on the relationship between HPA axis dysregulation and AD early onset in the Tg<sup>+</sup> mice. Dysregulated HPA axis was characterized by increased GC levels at 4 and 6 months of age and by loss of GC feedback inhibition in these mice. Secondly, we crossed Tg<sup>+</sup> mice with GRfloxed mice to generate GR<sup>lox/lox</sup> Tg<sup>+</sup> double mutant mice, which we characterized phenotypically. Even without removing GRs, these mice already exhibited high GRs levels from weaning period, exacerbated synaptic deficits, low body weight and low survival rate upon surgery. We speculate that, together, presence of the transgene and of the GR floxed allele were too detrimental for adequate development of these double-mutant mice. Hence, we discontinued using this new mouse model. Instead, to identify the functional relationship between GRs and oA $\beta$  at synapses, we shifted to acute oA $\beta$  treatment in neurons *in vitro* and *ex-vivo* hippocampus slices. In neuron cultures, we observed an increase in GR levels in the post synaptic density upon acute oA $\beta$  treatment. Using a specific GR antagonist in presence of oA $\beta$  on *ex-vivo* hippocampus slices, we observed that the oA $\beta$ -dependent LTP impairment was prevented. This finding was confirmed by reducing GR levels in CA1 neurons using local *in vivo* injections of Cre-GFP viruses in GR<sup>lox/lox</sup> mice and then inducing LTP in presence of oA $\beta$ . Hereby, we demonstrate that reducing GR function prevents the acute oA $\beta$  effect on LTP.

In conclusion, our results with the Tg<sup>+</sup> mice suggest that a neuroendocrine dysregulation occurs during the onset of AD pathology. Additionally, we provide evidence for a functional relationship between oA $\beta$  and GRs with GRs at the synapse playing an important role in acute A $\beta$ -induced synapto-toxicity.

## RESUME

La maladie d'Alzheimer (MA) est une maladie neurodégénérative caractérisée par une perte irréversible des fonctions cognitives. En début de maladie, il a été mis en évidence que la perte de fonction des synapses de l'hippocampe engendre la perte de mémoires de type épisodique. Les données actuelles suggèrent fortement que les formes oligomériques du peptide  $\beta$ -amyloïde (oA $\beta$ ), qui s'accumulent dans le cerveau des patients, sont toxiques pour la fonction de ces synapses. La MA est aussi associée à une dérégulation de l'axe du stress, l'axe hypothalamo-pituitaire-surrénal (HPA), comme observée chez les patients et les modèles animaux de la MA. Cette dérégulation engendre une augmentation de la production des glucocorticoïdes (GCs) qui activent les récepteurs associés (GRs). Nous avons récemment mis en évidence que l'inhibition de ces GRs dans un modèle murin de la maladie, les souris Tg2576 (Tg<sup>+</sup>), prévient les déficits de mémoire épisodique et de plasticité synaptique (Lanté et al. Neuropsychopharmacology. 2015).

Dans ce contexte, nous avons étudié l'étendue de la contribution des GRs dans la physiopathologie de la MA. D'abord, nous avons étudié la relation entre la dérégulation de l'axe HPA et le début de la pathologie dans les souris Tg<sup>+</sup>. Nous montrons que cette dérégulation était caractérisée par des niveaux élevés de GCs à 4 et 6 mois d'âge ainsi que par la perte de la boucle de rétroaction négative. Ensuite, nous avons croisé les souris Tg<sup>+</sup> avec des souris GR floxées pour générer des double mutants GR<sup>lox/lox</sup> Tg<sup>+</sup>, dont nous avons fait la caractérisation phénotypique. Alors même que les GRs étaient encore présents, ces double mutants exhibaient des niveaux élevés de GCs dès le sevrage, une exacerbation des déficits synaptiques, un poids faible et un taux de survie faible lors de chirurgies. Nous concluons, qu'ensemble, la présence du transgène et de l'allèle GR floxé sont trop nuisibles pour permettre un développement adéquat des souris double mutantes. Nous avons donc décidé de mettre fin à cette lignée de souris. A la place, pour identifier la relation fonctionnelle entre les GRs et oA $\beta$  à la synapse, nous avons utilisé des cultures de neurones et des tranches d'hippocampes soumises à un traitement aigu d'oA $\beta$ . Dans les cultures, ce traitement a favorisé une augmentation des niveaux de GRs à la synapse. Dans les tranches, ce traitement a provoqué une diminution de la potentialisation à long-terme (LTP), un effet totalement bloqué en présence d'un inhibiteur spécifique des GRs. Confirmant ce résultat, nous n'avons pas vu d'effet d'oA $\beta$  sur la LTP sur des tranches de souris GR<sup>lox/lox</sup> où l'expression génique des GRs dans les neurones CA1 de l'hippocampe avait été supprimée par transduction virale Cre-GFP in vivo. La réduction de la fonction des GRs prévient donc l'action aiguë d'oA $\beta$  sur la LTP.

En conclusion, nos résultats avec les souris Tg<sup>+</sup> suggèrent qu'une dérégulation neuroendocrine est présente en début de maladie. Aussi, nous mettons en évidence une relation fonctionnelle entre oA $\beta$  et les GRs à la synapse, les GRs jouant en rôle clé dans la synapto-toxicité induite par oA $\beta$ .

# Table of Contents

|   |           |
|---|-----------|
| <b>SUMMARY .....</b>  | <b>2</b>  |
| <b>1 ABBREVIATIONS.....</b>   | <b>13</b> |
| <b>2 INTRODUCTION .....</b>   | <b>16</b> |
| <b>2.1 Alzheimer’s Disease .....</b>  | <b>16</b> |
| 2.1.1 Aging, Dementia and AD .....  | 16        |
| 2.1.2 AD and its discovery .....  | 17        |
| 2.1.3 AD neuropathology: .....  | 17        |
| 2.1.3.1 Senile plaques .....  | 18        |
| 2.1.3.2 Tau neurofibrillary tangles .....   | 19        |
| 2.1.4 Two types of AD: .....  | 19        |
| 2.1.4.1 Familial AD .....   | 19        |
| 2.1.4.2 Sporadic AD.....  | 20        |
| 2.1.5 Environmental risk factors: .....   | 20        |
| 2.1.6 APP and its processing: .....   | 21        |
| 2.1.6.1 Function of APP:.....   | 21        |
| 2.1.6.2 APP processing: .....   | 22        |
| 2.1.6.3 Amyloid cascade hypothesis .....  | 24        |
| 2.1.6.4 Criticism and modifications to the amyloid hypothesis .....                         | 25        |
| 2.1.7 Evolution of AD in the brain .....  | 26        |
| 2.1.8 Treatments .....  | 28        |
| <b>2.2 Memory formation, synaptic plasticity and modulation by A<math>\beta</math>.....</b> | <b>30</b> |
| 2.2.1 Different types of memory .....   | 30        |
| 2.2.1.1 Declarative long term memory.....   | 31        |
| 2.2.2 Memory formation and its stages: .....  | 31        |
| 2.2.2.1 Encoding, Consolidation, Storage and Retrieval.....                                 | 31        |
| 2.2.3 Episodic memory is affected in AD.....  | 34        |
| 2.2.3.1 Episodic-like object recognition memory in rodents .....                            | 34        |
| 2.2.4 Hippocampus organization and pathways for memory formation .....                      | 37        |
| 2.2.5 Basal synaptic transmission and synaptic plasticity .....                             | 38        |
| 2.2.5.1 Glutamergic synapse .....   | 40        |
| 2.2.5.2 Post synaptic density .....   | 40        |
| 2.2.5.3 AMPAR and NMDAR.....  | 40        |
| 2.2.5.4 Different forms of synaptic plasticity.....   | 41        |
| 2.2.5.4.1 LTP.....  | 41        |
| 2.2.5.4.2 LTD.....  | 43        |

|            |   |           |
|------------|---|-----------|
| 2.2.6      | Modulatory action of A $\beta$ on synapse function and plasticity ..... | 43        |
| 2.2.6.1    | Physiological conditions .....  | 44        |
| 2.2.6.2    | Pathological conditions .....   | 45        |
| 2.2.7      | Modulatory action of A $\beta$ on memory .....                          | 47        |
| 2.2.8      | Putative mechanisms of A $\beta$ actions at synapses .....              | 48        |
| 2.2.9      | Mouse models of AD.....   | 49        |
| 2.2.9.1    | Different mouse models .....  | 49        |
| 2.2.9.2    | Tg2576.....   | 50        |
| 2.2.9.2.1  | A $\beta$ accumulation .....  | 50        |
| 2.2.9.2.2  | Memory deficits .....   | 51        |
| 2.2.9.3    | A $\beta$ local injections .....  | 51        |
| <b>2.3</b> | <b>Stress axis.....</b>   | <b>52</b> |
| 2.3.1      | Stress .....  | 52        |
| 2.3.1.1    | Definition .....  | 52        |
| 2.3.1.2    | Acute and Chronic stress.....   | 52        |
| 2.3.2      | Hypothalamus-Pituitary-Adrenal (HPA) axis.....                          | 53        |
| 2.3.2.1    | CORT release.....   | 54        |
| 2.3.2.2    | Effect of CORT on thymus .....  | 55        |
| 2.3.2.3    | ACTH release and its effect on adrenal glands .....                     | 55        |
| 2.3.2.4    | Negative feedback control of CORT.....                                  | 56        |
| 2.3.3      | GRs and MRs .....   | 57        |
| 2.3.3.1    | Gene sequence and structure of the receptors: .....                     | 58        |
| 2.3.3.2    | Functional role of the receptors: .....                                 | 59        |
| 2.3.3.2.1  | Membrane CORT receptors and their functions.....                        | 59        |
| 2.3.3.2.2  | Genomic action of receptors.....  | 60        |
| 2.3.4      | Techniques to study receptor function.....                              | 61        |
| 2.3.4.1    | Different GR agonist and antagonists and their drawbacks .....          | 61        |
| 2.3.4.2    | Genetic manipulation studies .....                                      | 62        |
| 2.3.5      | Role of the hippocampus in stress/HPA axis.....                         | 63        |
| 2.3.5.1    | Effect of stress on hippocampus: .....                                  | 63        |
| 2.3.5.2    | Effect of stress/CORT on synaptic plasticity .....                      | 64        |
| 2.3.5.2.1  | At intermediate CORT level/stress:.....                                 | 64        |
| 2.3.5.2.2  | High CORT level/stress .....  | 65        |
| 2.3.5.3    | Effect of CORT/ stress on memory .....                                  | 65        |
| 2.3.6      | GR modulators and their use as therapeutic in AD.....                   | 66        |
| <b>2.4</b> | <b>Link between AD and stress.....</b>                                  | <b>66</b> |

|            |   |           |
|------------|---|-----------|
| 2.4.1      | Stress is a major environmental risk factor for AD .....                      | 66        |
| 2.4.2      | HPA axis adaptive changes in human AD patients and AD mouse models .....      | 67        |
| 2.4.2.1    | CORT levels.....  | 67        |
| 2.4.2.2    | ACTH levels .....   | 68        |
| 2.4.2.3    | Stress related disorders in AD patients .....                                 | 68        |
| 2.4.3      | Tau and HPA axis.....   | 69        |
| 2.4.4      | Role of stress/CORT administration on A $\beta$ pathology.....                | 69        |
| 2.4.5      | Role of GRs in AD .....   | 70        |
| 2.4.6      | Relationship between A $\beta$ oligomers and GRs .....                        | 70        |
| 2.4.7      | Common link between A $\beta$ and CORT on the glutamatergic system.....       | 71        |
| <b>3</b>   | <b>OBJECTIVES .....</b>   | <b>73</b> |
| <b>4</b>   | <b>MATERIALS AND METHODS:.....</b>  | <b>75</b> |
| <b>4.1</b> | <b>Animal Breeding .....</b>  | <b>75</b> |
| <b>4.2</b> | <b>Genotyping.....</b>  | <b>76</b> |
| <b>4.3</b> | <b>Dissection of hippocampus, thymus and adrenal glands.....</b>              | <b>78</b> |
| <b>4.4</b> | <b>Biochemical Techniques .....</b>   | <b>79</b> |
| 4.4.1      | Estimation by ELISA.....  | 79        |
| 4.4.1.1    | Plasma corticosterone .....   | 79        |
| 4.4.1.2    | ACTH estimation .....   | 79        |
| 4.4.2      | Extraction of total proteins from hippocampus .....                           | 79        |
| 4.4.3      | Immunoblotting .....  | 80        |
| 4.4.4      | A $\beta$ oligomer (oA $\beta$ ) preparation .....                            | 80        |
| <b>4.5</b> | <b>Local <i>in vivo</i> ablation of GR in GR<sup>lox/lox</sup> mice .....</b> | <b>82</b> |
| 4.5.1      | Stereotaxic injections of AAV .....   | 82        |
| 4.5.2      | Immunofluorescence staining of GR .....                                       | 83        |
| 4.5.3      | Microscopy and estimation of GR intensity .....                               | 84        |
| <b>4.6</b> | <b>Electrophysiology .....</b>  | <b>84</b> |
| 4.6.1      | Slice preparation.....  | 84        |
| 4.6.2      | Field recordings by electrophysiology.....                                    | 85        |
| 4.6.2.1    | To measure basal synaptic plasticity.....                                     | 85        |
| 4.6.2.2    | For pharmacological studies .....   | 86        |
| 4.6.3      | Analysis of fEPSP response: .....   | 87        |

|            |   |            |
|------------|---|------------|
| <b>4.7</b> | <b>Behaviour</b> .....  | <b>88</b>  |
| 4.7.1      | Episodic-like object recognition memory.....  | 88         |
| 4.7.2      | Novel Object Recognition (NOR) after local <i>in vivo</i> injections.....   | 90         |
| <b>4.8</b> | <b>Statistical analysis</b> .....   | <b>92</b>  |
| <b>5</b>   | <b>RESULTS</b> .....  | <b>93</b>  |
| <b>5.1</b> | <b>Chapter 1</b> .....  | <b>93</b>  |
| 5.1.1      | Aim: Study of HPA axis dysregulation in Tg2576 (Tg <sup>+</sup> ) AD mouse model.....   | 93         |
| 5.1.1.1    | Comparison of CORT levels in WT and Tg <sup>+</sup> male mice at 3 and 6-month of age.....  | 95         |
| 5.1.1.2    | Comparison of plasma ACTH levels in WT and Tg <sup>+</sup> male mice at 4 and 6 months.....   | 96         |
| 5.1.1.3    | Comparison of body, thymus and adrenal gland weights between WT and Tg <sup>+</sup> male mice at 4 and 6 month of age.....                | 97         |
| 5.1.1.4    | Quantification of GR by immunoblotting from hippocampal total protein extract in 4 months male Tg <sup>+</sup> and WT mice.....           | 99         |
| 5.1.1.5    | Rescue of episodic memory deficits in 4 month Tg <sup>+</sup> male mice with GR antagonist RU486 treatment.                               | 100        |
| <b>5.2</b> | <b>Chapter 2</b> .....  | <b>102</b> |
| 5.2.1      | Aim 2: To check the specific role of GRs in AD like phenotypes in GR <sup>lox/lox</sup> Tg <sup>+</sup> mice.....                         | 102        |
| 5.2.1.1    | Generation of the GR <sup>lox/lox</sup> Tg <sup>+</sup> mice.....   | 103        |
| 5.2.1.2    | Basic characterization of the GR <sup>lox/lox</sup> Tg <sup>+</sup> mice.....   | 105        |
| 5.2.1.3    | Verification of AD like phenotypes in GR <sup>lox/lox</sup> Tg <sup>+</sup> as seen in Tg <sup>+</sup> mice.....                          | 106        |
| 5.2.1.4    | Increased CORT levels.....  | 107        |
| 5.2.1.5    | Exacerbated LTD phenotype.....  | 108        |
| 5.2.1.6    | Stereotaxic injections with Cre-GFP in GR <sup>lox/lox</sup> Tg <sup>+</sup> mice to ablate GR gene in CA1 neurons <i>in vivo</i>         | 109        |
| <b>5.3</b> | <b>Chapter 3</b> .....  | <b>111</b> |
| 5.3.1      | Aim 3: To investigate if A $\beta$ oligomers act via GRs to promote their acute synaptic effects at hippocampal synapses.....             | 111        |
| 5.3.1.1    | Effect of oA $\beta$ on levels of GR in PSD.....  | 112        |
| 5.3.1.2    | Effect of GR Antagonist compound 13 (C13) on synaptic transmission and LTP.....   | 113        |
| 5.3.1.3    | Effect of C13 on LTP impairment caused by oA $\beta$ .....  | 114        |
| 5.3.1.4    | Quantification of GR reduction in the CA1 of the GR <sup>lox/lox</sup> Tg <sup>-</sup> mice upon <i>in vivo</i> Cre-GFP transduction..... | 116        |
| 5.3.1.5    | Effect of GR reduction in CA1 on LTP.....   | 117        |
| 5.3.1.6    | Effect of GR reduction in CA1 neurons on the LTP impairment caused by oA $\beta$ .....  | 119        |

|            |  |            |
|------------|--|------------|
| 5.3.1.7    | NOR test after oA $\beta$ local injections .....   | 121        |
| <b>5.4</b> | <b>Chapter 4 .....</b>   | <b>124</b> |
| 5.4.1      | Discovery of $\eta$ -secretase APP processing pathway.....                                   | 124        |
| 5.4.2      | Aim 4: Effect of CHO derived A $\eta$ - $\alpha$ and A $\eta$ - $\beta$ peptides on LTP..... | 124        |
| <b>6</b>   | <b>DISCUSSION AND PERSPECTIVES .....</b>   | <b>127</b> |
| <b>7</b>   | <b>CONCLUSION .....</b>  | <b>139</b> |
| <b>8</b>   | <b>PERSONAL ACCOMPLISHMENTS.....</b>   | <b>141</b> |
| <b>9</b>   | <b>ANNEXE.....</b>   | <b>142</b> |
| <b>10</b>  | <b>REFERENCES.....</b>   | <b>171</b> |

## Index of Figures

|  |    |
|--|----|
| Figure 1: Photomicrograph of a section of the amygdala from an Alzheimer's patient showing the classical neuropathological lesions. .... | 18 |
| Figure 2: Scheme of amyloid precursor protein (APP) processing pathways and cleavage products.....                                       | 23 |
| Figure 3: Schematic of A $\beta$ assembly process.....   | 25 |
| Figure 4: Gross brain of late stage AD patient. ....   | 27 |
| Figure 5: Biomarkers of Alzheimer's pathological pathway.....  | 28 |
| Figure 6: Classification of the different memory systems into short and long term storage systems.....                                   | 31 |
| Figure 7: Functional overview of extended hippocampal-diencephalic memory system.....  | 32 |
| Figure 8: Standard consolidation model. ....   | 33 |
| Figure 9: Object recognition tasks. ....   | 36 |
| Figure 10: Basic anatomy of the hippocampus.....   | 38 |
| Figure 11: Simplified representative diagram of excitatory glutamatergic chemical synapse. ....  | 39 |
| Figure 12: A simplified scheme showing the two forms of synaptic plasticity, LTP and LTD. ....   | 42 |
| Figure 13: Bell shaped representation of the relationship between A $\beta$ level and synaptic activity.....                             | 43 |
| Figure 14: Differential dose-dependent effects of A $\beta$ on LTP in hippocampus.....   | 45 |
| Figure 15: Concentration dependent effects of A $\beta$ on synaptic function. ....   | 46 |
| Figure 16: The HPA axis is under the excitatory control of the amygdala and the inhibitory control of the hippocampus.....               | 53 |
| Figure 17: Typical superimposed ultradian (fine line) and circadian (thick line) circulating corticosterone plasma level in mice. ....   | 54 |
| Figure 18: The major physiological functions of cortisol in the human body.....  | 55 |
| Figure 19: Time domains of CORT feedback.....  | 56 |
| Figure 20: Structure of human GR gene and protein.....   | 59 |
| Figure 21: General mechanism of nuclear action of GRs in target cells. CORT.....   | 61 |

|  |     |
|--|-----|
| Figure 22: Specific sites of hippocampus indicating areas responsible for synaptic plasticity and regulation of HPA axis with respect to the site of GRs. ....                               | 63  |
| Figure 23: Link between A $\beta$ and GRs. ....  | 71  |
| Figure 24: Gel picture of PCR bands after amplification. ....  | 78  |
| Figure 25: Profile of the synthetic oA $\beta$ preparation. ....   | 81  |
| Figure 26: Summary of the protocol for the Cre-GFP injections in the GR <sup>lox/lox</sup> mice. ....  | 82  |
| Figure 27: Cross section of the hippocampus showing the synapses formed between the different sub-structures of the hippocampus.....   | 85  |
| Figure 28: Timeline used to check the preventive action of the GR Antagonist C13 on oA $\beta$ – mediated effect on LTP.....   | 87  |
| Figure 29: Representative fEPSP response in clamp fit software.....  | 87  |
| Figure 30: Scheme for What-When-Where object recognition protocol.....   | 88  |
| Figure 31: Scheme showing cannula implantation in the CA1 of the hippocampus for local injections of drug/peptide followed by Novel Object Recognition behaviour task.....                   | 90  |
| Figure 32: Scheme for Novel Object Recognition protocol. ....  | 91  |
| Figure 33: Timeline of Tg2576 mouse neuropathology showing gradual increase of A $\beta$ oligomers starting at the early stage (3-4 months) and developing plaques only at a later age. .... | 95  |
| Figure 34: Comparison of plasma CORT levels in WT and Tg <sup>+</sup> mice at 3, 4 and 6 months. .   | 96  |
| Figure 35: Comparison of plasma ACTH levels in WT and Tg <sup>+</sup> mice at 4 and 6 months of age. ....  | 97  |
| Figure 36: Comparison of body weights, thymus and adrenal gland weights of WT and Tg <sup>+</sup> male mice at 4 and 6 month of age. ....  | 98  |
| Figure 37: Quantification of GR by immunoblotting from hippocampal total proteins in 4 months male WT and Tg <sup>+</sup> mice. ....   | 100 |
| Figure 38: Four-month old Tg <sup>+</sup> mice display episodic memory deficits which were rescued by blocking glucocorticoid receptors.....   | 101 |
| Figure 39: Summary of the GR <sup>lox/lox</sup> Tg <sup>+</sup> mice breeding. ....  | 103 |
| Figure 40: Basic characterization of GR <sup>lox/lox</sup> Tg <sup>+</sup> mice .....  | 105 |
| Figure 41: Comparison of CORT levels in Tg <sup>+</sup> and GR <sup>lox/lox</sup> Tg <sup>+</sup> mice. ....   | 107 |
| Figure 42: Comparison of LFS-LTD in Tg <sup>+</sup> and GR <sup>lox/lox</sup> Tg <sup>+</sup> .....  | 108 |
| Figure 43: Deaths of animals upon surgery for stereotaxic injection. ....  | 110 |

|  |     |
|--|-----|
| Figure 44: Effect of oA $\beta$ on the GR levels in the post synaptic density.....   | 112 |
| Figure 45: Effect of C13 on basal synaptic transmission and LTP.....   | 113 |
| Figure 46: Effect of acute oA $\beta$ and C13 on LTP. ....   | 115 |
| Figure 47: Expression of Cre-GFP and reduction of nuclear GR expression in CA1 of GR <sup>lox/lox</sup> mice.....            | 116 |
| Figure 48: Effect of GR reduction on LTP. ....   | 118 |
| Figure 49: Effect of acute oA $\beta$ on eGFP- and Cre-GFP-transduced adult hippocampal sections.....                        | 120 |
| Figure 50: Discrimination ratio for oA $\beta$ versus vehicle mice. ....   | 121 |
| Figure 51: Effect of A $\eta$ - $\alpha$ (n=4) or A $\eta$ - $\beta$ (n=4) on baseline activity at the CA3-CA1 synapse. .... | 125 |
| Figure 52: A $\eta$ - $\alpha$ impairs LTP. ....   | 126 |
| Figure 53: Possible pathways contributing to the dissociation of ACTH and GC levels. ....                                    | 129 |
| Figure 54: Summary of HPA axis alterations in Tg2576 AD mouse model. ....  | 132 |

## Index of Tables

|  |     |
|--|-----|
| Table 1: Characteristic symptoms, neuropathology and proportion of the different types of dementia cases. ....   | 17  |
| Table 2: Comparison between effects of high levels of A $\beta$ and stress/ high levels of CORT/GR activation on the glutamatergic transmission, synaptic plasticity, dendrites and spines, and hippocampus-dependent memory processes. .... | 72  |
| Table 3: Primer list for APP transgene and GRloxP PCR .....  | 77  |
| Table 4: Details of primary and secondary antibodies used for immunoblotting with their respective conditions.....   | 80  |
| Table 5: Properties of Compound 13 (C13) as described in (Hunt et al., 2015) .....   | 86  |
| Table 6: Statistics table for unpublished data from Chapter 3.....   | 123 |

# 1 Abbreviations

ACTH: Adrenocorticotrophic hormone  
AD: Alzheimer's disease  
ADAM: A disintegrin and metalloproteases  
AICD: APP intracellular domain  
AMPA: Alpha-amino-3-hydroxy-5-methyl-4-isoxazole-propionate  
Amyloid- $\beta$  /A $\beta$ : Amyloid  $\beta$  peptide  
A $\eta$ - $\alpha$ : Amyloid eta- $\alpha$  peptide  
A $\eta$ - $\beta$ : Amyloid eta- $\beta$  peptide  
AP-1: Activated protein -1  
APH1: Anterior pharynx defective homolog 1  
APP /A $\beta$ PP: Amyloid precursor protein  
APLP1 and 2: Amyloid- $\beta$  precursor like protein 1 and 2  
APOE: Apolipoprotein E  
AR: Androgen receptor  
AVP: Vasopressin  
BACE1:  $\beta$ -site APP-cleaving enzyme  
BDNF: Brain derived neurotrophic factor  
BST: Bed nucleus of stria terminallis  
CA: Cornu ammonis  
cAMP: Cyclic adenosine monophosphate  
CAMKII: Calcium/calmodulin-dependent protein kinase II  
CBG: Cortisol binding globulin  
CD4<sup>+</sup>/CD8<sup>+</sup>: Cluster of differentiation  
CORT: Corticosteroids  
CREB: Cyclic AMP response element binding protein  
CSF: Cerebrospinal fluid  
CTF: C terminal fragment  
DBD: DNA-binding domain  
DG: Dentate gyrus  
DNA: Deoxyribonucleic acid  
EM: Episodic memory  
EphB2: Ephrin-type B2  
EPSC: Excitatory post synaptic current  
EPSP: Excitatory post synaptic potential  
ER: Estrogen receptor  
FAD: Familial Alzheimer's disease  
GABA: Gamma-Aminobutyric acid  
GCs: Glucocorticoids  
GFP: Green fluorescence protein

GluA1-4: AMPAR subunits  
GluN / NR1-3: NMDAR subunits  
GR: Glucocorticoid receptor  
GRE: Glucocorticoid response element  
Gsk3 $\beta$ : Glycogen synthase kinase-3 $\beta$   
HFS: High frequency stimulation  
HPA: Hypothalamus pituitary adrenal  
HSP: Heat-shock proteins  
KO: Knock-out  
LBD: Ligand-binding domain  
LTD: Long term depression  
LTM: Long term memory  
LTP: Long term potentiation  
MAPK-ERK: Mitogen-activated protein kinases / extracellular signal regulated kinase  
mGluR: Metabotropic glutamate receptors  
MMT: Multiple memory trace  
mPFC: Medial prefrontal cortex  
MR: Mineralocorticoid receptor  
MRI: Magnetic resonance imaging  
MT: Microtubules  
MT5-MMP: Membrane bound metalloproteinase  
MTL: Medial temporal lobe  
MWM: Morris water maze  
nAChR: Nicotinic acetylcholine receptors  
NF- $\kappa$ B: Nuclear factor-kappa B  
NFTs: Neurofibrillary tangles  
NMDA: N-methyl-D-aspartate  
NOR: Novel object recognition  
NR3C1: Nuclear receptor subfamily 3 group C membrane 1  
NT: Neurotransmitter  
NTD: N-terminal domain  
oA $\beta$ : Oligomers of amyloid- $\beta$   
p38MAPK: p38 mitogen activated protein kinase  
PEN2: Presenilin enhancer 2  
PET: Positron emission tomography  
PHF: Paired helically wound filaments  
PMCI: Pre-mild cognitive impairment  
PP2: Protein phosphatase 2  
PR: Progesterone receptor  
PrPc: Prion protein  
PRS: Perceptual representation system  
PSD: Post synaptic density

---

PSEN-1/ PS1: Presenilin 1  
PSEN-2 / PS2: Presenilin 2  
PVN: Paraventricular nucleus  
PVT: Paraventricular thalamus  
RAGE: Receptor for advanced glycation end products  
RNA: Ribonucleic acid  
sAPP $\alpha$ : Soluble APP alpha  
SM: Standard model  
SP: Senile Plaques  
STM: Short tern memory  
Tau: Tubulin associated unit  
Tg: Transgene/transgenic

## **2 Introduction**

---

### **2.1 Alzheimer's Disease**

#### **2.1.1 Aging, Dementia and AD**

Aging is a natural process of cognitive impairment in elderly people causing loss of executive functions as compared to younger people. A huge number of people in our current population are in this group. Eurostats (European statistical Institute) data show 18.9% of the European population in 2015 was 65 years and over. With aging, the incidence of neurodegenerative diseases like dementia increases.

Dementia is a chronic syndrome, characterized by a progressive deterioration in intellect, including memory, learning, comprehension and judgment (World Alzheimer's report, 2009). 46.8 million people worldwide were estimated to have dementia in 2015 and this is set to rise to 131.5 million people by 2050 (World Alzheimer report 2015). There are two important factual points to note here. First, much of the increase will take place in low and middle income countries. Secondly, the total estimated worldwide cost of dementia in 2015 is US \$ 818 billion (World Alzheimer report 2015). This high cost of treatment in lower income countries increases the burden of health care management, hence calling for extensive research in this field.

Dementia syndrome is linked to a large number of underlying brain pathologies. Alzheimer's disease (AD), vascular dementia, dementia with Lewy bodies and frontotemporal dementia are among the most common (Table 1). AD constitutes the leading cause of dementia in persons over 60 years, reaching 6.7% in subjects 75-79 years old and 31.15% in those over 85 years old (Tromp et al., 2015).

Table 1: Characteristic symptoms, neuropathology and proportion of the different types of dementia cases. Alzheimer’s disease is the most common form of dementia consisting of nearly 50-75% of dementia cases (World Alzheimer Report, 2009).

Table 1  
**Characteristics of dementia subtypes**

| Dementia subtype                       | Early, characteristic symptoms  | Neuropathology  | Proportion of dementia cases |
|--|---|---|------------------------------|
| <b>Alzheimer’s disease (AD) *</b>      | Impaired memory, apathy and depression<br>Gradual onset   | Cortical amyloid plaques and neurofibrillary tangles  | 50-75%                       |
| <b>Vascular dementia (VaD) *</b>       | Similar to AD, but memory less affected, and mood fluctuations more prominent<br>Physical frailty<br>Stepwise onset | Cerebrovascular disease<br>Single infarcts in critical regions, or more diffuse multi-infarct disease | 20-30%                       |
| <b>Dementia with Lewy Bodies (DLB)</b> | Marked fluctuation in cognitive ability<br>Visual hallucinations<br>Parkinsonism (tremor and rigidity)              | Cortical Lewy bodies (alpha-synuclein)  | <5%                          |
| <b>Frontotemporal dementia (FTD)</b>   | Personality changes<br>Mood changes<br>Disinhibition<br>Language difficulties                                       | No single pathology – damage limited to frontal and temporal lobes                                    | 5-10%                        |

\* Post mortem studies suggest that many people with dementia have mixed Alzheimer’s disease and vascular dementia pathology, and that this ‘mixed dementia’ is underdiagnosed

### 2.1.2 AD and its discovery

As mentioned above, AD is one of the most common forms of dementia contributing to almost 50-75% of cases (see Table 1). According to the Alzheimer’s foundation of America, AD is defined as a progressive, degenerative disorder that attacks the brain's nerve cells, or neurons, resulting in loss of memory, thinking and language skills, and behavioural changes. It was in 1906 that a German physician Alois Alzheimer first described the presence of lesions such as senile plaques and neurofibrillary tangles (NFTs) in the brain (Figure 1) of a patient Auguste Deter, who was suffering from dementia. Her symptoms included cognitive and psychosocial impairments, hallucinations and disorientation (Maurer et al., 1997).

### 2.1.3 AD neuropathology:

More than 100 years have passed since Alois Alzheimer’s discovery of neuropathological hallmarks of AD. Currently, the pathological features are known to include 1) Senile plaques

composed largely of amyloid- $\beta$  ( $A\beta$ ) peptides, 2) intracellular NFTs composed of hyperphosphorylated microtubule associated protein tau, 3) dysmorphic synapses and 4) neuronal loss (Hardy and Allsop, 1991, Goedert et al., 1991, Palop and Mucke, 2010).

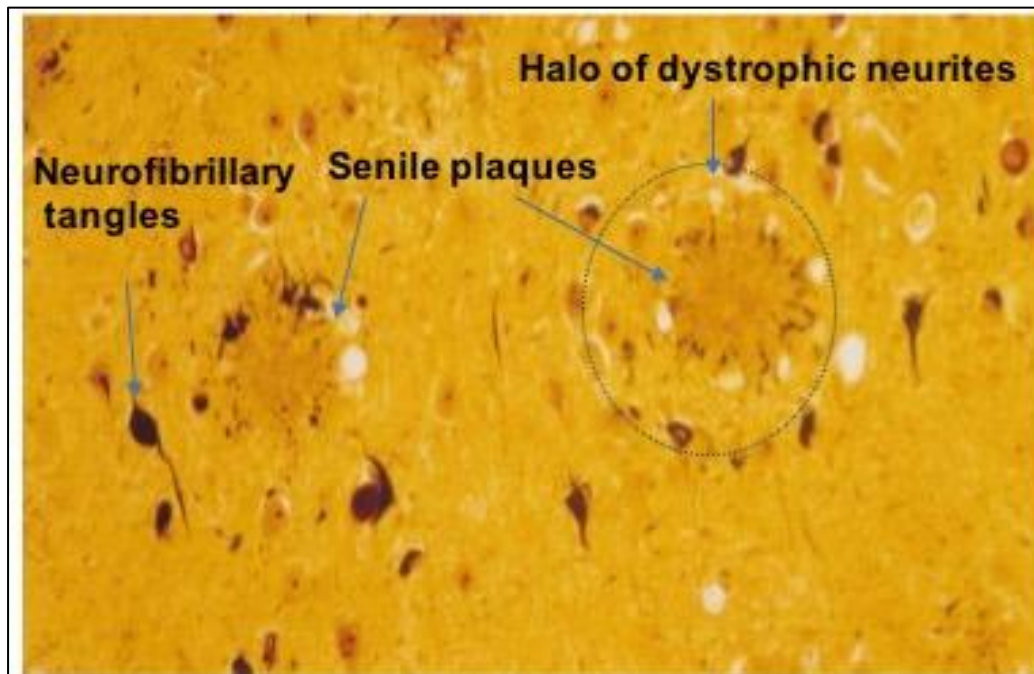


Figure 1: Photomicrograph of a section of the amygdala from an Alzheimer's patient showing the classical neuropathological lesions. Modified Bielschowsky silver stain demonstrates two senile plaques consisting of extracellular deposits of amyloid surrounded by halo of dystrophic neurites. Some of the pyramidal neurons contain neurofibrillary tangles. (Selkoe et al, 1999)

### 2.1.3.1 *Senile plaques*

Senile plaques (also called as neuritic plaques), are spherical lesions, microscopic foci of extracellular deposits of  $A\beta$  protein that include abundant amyloid fibrils (7-10 nm) intermixed with non-fibrillar forms of this peptide (Figure 1). They contain degenerating axons and dendrites and intimately surrounded with amyloid deposits. They characteristically contain activated microglia within and near the fibrillary amyloid core, as well as reactive astrocytes surrounding the core (Perlmutter et al., 1992). Plaques are generally found in the limbic and associated cortices.

Along with the neuritic plaques came the discovery of diffused plaques which were amorphous appearing non-fibrillar plaques. These were considered to be diffused “pre-amyloid” deposits.

### **2.1.3.2 *Tau neurofibrillary tangles***

These are intraneuronal cytoplasmic lesions consisting of non-membrane bound bundles of paired, helically wound approximately 10nm filaments (PHF), sometimes interspersed with straight filaments (Figure 1). Biochemical analysis of neurofibrillary tangles showed that they consist of microtubule associated protein tau in its hyperphosphorylated form. These tangles generally occur in large numbers in AD brain particularly in entorhinal cortex, hippocampus, amygdala and associated cortices of frontal, temporal and parietal lobes. Tau is a highly soluble protein with a predominant expression in the neurons (Trojanowski et al., 1989). A large proportion of this protein present in the axon, interacts with microtubules (MTs) through its C terminal microtubule-binding domain to promote MT polymerization and stabilization (Götz et al., 2013).

Neurofibrillary tangles can occur in multiple uncommon neurodegenerative diseases (like frontotemporal dementia) and in absence of A $\beta$  deposits and neuritic plaques. Therefore, the two classical lesions of AD can occur independently of each other.

## **2.1.4 Two types of AD:**

### **2.1.4.1 *Familial AD***

Familial AD (FAD) causes early onset of AD and account for 1-5% of all cases. FAD onset is due to autosomal dominant mutations in the following three genes: Amyloid precursor protein (APP), Presenilin 1, Presenilin 2 (PSEN-1 and 2; catalytic subunit of enzyme responsible for cleavage of APP to produce A $\beta$ ). These mutations shift the APP processing towards the amyloidogenic pathway resulting in long, toxic A $\beta$  peptide production (see section 1.1.6 below for more details on APP processing). However, there is an exception in one of the mutations of APP variant in the population of Iceland that does not increase the A $\beta$  peptide load. Instead, this mutation confers protection from AD (Jonsson et al., 2012). Several mutations have been identified supporting studies on FAD, with more than 20 autosomal-dominant APP mutations, ~ 80 mutations in presenilin-1 and 10 mutations in presenillin-2 have been linked to AD (Ashe and Zahs, 2010).

### **2.1.4.2 Sporadic AD**

Sporadic AD, which is the more common form of AD, also involves genetic risk factors. This form of AD is seen in patients above 60-65 years and hence generally called as late onset AD (LOAD). The most common mutation in this context is the  $\epsilon 4$  allelic variant of the APOE gene, which encodes for apolipoprotein E (APOE) (Bertram et al., 2010). This allele is one amongst the three alleles ( $\epsilon 2$ ,  $\epsilon 3$ ,  $\epsilon 4$ ), which exist for this protein. Approximately 20-25% of the population carries at least one copy of APOE  $\epsilon 4$  allele, which increases the risk of AD by ~4 fold (as compared to those with the more common APOE  $\epsilon 3/\epsilon 3$  genotype). On the other hand, 2% of the population carries two  $\epsilon 4$  alleles, imparting a ~12 fold increase risk. Studies in mice suggest that APOE regulates A $\beta$  levels in an APOE-isoform dependent manner, such that the  $\epsilon 4$  isoform promotes A $\beta$  build-up whereas the  $\epsilon 2$  isoform seems to enhance its clearance (Genin et al., 2011). In addition, a most recent study suggests that APOE isoforms differentially regulate APP transcription (Huang et al., 2017).

Hence both APP mutations and APOE isoforms can either increase A $\beta$  accumulation, which increases the susceptibility towards AD, or reduce its accumulation, which reduces susceptibility to AD. Thus, we can conclude that genetic data strongly support an important etiological role for A $\beta$  accumulation in AD.

Along with the widely studied APOE, recent large genome wide association studies (GWASs) have identified nine other genes/loci (CR1, BIN1, CLU, PICALM, MS4A4/MS4A6E, CD2AP, CD33, EPHA1 and ABCA7) for LOAD (Kamboh et al., 2012). BIN1 stands as the second most important risk locus in LOAD after APOE. Interestingly it is known to modulate tau pathology, amongst its other functions including endocytosis, calcium homeostasis and apoptosis (Tan et al., 2013).

Together, these data support the notion that LOAD, although neuropathologically and neuroclinically similar to FAD, harbours a complex aetiology.

### **2.1.5 Environmental risk factors:**

LOAD is also subject to environmental risk factors. Besides age, which is the most evident risk factor for LOAD, stress is one of the better known environmental risk factor (Sotiropoulos et al., 2011, Wilson et al., 2003) as there is evidence that it accelerates AD (see Introduction chapter 1.4 below). Also, a rare haplotype in the gene producing cortisol has

been associated with a six fold increased risk for sporadic AD (de Quervain et al., 2004), suggesting that genes implicated in stress biology could represent additional genetic risk factors. Other non-genetic risk factors, include hypertension (Kehoe, 2003), metabolic disorders such as diabetes (Sleegers et al., 2004) and diet (Rothman and Mattson, 2010).

### **2.1.6 APP and its processing:**

The etiological role for A $\beta$  accumulation in AD is currently questioned due to contradictory data obtained from AD patients and mouse models (Musiek and Holtzman, 2015, Herrup, 2015, Nelson et al., 2009). Nevertheless, sufficient evidence proves that A $\beta$  and its aggregates cause synaptic dysfunction and memory impairments, strengthening its role as a trigger to initiate AD. To understand better the role of the 4kDa A $\beta$  peptide and its production, it is important to first address the functional role of its precursor APP.

#### **2.1.6.1 *Function of APP:***

A $\beta$  is a proteolytic product derived from APP (also called A $\beta$ PP), which is a type-1 transmembrane glycoprotein expressed in several cells (e.g. neurons, glia, endothelial cells, fibroblasts). There are two other APP-like proteins, APLP1 and APLP2, which seem at least partly homologous in function to APP. However, they do not conserve the A $\beta$  region and till date no AD related mutation have been identified in these genes. To identify the physiological function of APP, different knock-out, knock-in and transgenic studies were created (Wolfe and Guénette, 2007). Single APP KO mice are viable, however, show several phenotypes, which include long term potentiation (LTP) and memory impairment (Dawson et al., 1999, Phinney et al., 1999). These mice do not exhibit any fundamental health problem, like early mortality as this may result due to compensatory action of ALPLs. By contrast, the double knockout APP-APLP2, APLP1-APLP2 and triple KO APP-APLP1-APLP2 result in mortality. Double knock out APP-APLP1 is the only exception that is viable due to the presence of essential APLP2 gene (Heber et al., 2000). These studies indicate that the APP gene family is vital in developmental stages. Overall, APP has been implicated in cell adhesion, cell signalling, protease inhibition and development (Wolfe and Guénette, 2007).

In addition, there is heterogeneity of APP which produces three different isoforms APP<sub>695</sub>, APP<sub>751</sub> and APP<sub>770</sub>. This is caused by alternative splicing as well as a variety of posttranslational modifications, including the addition of sugars and phosphate groups (Hung and Selkoe, 1994, Oltersdorf et al., 1990). The importance of these alternative splicing is unknown.

#### **2.1.6.2 APP processing:**

A $\beta$  peptides of 39-43 amino acids are generated from the sequential cleavage of APP. APP can be cleaved to produce A $\beta$  at the plasma membrane, the trans-golgi, the endoplasmic reticulum and within endosomal-lysosomal systems (Xu et al., 1997, Greenfield et al., 1999). The structure of APP includes the A $\beta$  domain with several cleavage sites for secretases enzymes. Two well-known pathways compete for the APP substrate, which either leads to amyloidogenic (A $\beta$  production) or non-amyloidogenic (no A $\beta$  production) processing of the protein.

In the **non-amyloidogenic pathway** (Figure 2), the APP is cleaved in the A $\beta$  domain by  $\alpha$ -secretases, belonging to the family of membrane glycoproteins called ADAM (a disintegrin and metalloproteases) or ADAM 10 and 17, releasing the soluble ectodomain sAPP $\alpha$  and the C-terminal fragment CTF $\alpha$  (Buxbaum et al., 1998, Lammich et al., 1999). It was shown that soluble APP $\alpha$  harbours numerous neuroprotective functions. These functions include, but are not limited to, proliferation, neuroprotection, synaptic plasticity, memory formation, neurogenesis and neuritogenesis in cell culture and animal models (Mattson et al., 1993, Turner et al., 2003). The subsequent cleavage of CTF $\alpha$  by the  $\gamma$ -secretase produces soluble extracellular p3 peptides and the APP intracellular domain (AICD) (De Strooper et al., 1999).  $\gamma$ -secretase is a member of the aspartyl protease family able to regulate intramembrane proteolysis for several type 1 integral membrane proteins, including APP, APLPs, Notch, E-cadherin and many others. Four main components of  $\gamma$ -secretase have been identified: Presenilin, nicastrin, anterior pharynx defective homolog 1 (APH1), and presenilin enhancer 2 (PEN2) (Steiner et al., 2002, Li et al., 2003). AICD has been reported to interact with different proteins and may be involved in several intracellular pathways including apoptosis, neuronal growth and has transcriptional activity (Cupers et al., 2001).

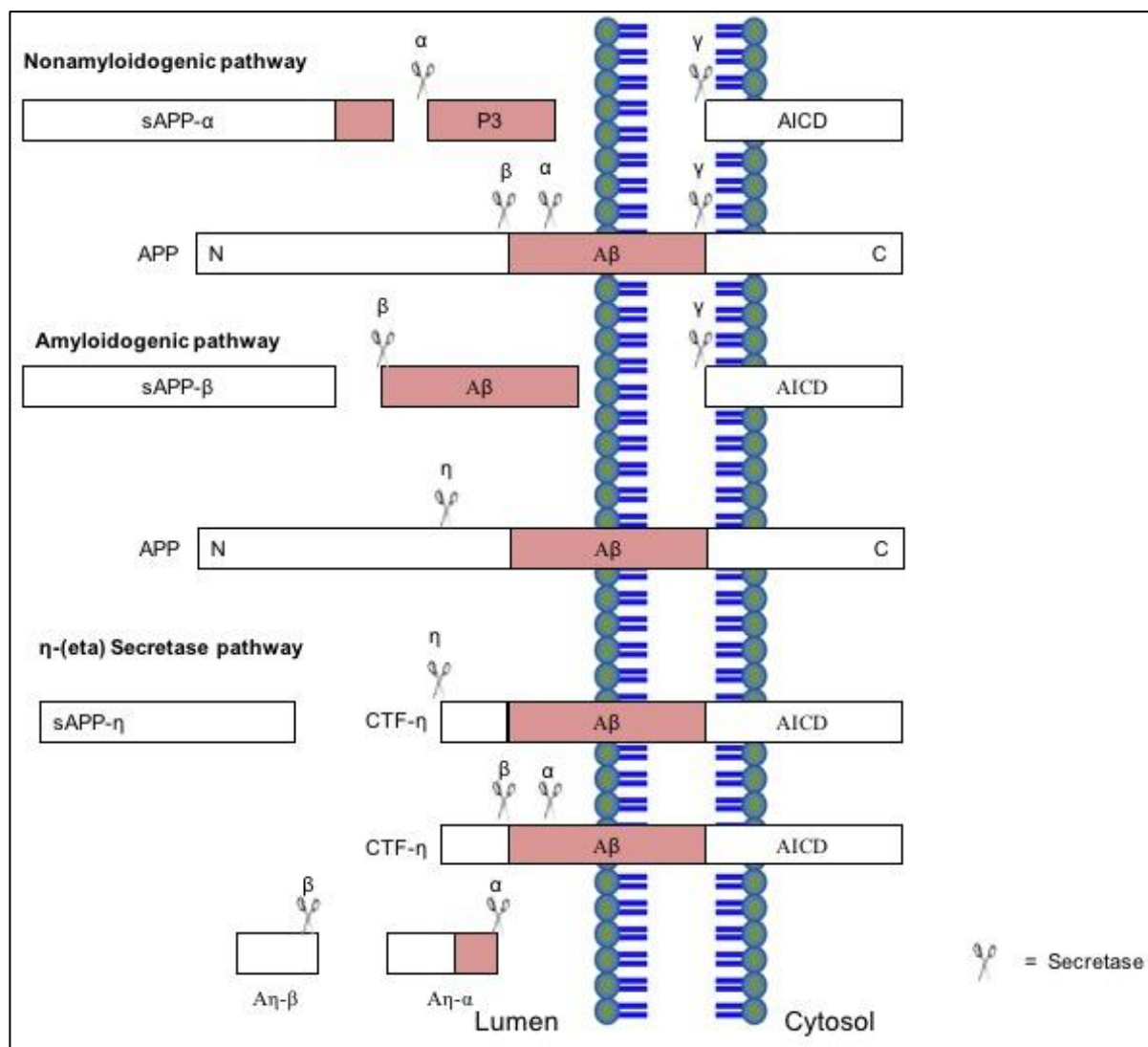


Figure 2: Scheme of amyloid precursor protein (APP) processing pathways and cleavage products. The nonamyloidogenic pathway (upper) involves first cleavage by  $\alpha$ -secretase to generate sAPP- $\alpha$  and C-terminal fragment CTF C83 (not shown). The subsequent cleavage of C83 by  $\gamma$ -secretase generates APP intracellular domain (AICD) and a short fragment P3. The amyloidogenic APP processing pathway (middle) involves first cleavage by  $\beta$ -secretase to generate sAPP $\beta$  and C-terminal fragment C99 (not shown). Subsequent cleavage of C99 by  $\gamma$ -secretase generates A $\beta$  peptides and AICD. In addition, a recent cleavage site of APP by  $\eta$ -secretase to generate sAPP $\eta$  and a membrane bound CTF $\eta$ . This is further cleaved by  $\alpha$ - and  $\beta$ -secretase to release a long A $\eta$ - $\alpha$  and a short A $\eta$ - $\beta$  peptide, respectively (Adapted from (Habib et al., 2016)).

On the other hand, the **amyloidogenic pathway** (Figure 2) involves APP cleavage by  $\beta$ -secretases (also known as BACE1,  $\beta$ -site APP-cleaving enzyme), (Hussain et al., 1999, Sinha et al., 1999), which releases the soluble ectodomain sAPP $\beta$  and CTF $\beta$ . Cleavage of CTF $\beta$  by  $\gamma$ -secretases yields A $\beta$  peptides of varying lengths as well as the AICD fragment. BACE1 (an aspartic protease), beside cleaving APP and its homologs APLP1 and APLP2, acts on

other important substrates involved in brain function and development, such as neuregulin and voltage-gated sodium channel (Prox et al., 2012).

There are two C-terminal variants of A $\beta$  (A $\beta$ <sub>1-40</sub> and A $\beta$ <sub>1-42</sub>) which arise from heterogenous proteolysis at the C terminal of A $\beta$  by  $\gamma$ -secretase. Physiologically, 90% of A $\beta$  produced is the shorter A $\beta$ <sub>1-40</sub>, but A $\beta$ <sub>1-42</sub> is more prone to aggregate as fibrils and is the main component of amyloid deposits (Selkoe, 2001, Esler and Wolfe, 2001, Cai et al., 1993, Jarrett et al., 1993). Also, because A $\beta$ <sub>1-42</sub> seems to be prone to aggregation and more toxic than the shorter A $\beta$ <sub>1-40</sub>, the ratio of A $\beta$ <sub>1-42</sub>/A $\beta$ <sub>1-40</sub> might predict the severity of AD (Hansson et al., 2007).

There are also new pathways for APP processing that are emerging. We contributed to the characterization of the new  $\eta$  (eta)-secretase pathway (see Results chapter 4), which yields novel APP fragments: A $\eta$ - $\alpha$  and A $\eta$ - $\beta$  (Willem et al., 2015) (Figure 2). In brief, a higher molecular mass carboxy-terminal fragment CTF- $\eta$  is generated by a membrane-bound metalloproteinases such as MT5-MMP, which is referred to as  $\eta$ -secretase activity.  $\eta$ -secretase cleavage occurs at amino acids 504-505 of APP<sub>695</sub>, releasing a truncated ectodomain. CTF- $\eta$  is further processed by ADAM-10 and BACE1 to generate long and short A $\eta$  peptides (termed as A $\eta$ - $\alpha$  and A $\eta$ - $\beta$ ). These CTF fragments were shown to be enriched in dystrophic neurites in AD patients and mouse models.

### **2.1.6.3 Amyloid cascade hypothesis**

Genetic studies from FAD indicate that different mutations in the APP, PS1, PS2 direct towards increasing the A $\beta$  production. In addition, evidence on problems associated with clearance of A $\beta$  load led to an imbalance in A $\beta$  levels. These two view points led to the hypothesis that A $\beta$  is the causative agent in AD pathology and that neurofibrillary tangles, cell loss, vascular damage and dementia follow as a direct result of this deposition. The original edition of the amyloid cascade hypothesis was proposed in 1992 by Hardy and Higgins (Hardy and Higgins, 1992).

In brief, it is widely believed that chronic elevation of A $\beta$ <sub>1-42</sub> in the brain extracellular fluid and inside the neurons slowly leads to oligomerization of the peptide, eventually fibril formation and its deposition as diffuse and then mature senile plaques (Figure 3). This is followed by a local microglial activation and other various inflammatory processes, which

cause oxidative injury to proteins and macromolecules in neurons hence affecting the surrounding neuronal tissue. This eventually gives rise to neuronal dysfunction, tangle formation and cell death. The hypothesis hence attributed dementia to nerve cell death caused by the toxicity of large insoluble amyloid fibrils.

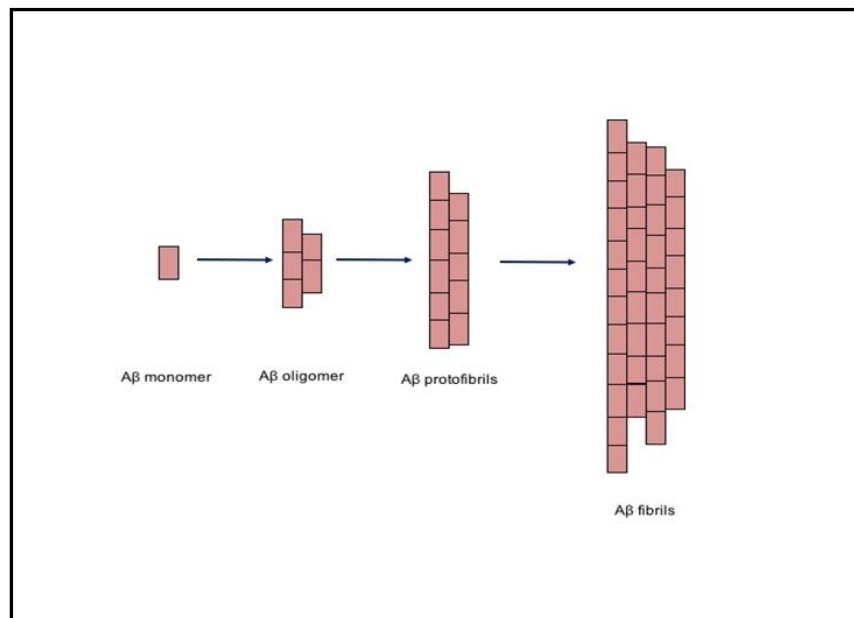


Figure 3: Schematic of Aβ assembly process. Aβ assembly starts from the monomer state to oligomers to protofibrils and fibrils (adapted from Yamin et al, 2009).

#### **2.1.6.4 Criticism and modifications to the amyloid hypothesis**

There is accumulating evidence indicating that this hypothesis is not sufficient to explain the multifaceted features of the disease as explained by (Herrup, 2015). The main criticism, which is very evident, is that a direct correlation between amyloid deposits and dementia severity has not been demonstrated, since some patients without amyloid deposition show severe memory deficits, while other patients with cortical Aβ deposits have no dementia symptoms (Terry et al., 1991, Arriagada et al., 1992, Herrup, 2015).

Another point, which arose with time, was the role of the soluble Aβ oligomers. As explained above, during pathological conditions, Aβ<sub>1-42</sub> peptide has a tendency to aggregate forming monomers, oligomers (which could include dimers, trimers, tetramers as aggregates) and later forming protofibrils and fibrils (simplified illustration in Figure 3). Amongst these aggregates, the small soluble Aβ oligomers (between 10 and 100 kDa) were discovered to be toxic and caused synaptic dysfunction and memory impairment (Lambert et al., 1998, Lue et al., 1999, Walsh et al., 2002). Hence these findings modified the hypothesis to the ‘oligomer

hypothesis'. It was suggested that A $\beta$  oligomers may have complex effects on surrounding neurons, microglia and astrocytes, the cumulative effect being to subtly alter synaptic function, and thus information storage and retrieval. Memory loss beginning earlier in the disease, was attributed to the oligomer-induced disruption of synaptic plasticity (Selkoe, 2002). The later stages of dementia were attributed to oligomer-induced cellular degeneration and death. The effect of amyloid- $\beta$  peptide/oligomers on synaptic plasticity and memory will be discussed in detail in Chapter 2.

One cannot conclude if it is the large, insoluble deposits or small soluble oligomers that represent the most prominent neurotoxic entity. Recent research shows that there is a dynamic balance between the two entities. The concentration of soluble A $\beta$  oligomers determines the size of the amyloid-beta aggregate, while concurrently this aggregate serves as a reservoir for the soluble amyloid oligomers (Koffie et al., 2009).

Also, although amyloid pathology is still generally considered as a key initiation factor in AD, we shall briefly mention the important contribution of tau. Indeed, the high degree of tau phosphorylation at early stages of AD as a key molecular signature of neurofibrillary degeneration in AD cannot be missed out (Buee et al., 2000). The conversion of physiological tau to pathological aggregates is believed to be a multi-faceted process. Detachment of tau from microtubules to unbound tau could be facilitated by either tau phosphorylation, A $\beta$ -mediated toxicity, oxidative stress, etc (Bramblett et al., 1993, Liu et al., 2005, King et al., 2006). In addition, recent research has opened new insights into the role of tau at the synapse (as mentioned in 2.2.6.2) and in the nucleus. Thus, in combination with amyloid pathology, tau pathology is likely to strongly contribute to neuron dysfunction early in AD progression.

### **2.1.7 Evolution of AD in the brain**

Clinically, the different stages of cognitive symptoms in AD can be divided into three phases: Pre-mild cognitive impairment (PMCI), MCI and AD. A long preclinical stage (PMCI) for almost 15-20 years before any sign of clinical symptoms has been suggested, followed by MCI where NFT and A $\beta$  pathology are increasing along with mild cognitive dysfunction in neuroclinical tests. MCI can be amnesic (aMCI) or multi-domain type (amnesic and other

cognitive domains), amongst which those with aMCI are at a higher risk to develop AD (Petersen, 2003).

AD neuropathology commences with thinning of cortex during asymptomatic stages (Dickerson and Wolk, 2012), proceeding with sequential atrophy in the entorhinal cortex, the hippocampus, the neocortex (Killiany et al., 2002, Raz et al., 2004) (Figure 4). In addition, quantitative morphological studies of temporal and cortical biopsies show significant loss of synapse density in AD patients (Davies et al., 1987) supported by low synaptic density and fewer dendritic spines. There is also evidence of a 25% decrease in the presynaptic marker synaptophysin in the cortex of MCI or mild AD patients (DeKosky and Scheff, 1990).

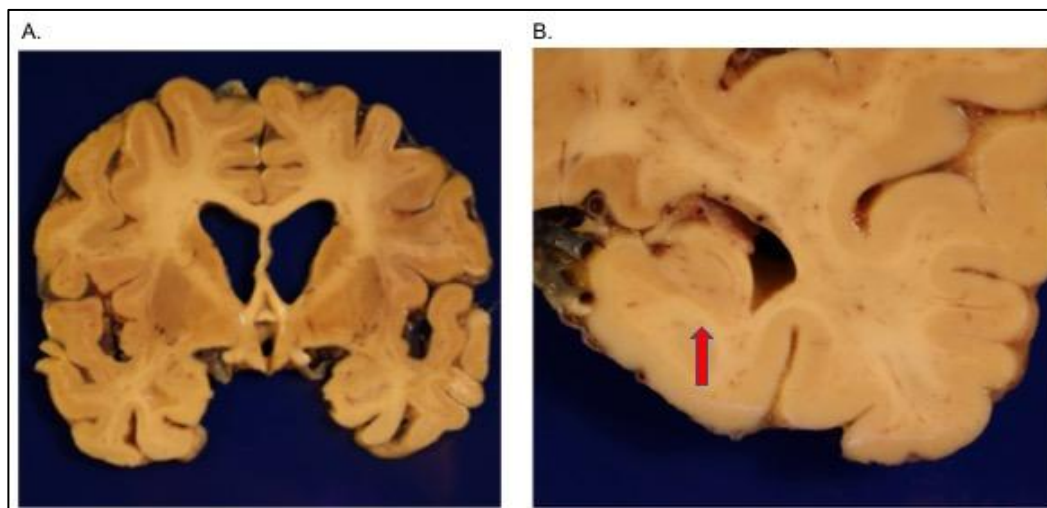


Figure 4: Gross brain of late stage AD patient. A). Generalised atrophy, ventricular dilation and medial temporal atrophy. B). Close up of hippocampal formation of the same patient, red arrow indicating hippocampal atrophy. (Castellani R et al., 2010)

The sequence of appearance of the two neuropathological hallmarks is known to be in a reverse order. Amyloid plaques are initiated in the neocortex and later spread to the entorhinal cortex and hippocampus (specifically, the CA1 sub region) and subcortical regions (Thal et al., 2002a). While NFTs develops sequentially from transentorhinal cortex to entorhinal cortex, hippocampus and neocortex (Thal et al., 1998). The hippocampus is one of the earliest brain structures to develop neurodegenerative changes. There is evidence showing that NFTs develop more profusely than the amyloid plaques in early AD (Arriagada et al., 1992). It is still under debate to determine which of the pathological features is best correlated with the disease state. Clinical studies indicate that NFTs correlate better than amyloid plaques with cognition in AD. Since the discovery that soluble A $\beta$  oligomers have

the ability to impair synaptic and memory function (Lesne et al., 2006), the idea is now changing to consider them along with amyloid plaques in pathological studies.

Recent advancement in biomarker research has also helped understand the sequence of abnormalities as the disease progresses. The earliest marker is that of an increase in cerebrospinal fluid (CSF)  $A\beta_{42}$  as shown in the graph below (Figure 5). These changes occur in preclinical phase and, by the time, the cognitive impairment is clinically detected,  $A\beta$  markers have reached a plateau. Subsequently, neuronal injury and neurodegeneration predominate. These are shown by CSF tau and cerebral atrophy on MRI. These markers, which become abnormal later in the disease, correlate more closely with clinical symptoms.

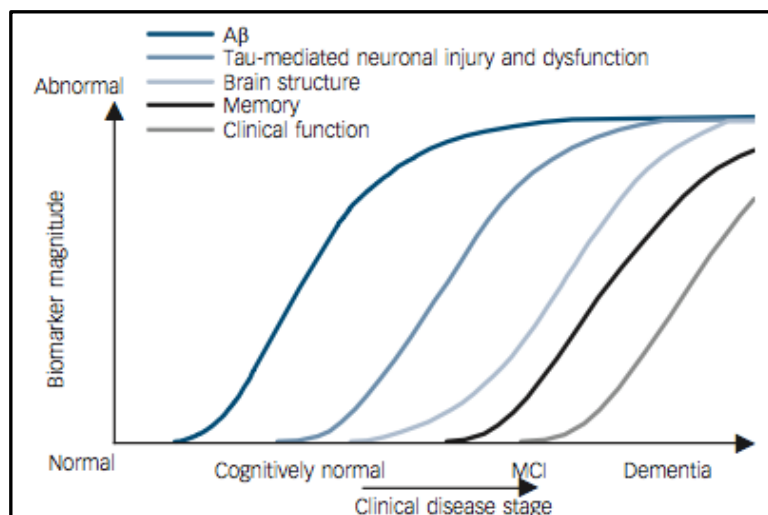


Figure 5: Biomarkers of Alzheimer's pathological pathway.  $A\beta$  is indicated by low CSF  $A\beta_{42}$  or positron emission tomography (PET)  $A\beta$  imaging. Tau neuronal injury and dysfunction is shown by CSF tau. Cerebral atrophy is measured with magnetic resonance imaging (Harrison J et al., 2016).

### 2.1.8 Treatments

AD has till date only a few different treatments targeting specific aspects. The two types of pharmacological therapeutics approved by the FDA are acetylcholine esterase inhibitors and NMDAR antagonist (memantine). In post-mortem AD brains, it was evident that there was cholinergic neuron loss (Whitehouse et al., 1981), although the mechanisms leading to this neuron loss remain largely unknown. Hence, to promote cholinergic signalling in early symptomatic AD patients, acetylcholine esterase inhibitors (donepezil, rivastigmine, and galantamine) have been used for decades to inhibit the acetylcholine degradation and thus maintain higher acetylcholine levels in the extracellular space (Zhu et al., 2013). On the other hand, memantine, an NMDA (N-methyl-D-aspartate) receptor antagonist is used for late

stage AD treatment. It is also not yet clear mechanistically how blocking NMDA receptors benefits the diseased brain, but use of memantine probably counteracts the effects of hyperactive excitatory circuits, evidenced in AD patients, and prevents high levels of glutamate from weakening synaptic strength. However, these drugs are only mildly effective and do not significantly halt cognitive deterioration or restore memory function (Zemek et al., 2014).

Other molecular treatments to restore cellular health and to repair circuit and network function are under development. Currently, to target high levels of A $\beta$ , several  $\beta$  and  $\gamma$ -secretase inhibitors and modulators are used in phase III clinical trials (Citron, 2010), but due to severe side effects these clinical trials were aborted (Schor, 2011). Also, active immunization against A $\beta$  is under development, but such endeavours have generally not been successful (Gilman et al., 2005). Indeed, 99% of the A $\beta$ -targeted phase 3 clinical trials in AD have not shown statistically significant benefit on its pre-specified clinical endpoints. These negative results have also largely contributed to question the validity of the amyloid hypothesis. Most recently, some hope was raised by a more positive outcome of a Biogen phase I clinical trial infusing aducanumab in mild AD patients with A $\beta$  pathology as measured by positron emission tomography (PET) (Sevigny et al., 2016). The 3 and 10mg/kg/month doses were effective in reducing brain A $\beta$  levels after 6 months and more so at 12 months. Mild positive effects of these doses on clinical outcome were reported, encouraging rapid transition to phase III trials. Because of the difficulties encountered with anti-A $\beta$  strategies, there resulted an increase of interest in drug trials directed towards tau aggregation (Morris et al., 2011) and APOE (Pedersen and Sigurdsson, 2015). Results of clinical trials using these alternative strategies should be disclosed within the next few years.

Directly targeting the activity of brain networks might also help to restore memory. Phase I clinical trials that used deep-brain stimulation techniques to directly manipulate network activity in individuals with AD reported positive memory outcomes (Laxton et al., 2010). This suggests that the development of non-invasive brain stimulation strategies could be a scalable and a safe route to restoring cellular health and network function.

Still, there is a strong urgency to develop new therapeutic strategies as none so far have showed strong benefits in preventing AD occurrence or slowing down AD progression. For this to occur, additional efforts are required to better understand the molecular and cellular mechanisms driving forward AD pathology.

---

## **2.2 Memory formation, synaptic plasticity and modulation by A $\beta$**

AD is a progressive neurodegenerative disease marked by a constellation of cognitive disturbances. The earliest form of memory affected in AD is episodic memory and is one of the most clinically relevant neurological symptom for AD patients. This form of memory helps us to function smoothly in our basic daily activities and to remember critical events. As the disease progresses the patient develops other cognitive abnormalities such as apraxia (inability to carry voluntary movements), aphasia (loss of ability to speak) and agnosia (inability to recognise objects and their use) eventually leading to global cognitive impairment.

### **2.2.1 Different types of memory**

There are mainly two forms of memory depending on the duration of recall: short and long term memory (STM and LTM) (Figure 6).

STM is known to hold a limited amount of information in a very accessible state temporarily (Cowan, 2008). STM mainly relies on cortical neuron activity in the lateral prefrontal cortex (Squire and Wixted, 2011). This structure is specifically known to perform higher executive functions, which include working memory and attention.

The LTM system is divided into two broad classes: explicit (declarative) memory, which requires the conscious recall of data, facts and events, and implicit (non-declarative) memory, which is based on non-conscious memory abilities. Implicit memory includes procedural or skilled-based kinds of learning and perceptual representation system (PRS) (Squire et al., 1987). PRS mainly involves priming effects (where one stimulus influences the response of the other stimulus) and operant or classical conditioning (which involves pairing of two stimuli). Long term memory is stored in the neocortex and distributed in different regions, where the area specific processing occurred at the time of learning.

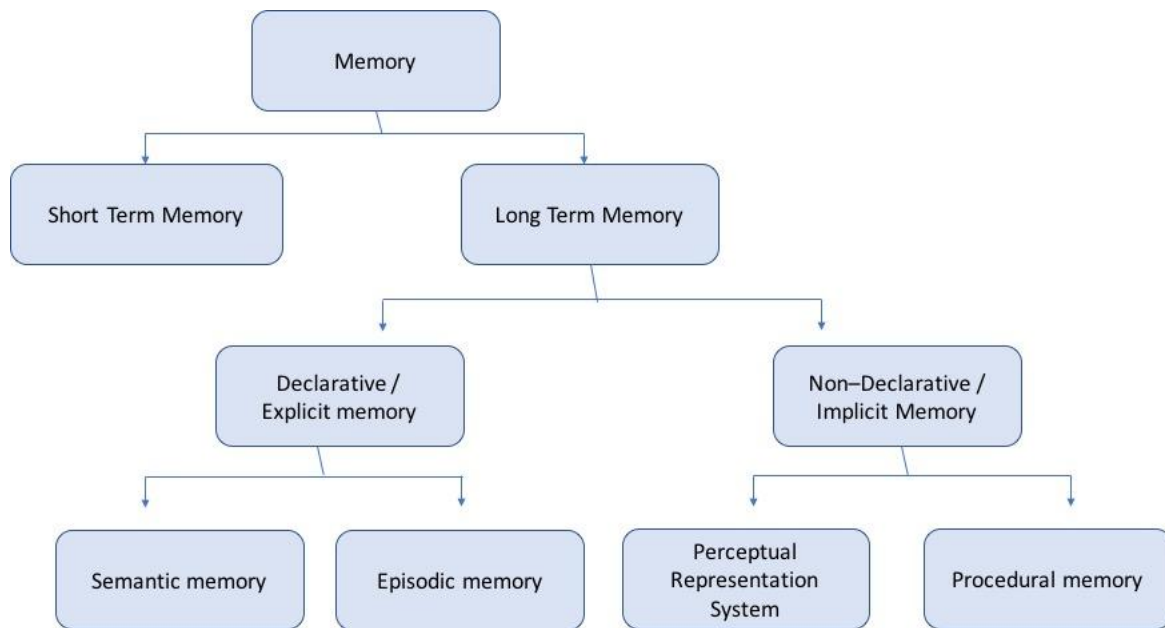


Figure 6: Classification of the different memory systems into short and long term storage systems. Long term memory is further divided into declarative and non declarative memory. Declarative memory represents explicit memory which can be declared and is further classified into semantic and episodic memory. Non declarative memory is the memory used in tasks and skills and can be divided in procedural and perceptual representation system. (Adapted from Tulving, 1995).

### 2.2.1.1 *Declarative long term memory*

Declarative memory is subdivided into semantic memory and episodic memory (EM). Semantic memory is related to storage of general facts and knowledge, such as the colour of fruits or the capital of countries. While EM is a system that enables an individual to encode, store, and retrieve information about personal experiences and the temporal and spatial contexts of those experiences (first defined by Tulving in 1972).

## 2.2.2 Memory formation and its stages:

### 2.2.2.1 *Encoding, Consolidation, Storage and Retrieval*

Memory formation and utilization can be divided into the following stages: Encoding, consolidation, storage and retrieval. The critical structures involved in these processes of memory involve hippocampus, the amygdala and the adjacent entorhinal, perirhinal and parahippocampal cortices, which make up the medial temporal lobe (MTL) and the prefrontal cortex (Squire and Wixted, 2011).

**Encoding** is the first stage of memory, and it is crucial for the storage and retrieval of voluntary stored information. Encoding begins with perception of sensory inputs that comes

from external stimuli. The MTL structures are involved and responsible for transforming these sensory inputs to a memory representation (Squire and Zola-Morgan, 2011). All these neuronal activities converge to the medial temporal lobe and specifically to the hippocampus, where they bind to form episodic memory (Figure 7) (Kessels and Kopelman, 2012). After binding, they are allocated to areas in the cortex for long-term storage as they are well protected from the influence of new incoming memories (Straube, 2012). The type of information processing that occurs during the encoding stage determines the quality of encoding and recovery of that information.

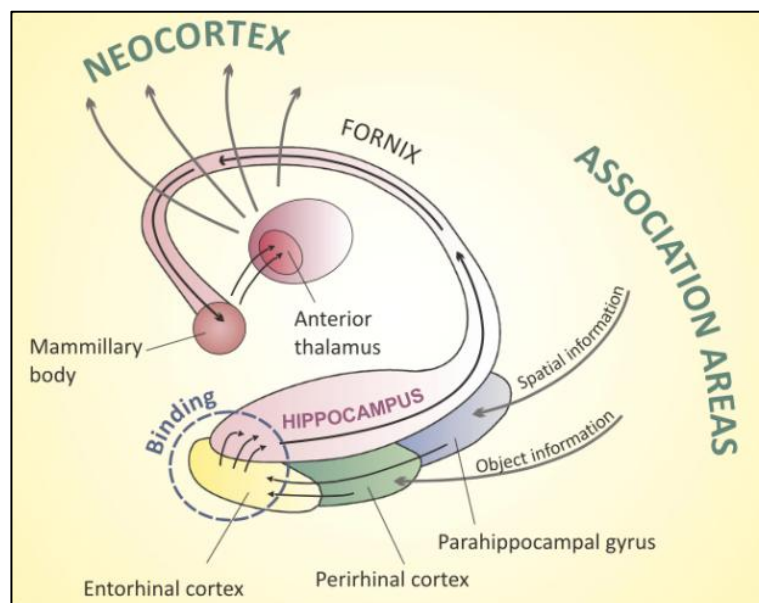


Figure 7: Functional overview of extended hippocampal-diencephalic memory system. Nonintegrated input from the association areas (such as spatial or object information) is processed in the parahippocampal and perirhinal cortices and then integrated as an “episode” in the entorhinal cortices. Storage then takes place through the hippocampi that are connected via the fornices to the mammillary bodies. Subsequently the thalamus projects to the neocortex where the episodic information is permanently represented (Kessels and Kopelman, 2012).

**Consolidation:** Encoded memory undergoes consolidation, a process by which short term memory trace is transferred to stable long term memory before directing it to neocortical areas for long term storage. There are two models of consolidation: the standard model (SM) and the multiple memory trace (MMT) (Nadel et al., 2007). The SM model, proposes that memory storage initially requires the hippocampus to link the different features of memory which are dispersed in several sites in the neocortex. Over time, however, the requirement of the hippocampus decreases and the representation of the memory is solely in the neocortex (Frankland and Bontempi, 2005) (Figure 8). In contrast, the MMT theory poses that all

memory traces are combined into a multiple-trace representation. In this model, both the hippocampus and the neocortex continue to interact with each other and that the hippocampus plays a permanent role for the storage and retrieval of the memory. CORT modulate memory consolidation of emotionally aroused experiences (McIntyre et al., 2012) and sleep also plays an active role in memory consolidation (Straube, 2012).

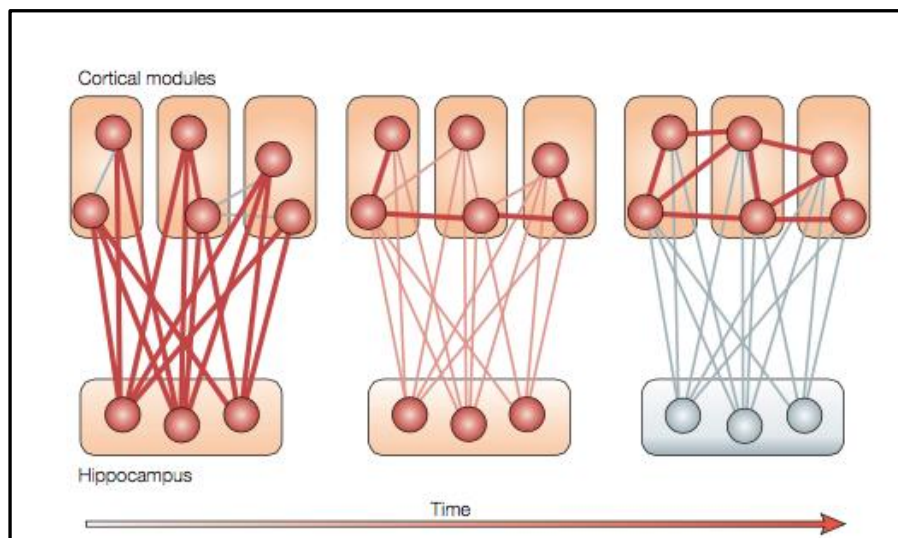


Figure 8: Standard consolidation model. The encoding of perceptual, motor and cognitive information initially occurs in the primary and associative cortical areas. The hippocampus integrates external information coming from specialized cortical areas and fuses them into a coherent memory trace. Successive reactivation of this hippocampal-cortical network leads to progressive strengthening of cortico-cortico connections and over time becomes independent of the hippocampus (Frankland and Bontempi, 2005).

### Storage and Retrieval

After the process of consolidation, memories are represented by networks of neurons distributed across the neocortex bound together for rapid storage. For retrieval of memory, MTL structures are necessary along with the cortical regions (Rugg and Vilberg, 2013). During recall of the memory, the representative map in the hippocampus is activated along with the other areas in the cortex, which were involved in forming the memory. While MTL brain structures are necessary for retrieval of recent episode-based memory associations, over time, these associations are expressed and can be recalled independently of the MTL structures (Squire and Wixted, 2011).

During aging, the encoding process seems to be affected, with encoding deficiencies predominating over retrieval deficits (Friedman et al., 2007). Patients with AD show deficits

in EM from very early stages of the disease. They show performance deficits in encoding, storing and retrieval (Pena-Casanova et al., 2012).

### **2.2.3 Episodic memory is affected in AD**

Episodic memory refers to the conscious recollection of a unique past experience / event in terms of “what”, “where” and “when” it happened. These three components identify a particular object or person (memory for what happened), the context or environment in which the experience occurred (memory for where it happened) and the time at which the event happened (memory for when it happened) (Nyberg et al., 1996, Clayton and Dickinson, 1998, Tulving and Markowitsch, 1998). It is the first form of memory, which is affected in Alzheimer’s patients (deToledo-Morrell et al., 2007). **Recall (free and cued) and recognition** are considered to provide two different ways to measure episodic memory. Recall depends on declarative memory and recognition on declarative and non-declarative memory. In a free recall experiment, an individual is given a list of items to study and is subsequently asked to recall the items (Arnold and McDermott, 2013), the results of which are noted. While in cued recall, the same protocol is followed with the help of cues. With this test, one can evaluate hippocampus-dependent memory encoding or consolidation. During a recognition experiment, the first phase, called the study phase, a subject is asked to memorize a series of items. Later, in the test phase, randomly ordered items, old and new, are presented and the individual is scored on his ability to distinguish them. In AD patients, both recall and recognition deficits seem to persist, which indicates inability to retrieve information. This could also be related to inability to encode target information (Gold and Budson, 2008).

#### **2.2.3.1 Episodic-like object recognition memory in rodents**

It has been challenging to study declarative forms of memory in mice since it is an integrative memory for “what”, “where” and “when” component and also it needs to be expressed non-verbally. Thus, in rodents, the equivalent studies done are hippocampus-dependent spatial and contextual memory tests. The most commonly used tasks to study spatial memory in AD mouse models are the Morris water maze (MWM), the Barnes Maze also called circular platform maze, the continuous and forced-choice spatial alternation task, and the radial arm water maze task (Stewart et al., 2011).

To integrate the component of familiarity of items along with recollection of contextual (spatial and/or temporal) information of items, the object recognition test was developed. The novel object recognition task measures spontaneous behaviour in rodents as they readily approach and explore novel objects (Frick and Gresack, 2003). This widely used task consists of a sample trial wherein two identical objects are explored by the mouse, followed by a delayed test trial wherein one familiar object presented during the sample test is replaced by a novel object (see Figure 9A). Animals with adequate memory spend longer time exploring the novel object. The NOR test could be interpreted as the study of the ‘What’ component of episodic memory. This task has been widely used for evaluation of memory in AD mouse models (Balducci et al., 2010). Two key points confirm that novel object recognition can be dependent on hippocampal activity. Firstly, it was noted that hippocampal lesions result in impaired object recognition and secondly a 24-hour inter-trial interval between the two phases (sample and test) confirms retrieval of long term memory consolidated via hippocampal activity (Reed and Squire, 1997). In NOR memory, particularly the dorsal hippocampus plays an important role, especially when spatial or contextual information is a relevant factor (Goulart et al., 2010).

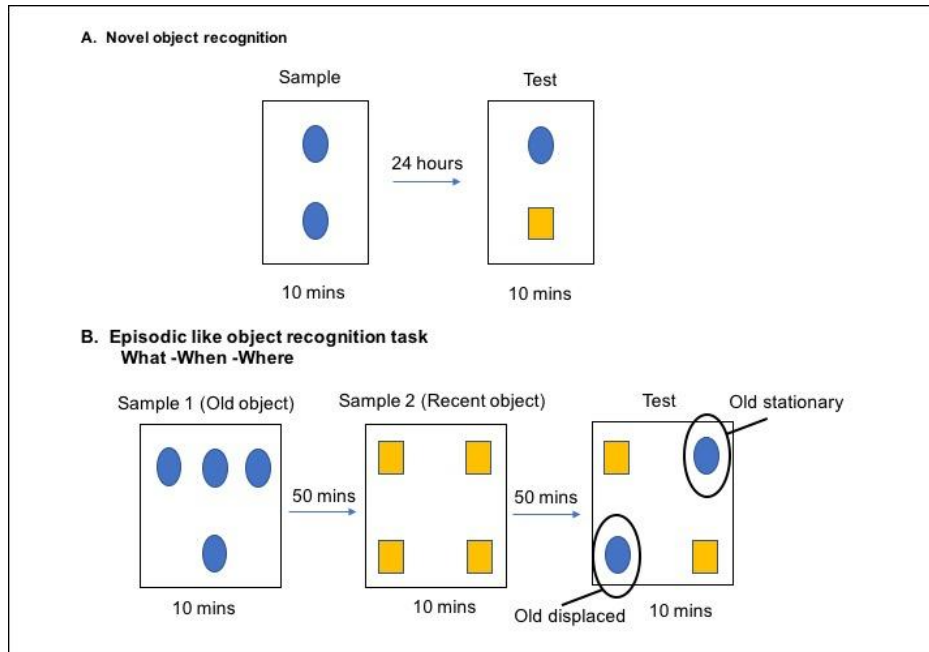


Figure 9: Object recognition tasks. A). Novel object recognition test which consist sample trial where the mouse explores for 10 mins two identical objects. After a delay of 24 hours, the mouse is subjected to the 10 min test trial, where one familiar object is replaced by a novel object. B). Elaborated episodic-like object recognition task, which involves the ‘What’, ‘When’, ‘Where’ components of EM. This task consists of three 10 min trials with a 50-min inter-trial interval. On sample 1, four novel objects are presented in a triangular orientation. On sample 2, another 4 objects are presented in another spatial arrangement. During the test trial, two ‘old familiar’ and two ‘recent familiar’ objects are presented as depicted. One amongst the two old familiar object is displaced (adapted from (Dere et al., 2005)).

To integrate the other ‘when’ and ‘where’ components of episodic behaviour, the NOR test was modified by (Dere et al., 2005). In this context, long-term memory for different objects, their spatial location and their order of presentation in an open field would incorporate all the components of episodic memory. The protocol included three 10 minute trials of object exploration task with a 50 minute inter-trial interval (Figure 9B). In the 1<sup>st</sup> trial, four novel objects were presented in a triangular spatial conformation while in 2<sup>nd</sup> trial, four different objects were presented in another spatial arrangement. During the 3<sup>rd</sup> trial (test), two ‘old familiar’ and two ‘recent familiar’ objects from the previous trials were presented. In this test, the mice were able to recognize the previous explored objects, to remember the location of the objects which were presented and lastly to discriminate the sequence (old/recent) in which the objects were presented. Thus, by changing the parameters to the object recognition test, different aspects of memory can be investigated.

Episodic memory system is supported by the MTL, especially the hippocampus. In AD patients, the hippocampus is one of the most severe sites to be affected. Studies have indicated evidence of hippocampal atrophy (Figure 4) accompanied by significant loss of

synaptic density and dendritic spines leading to memory impairment (Barnes et al., 2007, Scher et al., 2007, Wang et al., 2004).

#### **2.2.4 Hippocampus organization and pathways for memory formation**

The entorhinal cortex serves as a main interface between the hippocampus and neocortex. The hippocampus and the entorhinal cortex are connected via pathways which play an important role in declarative memory formation. The hippocampus is mainly subdivided into: 1). The dentate gyrus (DG) which is a tightly packed layer of small granule cells forming a v-shaped wedge. 2). Cornu Ammonis (CA) which mainly contain densely packed pyramidal cells (Hyman and Van Hoesen, 1987), emerge from the DG as: CA4, then CA3, then a very narrow transitional zone termed CA2 and then CA1 (refer Figure 10). The CA1 merges with the subiculum with projections leading back to the entorhinal cortex completing the circuit.

The entorhinal cortex contains 5 layers, amongst which Layer II/III contains the cell islands consisting of glutamatergic neurons. Layer II projects axons to the hippocampal DG and CA3 region via the perforant pathway (Stranahan and Mattson, 2010) while Layer III projects primarily to the hippocampal CA1. These layers receive inputs from surrounding areas like the perirhinal and parahippocampal cortices (as shown in Figure 10) as well as the prefrontal cortex. The DG sends projections to the pyramidal cells in the CA3 region through mossy fibres. Further, CA3 neurons relay the information to the CA1 neurons via the Schaffer collaterals. Lastly, CA1 neurons send back-projections to the deep-layer neurons in the EC completing the circuit.

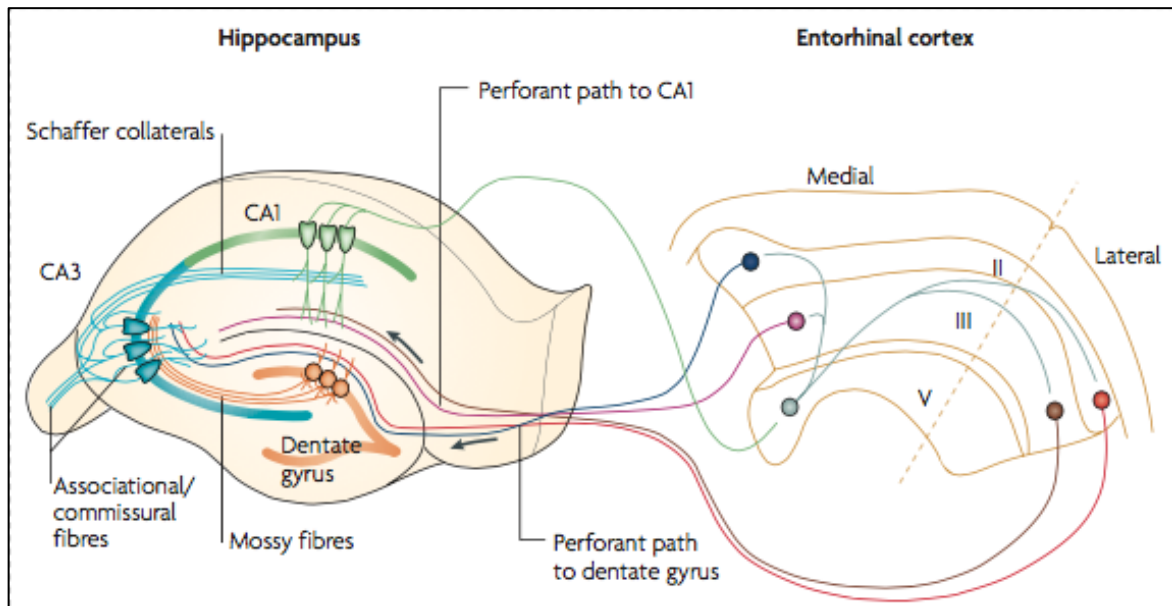


Figure 10: Basic anatomy of the hippocampus. The wiring diagram of the hippocampus is presented as a trisynaptic loop. The major input is carried by axons of the perforant path which convey sensory information from neurons in layer II of entorhinal cortex to the dentate gyrus. Perforant path axons make excitatory synaptic contact with dendrites of granule cells, which then project through the mossy fibers to the CA3 pyramidal cell which, in turn, project to the CA1 pyramidal cells through Schaffer collaterals. The distal apical dendrites of the CA1 pyramidal neurons receive a direct input from layer III cells of the entorhinal cortex (Neves G et al., 2012)

### 2.2.5 Basal synaptic transmission and synaptic plasticity

A synapse is an entity consisting of the communication point between a pre- and post-synaptic neurons. It is well established that learning and memory are based on dynamic regulation of synaptic connections between neurons. Neurons being highly plastic in their connections, organise themselves into groups, handling different type of information in response to one's experience to create new memories. At this point, we can refer to the Hebb's rule, which states that 'Cells that fire together wire together' (introduced by Donald Hebb in his book 'The organisation of behaviour' in 1949).

Synaptic strength and synaptic plasticity are main molecular events that constitute the neurobiological basis of memory formation (Sehgal et al., 2013, Papoutsi et al., 2013). Synaptic strength may be defined as the response in amplitude produced in the target neuron by the synapses of a connected neuron on initial stimulation. There are mainly two types of synapses: electrical and chemical synapses. In the fast acting electrical synapses, communication between the neurons occurs via direct ion exchange. In contrast, chemical synapses, which represent the majority of synapses in the brain, depend on the release of neurotransmitters (NTs) by the pre-synaptic neuron, which will influence NT receptors on the

post-synaptic neuron to open ion permeable channels. Basal synaptic strength is evaluated when the pre-synapse is stimulated with a unique stimulation pulse, which promotes a one-time release of NTs via generation of an AP. Synaptic plasticity refers to any up-regulation or down-regulation of this basal synaptic strength, involving mechanisms such as modulation of neurotransmitter release and changes in number of neurotransmitter receptors (Cortes-Mendoza et al., 2013).

There are mainly two forms of synaptic plasticity, which are believed to be implicated in memory formation: Long term potentiation (LTP) and long term depression (LTD). LTP is induced by a high frequency synaptic stimulation, which results in long lasting increase in synaptic strength and is the fundamental process in memory coding. It is most widely studied in the hippocampus and also in amygdala and cortex-dependent learning areas in the brain (Neves et al., 2008). On the contrary, long term depression (LTD) reduces the synaptic strength between neurons in several areas of the brain including the hippocampus.

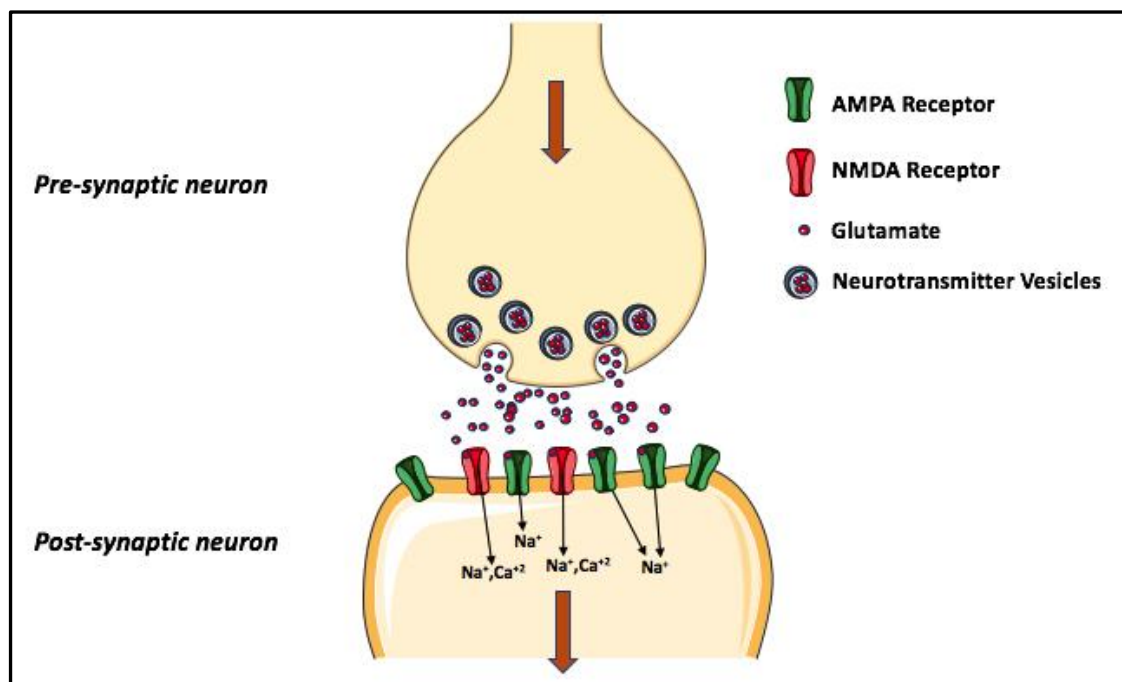


Figure 11: Simplified representative diagram of excitatory glutamatergic chemical synapse. Upstream activation (AP generation) potentiates the pre-synaptic neuron (upper brown arrow). This initiates the glutamate to be released from the pre-synapse by the vesicles. Glutamate activates the AMPAR present on the post synaptic neuron to allow sodium influx. This depolarizes the post-synaptic neuron and activates the NMDAR to allow influx of  $\text{Ca}^{2+}$  and  $\text{Na}^+$  thus transmitting the electric message downstream (brown arrow below). Kainate and metabotropic receptors, which also contribute to glutamatergic synaptic transmission, are not presented here for simplicity.

### **2.2.5.1 *Glutamergic synapse***

Glutamate is the major excitatory neurotransmitter in the nervous system and is particularly predominant in the hippocampus. It is involved in fast transmission and found as a part of the tripartite synapse which involves communication between pre-and post-synaptic neurons along with glial cells. The pre-synaptic release of glutamate and the activation of post synaptic glutamate receptors are essential mechanisms involved in LTP at glutamatergic synapses (Figure 11). Upon vesicular release, glutamate can act on ionotropic glutamate receptors, (AMPA, NMDA and kainate receptors), which are ligand-gated ion channels and allow direct ion influx when activated (Dingledine et al., 1999). AMPA stands for ( $\alpha$ -amino-3-hydroxy-5-methyl-4-isoxazole-propionate) and NMDA for (N-methyl-D-aspartate). Metabotropic glutamate receptors (mGluR) can also be activated by glutamate which are G-protein-coupled receptors and modulate secondary messenger pathways. In this chapter, focus will be given to AMPA receptors (AMPA) and NMDA receptors (NMDAR).

### **2.2.5.2 *Post synaptic density***

Post synaptic density (PSD) refers to the electron-dense region in the postsynaptic membranes of excitatory synapses which mainly contain proteins responsible for synaptic activity. The biochemical methodology of PSD purification was established in 1970s. In brief, initially the synaptosomes were isolated, followed by detergent treatment (Triton X) for purification of PSD fractions (Carlin et al., 1980). Due to their resistance to detergents they are isolated as detergent –insoluble fractions. From these biochemical PSD fractions, an array of structural membrane proteins (e.g. PSD-95 as a scaffolding protein), cytoskeletal proteins (e.g. actin and tubulin), receptors (NMDAR, AMPAR), ion channels, signalling molecules like calcium/calmodulin dependent protein kinase II (CAMKII) and other enzymes were identified (Matus et al., 1982, Chen et al., 2000, Valtschanoff and Weinberg, 2001). This receptor/enzymes system plays a major role in synaptic activity and PSDs are thus identified as one of the main machineries for synaptic transmission and plasticity.

### **2.2.5.3 *AMPA and NMDAR***

Within the PSD, one can find the AMPARs, which performs most of the fast-synaptic transmission in the brain. They are composed of GluA1-4 subunits (also previously called

GluR), which combine to form a heterotetramer (composed of 4 subunits, of more than one type). These tetramers can be formed of different subunits conferring different activity and channel permeability properties (Kessels and Malinow, 2009). When activated by glutamate, AMPAR allow  $\text{Na}^+$  influx.

NMDARs can be formed from various combinations of GluN1 (previously called NR1), GluN2(A-D) (previously called NR2(A-D)), and GluN3(A/B) (previously called NR3(A/B)) subunits. The most common form of NMDAR on hippocampal excitatory neurons is the heterotetrameric combination of GluN1 with GluN2 units (Paoletti and Neyton, 2007). Activation of these receptors requires the binding of glutamate to GluN2 and one of the co-agonists glycine or d-Serine to GluN1. NMDAR activation opens a non-selective ion channel through which  $\text{Ca}^{2+}$  and  $\text{Na}^+$  ions can enter the post synaptic neuron. NMDAR activation requires depolarization of the surrounding membrane, which removes  $\text{Mg}^{2+}$  ions from its pore, thus allowing for ion flux through its channel. This property makes NMDARs ideal coincidence detectors, coupling pre-synaptic and post-synaptic activation, and these receptors are thus crucial for information flow and memory processing (Nowak et al., 1984).

Both AMPAR and NMDAR are involved in synaptic plasticity processes of LTP and LTD.

#### **2.2.5.4 Different forms of synaptic plasticity**

##### **2.2.5.4.1 LTP**

LTP was first discovered by (Bliss and Lomo, 1973) and since then has consolidated its status as the pre-eminent synaptic model for investigating the molecular basis of memory (Figure 12).

Under rest or low levels of input activity, glutamate neurotransmitter, which is released from the presynaptic cell, binds to both AMPAR and NMDAR. At this resting membrane potential, the NMDAR is blocked by  $\text{Mg}^{2+}$ , while AMPAR open allowing  $\text{Na}^+$  ions to enter, hence only slightly depolarizing the cell. Only when the post-synaptic cell is sufficiently depolarized, e.g. by increased stimulation of the presynaptic cell, is the  $\text{Mg}^{2+}$  expelled out of the NMDAR. Its activation initiates an influx of sodium and calcium ions inside the post synaptic neuron. It is this calcium influx, which is thought to initiate LTP (Lynch et al., 1983). The two-major calcium-responsive signalling pathways activated are CAMKII-dependent signalling and cyclic adenosine monophosphate (cAMP)-dependent signalling

pathway. These molecules, locally phosphorylate non-synaptic AMPAR, which then integrate into the post-synaptic membrane, increase  $\text{Na}^+$  influx and further potentiate the neuron (Lisman et al., 2012). The other effect of the calcium responsive signalling pathways is to alter gene expression in the cell nucleus via transcriptional factors (Alberini et al., 1995). Calmodulin activates cyclicAMP response element binding protein (CREB) in the nucleus via MAPK-ERK (mitogen-activated protein kinases/ extracellular signal regulated kinase) and CAMK kinase pathways (Lisman et al., 2012).

CREB subsequently activates immediate early genes, such as c-fos, c-jun, zif268 (a zinc finger protein), BDNF (brain derived neurotrophic factor). Activation of these early genes is critical for inducing long term changes in plasticity and memory formation (Cortes-Mendoza et al., 2013).

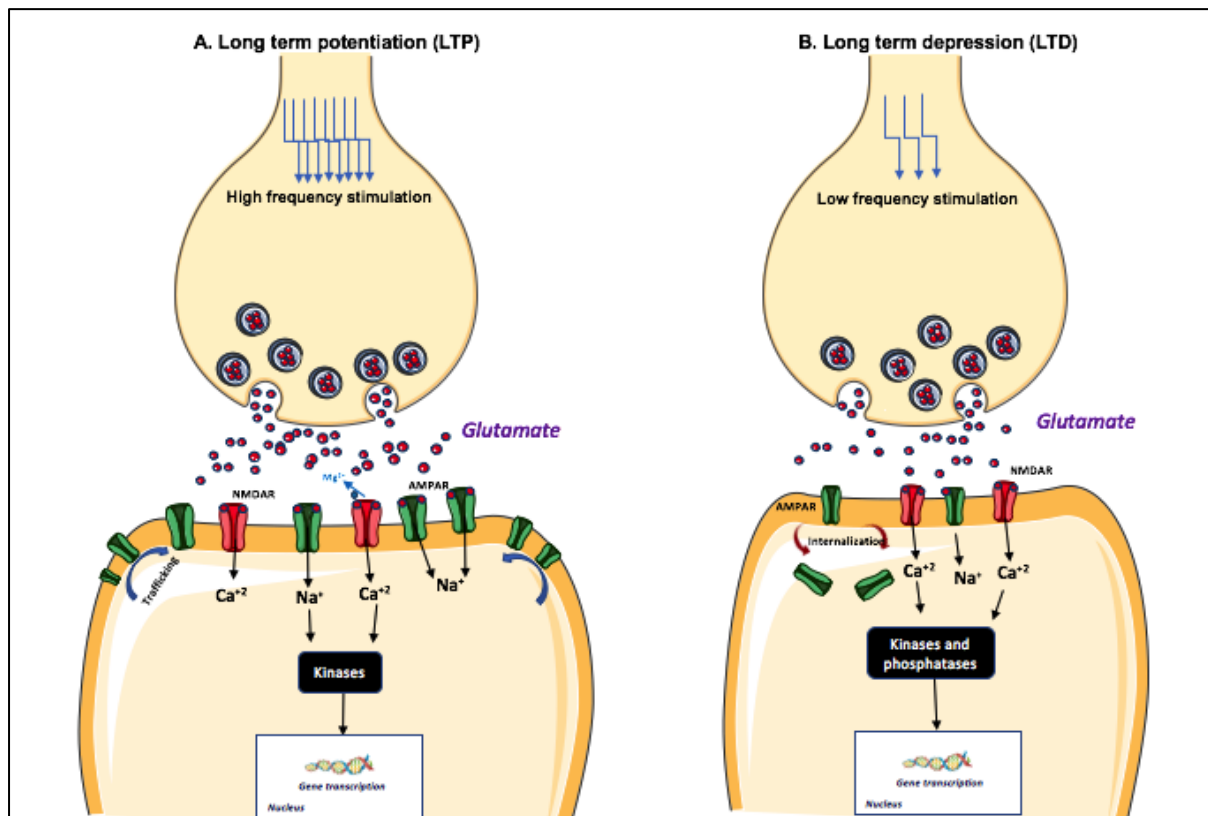


Figure 12: A simplified scheme showing the two forms of synaptic plasticity, LTP and LTD. A). Basic mechanisms involved in induction of LTP following high frequency stimulation. Activation of AMPARs by glutamate depolarizes the postsynaptic neuron which removes the  $\text{Mg}^{2+}$  block on the NMDAR allowing subsequent activation and influx of  $\text{Ca}^{2+}$ .  $\text{Ca}^{2+}$  along with activation of signalling pathways downstream of the receptor, activate a kinases such as CamKII and MAPK/ERK. This leads to rapid incorporation of AMPARs into the PSD. Also, these pathways ultimately transmit the signals to the nucleus, where changes in gene transcription and translation occur to enhance synaptic strength. Insertion of newly formed AMPAR at synaptic sites and formation of new spines occur post LTP. B). LTD is triggered by low frequency stimulation and various mechanisms are implicated in this induction. Most notably, LTD induction activates NMDAR receptors, which induce influx of  $\text{Ca}^{2+}$  activating both kinases and phosphatases leading to AMPAR endocytosis. Adapted from (Sandi, 2011).

#### 2.2.5.4.2 LTD

LTD is the converse process to LTP and results in long lasting decrease in synaptic strength (Figure 12). Like LTP, LTD is phenomenon important for memory formation as overall it counterbalances the LTP process. An extended low frequency stimulation induces activation of NMDAR, possibly via a metabotropic action of these receptors (Nabavi et al., 2013), and calcium-dependent molecular mechanisms are triggered by low concentrations of post synaptic calcium (Nishiyama et al., 2000). Calcium responsive phosphatases, such as calcineurin and protein phosphatase 1 (PP1), and kinases, like Gsk3 $\beta$  (Peineau et al., 2007), are implicated as effector molecules in the mechanisms of LTD. The main outcome of this LTD induction is internalization of AMPAR, mainly through endocytosis, hence leading to a depression of the synaptic strength. Moreover, the activation of G-protein–coupled metabotropic glutamate receptor (mGluR) can also induce LTD via reduction of AMPAR function (Palmer et al., 1997, Bellone et al., 2008).

Using NMDAR antagonists, it was concretely shown that NMDAR are necessary for induction of LTP and LTD, while they do not contribute much to baseline transmission (Morris et al., 1986). Comparatively, the trafficking of AMPAR through insertion and removal within the PSD is involved in post-induction response maintenance. AMPAR also move laterally within the plasma membrane during synaptic plasticity. In the context of AD, it has been extensively studied that these synaptic processes are impaired by A $\beta$ .

#### 2.2.6 Modulatory action of A $\beta$ on synapse function and plasticity

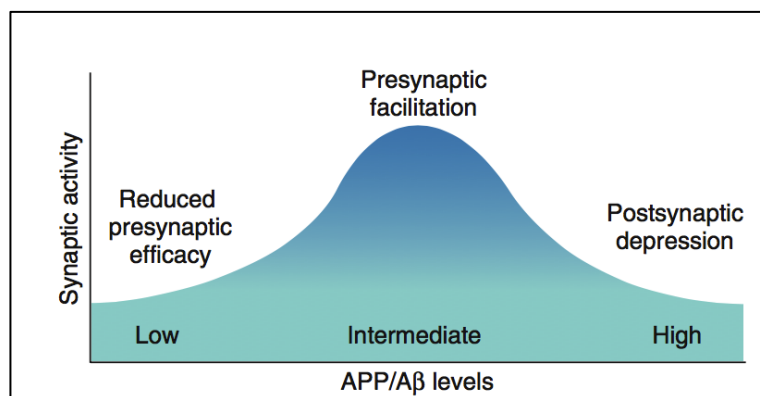


Figure 13: Bell shaped representation of the relationship between A $\beta$  level and synaptic activity. Intermediate levels of A $\beta$  enhance synaptic activity presynaptically, whereas abnormally high or low levels of A $\beta$  impair synaptic activity by inducing postsynaptic depression or reducing presynaptic efficacy, respectively (Palop and Mucke, 2010),

As shown in the above pictorial representation (Figure 13) by (Palop and Mucke, 2010), there is evidence that synaptic activity is differentially modulated depending on the APP/A $\beta$  levels. Intermediate levels of A $\beta$  potentiate presynaptic terminals, while low levels reduce presynaptic efficacy and high levels depress postsynaptic transmission. Abnormally low A $\beta$  level in mice deficient in APP, PS1 or BACE1 is associated with synaptic transmission deficits (Seabrook et al., 1999, Saura et al., 2004). Due to the extensive research currently carried on the pathological effects of high concentration of A $\beta$ , we tend to forget that the proteolytic pathway of production of amyloid- $\beta$  is a physiological process. And only when net A $\beta$  levels become excessive can this process be regarded as pathological condition.

#### **2.2.6.1 *Physiological conditions***

Normal levels (picomolar range) of A $\beta$  peptide via nicotinic acetylcholine receptors (nAChRs) in CA1 (Puzzo et al., 2008) positively increase presynaptic release at hippocampal synapses and facilitate LTP (see Figure 14, Figure 15). Parallel evidence indicates that A $\beta$  may have a role in controlling synaptic activity. Kamenetz et al. 2003 proved that evoked activity of hippocampal neurons in brain slices increased the A $\beta$  secretion at the cell membrane. In physiological conditions, this production of A $\beta$  seems to work as a negative feedback mechanism to controls synaptic activity. Without such a tight control, synaptic activity could become excessive leading to excitotoxicity. There are two evidences confirming this function:  $\gamma$ -secretase inhibition would lead to increased excitatory post synaptic current (EPSC) frequency (Kamenetz et al., 2003) and kainate-induced seizures are potentiated in APP knockout mice (Steinbach et al., 1998). Together these studies suggest that APP processing and presence of A $\beta$  are closely associated with synaptic activity. This may serve as a physiological control for guarding against excessive activity and preventing increased glutamate release.

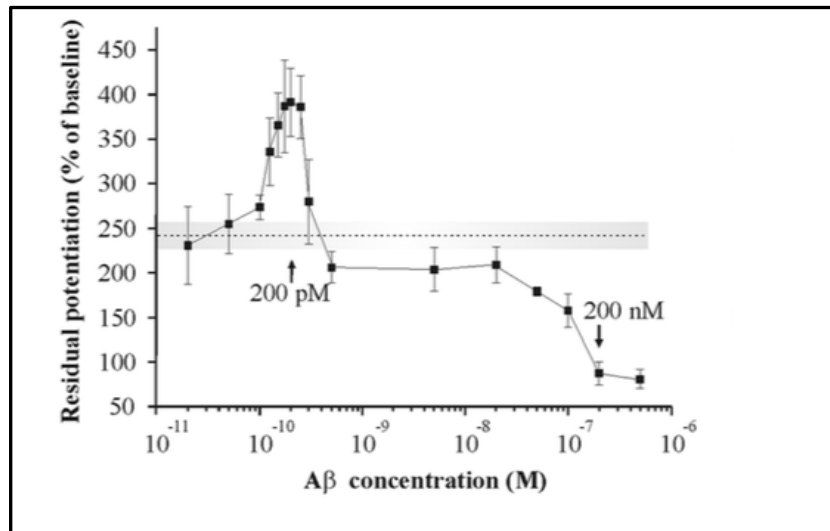


Figure 14: Differential dose-dependent effects of A $\beta$  on LTP in hippocampus. Concentration response curve for the effect of A $\beta_{42}$  on CA1-LTP indicating that the peptide has an enhancing effect with a peak around 200pM, whereas it has an opposite detrimental effect above 20nM, The dotted line and the shaded area corresponds to the amount of potentiation and the standard error range in vehicle treated slices (Puzzo et al., 2008).

### 2.2.6.2 Pathological conditions

Several studies point to abnormal synapse function in presence of elevated levels of A $\beta$ , but a consensus has yet to be reached on which mechanisms promote these A $\beta$ -mediated synaptic alterations (Figure 15). It is well known that elevated levels of A $\beta$  (in nanomolar concentration) influences synaptic plasticity processes i.e. it impairs LTP (Walsh et al., 2002, Lambert et al., 1998, Townsend et al., 2006, Shankar et al., 2008) and enhances LTD (Hsieh et al., 2006, Shankar et al., 2008, Li et al., 2009). One favoured hypothesis is that pathologically elevated A $\beta$  may block neuronal glutamate uptake at the synapses, leading to increased glutamate levels at the synaptic cleft (Li et al., 2009). This increase in glutamate would activate synaptic NMDARs (Snyder et al., 2005) resulting in desensitization of these receptors and further internalization of AMPAR and NMDAR leading towards LTD (Hsieh et al., 2006, Almeida et al., 2005). This could also further activate extra- or peri-synaptic NMDARs, mGluRs,  $\alpha$ 7-nAChRs due to increased glutamate spill over. This results in several downstream effects activating LTD-related pathways like on calcineurin-STEP-cofilin, p38MAPK, and GSK-3 $\beta$  signalling pathway, etc eventually leading to postsynaptic depression and dendritic spine loss (Shankar et al., 2007, Shankar et al., 2008, Wang et al., 2004, Li et al., 2009). A $\beta$ -induced LTD effects could be related to A $\beta$ -induced LTP deficits, as blocking of LTD related signalling cascades like mGluR or p38MAPK, prevents A $\beta$ -

dependent LTP impairment (Lambert et al., 1998, Walsh et al., 2002, Townsend et al., 2006, Shankar et al., 2008).

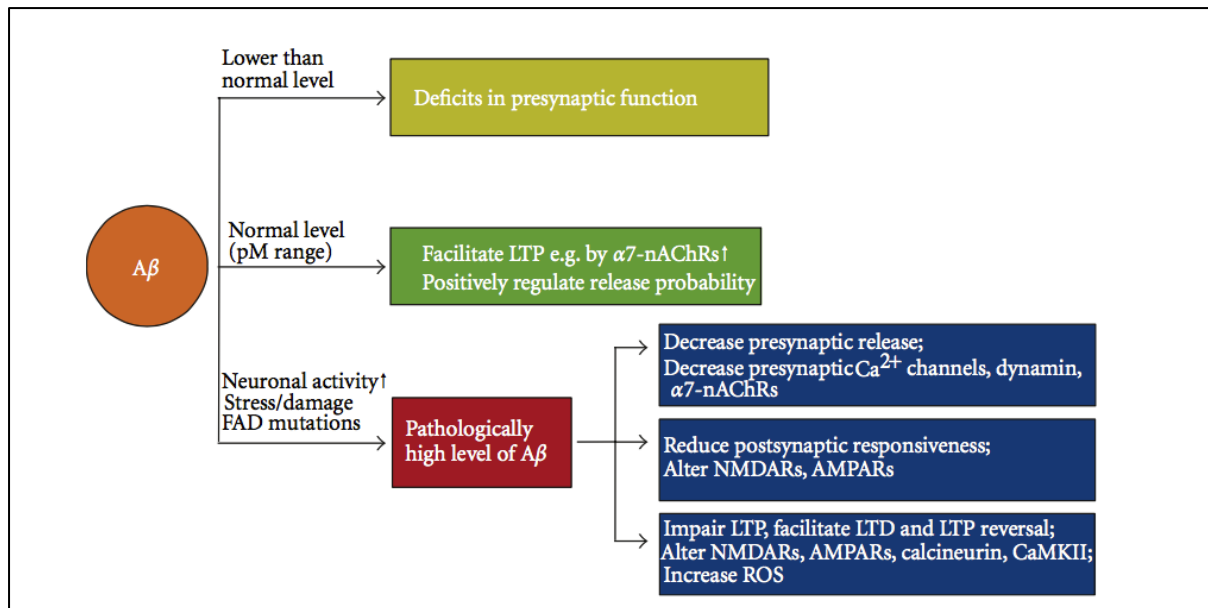


Figure 15: Concentration dependent effects of A $\beta$  on synaptic function. At normal physiological levels (picomolar levels), A $\beta$  peptides positively regulate presynaptic release probability and facilitate learning and LTP. At concentrations lower than normal A $\beta$  shows deficits in presynaptic function. While at high concentrations like those seen during pathology there is a decrease in presynaptic release and eventually leads to impairment in LTP and facilitates LTD (Wang et al., 2012).

### Evidence of A $\beta$ - tau at the synapse:

There has been recent evidence of an interaction between oligomers of A $\beta$  (oA $\beta$ ) and tau at the synapse. Tau protein is predominantly present in the axons as they stabilize the microtubules. Recently, it is known that in presence of oA $\beta$ , tau translocates to the somatodendritic compartments in association with loss of spines and microtubule breakdown (Zempel et al., 2010). The presence of tau at the synapses has both physiological and pathological significance (Pooler et al., 2014). Recent work using cortical neurons show that synaptic activation translocate tau to excitatory synapse, specifically dendritic spines and post-synaptic compartment (Frاندemiche et al., 2014). They also demonstrated that oA $\beta$  induced tau localization to the synapse, and phosphorylation of S404 residue on the tau protein is required. It is thus likely that Tau contributes to the A $\beta$ -mediated synapse alterations.

### **Caveat using oligomers of A $\beta$ :**

It has been shown that oA $\beta$  of synthetic origin are similar in toxicity to the natural oligomers, thus been considered as a model to study the assembly and the toxicity of A $\beta$  peptide and of its oligomeric form (Snyder et al., 1994). One main caveat about the oA $\beta$  studies is their tendency to aggregate hence occurring in different sizes. At present, it is uncertain as to which class amongst the aggregates is important for pathogenesis. Some groups suggest that dimers through tetramers are most critical (Shankar et al., 2007, Shankar et al., 2008, Townsend et al., 2006), while others suggest higher order oligomers are most important like 12mers (Lesne et al., 2006). It was demonstrated that monomers and A $\beta$  fibrils do not affect LTP (Walsh et al., 2002). Along with size, there are other factors like pH, temperature, ionic strength, which can change the conformation and aggregation size of these oligomers hence making it difficult to estimate the good concentration of the oA $\beta$  used in the studies and to assign synapse-modulating properties to a specific A $\beta$  species (Stine et al., 2003).

### **2.2.7 Modulatory action of A $\beta$ on memory**

A $\beta$  levels modulate memory processes in a way similar to how they regulate synaptic activity. At intermediate levels, they have a positive effect on memory formation, while as the concentration of A $\beta$  increases it can cause memory impairment. There have been multiple studies using AD transgenic mice (like Tg2576 mice and other APP mouse models) to study memory impairment in the context of abnormal APP processing and elevated A $\beta$  levels. Results from these mouse studies demonstrate that a chronic increase of A $\beta$  levels, but also possibly an increase of other APP fragments, correlate with spatial and contextual memory impairment (Hsiao et al., 1996, Higgins et al., 1994, Sandhu et al., 1991). These results indicate the role of APP/ APP processing/ A $\beta$  accumulation on memory processes. On the other hand, non-transgenic models of AD (mice/rats) have been used to study acute effect of *in vivo* application of A $\beta$  peptides or oligomers on memory processes. *In vivo* local injections have been mostly carried out using synthetic A $\beta$ <sub>25-35</sub> and A $\beta$ <sub>1-42</sub> in the intracerebral ventricle (icv) or intra-hippocampus. Using this acute model of AD, results have shown that, at intermediate concentrations (picomolar), A $\beta$  can enhance learning and memory retention (Morley et al., 2010). This has been confirmed by (Puzzo et al., 2008) where infusion of pM

concentration of A $\beta$ <sub>1-42</sub> improved reference and contextual memory. However, a single icv injection of nanomolar concentration of A $\beta$ <sub>1-42</sub> impairs memory consolidation within 24 hours, suggesting that A $\beta$  can also rapidly interfere with synaptic activity necessary for stabilization of new memories (Balducci et al., 2010). Whereas, when injected after memory consolidation, no such effects were seen indicating that A $\beta$  oligomers affect memory consolidation rather than retrieval (Balducci and Forloni, 2014). These results hence confirm the bell-shaped relationship between extracellular A $\beta$  and its effect on memory processes.

### **2.2.8 Putative mechanisms of A $\beta$ actions at synapses**

Elevated extracellular A $\beta$  levels particularly in the form of soluble oligomers can alter synaptic transmission and memory processing. However, the mechanism of action of these oligomers are currently unclear. Diverse lines of evidence show that extracellular oligomers can bind to pre- and post-synaptic elements on cultured neurons and in the cortex of AD patients. Cellular and animal studies have attempted to identify the molecular targets of the oligomers and have yielded an array of candidates. A $\beta$  has been reported to interact functionally and also sometimes structurally with several distinct types of plasma membrane-anchored receptors, including  $\alpha$ 7 nicotinic acetylcholine receptors (Snyder et al., 2005), NMDA and AMPA receptors (Lacor et al., 2007), insulin receptors, RAGE (the receptor for advanced glycation end products) (Deane et al., 2003), the prion protein PrP<sup>c</sup> (Um and Strittmatter, 2013), and the Ephrin-type B2 receptor (EphB2) (Lacor et al., 2007).

The extracellular nature of A $\beta$  assumes that the toxic effects are mediated via membrane-bound substrate and/or by internalization of A $\beta$  by affected neurons. Examples of such plasma membrane substrates are the metabotropic glutamate receptors (mGluR) and PrP<sup>c</sup> which interact with A $\beta$  at the synapse and these interactions are known to catalyze synaptic dysfunction and eventually cell death. Reports of capability of A $\beta$  to make holes in the lipid bilayers of membranes could also serve as sites for aberrant entry of Ca<sup>2+</sup> into cells (Capone et al., 2009).

It is important to reinforce here that when studying the different receptor /transporters, which are putative substrates for A $\beta$ , consideration must be given to the form of A $\beta$  used, its concentration and its relevance to physiology. Physiological concentrations of A $\beta$  peptides in

human brain, and cerebrospinal fluid are in low nanomolar range or below (Schmidt et al., 2005, Giedraitis et al., 2007). A $\beta$  concentrations in the most pathobiologically relevant sites of the AD brain, i.e. within and around the synaptic clefts are unknown and might be higher. Also, the binding capacity of monomers to certain receptors will not be the same as binding of oligomers. Hence since these questions are unanswered it is currently hard to conclude on the molecular mediators of A $\beta$  actions.

## **2.2.9 Mouse models of AD**

### **2.2.9.1 Different mouse models**

There are several mouse models of AD, both transgenic (Tg) and non-transgenic, which are currently being used to study potential molecular mechanisms related to dysfunctional synaptic plasticity and memory impairment. The advantage of using AD transgenic mice is that most develop A $\beta$ -related neuropathology in the hippocampus and the cortex, as seen in AD patients and typical behaviour phenotypes reminiscent of AD patients, e.g. alterations in memory processes are also detectable in these Tg mice. The identification of genetic forms of familial AD, involving mutations in APP, has enabled the creation of transgenic mouse models of AD. These genetically modified mice produce human APP well above the physiological level. They often exhibit high levels of soluble and insoluble forms of A $\beta$  peptide, neuropathological features such as neuritic plaques, glial activation, neuritic dystrophy but no paired helical filaments (PHF) or neuronal loss. They are generally considered to represent the early phase of the disease (Ashe and Zahs, 2010). Another widely used type of mouse model, the 3xTg mouse developed by (Oddo et al., 2003), is a triple transgenic mouse carrying mutations in APP, PS1 and Tau gene. The development of these transgenic mice is mostly based on the genetic form of AD (1-5% of AD patients), as these mouse models mainly express mutated forms of human APP and/or PS1 found in these genetic forms. As such, they do not concretely mimic AD in its complexity, which is mainly represented by sporadic forms of the disease. Well characterized mouse models mimicking sporadic AD do not yet exist. Additionally, transgenic models over-expressing APP do not only show elevation of A $\beta$ , but also elevation of full-length APP and other fragments of APP processing that might interfere with the phenotype observed and provide misleading results. Alternatively, the increased use of non-transgenic mice (eg. *in vivo* injections of peptides)

allows to specifically address the mechanisms of action of specific forms of A $\beta$  and help to find a new therapeutic approaches (Benilova et al., 2012).

### **2.2.9.2 Tg2576**

During the thesis, we have used the Tg2576 transgenic mouse developed by (Hsiao et al., 1996), which over-expresses the Swedish double mutant form of A $\beta$ PP<sub>695</sub> (K670N-M671L) under the hamster PrP promoter, on a background of C57Bl/6 and SJL hybrid mouse strain. This is a good APP-derived mouse model which mimic A $\beta$  accumulation in AD patients with a good correlation between A $\beta$  deposition, age and cognitive deficits (Stewart et al., 2011).

#### **2.2.9.2.1 A $\beta$ accumulation**

The Tg2576 mice expresses the mutant hA $\beta$ PP at around 5.5 times the level of endogenous A $\beta$ PP. The A $\beta$  (40 and 42) brain levels increase from 2-4 months of age while plaques appear later at 11-12 months of age. It is a good mouse model to study A $\beta$ -related early onset of AD as soluble A $\beta$  oligomers are high at 3 months in the Tg<sup>+</sup> mice as compared to the controls (Mustafiz et al., 2011). Other authors describe the mice by showing A $\beta$ <sub>42</sub> and A $\beta$ <sub>40</sub> elevation levels at 5 months of age, insoluble A $\beta$  at 7 months and amyloid plaques at 8-9 months onwards (Kawarabayashi et al., 2004). By 11-13 months, there are plaques in the frontal, temporal, entorhinal cortices, hippocampus, pre-subiculum and cerebellum of the brain. This model displays modest hyper phosphorylation of Tau but it does not develop neurofibrillary tangles. It also does not display neuronal loss even at an advanced age. One draw back of this model is that the position of the transgene insertion has never been mapped and its influence on nearby genes never studied. It is therefore not clear how this transgene insertion might influence mouse behaviour and metabolic processes. Also, survival of this model is highly influenced by mouse genetic background (Carlson et al., 1997). Indeed, these Tg2576 mice are generated on a hybrid background of C57Bl6 and SJL (Hsiao et al., 1996). Carlson et al., 1997 reported that when these Tg<sup>+</sup> mice are bred to C57Bl/6 for multiple generations, the proportion of mice dying prematurely increased and proportion of transgene positive mice were significantly reduced. Hence, for generating these mice the mixed

background of C57Bl6/SJL is preferred, but the reasons for this background sensitivity remain unclear.

#### **2.2.9.2.2 *Memory deficits***

(D'Amelio et al., 2011) characterized the onset of memory loss as early as 3 months of age in the Tg2576 mice by showing hippocampus-dependent memory deficits using the contextual fear conditioning task. This early memory deficit is interesting, as at this age there are high levels of soluble form of A $\beta$  oligomers and complete absence of A $\beta$  plaques. As the accumulation of A $\beta$  progressed further into pathology, ability to perform other tasks related to hippocampus-dependent spatial and contextual memories were affected (Hsiao et al., 1996, Arendash et al., 2001, King et al., 1999). The advantage of Tg2576 is their well-known characterization and their extensive usage in diverse behavioural tasks.

#### **2.2.9.3 *A $\beta$ local injections***

To overcome the shortcomings which arise from the transgenic AD mouse model, and to study A $\beta$  or Tau effects more specifically, the acute *in vivo* local infusion model was set up. These non-Tg mouse models of AD are obtained by injecting A $\beta$  or tau directly into the brain via intra-cerebroventricular (icv) or intra-hippocampal injection (Puzzo et al., 2014, Balducci and Forloni, 2014). In the context of A $\beta$ , this model of AD has been advantageous to study how the acute A $\beta$  injection impairs specific signalling pathways leading to synaptic and memory dysfunctions. In addition, the different oligomeric forms of A $\beta$  can be studied since they might exert a different role in synaptic plasticity and memory impairment. The disadvantage of using this acute model is non-reproducibility of gradual rise of A $\beta$  over the years as in AD patients.

Both acute A $\beta$  infusion models and transgenic APP models have limitations as they resemble some but not all aspects of human AD. When taking into consideration, these two types of approaches are, however, still very usefully to identify cellular and molecular processes that might be important for AD pathology. Using these tools in the context of this thesis, we have addressed the relationship between AD and stress, which has been shown to be a significant risk factor for AD (Wilson et al., 2003, Catania et al., 2009).

---

## **2.3 Stress axis**

### **2.3.1 Stress**

#### **2.3.1.1 *Definition***

It is evident by epidemiological and clinical studies that there is a very strong influence of stress in several neurological diseases (de Kloet et al., 2005). Stress can be understood as an aversive stimuli that is endowed with the short and long lasting consequence on the autonomic, neuroendocrine and /or behaviour profile of the subject. When an organism is confronted with a situation that is perceived as a threat, a number of events occur that prepare the organism for a response that is typically considered as “fight-or-flight”. These include increased heart rate, increased respiration and vigilance. These efforts are energy consuming but serve one important function, that is to maintain homeostasis and survival of the organism in a constantly changing environment. We need to consider that all stress consequences are not of the negative type and that stress can have positive effects for example on improving memory, etc.

#### **2.3.1.2 *Acute and Chronic stress***

When an organism is exposed to a stressful situation, the brain areas involved in perception gathers this information and transmits it to the hypothalamus. From there leads two systems, a rapidly acting sympatho-adrenomedullar system and the slower hypothalamo-pituitary-adrenal (HPA) system (de Kloet et al., 2005). As a result of this, the adrenals produce noradrenaline and glucocorticoids (GCs)/corticosteroids (CORT) (corticosterone in rodents, and cortisol in humans). These two hormones have peripheral effects preparing the body to have sufficient energy to face the challenge. Acute stress is normally an adaptive response of the organism to cope with the fluctuations of the environment and hence is essential for survival. By contrast, chronic stress is deleterious and leads to various diseases in vulnerable individuals. Its adverse effects on the brain and body result from dysregulation of the stress axis leading to elevated levels of CORT.

### 2.3.2 Hypothalamus-Pituitary-Adrenal (HPA) axis

The HPA axis activation occurs in response to circadian signalling pathways (Schibler and Sassone-Corsi, 2002) and in presence of a stressor, hence taking the name ‘stress axis’. HPA axis is mainly under the excitatory control of the amygdala and inhibitory control of the hippocampus. Once the hypothalamus receives the signal of the stimulus, the parvocellular neurons within the paraventricular nucleus (PVN) of the hypothalamus release corticotrophin-releasing hormone / factor (CRH/CRF) and vasopressin (AVP) into the portal vessels. Through these vessels, CRH and vasopressin reach the anterior pituitary. This signal further produces adrenocorticotropic hormone (ACTH) which regulates the adrenal cortex to release CORT (Figure 16).

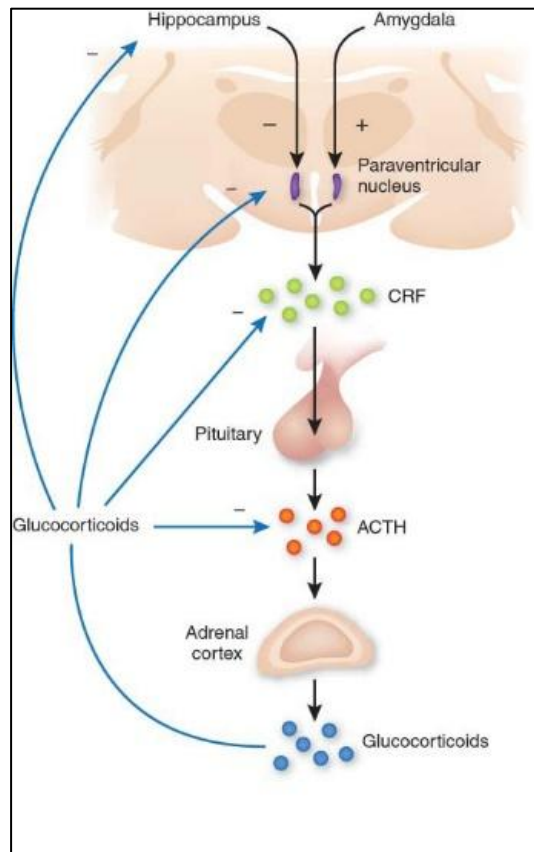


Figure 16: The HPA axis is under the excitatory control of the amygdala and the inhibitory control of the hippocampus. In the hypothalamus, the paraventricular nucleus releases CRF, which is transported to the anterior pituitary where it causes the release of ACTH into the blood stream. ACTH stimulates the adrenal cortex to synthesize and release glucocorticoids (cortisol (humans) or corticosterone (rodents)). CORT feedback at the level of the hippocampus, hypothalamus and pituitary to dampen the excess activation of the HPA axis (Hyman et al., 2009).

### 2.3.2.1 CORT release

There is a rhythmic pattern to the release of CORT. CORT release shows an endogenous circadian variation, which is carried out by brief hourly (ultradian) pulses (Lightman and Conway-Campbell, 2010) as shown in Figure 17. Pulse amplitudes steeply rise some hours before awakening and then slowly diminish again. Recent evidence shows that this pulsatory action is necessary for optimal GR transcriptional activity (Lightman and Conway-Campbell, 2010) to maintain essential body functions in preparation of the active phase. After the exposure of the stressful stimulus, CORT levels slowly increase and then normalize after 2 hours as a result of the negative feedback mechanism at the pituitary and hypothalamus (Ulrich-Lai and Herman, 2009).

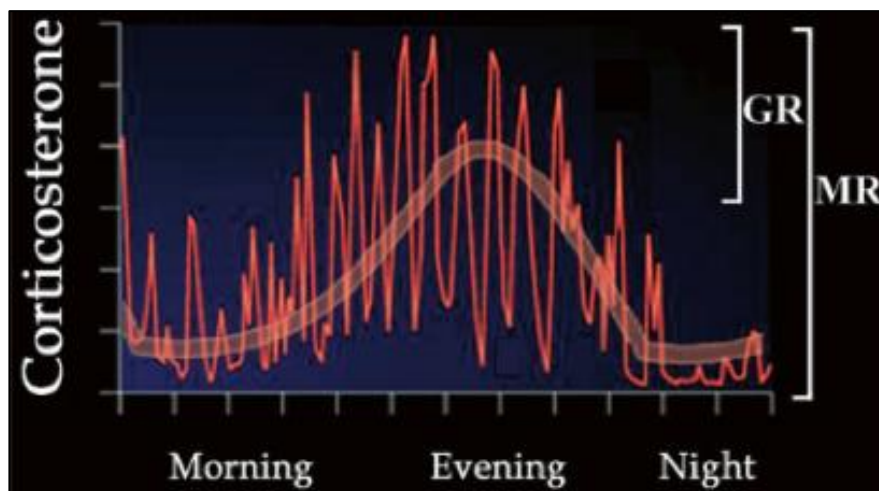


Figure 17: Typical superimposed ultradia (fine line) and circadian (thick line) circulating corticosterone plasma level in mice. MR are constantly activated due to their high affinity in contrary to GR which are activated only at secretion peaks (Lightman and Conway-Campbell, 2010).

CORT circulates in the blood in three main forms: protein-bound, “free” CORT or as CORT conjugates. “Free” CORT accounts to 5% of the total CORT and is the physiologically active form, which can directly target tissues. While the 95% of CORT is protein bound and there are two known CORT-binding factors in plasma. These are the high-affinity, low capacity  $\alpha_2$  globulins called transcortin or cortisol binding globulin (CBG) and the low-affinity, high capacity protein albumin (Funder, 1990).

CORT plays a multifunctional role and they regulate a range of physiological systems (see Figure 18). It plays a very important role in embryonic lung development and this is evident in mice lacking CORT receptors as they die at birth due to lung dysformation (Cole et al.,

1995). Along with maintaining homeostasis, CORT play major roles in immunological system, reproductive system, respiratory system, cardiovascular system, diabetes and many more vital systems showing how important CORT is to our body.

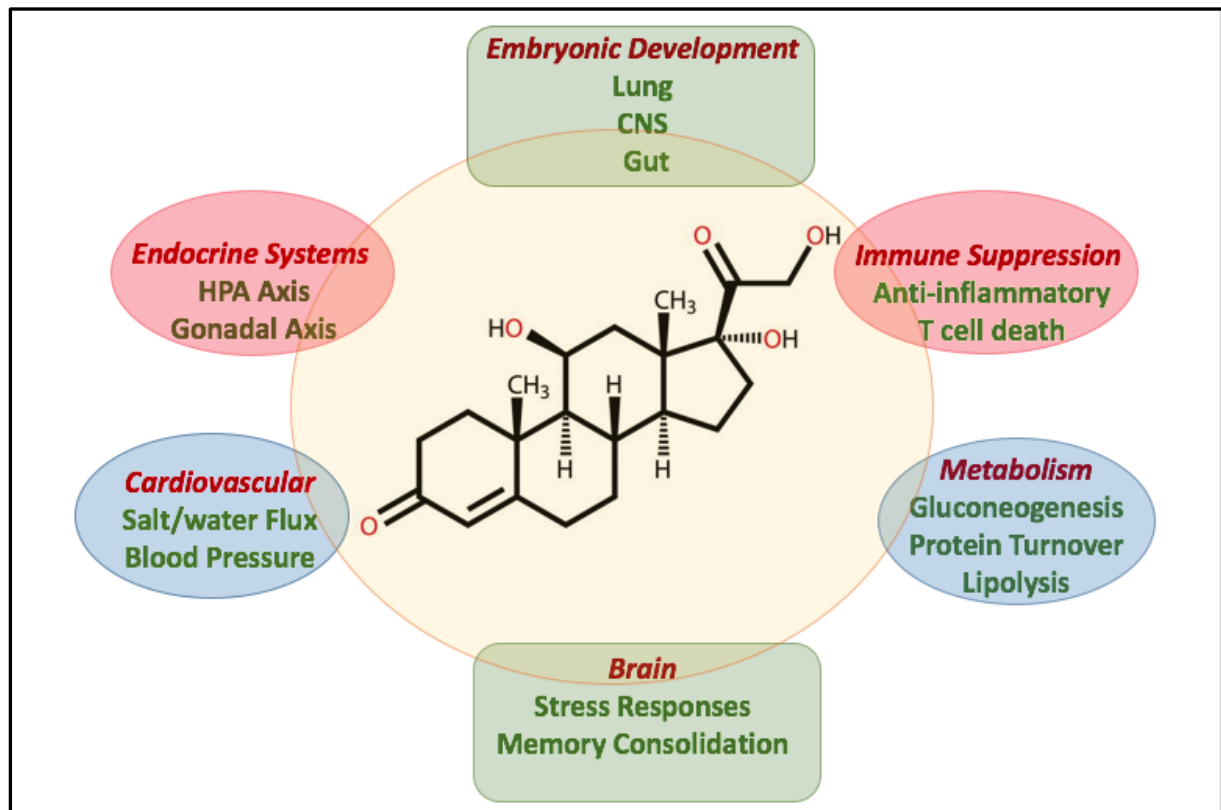


Figure 18: The major physiological functions of cortisol in the human body. CNS, central nervous system. (Adapted from (Cole, 2006)).

### 2.3.2.2 *Effect of CORT on thymus*

The thymus is the key organ in the immune system, which is responsible for maturation of T cells. Elevation of CORT due to chronic stress cause profound atrophy of the thymus (Scollay and Shortman, 1983). T cells especially the immature thymocytes ( $CD4^+/CD8^+$ ) are particularly sensitive to apoptosis induced by CORT. CORT plays a significant role in development, differentiation, homeostasis and function of the T cell (Sapolsky et al., 2000).

### 2.3.2.3 *ACTH release and its effect on adrenal glands*

The primary positive regulator of CORT synthesis and secretion is the ACTH which is released from the anterior pituitary gland. At the adrenal, chronic stress causes cellular

hypertrophy and hyperplasia in the zona fasciculata of the adrenal cortex, which causes elevated responsiveness to ACTH (Ulrich-Lai et al., 2006). ACTH further stimulates adrenocortical cells to synthesize CORT by binding to cell surface of ACTH receptor. cAMP is activated which increases the activity of intracellular biosynthetic enzymes which increase the formation of steroid hormones (Stewart, 2003). The release of ACTH from the pituitary is controlled by CRH produced and secreted by the hypothalamus.

#### 2.3.2.4 Negative feedback control of CORT

To maintain the homeostasis of the body the HPA axis is under tight regulation by circulating CORT. This can be carried out at the level of the hypothalamus (Evanson et al., 2010) and pituitary (Cole et al., 2000) as well as upper limbic structures such as hippocampus (Sapolsky et al., 1984), paraventricular thalamus (PVT) (Jaferi et al., 2003) and prefrontal cortex (Hill et al., 2011).

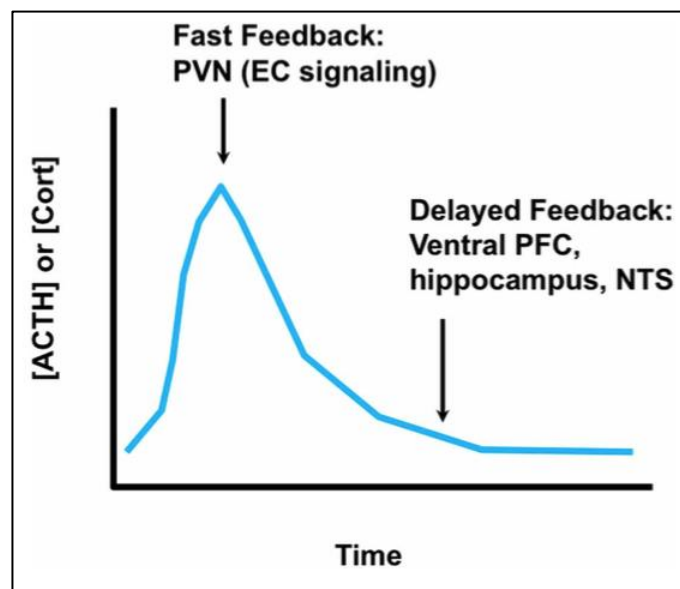


Figure 19: Time domains of CORT feedback. Fast CORT feedback occurs within seconds to minutes, and likely involves the membrane effects of CORT at the PVN. Delayed feedback controls return the CORT back to baseline levels involves the CORT feedback signals at multiple brain regions, including the hippocampus, prefrontal cortex and the NTS (nucleus of solitary tract). It is not clear whether delayed feedback mechanism is genomic, non-genomic or a combination of both (Herman JP., 2013)

There are two mechanisms of CORT feedback (Figure 19). The first is the fast feedback which is most certainly non-genomic and is mediated by inhibitory neurons in part by the direct feedback onto the PVN of the hypothalamus and the pituitary (Evanson et al., 2010). The second is the delayed feedback which eventually shuts off the HPA axis and returns the

system back to baseline. This is known to be mediated via the limbic circuitry including the hippocampus (Jacobson and Sapolsky, 1991). It is not clear whether the delayed feedback mechanism occurs via genomic, non-genomic action or a combination of both. The signalling from the various brain limbic regions are both excitatory and inhibitory. Lesioning of the hippocampus or hippocampectomy resulted in CORT production and /or ACTH suggesting that this region majorly provides inhibitory input to the PVN (Fendler et al., 1961). The outputs coming from the hippocampus to the PVN of the hypothalamus are through indirect innervations. In a stressful situation, the hippocampus sends an excitatory glutamatergic output to the intermediate synapse of the bed nucleus of stria terminallis (BST). Here, the inhibitory GABAergic neurons are activated which inhibit the PVN neurons, which in turn shut down the HPA axis response mediated by stress (Herman and Seroogy, 2006). The medial prefrontal cortex has also shown to have inhibitory action on the PVN (Diorio et al., 1993) while signalling from the amygdala activates the HPA axis (Redgate and Fahringer, 1973).

In the following section, the two CORT receptors will be introduced and their role in HPA axis regulation with respect to the hippocampus and their contribution to synaptic plasticity and memory will be discussed.

### **2.3.3 GRs and MRs**

There are two CORT receptors which have been distinguished in the brain: the mineralocorticoid receptor (MR) formerly called Type I receptors and the glucocorticoid receptor (GR) Type II receptors (Reul and de Kloet, 1985). Both these receptors belong to family of nuclear receptors, which bind to DNA response elements, thus modulating the action of responsive genes (Lu et al, 2009). MRs have high affinity towards the endogenous ligand CORT, such that low CORT levels, like between ultradian pulses of hormone (Young et al., 2004), are sufficient to bind to and activate MRs (see Figure 17). MRs also bind to mineralocorticoids such as adrenal steroid aldosterone with high affinity. MRs are enriched in limited number of limbic regions, particularly high expression in hippocampal subfields and central amygdala (de Kloet et al., 2005). By contrast, GRs are more ubiquitous than MRs and are expressed in the hypothalamus, hippocampus and amygdala, with highest expression in the hippocampus (Diorio et al., 1993). They display low affinity for CORT. These receptors

are only partially occupied under rest but become gradually activated when hormone levels rise, e.g. during an ultradian pulse or after stress (see Figure 17).

### **2.3.3.1 *Gene sequence and structure of the receptors:***

GR is translated from the NR3C1 (Nuclear Receptor Subfamily 3 Group C Member 1) gene located on chromosome 5 and comprises of 9 exons and 11 introns. The protein is encoded from the exon 2 to 9, as exon 1 and 9 undergo alternative splicing. There are 2 isoforms of GR: the most prevalent GR $\alpha$  and GR $\beta$ . GR $\alpha$  is majorly expressed and shuttles between the cytoplasm and the nucleus depending upon its activation by the ligand, while GR $\beta$  is permanently situated in the nucleus and acts as a gene regulator. There are other isoforms, which are generated via alternative translation which bind with same affinity to the ligand, but have different transcriptional activity. MR are nuclear hormone receptors of the NR3C2 gene which contain 10 exons with the first 2 exons remaining untranslated (Zennaro et al., 1995).

GR and MR are classified members under the nuclear receptors superfamily and steroid receptor subfamily. Hence they share a common domain structure (NTD-DBD-LBD) with other steroid hormones like progesterone receptor (PR), androgen receptor (AR), estrogen receptor (ER) (see Figure 20). Both GR and MR are characterized by a central DNA-binding domain (DBD), which functions to target the receptor to specific DNA sequences known as glucocorticoid response elements (GREs). As both the receptors have almost identical DBDs, they bind to identical GREs. The C-terminal end has a ligand-binding domain (LBD) which provides essential property of binding hormone, while the N-terminal part of the receptor, is involved in trans-activation of target genes after the receptor complex is bound to DNA.

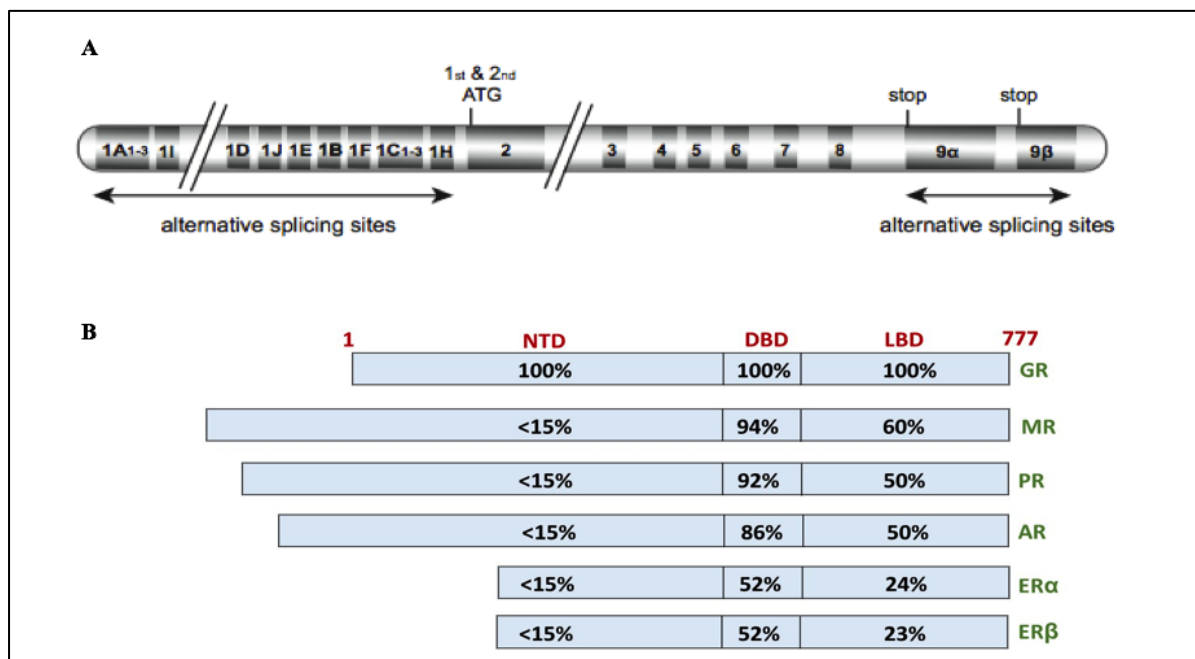


Figure 20: Structure of human GR gene and protein. A). The hGR gene is located on chromosome 5 (region 5q31p) and contains 9 exons of which exon 2 to 8 are translated for GR protein. Exon1 is composed of nine alternatives (1A-IH) and remains untranslated as ATG start codon lies with exon 2. B). Structural comparison of GR with the other members of the steroid receptor subfamily from the nuclear receptor superfamily. NTD: N-terminal domain; DBD, DNA-binding domain; LBD, ligand-binding domain; PR, progesterone receptor; AR, androgen receptor; ER $\alpha$ , estrogen alpha; and ER $\beta$ , estrogen beta. Percentage identity at the amino acid level is related to GR (set at 100%). (Adapted from (Joëls and Karst, 2012)).

### 2.3.3.2 Functional role of the receptors:

There are two modes of action of these receptors: the fast acting/non-genomic membrane receptors and the long lasting/genomic nuclear receptors.

#### 2.3.3.2.1 Membrane CORT receptors and their functions

There is accumulating evidence which implicates mechanisms involving membrane located GRs and MRs. The 'fast' feedback mechanism is speculated to pass through these membrane receptors. Increasing evidence suggests the non-genomic hypothesis of neuronal signalling through membrane-associated GRs and MRs (de Kloet et al., 2008). These receptors regulate second messenger systems, which can have direct effects on membrane potentials, including ion channels that regulate neuronal membrane potential (French-Mullen, 1995). Additionally, these membrane receptors can regulate gene transcription through second messenger cascades (Kino et al., 2005). Membrane GRs regulate dendrite spine growth while MR plays a

regulatory role in dendritic spine structure (Liston et al., 2013, Russo et al., 2016). Moreover, their implications in memory retention and learning come from the influential relationship that they have on spine formation during circadian CORT peaks and troughs. At the molecular level, GR was shown to regulate pre- and post-synaptic function (Tasker et al., 2006) and acutely regulate AMPAR trafficking, hence playing a role in synaptic transmission (Conboy and Sandi, 2010). Thus, fast acting membrane associated form of MR and GR have multiple roles, with a convergence of functions at synapses and dendritic spines. Recently, GR receptors have also been identified in the PSD as well as in dendritic spines, dendrites, soma, nuclei and also pre-synaptic terminal regions and glia processes (Johnson et al., 2005). It should be noted here that it is still not clear if the GRs and MRs found in the PSD are the fast-acting membrane receptors.

#### **2.3.3.2.2 *Genomic action of receptors***

In absence of the ligand, GRs and MRs form an inactive cytoplasmic multi-protein complex with heat-shock proteins, such as HSP90, HSP70, and HSP56 (see Figure 21 for diagram of activation of GRs). In presence of CORT, GRs or MRs are released from the chaperones and dimerize and translocate to the nucleus (Trapp et al., 1994). Here, they bind to specific DNA GREs at the promoter site of target genes and controls the rate of gene transcription through transactivation. On the other hand, transrepression activity requires the monomeric form of GR to interact with other transcriptional factors through protein-protein interaction and involves activated protein-1 (AP-1), nuclear factor-kB (NF-kB), and cAMP-responsive element binding protein (CREB). GR and MRs also have the ability to heterodimerize in tissues co-expressing the two receptors (Trapp et al., 1994). In general, these nuclear receptors are necessary for normal cellular activity, and crucial for many central nervous system functions, including learning and memory (Roozendaal, 2000). There has also been recent discovery of the mitochondrial GR nuclear receptors whose functional role is still not discovered.

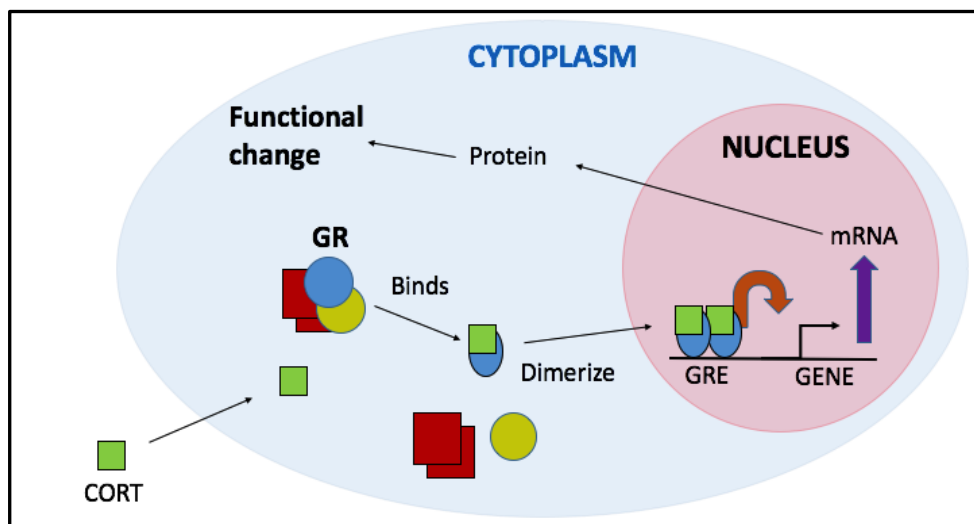


Figure 21: General mechanism of nuclear action of GRs in target cells. CORT enters target cell by passive diffusion across the cell membrane. The GR dissociates from its bound form with the chaperones and undergoes conformational changes optimal for hormone binding. Upon binding to ligand, GR dimerizes and translocates to the nucleus. The activated GR dimer binds to the specific glucocorticoid response element (GRE) and increases the rate of transcription. This produces an elevation of protein level in the cell and eventually produce physiological adaptations (Adapted from Cole T., 2006)

## 2.3.4 Techniques to study receptor function

To understand the mechanism of action of CORT via their receptors GR and MR, there are two major techniques: Pharmacological and genetic manipulation studies which are currently carried out. These techniques will be reviewed with respect to GR.

### 2.3.4.1 Different GR agonist and antagonists and their drawbacks

Synthetically prepared CORT, like prednisone and dexamethasone, are extensively used in pharmacological studies as agonists to facilitate understanding the mode of action of CORT. For example, dexamethasone, an agonist for cortisol is routinely run on patients to verify the proper functioning of the feedback mechanism. Injection of this potent agonist, normally triggers the negative feedback mechanism resulting in a reduction of plasma cortisol levels within hours (Raff et al., 2014).

Excessive or chronic exposure to CORT levels increases the vulnerability towards psychopathologies like major depressive disorder and neurodegenerative diseases like AD. For this reason, full GR antagonists have been currently been used as potential therapeutics in clinical research (Wulsin et al., 2010). Also GR antagonists are mainly used to treat

Cushings Syndrome, where patients exhibit abnormally high levels of CORT (van der Lely et al., 1991).

There are two main types of GR antagonists: steroidal and non-steroidal (Cole, 2006). Amongst the steroid GR antagonists, the RU486 / mifepristone is the most commonly prescribed and has been used in the treatment of some psychiatric disorders (Baulieu, 1997). The disadvantage of using RU486 is its lack of specificity to GRs as it cross reacts with PRs as well as GR, thus preventing its wide spread use. Also, because of its ability to bind to PR, it is used as an abortion pill for treatment of early pregnancy. To circumvent the issue of lack of specificity towards GR, there are currently new nonsteroidal GR antagonists (e.g. Compound 13; Corcept Therapeutics, USA) being tested, which bind specifically to GRs and not PRs (Hunt et al., 2015) (for properties of C13 refer to Table 5 in Material and methods).

There have also been efforts to generate GR modulators, which do not have complete antagonist like actions but act as partial agonist-antagonist (Zalachoras et al., 2013). With this approach, only the excessive GRs are inhibited while the basal GRs required for normal function are not disturbed. CORT 108297 and CORT 113176 are representatives of a series of novel, selective non-steroidal GR modulators developed by Corcept Therapeutics, USA. These compounds exhibit excellent affinity for GR with no measurable affinity for other nuclear hormone receptors PR, AR (androgen receptor), MR and ER (estrogen receptor) (Hunt et al., 2015).

#### **2.3.4.2 Genetic manipulation studies**

In addition to pharmacological studies, a number of studies were carried out on mice in which GR was genetically manipulated to determine its role in HPA axis regulation and in different behaviours (especially to study depression) (Chourbaji et al., 2008). Mice homozygous for GR null allele ( $GR^{-/-}$ ) die shortly after birth as they exhibit a lung dysfunction. Hence, there are transgenic mice with decreased GR expression with antisense RNA (Pepin et al., 1992) and mice with GR over-expression (Reichardt et al., 2000). Specific conditional knock-out mice for GR have also been generated using the Cre/loxP recombination system under the control of a rat nestin promoter ( $GR^{NesCre}$  mice) (Tronche et al., 1999). For this, two mouse lines were generated. In one mouse line, which we call here  $GR^{lox/lox}$ , exon 3 of the GR gene was flanked by loxP sites to promote recombination in

presence of cre recombinase. This mouse was crossed with a mouse expressing cre recombinase under the nestin (Nes) promoter allowing for cre recombinase expression in all neuron and glial cells of the CNS. These mutants lacked the GR in all neurons and glial cells throughout the CNS. Analysis of these mutants evidenced over-activation of the HPA axis as there was no negative feedback exerted at the PVN via the GRs, and reduced anxiety (Tronche et al. 1999).  $GR^{lox/lox}$  mice are perfect for conditional ablation of GRs in area specific region by injection of Cre recombinase encoding viruses with neuronal specific promoter. For example, these mice have been used to remove GRs specifically in dopamine neurons *in vivo* to study their roles in addiction and stress (Ambroggi et al., 2009, Barik et al., 2013).

### 2.3.5 Role of the hippocampus in stress/HPA axis

#### 2.3.5.1 Effect of stress on hippocampus:

Increase in CORT due to chronic stressors can have some deleterious effects on the structural and functional integrity of corticosteroid-responsive brain regions especially the hippocampus. Adverse stress and administration of CORT cause alterations in hippocampal plasticity, including shortening of dendrites, altered neurogenesis and impairment in LTP and memory formation (Figure 22).

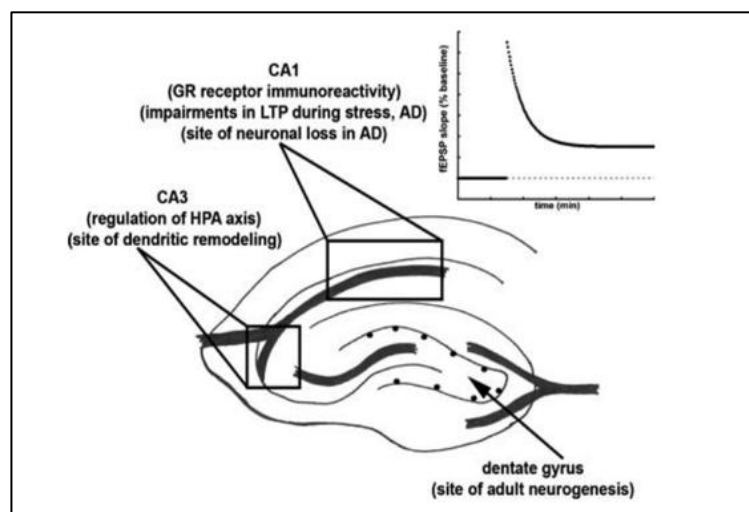


Figure 22: Specific sites of hippocampus indicating areas responsible for synaptic plasticity and regulation of HPA axis with respect to the site of GRs. (Rothman and Mattson, 2010)

In rodents, reduction in dendritic spines occurs in the CA3 region after exposure to chronic stress (Sousa et al., 2000). Moreover, increased levels of CORT significantly decrease neurogenesis in DG, which is a major site of adult neurogenesis (Gould and Tanapat, 1999). Lastly, long term elevations in corticosteroid CORT levels can have negative effects on neuroplasticity and cell survival (Sapolsky, 1985). There is atrophy of neuronal dendrites within the CA1 of the hippocampus followed by deficits in spatial memory after exposure to chronic behavioural stressor or administration of CORT. Additionally, the hippocampus is playing an important role in inhibiting the activity of the HPA axis and damage to the hippocampus could provide a repetitive cycle of increasing the HPA axis dysregulation and hippocampal injury (Sapolsky, 1992).

Overall, CORT has been shown to heavily influence the structure and function of the hippocampus. They seem to mediate their regulation via the rapid non-genomic mechanism and the long lasting genomic mechanism. These in turn directly affect synaptic transmission, plasticity, learning and memory (Popoli et al., 2011).

### ***2.3.5.2 Effect of stress/CORT on synaptic plasticity***

#### ***2.3.5.2.1 At intermediate CORT level/stress:***

CORT regulates glutamate transmission by the both genomic and non-genomic actions. It is known that CORT enhances rapidly presynaptic glutamate release in the hippocampus, amygdala and medial prefrontal cortex (mPFC) (Lowy et al., 1993). CORT also rapidly increase the trafficking of AMPARs at the post-synapse via genomic-independent mechanisms (Groc et al., 2008). Also, it was shown that activation of MRs leads to lateral diffusion of GluA1 and GluA2 subunits to the post synaptic sites, thus increasing the frequency of hippocampal AMPAR-mediated current in CA1 neurons (Krugers et al., 2010, Groc et al., 2008). These results suggest that rapid effects of GCs should facilitate LTP.

Genomic actions of CORT have similar effect on glutamate neurotransmission (Yuen and Yan, 2009, Yuen et al., 2011). Like the non-genomic effect, genomic actions lead to increase in GluA2 containing AMPAR and enhance synaptic transmission (Martin et al., 2009). This in turn leads to spine formation, and long term memory formation. In line with these findings, genomic mediated effects of GR also regulate calcium signalling in hippocampal neurons leading to high frequency LTP. GR-mediated increase in intracellular calcium levels was

found to be dependent on activation of NMDARs (Takahashi et al., 2002). Together, these data support an important activity of GRs at synapses, but little is known about the local synaptic partners of GRs, which allow for these synapse alterations.

#### **2.3.5.2.2 High CORT level/stress**

In conditions of high CORT /high prolonged stress, activation of GRs can have a negative effect through activation of NMDAR (Coussens et al., 1997). This action mainly activates the extrasynaptic NR2B-containing NMDARs (Yang et al., 2005) and endocytosis of AMPAR, leading to exacerbation of LTD and impairment of spatial memory (Howland and Cazakoff, 2010).

In line with these observations, several studies investigated the role of GR and MR in GR-mediated synaptic plasticity (Diamond et al., 1992). In particular, activation of MRs was found to enhance hippocampal LTP, whereas saturation of GRs after treatment with high doses of CORT attenuated LTP and enhanced LTD (McEwen and Sapolsky, 1995).

#### **2.3.5.3 Effect of CORT/ stress on memory**

In both humans and rodents, it is well established that stress intensity and memory are known to follow an inverted U-shaped relationship, with maximum memory strength at an intermediate level of stress.

CORT-mediated effects engage both GR and MR play a different role in acquisition, storage, consolidation and retrieval of information. MRs play a role in the initial phase of memory encoding including response to novelty, while GRs are important in memory consolidation (Ter Horst et al., 2012). GRs activation affects hippocampal functions thus modulating the consolidation of several types of hippocampus-dependent memories, including spatial and contextual memories in rodents and declarative memory in humans (Donley et al., 2005). Mild stress during or after learning was shown to have a positive effect on consolidation of long term memory (Roosendaal, 2000). However, several studies in mice and humans have shown stress exposure or CORT administration shortly before retention testing impairs retrieval of memory (de Quervain et al., 1998). These are mainly caused by the action of the non-genomic membrane GRs. Hence there is now strong evidence that the timing of the stressor and the intensity can have a differential impact on memory retention. Consolidating a

strong memory after a salient or stressful event is an adaptive response that is necessary for appropriate reactions to similar demands in the future.

GRs regulate several intracellular signalling pathways known to be required for memory consolidation. These include the pathways activated by CREB, MAPK, CamKII and BDNF (Chen et al., 2012). These signalling pathway and GR-mediated action are involved in controlling epigenetic modifications that influence long-term memory processes (Finsterwald and Alberini, 2014).

### **2.3.6 GR modulators and their use as therapeutic in AD**

Recent research has used GR modulators in rodent models to check for rescue of principal hallmarks of AD phenotypes and have shown promising results (Pineau et al., 2016).

Report that these GR modulators (CORT 108297 and CORT 113176) reverse the hippocampal amyloidogenic pathways induced by icv injection of A $\beta$ <sub>25-35</sub> through inhibition of BACE1 and increase clearance of A $\beta$ . In addition, they restore synaptic marker levels in hippocampus, reverse neuroinflammation and apoptotic processes and restore cognitive functions. These results are promising and form the bases of using these GR modulators as therapeutics in AD. Overall, these modulators seem to have promising therapeutic potential to tackle diseases associated with dysregulated HPA axis and stress related disorders.

For this thesis, we will now focus on the specific relationship between AD and stress as risk factor.

---

## **2.4 Link between AD and stress**

### **2.4.1 Stress is a major environmental risk factor for AD**

The cause and mechanism of development of AD remains unclear. There are multitudes of environmental risk factors leading to AD amongst which stress is the most common. Indeed, patients who are susceptible to stress are 2.7 times more likely to develop AD than others (Wilson et al., 2003, Wilson et al., 2007). This can also be seen in cases where stress lowers the age of onset of FAD (Mejia et al., 2003). As mentioned earlier, an increased risk of AD arises from mutations affecting CORT production (de Quervain et al., 2004). On the other hand, there could be a decreased risk of AD from GR variants cumulating in CORT

resistance (van Rossum et al., 2008). Interestingly, *in vivo* and *in vitro* studies have shown that stress and CORT induce the production of A $\beta$  by neural cells (Green et al., 2006, Baglietto-Vargas et al., 2013) whereas stress and CRH promote hyperphosphorylation of tau by activation of CRFR1 receptor (Rissman, 2009). Furthermore, CORT was shown to trigger APP misprocessing, increased A $\beta$  production, reduced A $\beta$  clearance, tau phosphorylation and accumulation and cognitive decline (Jeong et al., 2006).

Together these data consolidate the link between HPA axis hyperactivity and AD. Moreover, there seems to be an establishment of a viscous circle whereby the pathology increases secretion of CORT, which further increases the pathology (Notarianni, 2013).

## **2.4.2 HPA axis adaptive changes in human AD patients and AD mouse models**

An association is recognized between AD and hyperactivity of the HPA axis, but the precise role played by HPA axis dysfunction in AD development is undefined. The foremost evidence in this context is dysregulation in the negative CORT feedback as well as high production of CORT levels as seen in both AD patients and mouse models. This leads to or is causal for other stress related molecules in the HPA axis to be involved in modifying vulnerability to AD. These include CRH levels, ACTH levels, gene expression level of GR and MR in different brain regions known to exert control over the HPA axis. In this chapter, focus will be on CORT levels and ACTH levels in AD cases.

### **2.4.2.1 CORT levels**

Clinical studies have reported that there is an increase in plasma CORT levels in patients with early phase of AD (Rasmuson et al., 2001). Here, it is interesting to note that while AD patients show basal hypercortisolemia, their circadian rhythm of CORT variation seems to be intact (Giubilei et al., 2001). This contrasts with the continuously elevated levels of CORT that are characteristic of other hypercortisolemia states like Cushing's disease or major depression.

In addition, there is a decreased negative feedback of CORT in AD patients, which is confirmed by a low-dose dexamethasone suppression test (Näsman et al., 1995). In AD

patients, due to dysregulation of the HPA axis the levels of CORT cannot be reduced. This phenotype of hypercortisolemia is also seen in 3xTg mouse model at late stages of the disease (Green et al., 2006).

There are many studies correlating the relationship between plasma CORT levels and clinical /cognitive measures of the rate of progression of AD. Of interest was the finding that, although AD patients had elevated basal CORT levels, HPA axis dysfunction did not worsen with additional cognitive decline (Swanwick et al., 1998).

#### **2.4.2.2 ACTH levels**

CORT levels depend on the upstream secretion of ACTH by the pituitary gland. In AD patients, it has been reported that despite high production of CORT there is an absence of ACTH drive (Umegaki et al., 2000). This lower or equal level of ACTH could be due to several reasons. Primarily, studies revealed that an increased central drive by CRH could result in down-regulation of pituitary receptors. Secondly, there might be a concomitant inhibition of corticotrophs due to increased CORT levels and lastly it might be due to an increased peripheral sensitivity of the adrenal gland to ACTH (Amsterdam et al., 1989). There is also evidence of increased adrenocortical sensitivity to ACTH in AD patients (O'Brien et al., 1996).

#### **2.4.2.3 Stress related disorders in AD patients**

Sleep is highly sensitive to stress and sleep disorders are often associated to stress-related disorders. Amongst the AD patients, 44% are affected with a sleep disorder and the prevalence and severity of the sleep disorders increase with dementia severity (McCurry et al., 1999). Their sleep patterns are known to be affected from early stages of AD and characterized by short sleep durations and worse sleep qualities (Ju et al., 2014). There is known to be a bidirectional relation between amyloid plaque accumulation and sleep disturbances (Ju et al., 2014). There are other sleep disturbances seen in AD which include daytime hypersomnia, delayed circadian phase and adverse effects of dementia medication such as acetylcholinesterase inhibitors (Dauvilliers, 2007).

Stress related psychiatric disorders (like anxiety and depression) have been identified as a risk for developing AD (Caraci et al., 2010). Anxiety in dementia is common. The risk of developing AD may be 30 times higher amongst people with MCI and anxiety.

### **2.4.3 Tau and HPA axis**

Clinical data shows that cognitive deficits in AD patients correlate better with NFT than to amyloid- $\beta$  profiles (Guillozet et al., 2003). This is also supported by the fact that the development of NFTs start earlier in the hippocampus than the amyloid plaques. These evidences support the essential role of tau in establishment of AD pathology.

*In vivo* data shows that high stress levels increase APP processing towards A $\beta$  formation and subsequent aberrant hyperphosphorylation of tau protein, NFT formation and eventually neuronal loss (Lee et al., 2009). For example, 3xTg mice injected with dexamethasone leads to somatodendritic accumulation of tau in the hippocampus, amygdala and cortex (Green et al., 2006). Furthermore, the stress related molecule CRH is commonly associated with tau phosphorylation and this is confirmed by the fact that deletion of receptor CRFR1 abolishes the detrimental effects of tau phosphorylation (Carroll et al., 2011). In addition, a new mechanism linking tau processing and stress was recently studied using the P301L tau transgenic mouse. In female mice, chronic stress elevated levels of caspase-3-truncated tau and insoluble tau aggregates altered expression of chaperones Hsp90, Hsp 70 and Hsp 105 (Sotiropoulos et al., 2015).

### **2.4.4 Role of stress/CORT administration on A $\beta$ pathology**

Several studies in transgenic mice indicate that both A $\beta$  production through APP processing and amyloid plaque formation are accelerated in response to chronic stress. Social isolation for 6 months in the Tg2576 increased A $\beta$  plaques (Dong et al., 2008) and a similar increase in extracellular and neuronal A $\beta$  in other transgenic mice were observed as a result of immobilization stress (Jeong et al., 2006). Concurrently, in 3xTg AD, chronic stress triggered APP misprocessing, which increased A $\beta$  level, tau phosphorylation and accumulation (Green et al., 2006). This study further showed that CORT and dexamethasone application *in vitro* also increased A $\beta$ 40 and A $\beta$ 42 level, implying that CORT can directly affect APP

processing. Collectively, these data strongly implicate that stress or CORT administration is linked to A $\beta$  pathology. Yet, the role of GRs in AD pathology remains mostly unknown.

### **2.4.5 Role of GRs in AD**

Hippocampal GRs and MRs are involved in the basal neuronal function and negative feedback regulation of the HPA axis (Sousa et al., 2008). The GC cascade hypothesis relates the relationship between CORT and hippocampus with aging. This hypothesis states that CORT secreted during periods of stress, desensitize the hippocampus to further CORT exposure, by downregulating the GRs (Sapolsky et al., 1984). However, biochemical results from AD patients, indicates that GR and MR levels in the hippocampus are maintained. This may be possible due to the maintained circadian hypercorticoïdism in AD patients (Hartmann et al., 1996). On the other hand, the single injected A $\beta$ <sub>(25-35)</sub> acute AD model, demonstrated a strong, long lasting activation of the HPA axis associated with a modification of the balance between GR and MR expression in the hippocampus, amygdala and hypothalamus. Subsequently a disruption of the GR nuclear-cytoplasmic translocation occurred, leading to its accumulation in the nucleolus (Brureau et al., 2013). *In vivo* studies show that young 3xTg AD mice exhibit an active HPA axis and higher GR mRNA levels in the hippocampus. Moreover, increased CORT levels are sufficient to exacerbate A $\beta$  deposits and it was shown that antagonism of GR could prevent this effect (Baglietto-Vargas et al., 2013).

Recently, one week of treatment with a novel potent GR modulator CORT 108297 has been effectively used to reverse memory deficits, CORT increase, hippocampal synaptic impairment and APP misprocessing caused by A $\beta$  toxicity, as tested by acute *in vivo* A $\beta$ <sub>25-35</sub> injections (Pineau et al., 2016).

### **2.4.6 Relationship between A $\beta$ oligomers and GRs**

With all the above evidence, it seems clear that GR signalling is altered in AD via increased CORT. On the other hand, there is a strong association of A $\beta$  accumulation in manifesting AD phenotypes like synaptic dysfunction and memory impairment (see chapter 1.2.7 above). But, till date, there is not much evidence functionally linking A $\beta$  oligomers and GRs at synapses and confirming the possibility of a combined effect on synaptic plasticity (Figure

23). Recently, it was reported that *in vivo* intra-cerebroventricular  $A\beta_{25-35}$  injections promoted accumulation of GRs in the nucleus of CA1 neurons in the hippocampus (Brureau et al., 2013). This strongly suggests an intricate functional relationship between  $A\beta$  and GRs at the nucleus, but there remains a paucity of data on the relationship between  $A\beta$  and GRs at synapses.

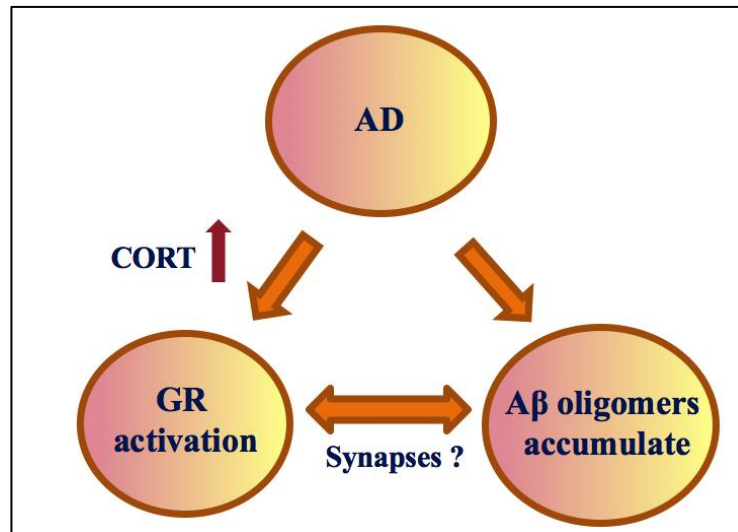


Figure 23: Link between  $A\beta$  and GRs. GR activation is known to act at synapses and is likely to be involved in AD due to increased levels of CORT. Simultaneously,  $A\beta$  is known to aggregate to oligomeric form and to modify synapse function as AD develops. Yet, there is not much data regarding the relationship between GRs and  $A\beta$  at synapses.

#### 2.4.7 Common link between $A\beta$ and CORT on the glutamatergic system

In the previous chapters, we described how elevated levels of  $A\beta$  and CORT, two phenotypes observed in AD, individually modify glutamate synaptic transmission. It is interesting to note that their effects in a bell-shaped fashion which is concentration-dependent. This illustrates the fine sensitivity of the glutamatergic system to these modulators. Also, when comparing the effects of  $A\beta$  and CORT/GRs on the hippocampus, they are surprisingly similar as summarized in Table 2. This comparative analysis, that I personally made, suggests that there might be an intricate relationship between the  $A\beta$  and CORT/GRs with important, but yet unidentified, implications in hippocampus dysfunction in AD.

Table 2: Comparison between effects of high levels of A $\beta$  and stress/ high levels of CORT/GR activation on the glutamatergic transmission, synaptic plasticity, dendrites and spines, and hippocampus-dependent memory processes.

| <b>Read out</b>              | <b>High levels of Amyloid-<math>\beta</math></b>  | <b>Stress/ High level of CORT/GR activation</b>   |
|------------------------------|---|---|
| Glutamate levels at synapses | Increases release and uptake is less<br>( <i>Li et al., 2009; Synder et al., 2005</i> )   | Increases release and blockade of uptake<br>( <i>Venero C, Borrell J., 1999; Yang et al., 2005</i> )  |
| AMPA                         | Internalisation of AMPAR<br>( <i>Almeida et al., 2005; Hsieh et al., 2006, Zhao et al., 2010</i> )  | Internalization of AMPAR<br>( <i>Wong et al., 2007; Fox C et al., 2007</i> )  |
| NMDAR                        | Internalisation of synaptic NMDAR , activation of extrasynaptic NMDAR<br>( <i>Synder et al., 2005; Lacor et al., 2007; Li et al., 2011; Talontova et al., 2013</i> )      | GR-mediated activation of extrasynaptic NMDAR, hamper NMDAR synaptic plasticity<br>( <i>Yang., 2005; Wong et al., 2007; Fox et al., 2007; Massey et al., 2004; Weigert et al., 2005</i> ) |
| LTP                          | Impairment of LTP<br>( <i>Lambert et al., 1998; Walsh et al., 2002; Townsend et al., 2006; Shankar et al., 2008</i> )   | Impairment of LTP<br>( <i>Diamond et al., 1992; Zhou et al., 2000; Alfarez et al., 2002</i> )   |
| LTD                          | Enhancement of LTD<br>( <i>Wang et al., 2002; Shankar et al., 2008; Li et al., 2009</i> )   | Increases hippocampal LTD<br>( <i>Wong et al., 2007</i> )   |
| Memory                       | Impairment in spatial and contextual memory<br>( <i>Hsiao et al., 1996; Higgins et al., 1994</i> )  | Impairment spatial memory retrieval<br>( <i>Howland &amp; Cazakoff, 2010; Wong et al., 2007; Howland al., 2010</i> )  |
| Dendritic atrophy            | Reduction in dendritic spine density, number of synapses decreased<br>( <i>Selkoe et al., 2002; Jacobsen et al., 2006; Shankar et al., 2007/2008; Zhao et al., 2010</i> ) | Shortening of dendrites<br>( <i>Magarinos et al., 1998; Sousa et al., 2000</i> )  |

It is within this context that I have pursued my PhD thesis, which focused on identifying the physiopathological relationship between AD and the HPA, focusing mostly on GR signalling.

### 3 Objectives

My first objective was to study in detail the relationship between HPA axis dysregulation and early onset of AD phenotypes using the Tg2576 mice (Tg<sup>+</sup> mice). At 4 month of age in these mice, my team had observed high CORT levels and a non-functional negative feedback mechanism shown by dexamethasone suppression test indicating a dysregulated HPA axis (detailed in (Lanté et al., 2015)). This led us to investigate the onset and progression of this dysregulation and its effect on other HPA axis regulators and peripheral organs at different time points in the early symptomatic stage of these mice. In addition, we wanted to quantify the level of hippocampal total GRs at 4 months of age, to check if high CORT levels affected GRs due to the HPA axis dysregulation or due to accumulation of A $\beta$  peptides and oligomers. My team had also previously observed alterations in hippocampal LTD in these mice at this same age and a rescue by the GR antagonist RU486 (detailed in (Lanté et al., 2015)). To place these findings in the context of memory loss in AD they had decided to investigate episodic-like memory in these Tg<sup>+</sup> mice. Lab members had optimized a version of the object recognition test that could test episodic-like memory in these mice based on (Dere et al. 2005) and had observed a deficit in this type of memory in 4 months old Tg2576 mice. In light of the dysregulation of the HPA axis and LTD rescue by GR RU486, we hypothesized that GR antagonism might rescue this memory deficit.

My second objective was to further investigate the specific role of GRs in driving AD phenotypes in these Tg<sup>+</sup> mice by creating double mutant mice, which harboured the APPswe transgene and a floxed GR gene (GR<sup>lox/lox</sup> mice; (Tronche et al., 1999)). This would allow for specific ablation of GRs in a spatially and temporally dependent manner. For this, we would cross the Tg<sup>+</sup> mice with the GR<sup>lox/lox</sup> mice. Upon obtaining these double mutants, we would verify that by injecting an AAV virus expressing Cre recombinase into the CA1 region of the hippocampus of these double mutant mice, we could efficiently remove GRs from neurons. We would then use these transduced mice to investigate if removing GRs could reverse the AD like phenotypes seen previously in the Tg<sup>+</sup> mice, namely exacerbated CORT levels, enhanced LTD and episodic-like memory deficit.

In collaboration with Dr. Frandemiche, my third and highly-related objective involved studying more specifically the functional relationship between oA $\beta$  and GRs at excitatory synapses. For this, we would mainly work with *in vitro* and *ex vivo* acute application of

synthetic oligomers of A $\beta$  (oA $\beta$ ). Using a well standardized protocol established by Dr. Frandemiche (Frandemiche et al., 2014), we would investigate if oA $\beta$  could modulate GRs at synapses in *in vitro* hippocampal neuron cultures. Moreover, the molecular mechanism through which oA $\beta$  acts to modify synapse function remains uncertain. We therefore decided to ask if GRs could be involved in these oA $\beta$ -mediated synaptic effects. For this, we would use *ex vivo* hippocampal sections acutely treated with oA $\beta$  to check if GRs could be implicated in oA $\beta$ -mediated LTP impairment. Using this *ex vivo* system, we would block GRs either pharmacologically using a specific GR antagonist C13 (provided by CORCEPT Therapeutics) or ablate GRs in the CA1 neurons using the *in vivo* transduction of a virus expression cre recombinase in GR<sup>lox/lox</sup> mice.

Overall, using different approaches, the main goal of this thesis was to identify the role of GRs in early AD-associated dysregulation of HPA axis, hippocampal-dependent memory deficits and impaired synaptic activity. I successfully fulfilled some of these objectives to highlight the functional role of GR in the physiopathology of AD.

## 4 Materials and Methods:

### 4.1 Animal Breeding

Different strains of mice were used during the thesis project:

The **Tg2576 (Tg<sup>+</sup>)** mice harbour the human Swedish mutation (hAPP<sup>swe</sup> transgene: APP<sub>695</sub> isoform with double mutations at KM670/671NL) and overexpress approximately 5 times more APP than their control littermates (Wildtype WT) (Hsiao et al., 1996). The Tg2576 mice were bred on C57Bl6/SJL hybrid background and are backcrossed to C57BL6 breeders before being deposited at Taconics (Carlson et al., 1997). The hemizygous Tg2576 male mice, purchased from Taconics, were mated with hybrid Bl6/SJL females and the F1 generation were used for all experiments. 4 and 6-month old Tg<sup>+</sup> and WT mice were used for dissections of hippocampus, thymus, adrenal glands, estimation of CORT and ACTH levels from blood plasma. The Episodic memory behaviour paradigm was also carried on 4-month old mice.

**GR<sup>lox/lox</sup> Bl6 mice** (from (Tronche et al., 1999)) have the exon 3 of the GR gene flanked with the loxP site and are bred on pure C57Bl6 background.

Two-month old mice were injected using a stereotaxic apparatus with Cre-GFP or control GFP virus in the CA1 region of the hippocampus. Mice were given a recovery period of 4 weeks to allow sufficient time for recombination followed by electrophysiological recordings.

To study the functional role of glucocorticoid receptors (GRs) in AD, we crossed the GR<sup>lox/lox</sup> with the Tg2576 to produce **GR<sup>lox/lox</sup> Tg<sup>+</sup>** mice. As mentioned above, the Tg2576 mice were bred on Bl6/SJL background and hence it was necessary to bring the GR<sup>lox/lox</sup> on the same background before starting the cross. Multiple crossings were required to finally generate the GR<sup>lox/lox</sup> Tg<sup>+</sup> mice with their controls GR<sup>lox/lox</sup> Tg<sup>-</sup> mice. The details of the cross will be explained in the results section of Chapter 2.

One, 2 and 3-month old mice were used for estimation of plasma CORT levels and exacerbated LTD phenotype was verified on 3-month old mice. 2-month old mice were stereotaxically injected with control eGFP or Cre-GFP virus. After 4 weeks of recovery period, electrophysiological recordings were carried out. Hippocampal sections of eGFP and Cre-GFP injection in GR<sup>lox/lox</sup> Tg<sup>-</sup> mice were used for GR immunofluorescence.

**C57Bl/6**, 2-month old C57Bl/6 mice (Janvier, France) were used for *ex-vivo* electrophysiological recordings and for *in-vivo* local injections followed by the Novel Object Recognition (NOR) behavioral task.

**Swiss mice**, 3-4 weeks old Swiss mice (Janvier, France) were used to test for CHO medium enriched in A $\eta$ - $\alpha$  or A $\eta$ - $\beta$  peptides purified by size exclusion chromatography (SEC fractions) by our collaborators (for details see (Willem et al., 2015)).

All experiments were done according to policies on the care and use of laboratory animals of European Communities Council Directive (2010/63). The protocols were approved by the French Research Ministry following evaluation by a specialized ethics committee (protocol number 01141.01). The animals were housed under controlled laboratory conditions with a 12-h dark light cycle and a temperature of  $22 \pm 2^\circ\text{C}$ . Mice had free access to standard rodent diet and tap water.

---

## 4.2 Genotyping

DNA samples were prepared from tail tips or fingers of less than post-natal day 8 (PND8) of individual mice. Each tail tip or finger was placed in Lysis buffer (50mM Tris HCL pH 8, 100mM EDTA pH 8, 100mM NaCL, 1% SDS) with proteinase K at 1 mg/ml. The samples were digested overnight at  $56^\circ\text{C}$ . They were centrifuged at  $15,000 \times g$  for 10 minutes to remove debris and the supernatant was transferred to new eppendorfs. Saturated NaCL was added to lyse the cells and access the genomic DNA. This was incubated for 10 minutes on a rocking platform and then centrifuged at  $15,000 \times g$  at  $4^\circ\text{C}$  for 10 minutes to get rid of cell debris. The supernatant was aspirated into a new tube and equal volume of iso-propanol was added to precipitate the DNA. After centrifugation, the pellet was washed in 70% EtOH. The pellet was air dried and then suspended in 200 $\mu\text{l}$  TE (10mM Tris HCl pH 7.5, 1mM EDTA pH 8.0) and left overnight at  $4^\circ\text{C}$ . For the PCR reaction, 1 $\mu\text{l}$  of diluted DNA was added to Master mix (25 $\mu\text{l}$ ). Oligonucleotide primers (5'-3') and PCR conditions for hAPPswe transgene and GR loxp DNA sequence are described briefly below. The list of primers used are provided in Table 3.

Table 3: Primer list for APP transgene and GRloxP PCR

| Primers          | Sequence                               |
|------------------|--|
| APP 1503         | CTG ACC ACT CGA CCA GGT TCT GGG T      |
| APP 1502         | GTG GAT AAC CCC TCC CCC AGC CTA GAC CA |
| Myosine sens     | CCA AGT TGG TGT CAAAAG CC              |
| Myosine antisens | CTC TCT GCT TTA AGG AGT CAG            |
| GR12             | CAT GCT GCT AGG CAA ATG ATC TTA C      |
| GR15             | CTT CCA CTG CTC TTT TAAAGAAGA C        |
| GR30             | GAA TGA GAA TGG CCA TGT ACT AC         |

For **APP transgene** amplification, detection of Myosin was used as an internal DNA control along with transgene positive and negative samples for controls. In addition to the primers, Buffer 5x with MgCl<sub>2</sub>, dNTPs and Taq polymerase were added to the master mix. PCR was performed on Biometra Personal Thermocycler by denaturing DNA at 96°C for 15 minutes, followed by 30 cycles of amplification: 95°C for 45 seconds, 55°C for 1 minute, 72°C for 1 minute and a final extension step at 72°C for 5 minutes. PCR samples were stored at 4°C until run on a gel.

Similarly, for **GR loxp** DNA amplification, the controls used were wildtype (GR<sup>+/+</sup>), heterozygous (GR<sup>lox/+</sup>) and homozygous (GR<sup>lox/lox</sup>). The PCR conditions were as follows, 95°C for 5 minutes, 35 cycles of amplification: 95°C for 5 minutes, 60°C for 45 seconds, 72°C for 1 minute and final extension at 72°C for 5 minutes. PCR samples were stored at 4°C until run on gel.

Following amplification, 10µl of PCR products were run on a 2% agarose gel for Tg2576 and 1.5% for GR loxp gene and staining with Ethidium bromide. Bands were photographed under UV light with a Syngene Camera (Figure 24).

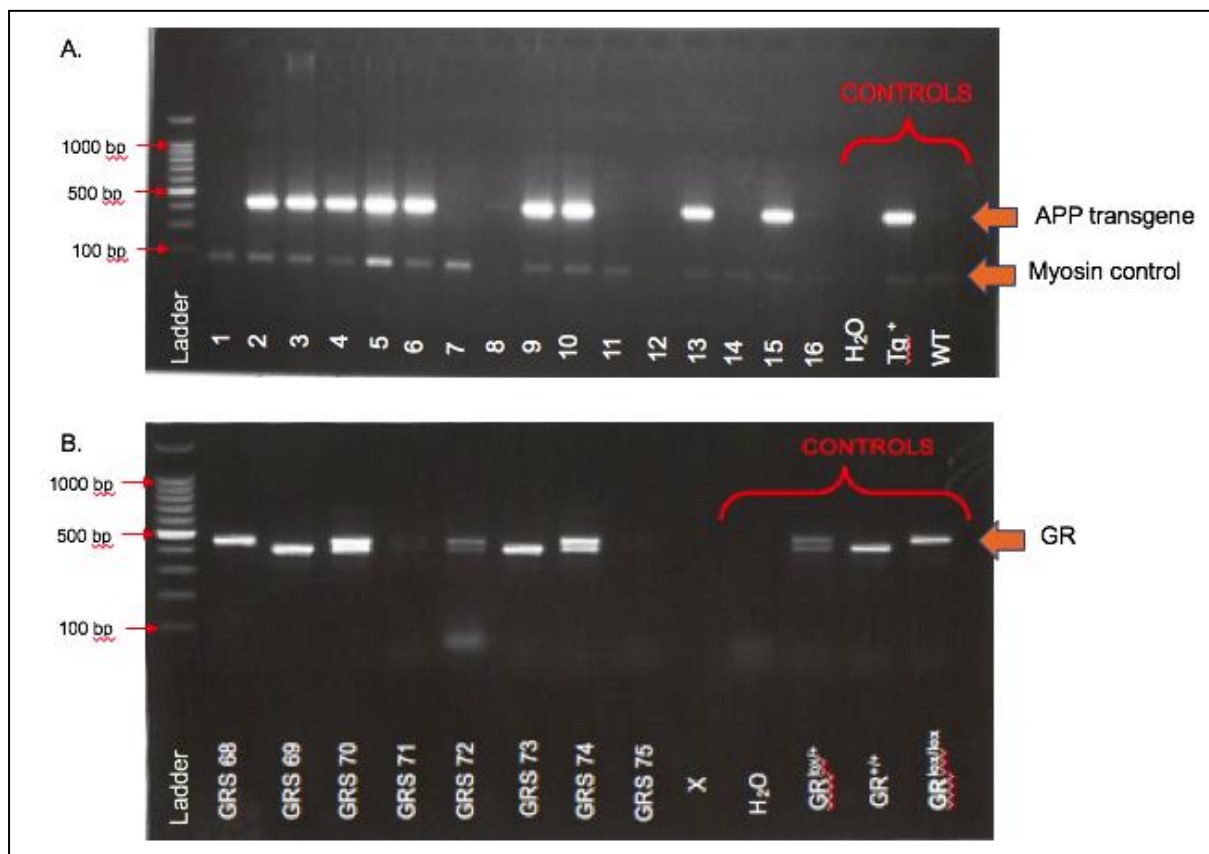


Figure 24: Gel picture of PCR bands after amplification. A) The absence or presence of the APP transgene marking the animal as WT or Tg<sup>+</sup>. Positive, negative and water control was run along with the samples. Myosin band was detected as an internal DNA control. B) Animals were identified as wildtype (GR<sup>+/+</sup>), heterozygous (GR<sup>+/-</sup>) or homozygous (GR<sup>lox/lox</sup>) depending on the number and position of the bands. Positive, negative and water control were run simultaneously.

### 4.3 Dissection of hippocampus, thymus and adrenal glands

Four and 6-month old WT and Tg<sup>+</sup> mice were sacrificed by decapitation. The brains were quickly collected on ice and the hippocampus were dissected. These were placed in special tight locked eppendorfs which were snap frozen in liquid nitrogen followed by storage at -80°C until proteins were extracted.

Adrenal glands and thymus were dissected, cleaned and weighed as general indices of HPA axis tone. For the dissection of the adrenal glands, it was important to remove the fat attached to the glands and this was done under a dissecting microscope. Care was taken not to let the glands burst or dry. These weights were normalized to the body weights which differed between the transgenic and wildtype mice. The weights inter-group were pooled and represented in mg/g ± S.E.M.

---

## 4.4 Biochemical Techniques

### 4.4.1 Estimation by ELISA

#### 4.4.1.1 *Plasma corticosterone*

To determine plasma corticosterone levels, blood samples were collected from WT, Tg<sup>+</sup>, GR<sup>lox/lox</sup> Tg<sup>-</sup>, GR<sup>lox/lox</sup> Tg<sup>+</sup> mice at different ages during the dark phase (8 pm). Sub-mandibular blood collection was carried out using microvettes, which are coated with Lithium Heparin. After 15 minutes of centrifugation at 1700 X g at 4°C, plasma samples were stored at -80°C. Plasma corticosterone concentrations were measured using an Enzyme Immunoassay (EIA) kit following the manufactures instructions (Enzo Life Science, France). Samples were diluted 20 times to fit into the standard graph. The concentration of CORT was represented in ng/ml ±S.E.M.

#### 4.4.1.2 *ACTH estimation*

Similarly, for ACTH estimation, sub-mandibular blood collection was done from 4 and 6-month old WT and Tg<sup>+</sup> mice. Undiluted samples and standards were deposited in duplicate on a 96 well plate with the competitor and incubated at 37°C for 1 hour. After washing and 30 minutes incubation with the enzyme horseradish peroxidase (HRP), TMB enzyme substrate was added. The colorimetric reaction was stopped using the stop solution and then read at 450nm. ACTH was measured in pg/ml ±S.E.M.

### 4.4.2 Extraction of total proteins from hippocampus

For extraction of **total proteins**, hippocampus tissue was lysed in cold buffer containing 20mM HEPES, 0.15mM NaCl, 1% Triton-X100, 1% deoxycholic acid, 1%SDS, pH 7.4 including phosphatases and protease inhibitors. This was done using a 1ml insulin syringe and care was taken not to introduce many air bubbles. Samples were left at 4°C on the rotor for 2 hours and later centrifuged at 1000 X g for 15 minutes. The supernatant was used to estimate the amount of protein using Bradford's reagent and BSA as the standard control. The samples were stored at -20°C.

### 4.4.3 Immunoblotting

Lysates were re-suspended in loading buffer (50% Sucrose, 6% SDS, 0.18% bromophenol blue, 12.5%  $\beta$ -mercaptoethanol) and were boiled at 90°C for 5 minutes. Equal amount of proteins (50 $\mu$ g for total hippocampal proteins and 5-10  $\mu$ g for PSD) were resolved on 10% SDS gel in denaturing conditions. Since PVDF (polyvinylidene difluoride, Millipore, France) membrane is hydrophobic in nature it needs to be activated by soaking for few seconds in 100% ethanol. Thereafter, transfer of proteins was carried out for 1 hour at 350 mA at 4°C. Blocking of the membrane proteins was carried out with Tris-buffered saline (10mM Tris, 150mM NaCl, pH 7.4) containing 0.01% Tween-20, 5% non-fat milk for 20-30 minutes at room temperature. For GR in particular, membranes were incubated at 4°C with primary antibody against GR (1:1000 dilution, Santa Cruz Biotechnology, anti rabbit) in 1% non-fat milk. HRP-conjugated secondary antibody (1:30,000 rabbit, Sigma) with 5% non-fat milk was incubated for 1 hour at room temperature. Specific proteins were visualized using enhanced chemiluminescence ECL detection system (Biorad, France). The relative levels of immunoreactivity were determined using the LAS-3000 imaging system (Fuji, Japan) and quantified by densitometry using ImageJ software. Similarly, immunoblotting was carried out for other proteins (See Table 4 for details).

Table 4: Details of primary and secondary antibodies used for immunoblotting with their respective conditions.

| Primary Antibody         | Company                  | Concentration | non-fat milk |
|--------------------------|--------------------------|---------------|--------------|
| rabbit anti-GR           | Santa Cruz Biotechnology | 1:1000        | 1%           |
| mouse anti-Actin         | Sigma-Aldrich            | 1:2000        | -            |
| rabbit anti-PSD95        | Millipore                | 1:1000        | -            |
| mouse anti-synaptophysin | Millipore                | 1:2000        | -            |
|                          |                          |               |              |
| Secondary Antibody       | Company                  | Concentration | non-fat milk |
| Goat anti-Rabbit IgG     | Jackson Immunoresearch   | 1:30000       | 5%           |
| Goat anti-mouse IgG      | Beckman Coulter          | 1:5000        | 1%           |

### 4.4.4 A $\beta$ oligomer (oA $\beta$ ) preparation

Recombinant A $\beta$ <sub>1-42</sub> peptide (Bachem, Bubendorf, Switzerland) was re-suspended in 1,1,1,3,3,3-hexafluoro-2-propanol (HFIP) to 1 mM until complete re-suspension as described in (Stine et al., 2003). This was quickly aliquoted into smaller volumes in cold room followed

by vaporisation to dry state under the hood. These aliquots were stored at -80 °C. A $\beta$  oligomers (oA $\beta$ ) were prepared from these aliquots by diluting A $\beta$  to 1 mM in DMSO then to 100  $\mu$ M in ice-cold HEPES and Bicarbonate-buffered saline solution (HBBSS) with immediate vortexing and bath sonication followed by incubation at 4°C for 24 h with mild agitation. Final concentration used was 100nM for electrophysiology, biochemical assays and behaviour. 1 $\mu$ l of 100  $\mu$ M oA $\beta$  were run on 10% SDS gel (as explained above) to verify their profiles. The primary antibody used was Beta-amyloid (1:1000, D54D2 rabbit monoclonal ab, Cell Signaling). The oA $\beta$  contained mainly monomers, dimers, trimers and tetramers (Figure 25).

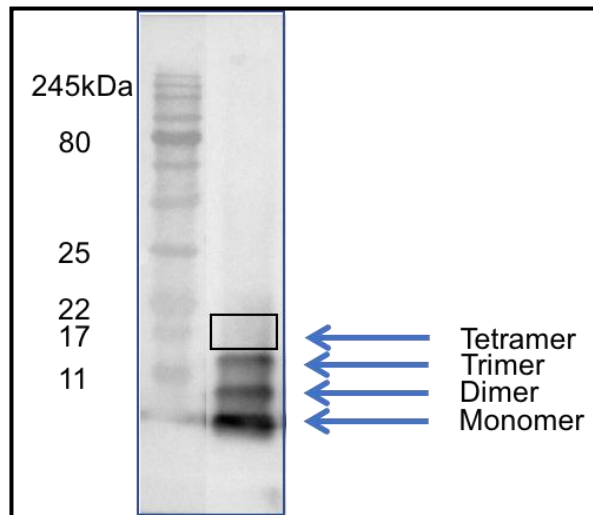


Figure 25: Profile of the synthetic oA $\beta$  preparation. 1 $\mu$ l of 100 $\mu$ M stock was run on a 10%SDS gel displaying low weight oligomers consisting of monomers, dimers, trimers, few tetramers of synthetic oA $\beta$  preparation.

## 4.5 Local *in vivo* ablation of GR in $GR^{lox/lox}$ mice

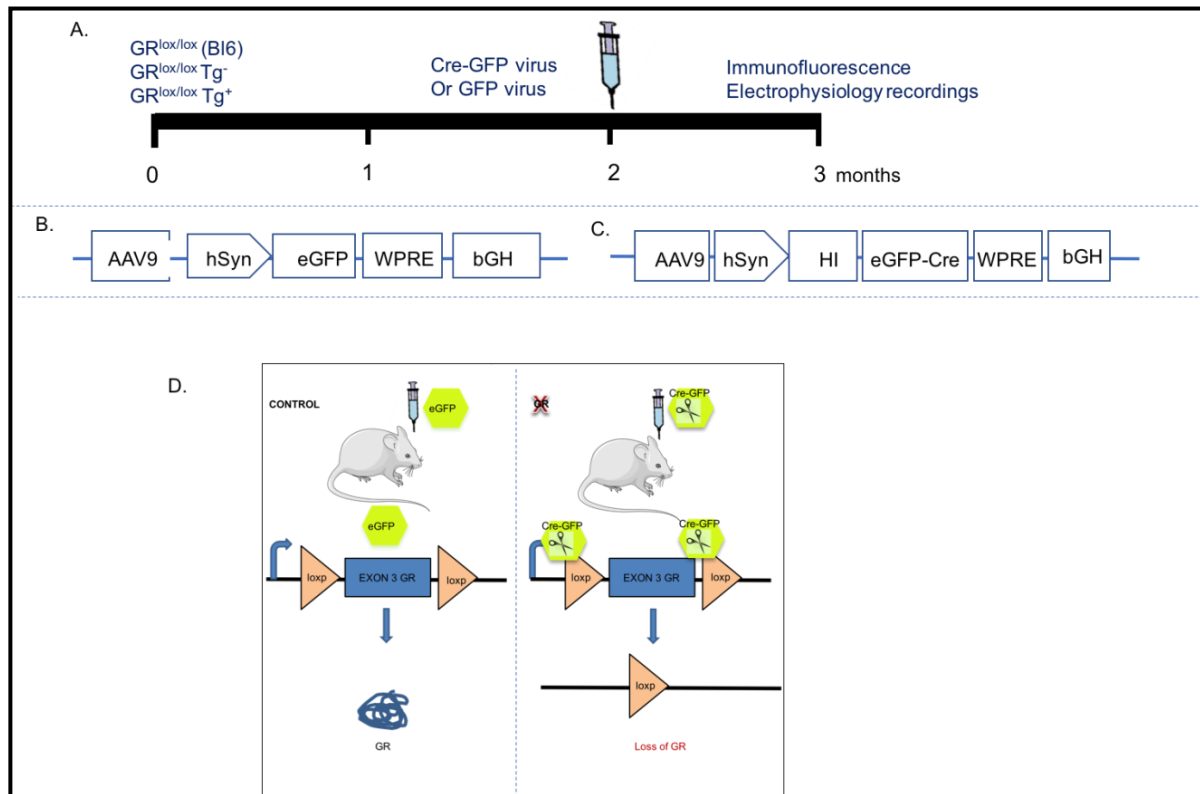


Figure 26: Summary of the protocol for the Cre-GFP injections in the  $GR^{lox/lox}$  mice. A) Timeline of the  $GR^{lox/lox}$  mice showing stereotaxic injections of eGFP or Cre-GFP virus in the CA1 of the hippocampus at 2 months of age. This was followed by 4 weeks of recovery time for complete expression of Cre recombinase and ablation of GR before performing immunofluorescence staining and electrophysiological recordings. B). Vector map of the eGFP control virus wherein Adeno-associated virus serotype 9 (AAV9) was used under human synapsin promoter (hSyn). To enhance the expression, woodchuck hepatitis virus posttranscriptional regulatory element (WPRE) was introduced and bGH bovine growth hormone as a terminator (Penn Vector Core Facility, USA). C). Vector map of the Cre-GFP virus (Penn Vector Core Facility, USA) indicating production of Cre recombinase and GFP as a fused protein specifically in neurons as under hSyn. D). Pictorial representation of the working of the Cre-lox system showing loss of GR.

### 4.5.1 Stereotaxic injections of AAV

We used 8-9 weeks old  $GR^{lox/lox} Tg^-$ ,  $GR^{lox/lox} Tg^+$  and  $GR^{lox/lox}$  mutants in C57Bl6 background for stereotaxic injections. AAV9.hSyn.HI.eGFP-Cre.WPRE.SV40 (called herein CreGFP virus) or AAV9.hSyn.eGFP.WPRE.bGH as the control virus (called herein eGFP virus) (Figure 26B and C) (ordered from Penn Vector Core Facility, USA) were injected into the CA1 region of the hippocampus by stereotaxic injections (see summary of protocol in Figure 4). AAV9 serotype with hSyn promoter was specifically chosen to ensure expression of virus in the neurons (Aschauer et al., 2013). Before surgery, mice were assigned to the 4

different groups: eGFP injected  $GR^{lox/lox} Tg^+$  or  $GR^{lox/lox} Tg^-$  and Cre-GFP injected  $GR^{lox/lox} Tg^+$  or  $GR^{lox/lox} Tg^-$ . Mice were anesthetized with chloral hydrate 400mg/kg (Restivo et al., 2009). Use of this anaesthetic was necessary particularly for the  $GR^{lox/lox} Tg^+$  mice as they would get seizures if ketamine-xylazine was injected. The mice were placed in stereotaxic frame well fixed between the ear bars. The scalp was incised and retracted and with a scalpel blade the skull was scraped to see the bregma clearly. Cannula was placed at the Bregma to calculate the co-ordinates for the CA1 area of the hippocampus. Holes were drilled through the skull above the hippocampus. A stainless steel cannula (0.1mm in diameter) was inserted bilaterally while infusing at a speed of 250nl/min until it reached the CA1 stereotaxic coordinates. 500nl of virus ( $\sim 5.54 \times 10^{11}$  genome copy/ml in PBS without  $Mg^{2+}$ ) was injected in the CA1 (A/P: -2.2 M/L:  $\pm 1.3$  D/V: -1.5) at 100nl/min. Mice were placed on a warm pad while they recovered from the surgery and later returned to their home cages. These virus-injected mice were given a recovery time of 4 weeks for complete cre recombinase expression followed by immunofluorescence staining of GR or electrophysiology recordings.

#### **4.5.2 Immunofluorescence staining of GR**

For immunostaining of GR, the protocol was adapted from (Barik et al., 2013). Mice were deeply anaesthetized with 400mg/kg chloral hydrate or 436.8mg/kg of pentobarbital (Centravet, France) and transcardially perfused with cold phosphate buffer (PB: 0.1 M  $Na_2HPO_4/NaH_2PO_4$ , pH 7.4), followed by 4% PFA in PB. Brains were post-fixed overnight in 4% PFA-PB. Free-floating vibratome sections (50  $\mu m$ ) were rinsed twice with PBS (20 min) and incubated (30 min) in PBS-BT (PBS 0.5% BSA, 0.1% Triton X-100) with 10% normal goat serum (NGS). Sections were incubated (4°C) in PBS-BT, 1% NGS, with rabbit anti-GR (1:500, Santa Cruz Biotechnology, Santa Cruz, USA) over 2 nights. Sections were rinsed in PBS and incubated (2 h) in Cy3-conjugated goat anti-rabbit antibody (1:2000, Vector Laboratories, Burlingame, USA). Sections were rinsed and incubated 5 min in DAPI to counterstain nuclei. These were then mounted for examination under Olympus Confocal microscope.

### 4.5.3 Microscopy and estimation of GR intensity

eGFP and Cre-GFP infected CA1 cells of the hippocampus were z scanned at 60x zoom 3 magnification under eGFP, cy3 and dapi lazer. Using Image J and CTCF (corrected total cell fluorescence) method (McCloy et al., 2014), the GR intensity per cell was calculated in GFP positive and nearby negative cells in both GFP and Cre-GFP virus infected sections. From each section, first GFP positive and negative cells were identified, stacked and selected. In addition, a small background area was defined near the cells. For all these regions, the area, integrated density and mean gray value were measured in the cy3 filter. Further, to calculate the corrected total cell fluorescence the following formula was used:

**CTCF= (Integrated density) – (Area of selected cell x Mean fluorescence of background readings)**

This value was considered as the relative value of the GR intensity per cell.

---

## 4.6 Electrophysiology

### 4.6.1 Slice preparation

Hippocampal slices were prepared as described in (Marchetti et al., 2010). Slices (350 or 400  $\mu$ m for field recordings) were cut in ice-cold oxygenated (95% O<sub>2</sub>/ 5%CO<sub>2</sub>) solution containing (in mM): Sucrose 234, KCl 2.5, NaH<sub>2</sub>PO<sub>4</sub> 1.25, MgSO<sub>4</sub> 10, CaCL<sub>2</sub> 0.5, NaHCO<sub>3</sub> 26, glucose 11 (pH 7.4). For recovery, slices were then incubated for one hour in warm (37 $\pm$  1  $^{\circ}$ C) oxygenated standard artificial cerebrospinal fluid (ACSF) containing (in mM): NaCl 119, KCl 2.5, NaH<sub>2</sub>PO<sub>4</sub> 1.25, MgSO<sub>4</sub> 1.3, CaCL<sub>2</sub> 2.5, NaHCO<sub>3</sub> 26, glucose 11 and then stored at room temperature.

Slices were visualized in a chamber on an upright microscope (Slicescope, Scientifica Ltd) with IR-DIC illumination and were perfused with oxygenated ACSF.

## 4.6.2 Field recordings by electrophysiology

Field excitatory post-synaptic potentials (fEPSPs) were recorded in the stratum radiatum of the CA1 region (using a glass electrode filled with 1M NaCl and 10mM HEPES, pH 7.4) and the stimuli were delivered at to the Schaffer collateral pathway by a monopolar glass electrode filled with ACSF (Figure 27).

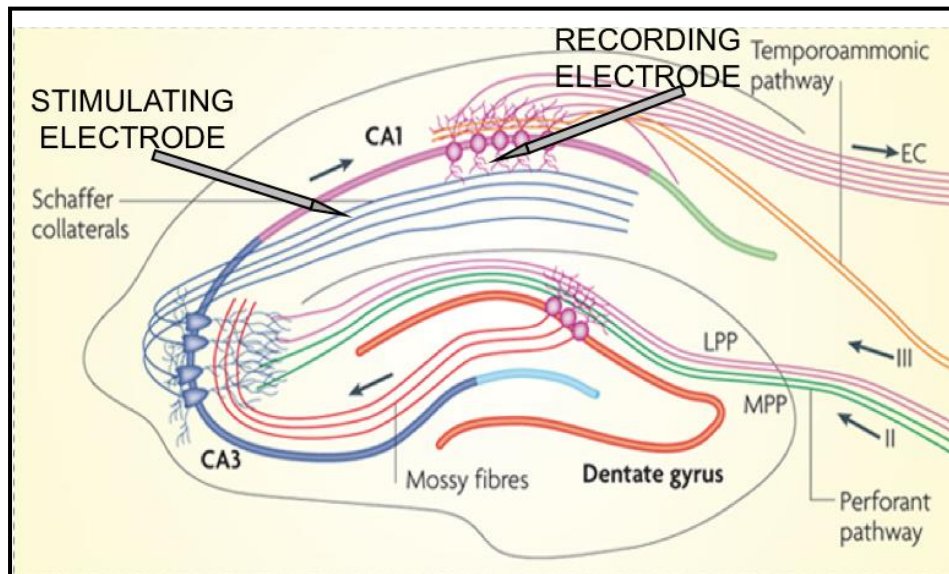


Figure 27: Cross section of the hippocampus showing the synapses formed between the different sub-structures of the hippocampus: CA1, CA3 and DG. fEPSP recordings were carried out by stimulating the Schaffer collaterals and recording within the CA1 neurons area (modified from (Deng et al., 2010)).

To check the health of the sections, the sections were highly stimulated to evoke strong fEPSP response (ideally between 0.8- 1 mV). Then for LTP recordings, fEPSP response was set to approximately 30% of the maximal fEPSP response (i.e. approx. 0.2-0.3mV).

### 4.6.2.1 To measure basal synaptic plasticity

For LTP, a minimum of 20 minutes stable baseline of fEPSP response was first obtained followed by an induction of a high frequency stimulation (HFS) protocol consisting of 2 pulses at 100 Hertz for 1 sec with a 20 sec interval between pulses. fEPSP response was further recorded for one hour.

For LTD experiments, ACSF containing 4mM  $\text{MgCl}_2$  and 2mM  $\text{MgSO}_4$  (otherwise identical to standard ACSF described above) was used during recording. fEPSP recordings were

carried out as explained for LTP with the only difference being the LFS LTD protocol, which consisted of 900 pulses at 1 Hertz.

#### 4.6.2.2 For pharmacological studies

To measure basal synaptic transmission, fEPSPs were recorded in standard ACSF to obtain a 20 minutes baseline followed by another 20 minutes of bath application of ACSF containing drug (1  $\mu$ M GR antagonist compound 13 (C13) (for properties see Table 5) or 0.1 % DMSO vehicle) or 100 nM oA $\beta$ . The ACSF/drug/oligomers were in re-circulation with a peristaltic pump while being continuously aerated with 95% oxygen. For all pharmacological studies, the electrodes were placed superficially to maximize exposure to drug or peptides.

Table 5: Properties of Compound 13 (C13) as described in (Hunt et al., 2015)

| Compound 13         | Assay                             | Properties       |
|---------------------|-----------------------------------|------------------|
| GR Binding $K_i$    | fluorescence polarization assay   | 0.29 nM          |
| GR antagonism $K_i$ | human HepG2 cells-TAT assay       | 19 nM            |
| GR antagonism $K_i$ | rat H4-II-EC4 cells- TAT assay    | 6.1 nM           |
| PR Binding          | radio-ligand binding assay        | 6% @ 10 $\mu$ M  |
| AR Binding          | radio-ligand binding assay        | 17% @ 10 $\mu$ M |
| ER Binding          | radio-ligand binding assay        | 27% @ 10 $\mu$ M |
| Selectivity for MR  | protein-protein Interaction assay | 0% @ 10 $\mu$ M  |
| Selectivity for GR  | protein-protein Interaction assay | $K_i$ = 51nM     |

#### To study the effect of C13 and A $\beta$ oligomers (oA $\beta$ ) on LTP:

To check the effect of the GR antagonist C13 on LTP, fEPSPs were recorded to reach a stable 20 minutes baseline in 15 ml of 1 $\mu$ M GR antagonist or 0.1% DMSO. Once achieved, HFS protocol (as explained above) was applied and responses 1 hour post induction were recorded.

To check the effect of the oA $\beta$  on LTP (Figure 28), sections were first recorded for a 20 min stable baseline in 15 ml of 0.1% DMSO followed by 20 minute of recordings in 15 ml of 0.1 % DMSO + 100nM oA $\beta$ . Once this was achieved, a HFS protocol was induced. Similarly, to check the effect of the GR antagonist and oA $\beta$ , 20 minutes baseline was recorded with 15 ml of 1 $\mu$ M C13 followed by 15 ml of 1 $\mu$ M C13 + 100nM oA $\beta$  and then HFS was induced.

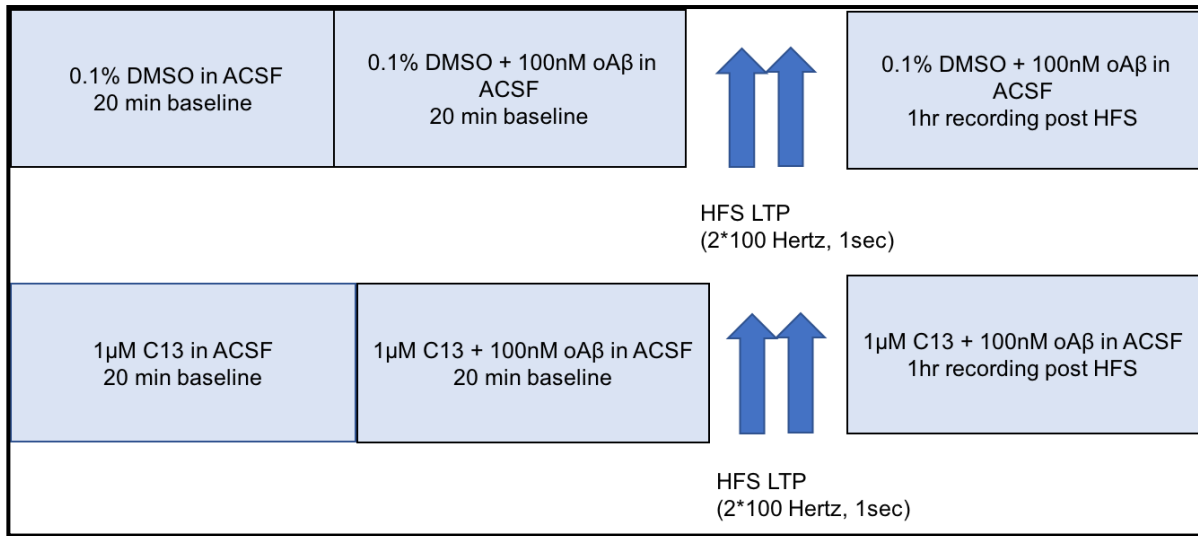


Figure 28: Timeline used to check the preventive action of the GR Antagonist C13 on oA $\beta$  –mediated effect on LTP.

### 4.6.3 Analysis of fEPSP response:

For the analysis of fEPSPs, the first third of the fEPSP slope was calculated (see Figure 29) in baseline condition (20 minutes prior to induction protocol delivery) and for 60 minutes post-induction. The average baseline value was normalized to 100% and all values of the experiment were normalized to this baseline average (one minute bins). Experiments were pooled per condition and presented as mean  $\pm$  S.E.M. Statistical analysis was used to compare the 20 minutes of baseline with the last 15 minutes of the recordings. Data analysis was performed with the clamp fit software (Molecular Devices).

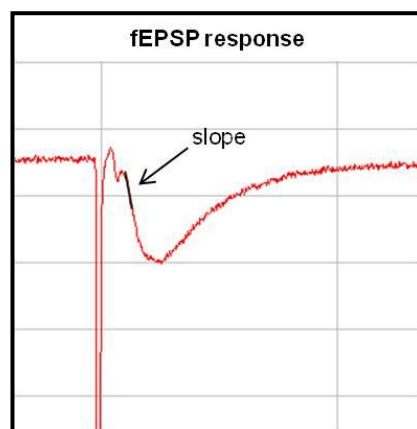


Figure 29: Representative fEPSP response in clamp fit software. The slope is marked as the first third of fEPSP response.

---

## 4.7 Behaviour

### 4.7.1 Episodic-like object recognition memory

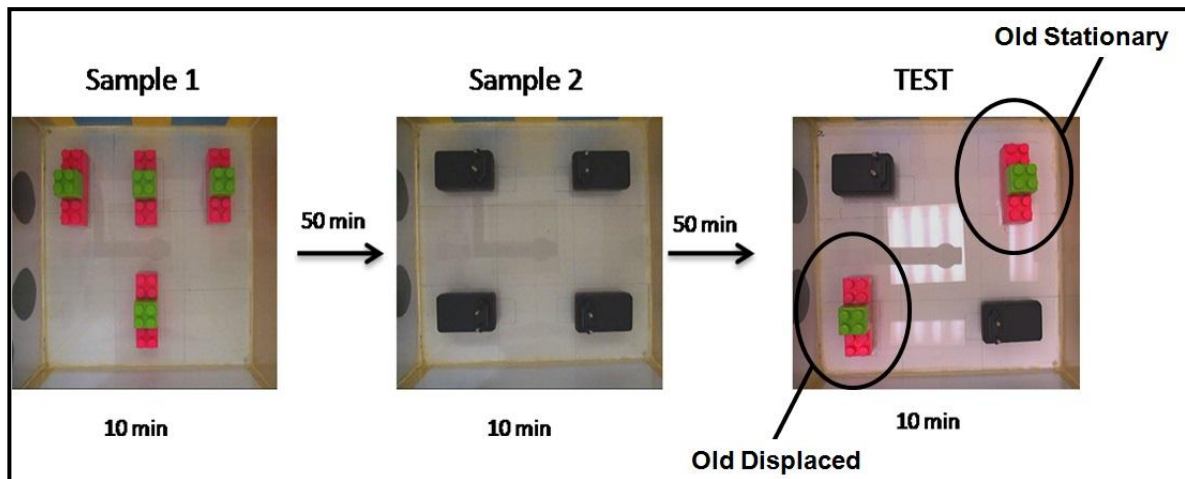


Figure 30: Scheme for What-When-Where object recognition protocol. The test day consisted of a three trial procedure (two sample trials and a test trial of 10 min each with 50 min inter-trial interval).

Episodic-like object recognition memory was performed as described in (Dere et al., 2005) with minor variations to minimize the stress levels. This task is based on the paradigm that episodic memory is the memory of personal experiences and specific events including what happened ('What' component), location ('When' component), and time ('When' component). Object exploration was assessed in a clear perspex open-field with wall-covered cues (30x30x30cm). A set of 4 identical black charger plugs and a set of 4 identical plastic pink and green legos were used for this paradigm (See Figure 30). For the habituation, two different objects were used to familiarize animals to objects inside the arena.

The **protocol** was as follows: After 3 days of handling, animals were familiarized to the apparatus during four consecutive days. During this habituation, animals were exposed for 5 min per day to the open field without objects for the first two days, followed by two days where mice were subjected to two objects in the box for 3 daily sessions of 10 min with 50 min inter-trial interval (ITI). For the test day, the mice were introduced to three trial procedure (two sample trials and a test trial of 10 mins each, with 50 mins ITI). During Sample 1, mice were exposed to four identical novel objects (coloured legos) in a triangle configuration. Following a delay of 50 mins, mice were then introduced to Sample 2, where

four new identical objects (adaptor plugs, which are of different colour, shape and texture from the previous object) were placed in a square arrangement. After a 50 minutes ITI delay, mice were submitted to the test trial. In this, two 'old' (coloured legos) and two, 'recent' (black adaptor plugs) were presented from the previous trials. One of the 'old' objects was spatially displaced (object displaced) during the test trial, whereas one 'old' (stationary) and the two 'recent' objects were presented at the same location at which they were already encountered during sample trials. The exploration time was measured for each object during this test trial. It is defined as the time spent actively sniffing or interacting with the object at a distance no greater than 2 cm.

**Analysis:** Using these test trial exploration data, we estimated three components of episodic-like memory:

**What** = (exploration time (ET) 'olds' - ET 'recents')/(ET 'olds' + ET 'recents')

**When** = (ET 'old stationary' - ET 'recents')/(ET 'old stationary' + ET 'recents')

**Where** = (ET 'old displaced' - ET 'old stationary')/(ET 'old displaced' + ET 'old stationary').

A positive discrimination ratio represents a good memory, whereas a negative ratio indicates memory impairment.

For the RU486 treatment, 40mg/kg was dissolved in water containing a droplet of Tween-20 and injected twice daily subcutaneously for 4 days and once on the 5<sup>th</sup> day, one hour before performing the behaviour paradigm. The appropriate vehicle solution (H<sub>2</sub>O/Tween-20) was administered appropriately.

## 4.7.2 Novel Object Recognition (NOR) after local *in vivo* injections

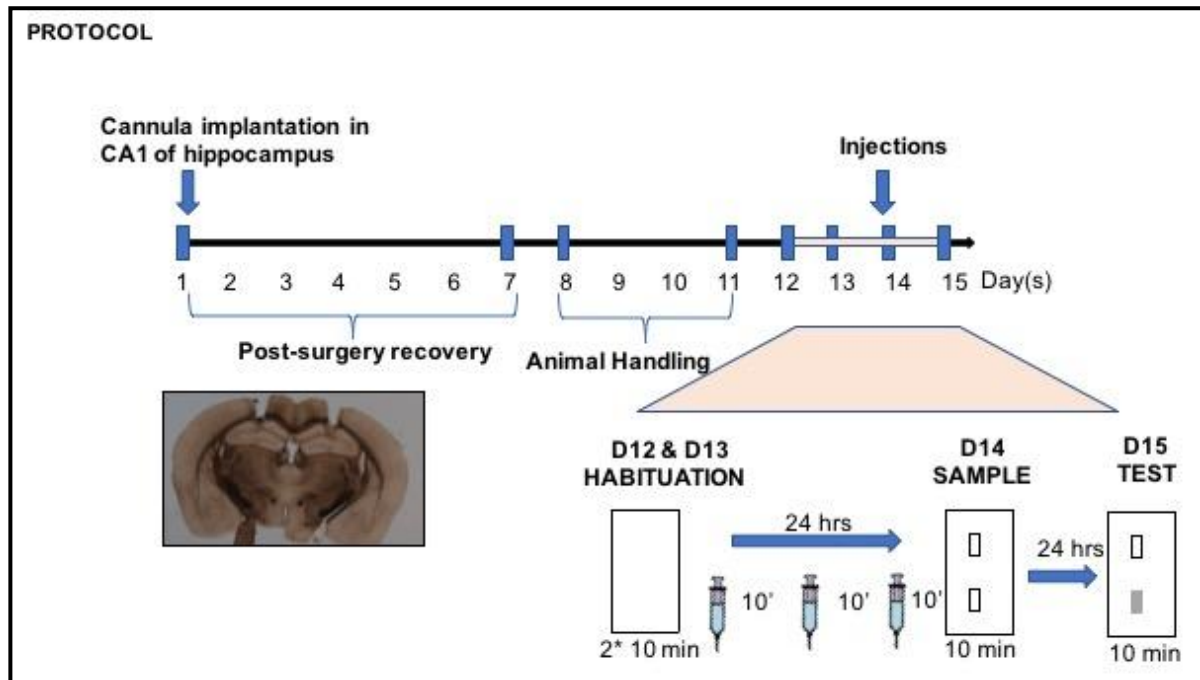


Figure 31: Scheme showing cannula implantation in the CA1 of the hippocampus for local injections of drug/peptide followed by Novel Object Recognition behaviour task.

### **Surgical procedures for cannula implantation:**

Bilateral cannulae (Bilaney Consultants, PlasticsOne) were stereotaxically implanted into the CA1 of the hippocampus (coordinates with respect to bregma: -2.2mm anteroposterior (AP),  $\pm$  1.5mm mediolateral (ML), -1.3mm dorsoventral (DV), according to Paxinos and Franklin mouse brain atlas (Paxinos and Watson, 2005) in anesthetized C57Bl/6 2-month-old mice (11.25 mg/kg of ketamine and 7.5 mg/kg of xylazine, i.p.).

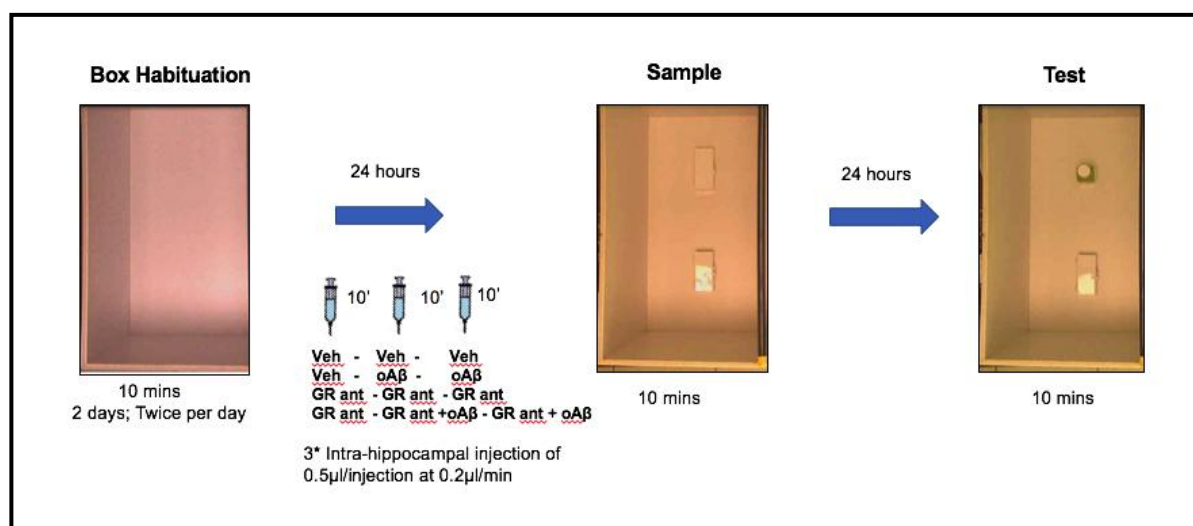


Figure 32: Scheme for Novel Object Recognition protocol. 24 hours after last box habituation, 3 intrahippocampal injections were given to the mice interspaced by 10 mins each. 10 mins after the last injection, mice were submitted to 10 mins exploration of 2 identical objects in Sample. 24 hours after, mice were exposed to 10 minutes in the test phase, where one familiar object was replaced by a novel object.

### Local injections and behaviour:

After one week of recovery, the mice were handled for 4 days followed by 2 days of box habituation, twice per day for 10 minutes in an empty open arena measuring 20X40 cm, 30cm high. The next day the mice were injected with 0.5μl volume of either vehicle (0.0004% DMSO), 100nM oAβ (0.23ng/0.5μl), 1μM GR Antagonist (C13) or 1 μM C13 +100nM oAβ. For each group, in total 3 local injections were interspaced by 10 minutes, in the order as shown in Figure 31. The rate of injection was at 0.2μl/min via cannulae PE50 tubing (Bilaney, Germany) connected to a 10μl Hamilton syringe pump system. The tubing was left in place for 3 minutes at the end of each injection, and the cannulae capped with the dummy cannulae to prevent reflux of the injected solutions.

10 minutes after the last injection the mice were placed in the same arena containing two identical objects i.e. named as Sample (Figure 32). 24 hours later, the Test phase was run as the mice are reintroduced into the arena containing two objects, one of which is presented previously (familiar) and the other which is a novel object. Exploration was recorded for 10 minutes. Analysis was carried out by an experimenter blinded to the treatment. Sniffing and nose pokes towards the objects at a distance of no more than 2 cms were scored as object investigation. Results were expressed as discrimination index (DI), i.e. (seconds spent on novel- seconds spent on familiar) / (total time spent on objects). Animals with adequate memory spent longer time exploring the novel object, hence giving a higher DI.

---

## 4.8 Statistical analysis

Statistical analysis was performed using unpaired two-tailed Student's t-test for studies involving weights, biochemical and electrophysiological experiments to probe for a difference between genotypes (WT; Tg<sup>+</sup>, GR<sup>lox/lox</sup> Tg<sup>-</sup>, GR<sup>lox/lox</sup> Tg<sup>+</sup>) or between treatments (GR antagonist versus Vehicle or Cre-GFP versus eGFP). Two-way analysis of variance (ANOVA) test was used to measure differences in GR intensity per cell in GFP positive and negative cells in eGFP and Cre-GFP virus infected sections. This test was also used for effect of treatment (vehicle, RU486) or difference in genotype (WT, Tg<sup>+</sup>) for episodic memory behaviour. For NOR test, one sample t-test was used to check the difference of sample mean from a theoretical mean (chance level). For the electrophysiological experiments involving effect of oAβ in presence of GR antagonist or reduction of GR with Cre-GFP, ANOVA test could not be carried out as its assumptions for normality and homogeneity of variances could not be fulfilled. Hence, approximative Kruskal-Wallis test was used followed by post-hoc permutation t-test analysis with False Discovery Rate (FDR) correction.

All statistical analysis was done using Prism 6 (Graph Pad). All results are expressed as mean ± S.E.M. P<0.05 was considered to be statistically significant.

## 5 Results

---

### 5.1 Chapter 1

#### 5.1.1 Aim: Study of HPA axis dysregulation in Tg2576 (Tg<sup>+</sup>) AD mouse model

The early phase of AD is characterized by hippocampus-dependent memory deficits and impaired synaptic plasticity. Strong evidence suggests that the oligomeric forms of the amyloid- $\beta$  peptide (oA $\beta$ ) are responsible for these synapse dysfunctions and subsequent memory loss (Shankar et al., 2008, Puzzo et al., 2008). However, the exact cellular mechanism contributing to onset of early synaptic failure and memory impairment in AD remains unclear. Stress is known as a major risk factor triggering AD (Rothman and Mattson, 2010). In presence of a stressful stimulus, the HPA axis is triggered and releases CORT which further binds to glucocorticoid receptor (GR). There has been multiple evidence implicating HPA axis dysfunction in AD, reflected by markedly elevated basal levels of circulating cortisol in human patients and mouse models (Näsman et al., 1995, Swanwick et al., 1998, Csernansky et al., 2006, Hebda-Bauer et al., 2013, Lanté et al., 2015). Interestingly, the HPA axis dysfunction only seemed relevant in the early stages of Alzheimer's disease (Swanwick et al., 1998) as it did not worsen with additional cognitive decline. Hence, in the first aim we focussed in detail on the relationship between HPA axis dysregulation and early onset of AD using the Tg2576 mice.

We used the Tg2576 (Hsiao et al., 1996), which is a good mouse model to study the early onset of AD with relation to the amyloid- $\beta$  protein accumulation. This is because at 3-month age there is high presence of different soluble oligomers (Mustafiz et al., 2011) and absence of tau phosphorylation. My team had previously characterized the onset of memory loss starting at 3 months of age in this mouse model (Figure 33) (D'Amelio et al., 2011). At the 4 month of age time point, my team had observed high levels of CORT and a non-functional negative feedback mechanism as shown by the Dex suppression test indicating a dysregulated HPA axis (detailed in Lanté et al. 2015). This helped us link the neuroendocrinological dysfunction in this early symptomatic AD mouse model. Onset and progression of this dysregulation of the HPA axis had however not been investigated in this model.

To answer this, we measured CORT levels at 3 months in the Tg<sup>+</sup> mice, to verify if the HPA axis dysregulation had already been triggered at this earlier time point and later at 6 months to check if CORT alterations persisted at this more advanced stage of pathology. Further, we estimated ACTH levels at 4 and 6 months in the Tg<sup>+</sup> mice. Analysis of ACTH levels were warranted as there was evidence of an absence of increased ACTH drive despite the high cortisol levels in AD patients (Umegaki et al., 2000).

High CORT levels are known to have an effect on peripheral organs like thymus, hence we were interested to check thymus weights in the Tg<sup>+</sup> mice at 4 and 6 months of age. In addition, we checked for adrenal glands weights at these time points to correlate it to the chronic over production of CORT in the Tg<sup>+</sup> mice. GRs are highly expressed in the hippocampus and negatively regulate the HPA axis (Herman and Cullinan, 1997, Jacobson and Sapolsky, 1991, Herman et al., 2005). Additionally, the hippocampus being a key structure involved in memory formation, it develops substantial AD neuropathology in the early stage of the disease (Braak and Braak, 1991, Thal et al., 2002b). Hence, we also estimated the GR protein level in the hippocampus of 4 month Tg<sup>+</sup> mice.

Lastly, we confirmed memory deficits in the Tg<sup>+</sup> mice at this 4 months time point. My team had optimized a memory task based on recognition of objects (see material and methods section for details), which allows for probing episodic-like memory in mice. This task was chosen as it was deemed fully relevant to study AD pathology as the first clinical sign of memory loss in the disorder is generally loss of hippocampus-dependent episodic memories (deToledo-Morrell et al., 2007, Salmon and Bondi, 2009). In light of HPA axis impairment and excessive CORT levels observed in the Tg2576 mice, we questioned if these episodic-like memory deficits could be rescued using a GR antagonist.

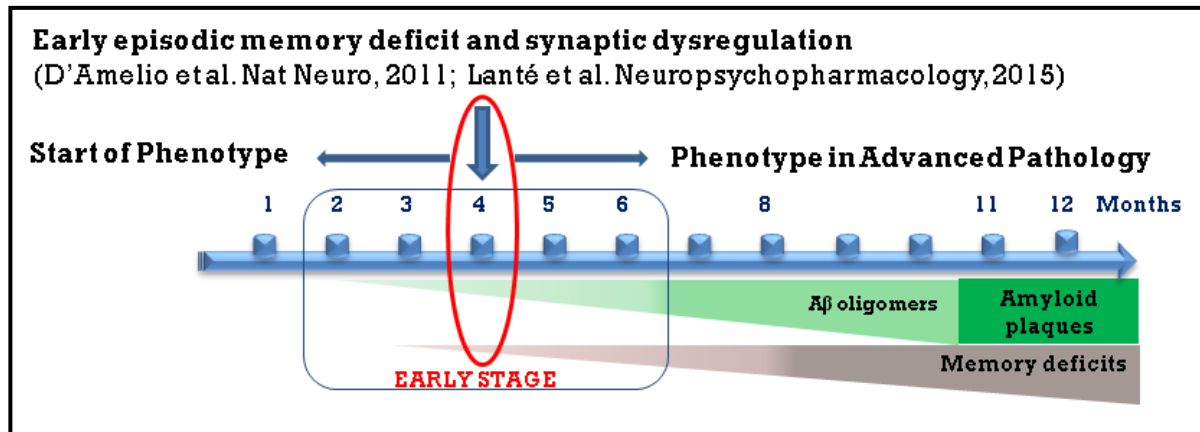


Figure 33: Timeline of Tg2576 mouse neuropathology showing gradual increase of A $\beta$  oligomers starting at the early stage (3-4 months) and developing plaques only at a later age. This is also accompanied by early memory deficits first observed at 3 months of age. In our study, we focus on the early stage of AD, particularly at 4 months as our lab has characterised high CORT levels, episodic-like memory deficit and synaptic dysregulation at this age. We also checked some phenotypes and measured organs and hormones related to HPA axis at earlier time points and at a later age with more advanced pathology.

Following up on previous results from the team, the **objectives** of this aim were as follow:

- To estimate CORT levels at 3 and 6 months in the Tg<sup>+</sup> mice
- To estimate ACTH levels at 4 and 6 months in the Tg<sup>+</sup> mice
- Global effect of HPA axis dysregulation on thymus and adrenal glands weights at 4 months age
- Effect of dysregulated HPA axis on total GRs in the hippocampus at 4 months age
- Check episodic memory test in the Tg<sup>+</sup> mice and its rescue by GR antagonist.

#### 5.1.1.1 Comparison of CORT levels in WT and Tg<sup>+</sup> male mice at 3 and 6-month of age

We demonstrated chronically elevated levels of circulating CORT in Tg<sup>+</sup> mice at 4 months, establishing an association between early onset AD and HPA axis dysregulation. This difference in CORT levels was only during the active phase (20:00) (Lanté et al., 2015). Hence, to dissect out in more detail the time point of the trigger and the extent of this dysregulation, we measured CORT levels during the active phase in 3 and 6-month old Tg<sup>+</sup> mice using ELISA method. At 3 months, there was no difference seen in the CORT levels between the WT and Tg<sup>+</sup> mice (WT: 128ng/ml  $\pm$  18,21; Tg<sup>+</sup>: 110.19 ng/ml  $\pm$  16.38; p> 0.05) Figure 34, while at 6 months, the levels of CORT were higher in the Tg<sup>+</sup> mice (WT: 152ng/ml  $\pm$  9.0; Tg<sup>+</sup>: 210.7 ng/ml  $\pm$  22.43; p< 0.05) (Figure 34). This suggests that, in this

AD mouse model, hypercortisolemia begins after 3 months and persist even at 6 months of age.

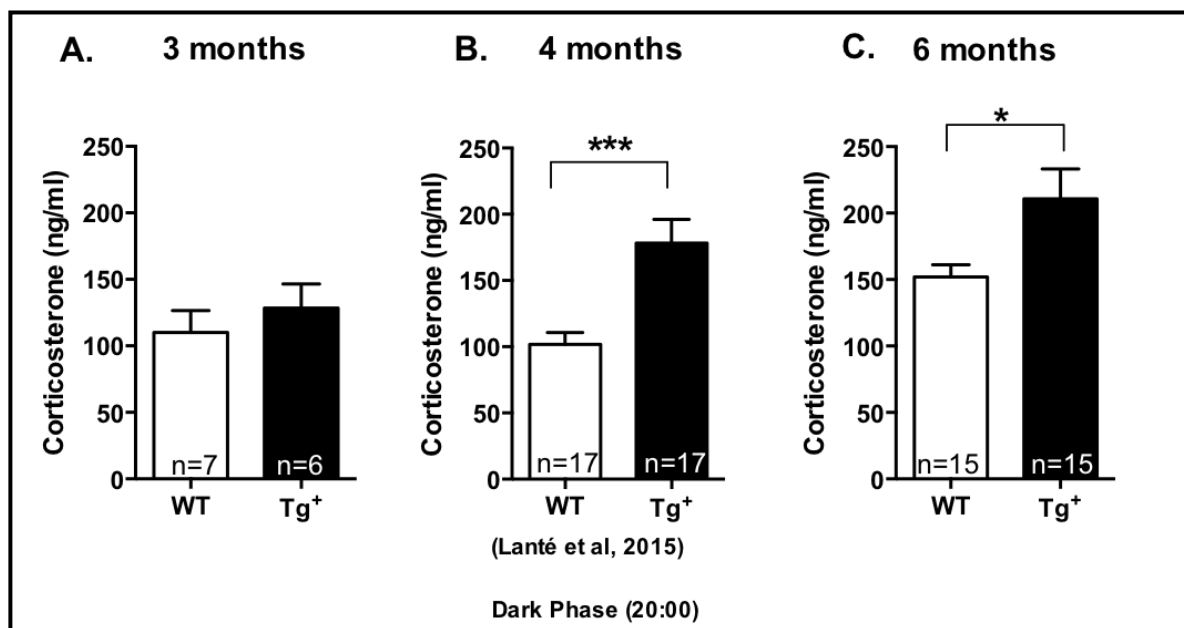


Figure 34: Comparison of plasma CORT levels in WT and Tg<sup>+</sup> mice at 3, 4 and 6 months. A) Corticosterone levels (ng/ml) were measured by ELISA at the dark phase (20:00) in 3 months WT and Tg<sup>+</sup> mice. B) Similarly CORT was measured at 4 months and C) at 6 months in WT and Tg<sup>+</sup> mice. All data plotted Mean  $\pm$  S.E.M. (\*)  $p < 0.05$ ; (\*\*\*)  $p < 0.001$ .

#### 5.1.1.2 Comparison of plasma ACTH levels in WT and Tg<sup>+</sup> male mice at 4 and 6 months

Secretion of CORT depends on the upstream secretion of ACTH by the pituitary gland. Observing excess levels of CORT at 4 and 6 months of age, we attempted to determine if this dysregulation would be related to ACTH levels. At 4 months, there was no change in plasma ACTH levels between Tg<sup>+</sup> and WT mice (WT:  $37.66 \pm 6.36$  pg/ml; Tg<sup>+</sup>:  $39.00 \pm 4.07$ ). In contrast, at 6 months there was a significant decrease in plasma ACTH levels observed in the Tg<sup>+</sup> mice (WT:  $20.98 \pm 3.80$  pg/ml; Tg<sup>+</sup>:  $9.52 \pm 1.50$  pg/ml;  $p < 0.01$ ) (Figure 35). This result suggests that in presence of high CORT levels, at 4 months, ACTH levels do not change whereas at 6 months ACTH levels decrease in Tg<sup>+</sup> mice. This decreased ACTH levels occurring after CORT increase in the Tg<sup>+</sup> is in concord with previous clinical studies from Umegaki et al., 2000, who report an absence of increased ACTH drive in early AD pathology in patients, and with Nasman et al., 1995, where lower levels of plasma ACTH levels were seen in the early phase of AD.

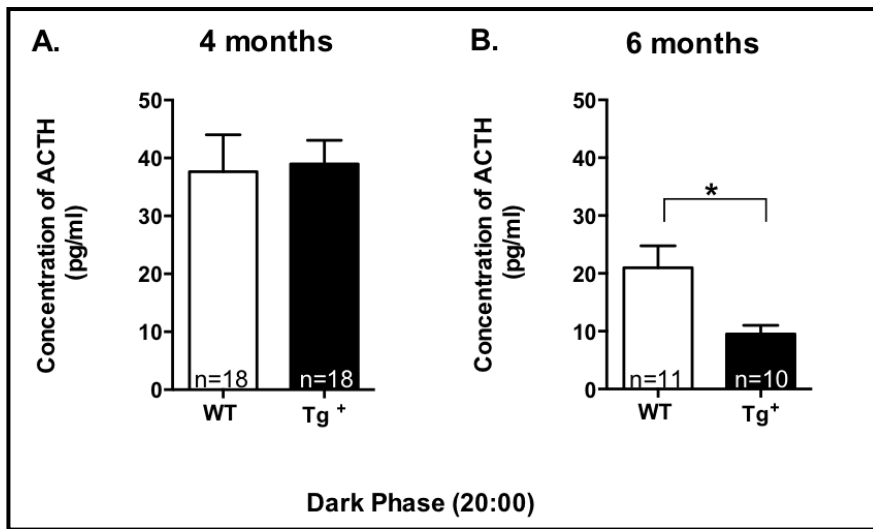


Figure 35: Comparison of plasma ACTH levels in WT and Tg<sup>+</sup> mice at 4 and 6 months of age. A) ACTH levels (pg/ml) were measured by ELISA at the dark phase (20:00) in 4 months WT and Tg<sup>+</sup> mice. B). Similarly, ACTH levels were measured from 6 months WT and Tg<sup>+</sup> mice. All data plotted Mean ± S.E.M. (\*) p < 0.05.

### 5.1.1.3 Comparison of body, thymus and adrenal gland weights between WT and Tg<sup>+</sup> male mice at 4 and 6 month of age

To further characterise the effect of high plasma CORT levels in this AD model, we investigated the peripheral organs in relation to the HPA axis. In this regard, we measured the weights of adrenal glands, the site of CORT production, at 4 and 6 month of age. In order to avoid the variations in the body weight linked to the genotype, the weight of the animals were recorded at the time of dissection and used as a normalisation factor. The ratios were expressed as mg of organ/ weight of animal in grams.

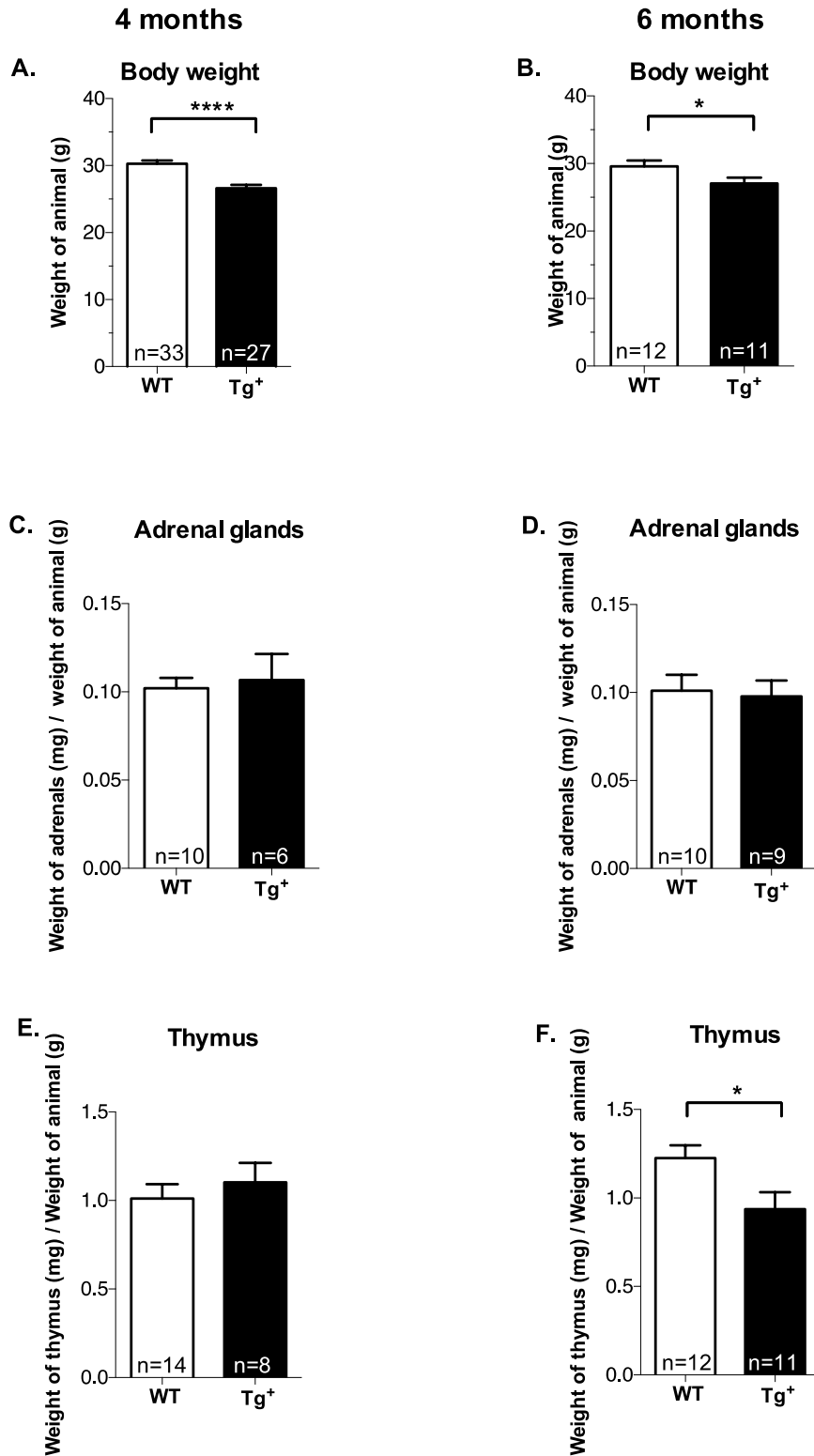


Figure 36: Comparison of body weights, thymus and adrenal gland weights of WT and Tg<sup>+</sup> male mice at 4 and 6 month of age. A) and B) represent body weights in grams. C) and D) represent thymus weights normalized to body weight (mg/g). E) And F) represent adrenal gland weights normalized to body weight (mg/g). All data plotted mean  $\pm$  S.E.M (\*)  $p < 0.05$ ; (\*\*)  $p < 0.01$ ; (\*\*\*)  $p < 0.001$ .

Animals were weighed at 4 and 6 months of age and at both these time points the Tg<sup>+</sup> mice were significantly smaller in weight as compared to their age matched WT mice ((4 months WT: 30.27 ± 0.48g; Tg<sup>+</sup>: 26.62 ± 0.5g; p < 0.0001), 6 months WT: 29.59 ± 0.86g; Tg<sup>+</sup>: 27.05 ± 0.88g; p < 0.05)) (Figure 36 A and B). However, neither at 4 nor at 6 months, did we find any significant difference in weight of the adrenal glands between the WT and Tg<sup>+</sup> mice (Figure 36 C and D). One of the remarkable effects of state of stress is the action of the CORT on the immune system. Hence, we also studied the thymus, which is the central organ involved in immunity.

Figure 36 E and F reports that, at 4 months, there was no significant difference between the mean thymus weight of the WT and Tg<sup>+</sup> mice (WT: 1.01 ± 0.08 mg/g; Tg<sup>+</sup>: 1.10 ± 0.11 mg/g), while at 6 months the average Tg<sup>+</sup> thymus weight was significantly lower than the corresponding age matched WT mice (WT: 1.23 ± 0.07 mg/g; Tg<sup>+</sup>: 0.94 ± 0.10 mg/g; p<0.05). Together, these results suggest that high CORT levels, seen at 4 and 6 months in Tg<sup>+</sup> mice, do not affect the weight of the adrenal glands, but affects thymus weight at 6 months.

#### **5.1.1.4 Quantification of GR by immunoblotting from hippocampal total protein extract in 4 months male Tg<sup>+</sup> and WT mice.**

On continuing our analysis of the effect of high CORT at different levels in the HPA axis, we next focused our attention to the hippocampal GR levels. CORT levels are maintained to homeostasis through the negative feedback mechanism regulated by various structures of the HPA axis. Besides tight regulation at the pituitary and the hypothalamus, the CORT levels are also negatively regulated by the hippocampus, the main structure of interest in our laboratory. Since the feedback mechanism is dysregulated in the Tg<sup>+</sup> mice at 4 months as shown by the Dexamethasone suppression test (Lanté et al., 2015), we speculated that this dysregulation would influence the hippocampal GR levels and hence we measured GR levels in hippocampal total proteins. Surprisingly, at 4 months, the total hippocampal GR levels (normalised to the endogenous actin control) were unchanged between the WT and Tg<sup>+</sup> mice (WT: 1.06 ± 0.09; Tg<sup>+</sup>: 1.03 ± 0.10, Figure 37). This data demonstrates that despite high CORT levels and a non-functional feedback loop, the total GR protein levels in the hippocampus remained unchanged.

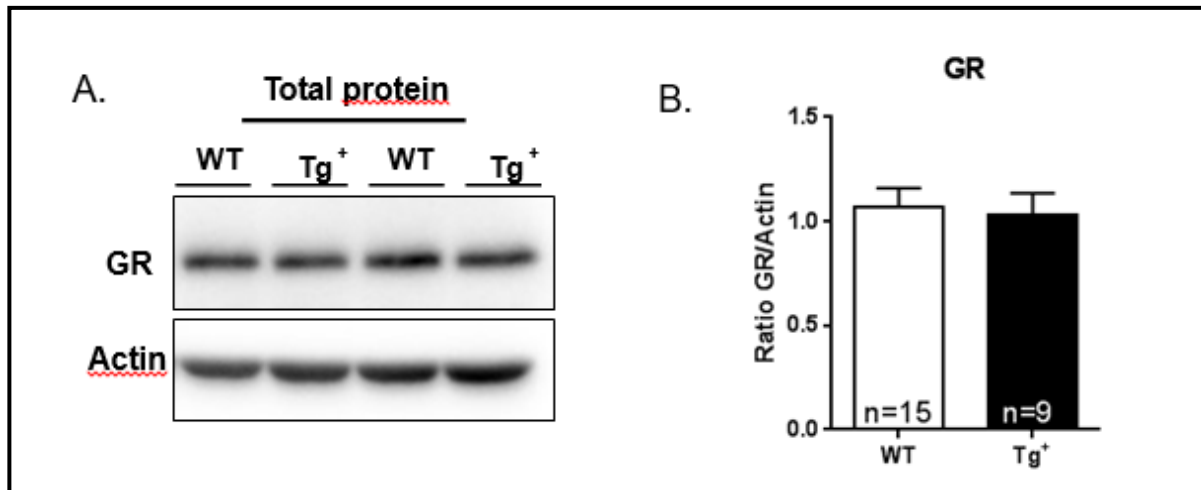


Figure 37: Quantification of GR by immunoblotting from hippocampal total proteins in 4 months male WT and Tg<sup>+</sup> mice. A). Representative western blot of GR and actin proteins in WT and Tg<sup>+</sup> mice. B). Graphical representation of relative intensity of GR and actin in total proteins from 4 months old WT and Tg<sup>+</sup>. All data plotted mean  $\pm$  S.E.M (\*)  $p < 0.05$ .

#### 5.1.1.5 *Rescue of episodic memory deficits in 4 month Tg<sup>+</sup> male mice with GR antagonist RU486 treatment.*

We next moved from molecular level to a more integrative level of memory processes. We had proof that this early stage of pathology in the Tg<sup>+</sup> mice was associated to changes in synaptic plasticity, like enhanced LTD and memory deficits in the contextual fear conditioning task (D'Amelio et al., 2011). To increase the relevance of our findings in the context of AD, we focussed our investigation on memory deficits by analysis of episodic-like memory, the first type of memory to be affected in AD patients (deToledo-Morrell et al., 2007, Salmon and Bondi, 2009). To specifically assess this type of memory in Tg<sup>+</sup> mice, my team had previously optimized an elaborated version of the object recognition test, which can probe for the 'What', 'When', 'Where' components of episodic memory (Dere et al., 2005). Exploration time for all objects was recorded and a discrimination ratio was calculated during the test trial. We observed that mice from both genotypes display a similar total exploration time during the 10 minute test trial (WT:  $63.56 \pm 5.73$ s; Tg<sup>+</sup>:  $59.62 \pm 6.11$  s;  $p > 0.05$ , data not shown). We evaluated discrimination ratios for the 'What', 'When', and 'Where' components of episodic memory. For the 'What' and the 'When' components the positive discrimination ratio for the two genotypes did not differ ('What' WT:  $0.327 \pm 0.028$ ; Tg<sup>+</sup>:  $0.242 \pm 0.046$ , 'When' WT:  $0.259 \pm 0.037$ ; Tg<sup>+</sup>:  $0.255 \pm 0.048$ ) (Figure 38). However, for the 'Where' component, while WT control animals (untreated/ vehicle-treated mice) displayed a positive

discrimination, Tg<sup>+</sup> group displayed a marked negative discrimination ratio, significantly different from the WT (WT: 0.126 ± 0.033; Tg<sup>+</sup>: -0.059 ± 0.068; p<0.001) (Figure 38). This data indicated that the WT mice displayed a good episodic memory in this refined object recognition paradigm, while the Tg<sup>+</sup> mice failed to process the ‘Where’ component (which integrates all the aspects of episodic memory i.e. object, time and location).

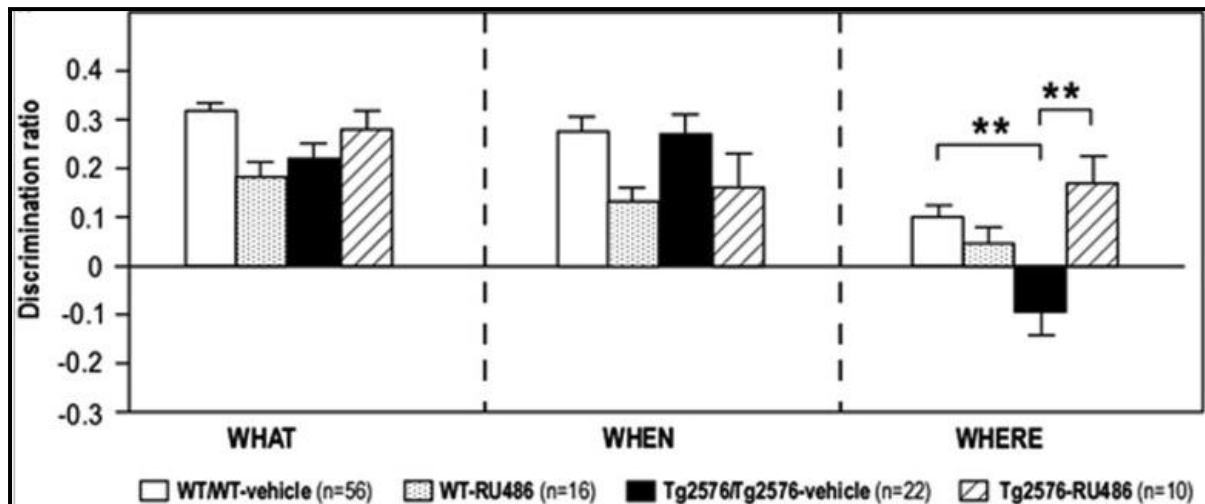


Figure 38: Four-month old Tg<sup>+</sup> mice display episodic memory deficits which were rescued by blocking glucocorticoid receptors. A) Scheme of the episodic memory paradigm including the what-when-where components. B) Episodic memory in 4-month old untreated/vehicle treated WT (white bars), in 4 day in-vivo RU486 treated WT (dotted bars), in untreated/vehicle treated Tg<sup>+</sup> (black bars) and in 4 days in-vivo RU486 treated Tg<sup>+</sup> (hashed black bars) mice. Discrimination ratios for each component of episodic-like memory are indicated. (\*\*) p<0.01; n= number of mice.

Since there was clear dysregulation of the HPA axis and memory deficits in the Tg<sup>+</sup> mice at 4 months, we were interested to check if blocking the GRs using its antagonist could rescue the memory deficit. WT and Tg<sup>+</sup> mice received twice daily sub-chronic (4 days) injections of GR antagonist RU486 before being exposed to the episodic memory paradigm. Figure 5, reports that RU486 did not significantly alter episodic memory in wildtype littermates, while it fully rescued the deficit in the ‘Where’ component of the episodic memory, which was seen in the Tg<sup>+</sup> mice (Tg<sup>+</sup>/Tg<sup>+</sup>vehicle: 0.095 ± 0.06; Tg<sup>+</sup>RU486: 0.18 ± 0.06; p<0.01) (see Figure 38). Hence, together these data suggest that GR activity is involved in impairment of episodic memory formation in these early symptomatic mice.

Part of these data were included in Lanté et al. 2015, for which I contributed as co-author (see full publication PDF in Annexe).

---

## 5.2 Chapter 2

### 5.2.1 Aim 2: To check the specific role of GRs in AD like phenotypes in $GR^{lox/lox} Tg^+$ mice.

As explained above and as published in Lanté et al 2015, promising results suggest that GRs activity might contribute to early AD onset phenotypes like episodic memory and synaptic deficits. Indeed, both these phenotypes were rescued in the  $Tg^+$  mice after chronic treatment with RU486, a commonly used GR antagonist. However, the major disadvantage of this antagonist is its unspecific binding affinity towards progesterone receptor (Baulieu, 1997). Hence, to confirm these data, the need for a more specific method to block GRs was required. To address this, we crossed the  $Tg^+$  mice (harbouring the hAPP<sup>swe</sup> transgene) with GRfloxed mice (Tronche et al., 1999) to generate  $GR^{lox/lox} Tg^+$  mice and their control  $GR^{lox/lox} Tg^-$ . We anticipated that at 4 months the  $GR^{lox/lox} Tg^+$  double mutant mice would exhibit phenotypes we had previously characterised in single mutant  $Tg^+$  mice i.e. increased CORT levels, exacerbated LTD and episodic like memory deficits. Then, using a Cre recombinase virus, we would have the possibility to remove the GRs from the CA1 neurons of the hippocampus *in vivo* and investigate if loss of GR would prevent the occurrence of these AD phenotypes.

Hence, by generating this conditional ablation model of GR, we could specifically address its role in the occurrence of AD phenotypes in this  $Tg^+$  AD mouse model.

The **objectives** in this aim were:

- To generate the  $GR^{lox/lox} Tg^+$  mice
- To characterise the  $GR^{lox/lox} Tg^+$  for survival rate, size and body weight
- To validate for AD phenotypes i.e. high CORT levels, exacerbated LTD phenotype before removing GR.
- To remove GR by Cre-GFP virus in the CA1 region of the hippocampus and to check for prevention of AD phenotypes.

### 5.2.1.1 Generation of the $GR^{lox/lox} Tg^+$ mice

To generate the  $GR^{lox/lox} Tg^+$  mice we crossed the  $GR^{lox/lox}$  mice with the  $Tg^+$  mice. The main goal of the breeding was to have all the animals with the GR floxed allele and half of these animals would be positive for the transgene. Due to the difference in background strains between the  $Tg^+$  and  $GR^{lox/lox}$  mice, several crossings were required.

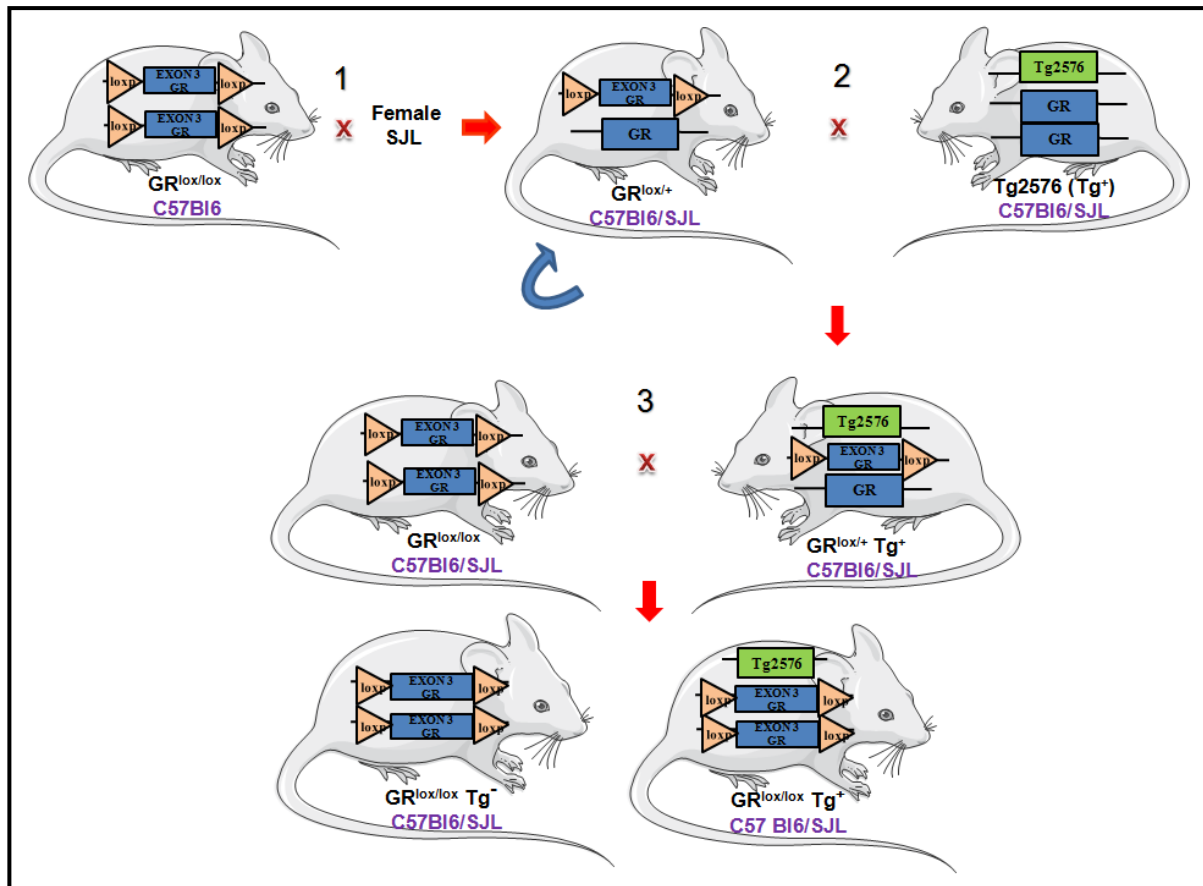


Figure 39: Summary of the  $GR^{lox/lox} Tg^+$  mice breeding. The first step (1) involved crossing the  $GR^{lox/lox}$  which is in the C57B16 background with a WT mouse of the SJL background to obtain a  $GR^{lox/+}$  in mixed C57B16/ SJL background. Second step (2) involved crossing the  $GR^{lox/+}$  obtained in the mixed background with the  $Tg^+$  mouse to obtain  $GR^{lox/+} Tg^+$  double mutants. In parallel, we also crossed  $GR^{lox/+}$  (C57B16/SJL) amongst each other to obtain  $GR^{lox/lox}$  (C57B16/SJL) (blue U arrow). In the third step (3), the  $GR^{lox/lox}$  (C57B16/SJL) was crossed with the  $GR^{lox/+} Tg^+$  to have all the mice with the  $GR^{lox/lox}$  (homozygous for  $GR^{lox/lox}$ ) and half of the mice transgenic for the APP<sup>swe</sup> transgene ( $Tg^+$ ).

The crossings were divided into 3 main steps (see Figure 39):

- To bring the GR<sup>lox/lox</sup> mouse in C57Bl6/SJL background, which is the Tg<sup>+</sup> background used in Lanté et al. 2015.
- To cross heterozygous GR<sup>lox/+</sup> in mixed background with Tg<sup>+</sup> mice
- To obtain mice homozygous GR<sup>lox/lox</sup> Tg<sup>+</sup> and their respective control (GR<sup>lox/lox</sup> Tg<sup>-</sup>)

The Tg2576 mice are bred in the C57Bl6/SJL background (Hsiao et al., 1996, Lanté et al., 2015) and hence it was important to bring the GR<sup>lox/lox</sup> mice originally in the pure C57Bl6 background to the mixed C57Bl6/SJL background. Secondly, we mated this heterozygous GR<sup>lox/+</sup> mouse with a male Tg<sup>+</sup> mouse to obtain GR<sup>lox/+</sup>Tg<sup>+</sup> mice. It is important to note here that for the mating, we introduced the transgene via the male mouse to avoid the effects of high CORT production during maternal care. The last step in this breeding was to obtain a homozygous GR floxed mice with the transgene (GR<sup>lox/lox</sup>Tg<sup>+</sup>). It took three generations of breeders to obtain this double mutant mouse and the probability was only 4% (i.e. 7 out of 148 GR<sup>lox/lox</sup> mice were Tg<sup>+</sup>).

### 5.2.1.2 Basic characterization of the $GR^{lox/lox} Tg^+$ mice

On obtaining the double mutant mice, several aspects were characterized by comparison between the  $GR^{lox/lox} Tg^+$  (double mutant) and its control, the  $GR^{lox/lox} Tg^-$  (single mutant), namely the survival percentage, weight and size of the mouse.

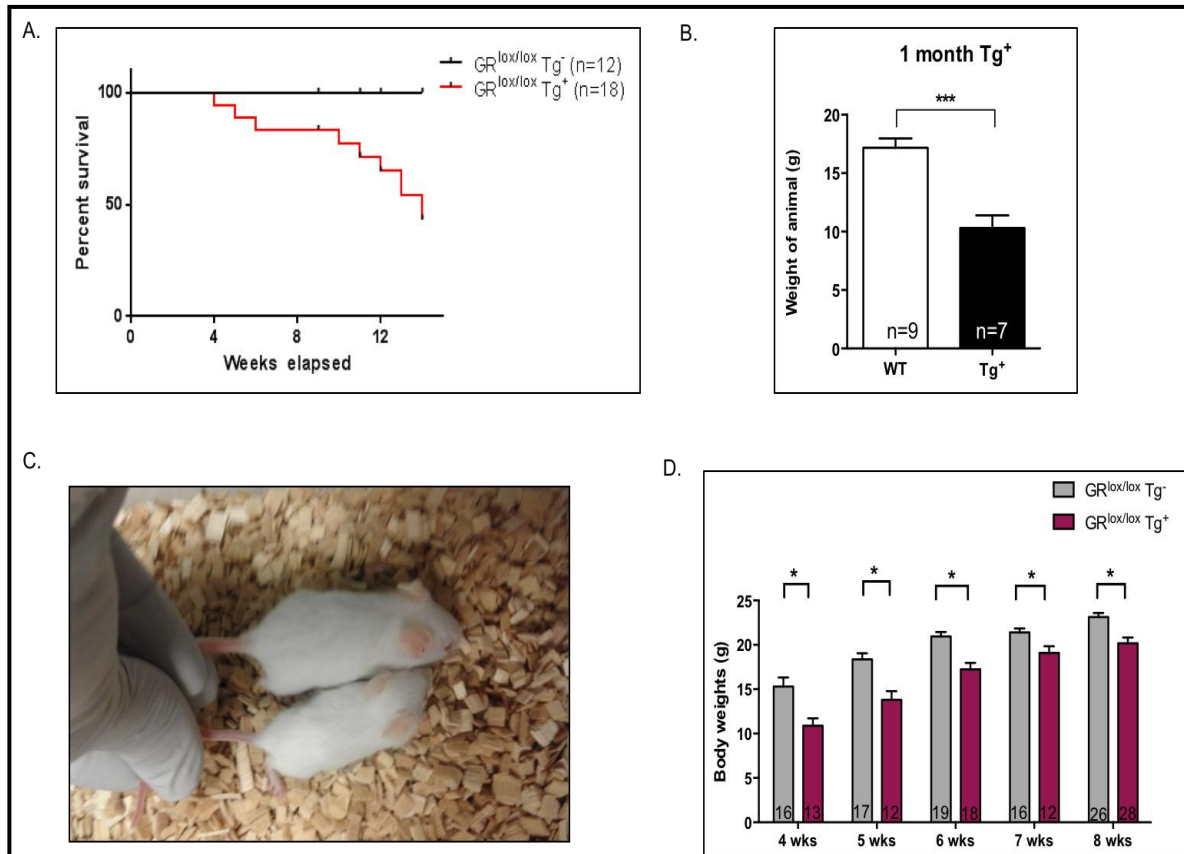


Figure 40: Basic characterization of  $GR^{lox/lox} Tg^+$  mice: A) Survival percentage of  $GR^{lox/lox} Tg^+$  mice as compared to their controls B) Comparison of body weights of  $Tg^+$  and WT male mice at 1 month of age. C) Photo of the  $GR^{lox/lox} Tg^+$  and  $GR^{lox/lox} Tg^-$  mice at the time of weaning to show size difference. D) Body weights of  $GR^{lox/lox} Tg^+$  and  $GR^{lox/lox} Tg^-$  male mice from 4 weeks to 8 weeks. All data plotted mean  $\pm$  S.E.M (\*)  $p < 0.05$ ; (\*\*)  $p < 0.01$ ; (\*\*\*)  $p < 0.001$ .

On obtaining the double mutant mice, it quickly became apparent that survival of these mice was low (See Figure 40A) and they looked weaker as compared to their controls. As shown using a Kaplan-Meier survival curve, the survival rate of these mice decreased to 50% within 12 weeks' time ( $p < 0.05$ ). This could probably be due to the C57Bl6 background incompatibility with the transgene leading to high lethality. It is known that breeding the Tg2576 mice into the mixed C57Bl6/SJL background allows for better long-term survival as the SJL alleles protect against the lethal effects of the APP over-expression (Carlson et al.,

1997). While working on the single  $Tg^+$  mice in the mixed C57Bl6/SJL background, we had previously observed that they already exhibited a body weight difference at 1 month as compared to their WT control (see Figure 40B). Similarly, this weight difference was observed in  $GR^{lox/lox} Tg^+$  double mutants (4 weeks,  $GR^{lox/lox} Tg^-$ :  $15.3 \pm 1.1g$ ;  $GR^{lox/lox} Tg^+$ :  $10.9 \pm 0.8g$ ;  $p < 0.01$  and 8 weeks,  $GR^{lox/lox} Tg^-$ :  $23.12 \pm 0.47 g$ ;  $GR^{lox/lox} Tg^+$ :  $20.17 \pm 0.65g$ ;  $p < 0.01$ ) when compared to their controls (Figure 40 D). The variation in size between the littermates is exemplified in the photo above (Figure 40C). To summarize this data, the  $GR^{lox/lox} Tg^+$  double mutant mice showed low survival rate, were weaker in health and had smaller body weight as compared to their controls.

### **5.2.1.3 Verification of AD like phenotypes in $GR^{lox/lox} Tg^+$ as seen in $Tg^+$ mice.**

Before proceeding to ablation of GR from the CA1 with Cre recombinase in the  $GR^{lox/lox} Tg^+$  mice, it was important to verify if these double mutants still exhibited the  $Tg^+$  phenotypes i.e. increased CORT levels and exacerbated LTD as compared to their control  $GR^{lox/lox} Tg^-$  mice.

### 5.2.1.4 Increased CORT levels

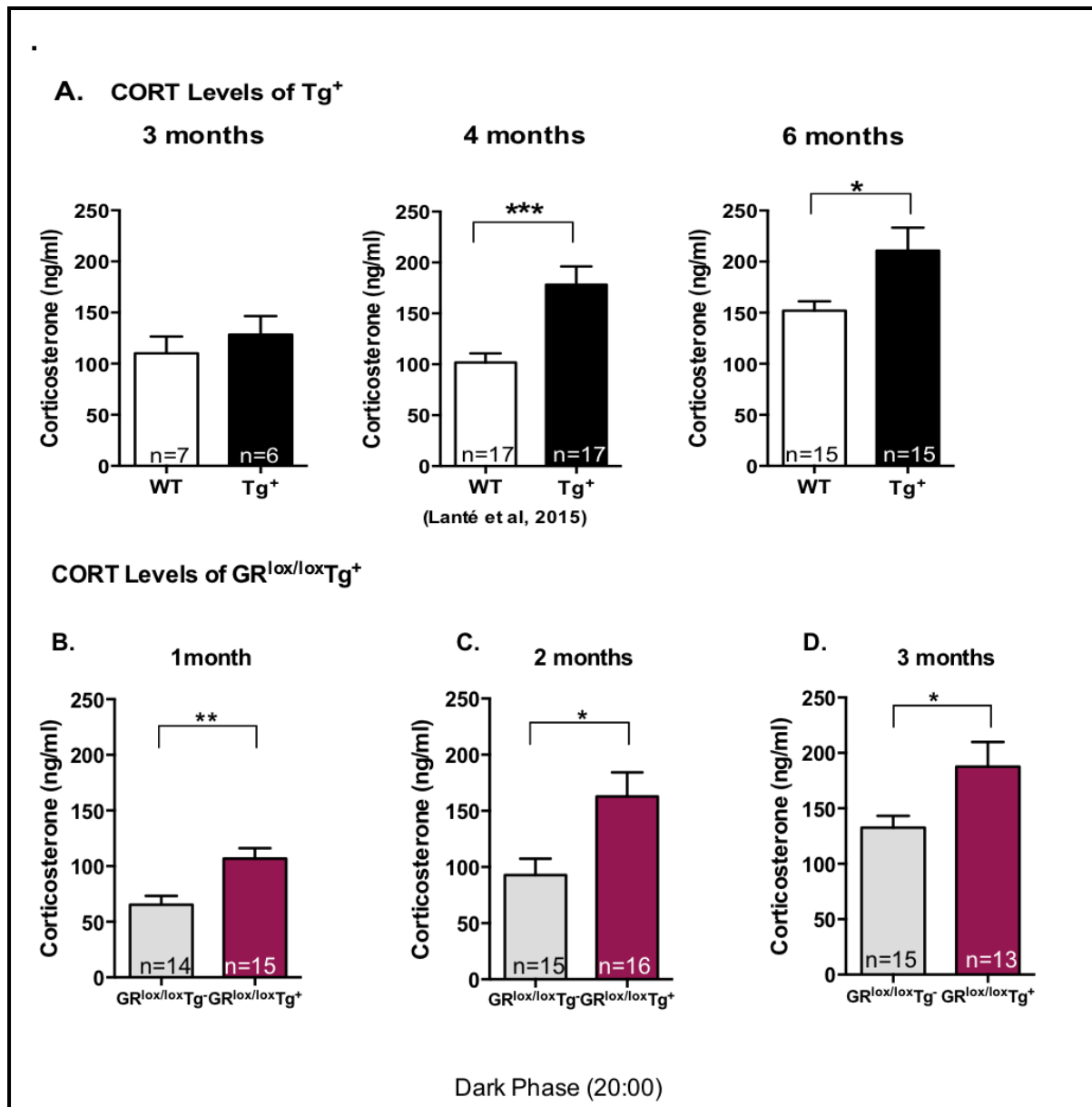


Figure 41: Comparison of CORT levels in Tg<sup>+</sup> and GR<sup>lox/lox</sup> Tg<sup>+</sup> mice. A) Plasma corticosterone levels (ng/ml) were measured by ELISA at the dark phase (20:00) in 3, 4 and 6 months WT and Tg<sup>+</sup> mice (as in figure 1 of chapter 1). B) Plasma corticosterone levels (ng/ml) were measured by ELISA at the dark phase (20H00) in 1, 2 and 3 month GR<sup>lox/lox</sup> Tg<sup>-</sup> mice and GR<sup>lox/lox</sup> Tg<sup>+</sup> mice. All data plotted Mean ± S.E.M. (\*) p < 0.05; (\*\*) p < 0.01; (\*\*\*) p < 0.001.

In Tg<sup>+</sup> single mutant mice, we had observed increased CORT levels at 4 and 6 months of age, but not at 3 months (Figure 34 chapter 1 and reproduced here in Figure 41A for ease of comparison with double mutant data). Due to the high mortality of the GR<sup>lox/lox</sup> Tg<sup>+</sup> mice, we had to shift the latest time point of measuring CORT from 4 months to 3 months. Unlike the Tg<sup>+</sup> mice, increased CORT levels was already seen at 3 month in the GR<sup>lox/lox</sup> Tg<sup>+</sup> mice as

compared to  $GR^{lox/lox} Tg^{-}$  ( $GR^{lox/lox} Tg^{-}$ :  $132.5 \pm 10.76$  ng/ml;  $GR^{lox/lox} Tg^{+}$ :  $187.7 \pm 22.20$  ng/ml;  $p < 0.05$ ). To identify how early this elevation of CORT occurred, we measured the CORT levels at earlier time points of 1 and 2 months. Surprisingly, at 2 months the  $GR^{lox/lox} Tg^{+}$  mice showed increase CORT levels as compared to the  $GR^{lox/lox} Tg^{-}$  mice ( $GR^{lox/lox} Tg^{-}$ :  $92.81 \pm 14.61$  ng/ml;  $GR^{lox/lox} Tg^{+}$ :  $162.8 \pm 21.47$  ng/ml;  $p < 0.05$ ). Similarly, this difference was also seen in 1 month old mice ( $GR^{lox/lox} Tg^{-}$ :  $65.31 \pm 8.0$  ng/ml;  $GR^{lox/lox} Tg^{+}$ :  $106.7 \pm 9.4$  ng/ml  $p < 0.01$ ) (Figure 41 B, C, D).

### 5.2.1.5 Exacerbated LTD phenotype

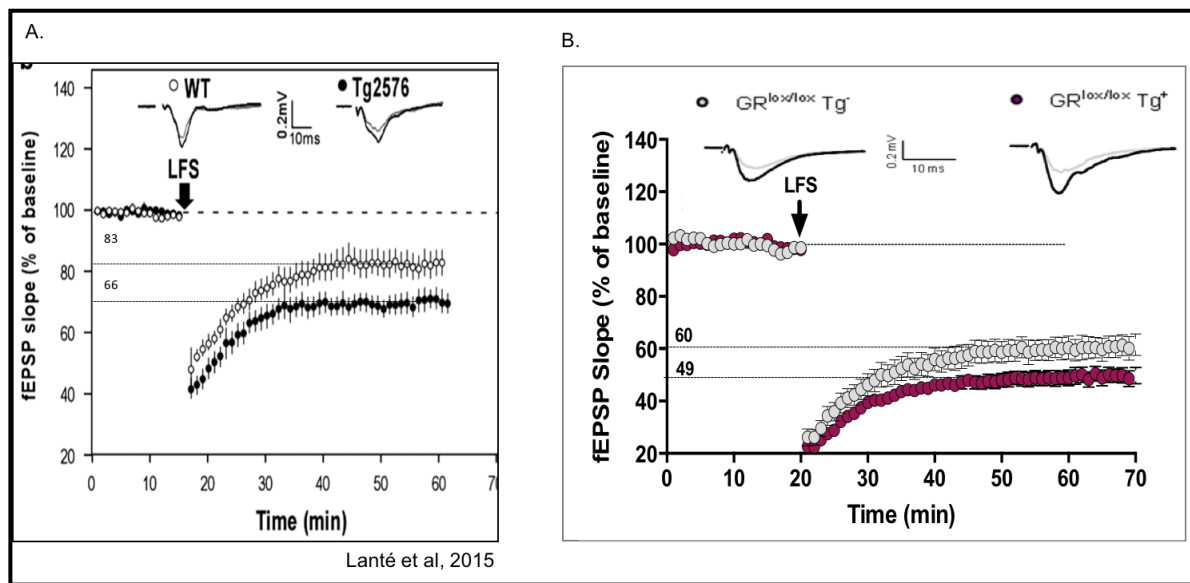


Figure 42: Comparison of LFS-LTD in  $Tg^{+}$  and  $GR^{lox/lox} Tg^{+}$  A) Summary graph (as percentage of fEPSP baseline) electrically induced LFS-LTD (arrow) is enhanced at the CA3-CA1 synapse in the 4-month old  $Tg^{+}$  mice ( $N=3$  mice,  $n=9$  slices) compared to the wild type littermate mice ( $N=3$ ,  $n=8$ ). B) Summary graph of electrically induced LFS- LTD (arrow) is enhanced in 3-month old  $GR^{lox/lox} Tg^{+}$  ( $N=6$ ,  $n=13$ ) mice compared to  $GR^{lox/lox} Tg^{-}$  ( $N=5$ ,  $n=13$ ) mice. All data plotted mean  $\pm$  S.E.M. (\*)  $p < 0.05$ .

We have previously demonstrated that, at 3 and 4 months, the  $Tg^{+}$  mice displayed an exacerbation of the LTD in at the CA3-CA1 synapses (Figure 42 left) (D'Amelio et al., 2011, Lanté et al., 2015). We were expecting to see a similar phenotype in the  $GR^{lox/lox} Tg^{+}$  mice. We indeed observed an increased LTD phenotype in 3-month-old  $GR^{lox/lox} Tg^{+}$  mice ( $49.27 \pm 2.841$ ) as compared to  $GR^{lox/lox} Tg^{-}$  ( $60.34 \pm 4.102$ ) ( $p < 0.05$  Figure 42 right). It was however noticed that the  $GR^{lox/lox} Tg^{-}$  mice showed a higher LTD (40%) compared to WT control (20%) (comparison of  $GR^{lox/lox} Tg^{-}$  LTD in Figure 42B and WT LTD in Figure 42A). Also, it was noticed that the double mutants exhibited slightly stronger LTD (Figure 42B, 49%

response remaining) than single  $Tg^+$  mutant (Figure 42A, 66% response remaining), suggesting exacerbation of LTD phenotype. However, as these two sets of LTD data were not obtained within the same timeframe, statistical comparison would be inappropriate.

Nonetheless, we decided to continue using the double mutant mice for stereotaxic injections with an AAV virus encoding a Cre-recombinase/GFP fusion protein (Cre-GFP virus) to proceed to local in vivo ablation of the GR gene (see Material and Methods section (Figure 26) for details on in vivo ablation procedure.

#### **5.2.1.6 Stereotaxic injections with Cre-GFP in $GR^{lox/lox} Tg^+$ mice to ablate GR gene in CA1 neurons in vivo**

To validate the Cre-Lox system for GR ablation, it was important to standardize the concentration of the Cre-GFP virus and the time of recombination after stereotaxic injection for complete expression of the Cre recombinase. CA1 cells transduced in vivo with diluted Cre-GFP of titre value  $5 \times 10^{12}$  had a morphology peculiar to apoptotic cells (data not shown). To avoid this, Cre-GFP was diluted to titre of  $5 \times 10^{11}$  and CA1 neurons were transduced in vivo. Animals were left alive for 4 weeks to allow for sufficient recombination. Identical in vivo transduction was performed using the control AAV virus expressing only GFP (eGFP virus). Immunofluorescence images of GR protein after Cre-GFP or eGFP injections will be shown later in Chapter 3, Figure 47).

When injecting the Cre-GFP virus in the CA1 of the hippocampus of  $GR^{lox/lox} Tg^+$  mice and control  $GR^{lox/lox} Tg^-$  mice, we encountered an additional problem with the survival rate after surgery especially for the  $GR^{lox/lox} Tg^+$  mice which were transduced with Cre-GFP (most relevant group for our study). As shown in Figure 43, we noted that, in all the four groups, a fraction of mice were, dying upon surgery, as can be sometimes observed for such heavy cranial surgeries. Yet it was clear that the double mutant  $GR^{lox/lox} Tg^+$  group was particularly sensitive to this surgery in combination with the Cre-GFP virus exhibited increased death (see Figure 43).

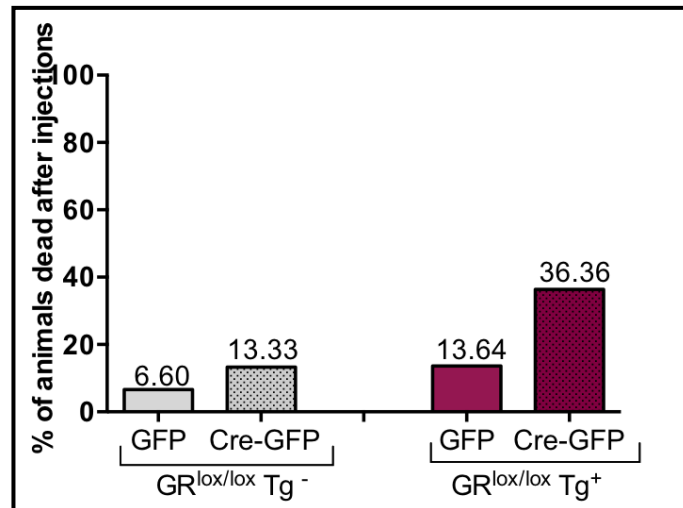


Figure 43: Deaths of animals upon surgery for stereotaxic injection. Prominent numbers of deaths were observed amongst the groups especially for GR<sup>lox/lox</sup> Tg<sup>+</sup> mice injected with Cre-GFP.

Although it had taken us a year to obtain these double mutant mice, their exacerbated CORT and LTD phenotypes as well as their low survival during surgery prompted us to abort the use of this strategy to explore the role of GRs in AD. This was a hard decision to take, but we were worried that: 1) it would be difficult to obtain sufficient mice with GR ablation in the CA1 in this double mutant background with this increase mortality after surgery, and 2) future phenotypical and mechanistic data that we would obtain in this context could not be correctly interpreted considering the exacerbated phenotypes that appear very early in the life of the mouse and that might not specifically be linked to APP fragment accumulation (e.g. weight, CORT levels). Instead, in collaboration with Dr Frandemiche and using the tools we have developed during this thesis and in the lab, we decided to address the functional relationship between A $\beta$  oligomers and GRs focussing on the acute actions of A $\beta$  at synapses (see next chapter).

---

## 5.3 Chapter 3

### 5.3.1 Aim 3: To investigate if A $\beta$ oligomers act via GRs to promote their acute synaptic effects at hippocampal synapses.

We established a link between enhanced CORT signalling via GRs and its contribution to early AD phenotypes using the Tg2576 mouse model, as described above. Strong evidence suggests that the oligomeric forms of the amyloid- $\beta$  peptide (oA $\beta$ ) are causal to development of AD pathology (Selkoe, 2002). These oligomeric forms are known to target excitatory synapses where they diminish synaptic functions and cause memory impairment (Walsh et al., 2002, Townsend et al., 2006, Shankar et al., 2007, Selkoe, 2008). However, the functional relationship between GRs and amyloid- $\beta$  oligomers (oA $\beta$ ) at the synapses remained mostly unexplored.

GRs are present in the cytoplasm in their inactive form and when activated in presence of the CORT ligand they translocate to the nucleus for transcriptional activity. Recently, GRs were however also found in PSDs of synapses as well as in dendritic spines (Johnson et al., 2005). It is not clear if these represent membrane GRs, which are known for their fast non-genomic action. Recently, it was reported that *in-vivo* intra-cerebroventricular A $\beta$ <sub>25-35</sub> injections in rat promoted accumulation of GRs in the nucleus of the CA1 neurons in the hippocampus (Brureau et al., 2013). This strongly suggested an intricate functional relationship between A $\beta$  and GRs at the nucleus, but there remained a paucity of data on the effects of A $\beta$  on the GRs present at the synapses.

There are numerous evidences in literature proposing amyloid- $\beta$  oligomers as key mediators of synaptic dysfunction. These oligomers (extracted from patients or synthetically prepared peptides) were shown to acutely impair hippocampal LTP in the hippocampus (Puzzo et al., 2008, Shankar et al., 2008, Townsend et al., 2006, Dineley et al., 2010) and to increase hippocampal LTD (Shankar et al., 2008, Li et al., 2009). The molecular mechanism through which oA $\beta$  acts to promote synaptic alterations remains uncertain. Interactions have been reported with several receptors such as glutamatergic, nicotinic acetylcholine receptors and PrPc (Yamin, 2009, Dineley et al., 2001, Laurén et al., 2009, De Strooper and Karran, 2016), but a consensus still needs to emerge on this issue. In this context, we were interested to check if the LTP impairment caused by oA $\beta$  occurred via GRs.

We specifically tackled three questions. In collaboration with Dr Frandemiche, we used acute oA $\beta$  treatment on hippocampal neuron cultures *in vitro* followed by biochemical analysis to ask if oA $\beta$  could modulate GR levels at synapses. We also used ex-vivo hippocampal sections acutely treated with oA $\beta$  to check if GRs are implicated in oA $\beta$ -mediated LTP impairment. In this ex-vivo context, we either blocked GRs with a specific GR antagonist or first ablated GRs in the CA1 neurons *in vivo* using the GR<sup>lox/lox</sup> mice described in the previous chapter. Finally, we further extended our research by moving from the synapses to a more integrated level of memory processing. To do this, we set up a protocol to assess how acute oA $\beta$  intra-hippocampal injections could modulate hippocampus-dependent memory deficits.

### 5.3.1.1 Effect of oA $\beta$ on levels of GR in PSD

In collaboration with Dr. Frandemiche we showed that oA $\beta$  can modulate GRs within the PSD. We have evidence that acute exposure (30 mins) of 100nM oA $\beta$  on *in vitro* hippocampal neuron cultures (14-15 DIV) increased the GR levels at the synapses, precisely at the PSDs (see Figure 44, oA $\beta$ : 1.8 times more than control;  $p < 0.01$ ). With this data, we established a relationship between acute oA $\beta$  and GRs at the PSD.

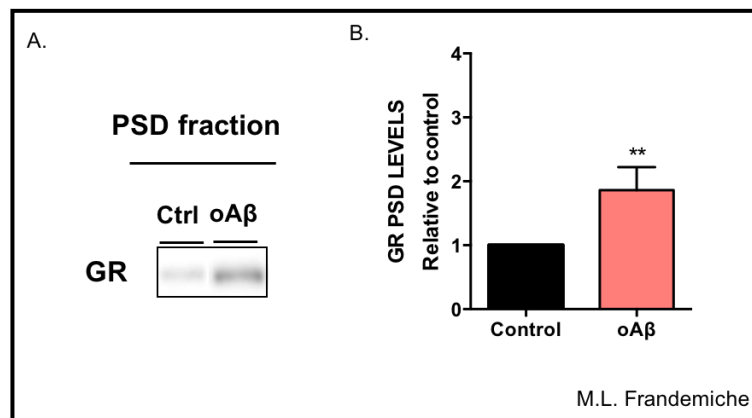


Figure 44: Effect of oA $\beta$  on the GR levels in the post synaptic density. A). Representative western blot image of GR levels in PSD in control and after 100 nM oA $\beta$ - treated hippocampal neurons. B). Graphical representation of GR level in PSD in control and oA $\beta$  treated neurons. All data plotted mean  $\pm$  S.E.M. (\*\*) $p < 0.01$ .

### 5.3.1.2 Effect of GR Antagonist compound 13 (C13) on synaptic transmission and LTP

To understand better the relationship of GR in acute  $\alpha\beta$ -mediated synaptic effects, we took to a pharmacological approach of exogenously adding specific GR antagonist compound 13 (C13; CORCEPT Therapeutics, USA, see characteristics in Table 5 in Materials and Methods) (Hunt et al., 2015) and 100 nM synthetic  $\alpha\beta$  as prepared in (Stine et al., 2003, Frandemiche et al., 2014).

We first studied the effect of C13 on basal synaptic transmission and synaptic plasticity *per se* as effects of this compound on these measures had not been described before. These data were necessary for correct interpretation of C13 effects on LTP with  $\alpha\beta$ . We used *ex vivo* hippocampal slices and exogenously perfused 1  $\mu$ M C13 or 0.1% DMSO (Vehicle) in ACSF.

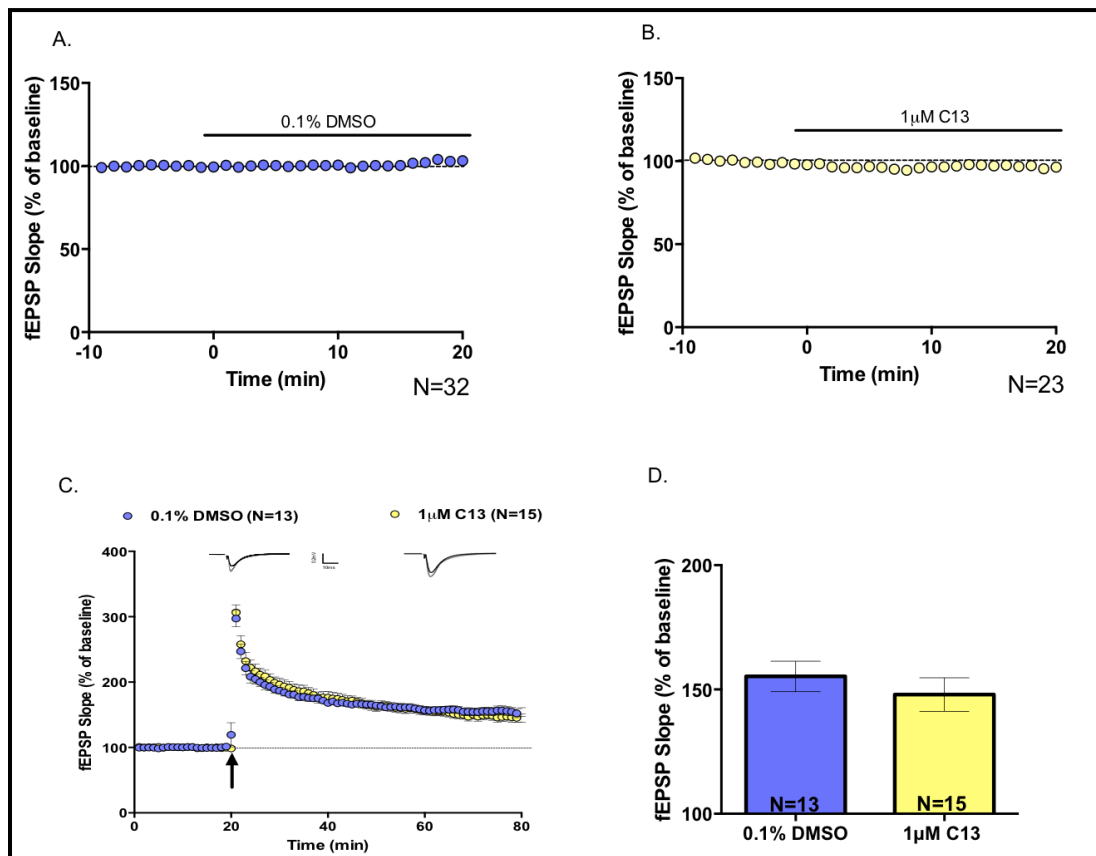


Figure 45: Effect of C13 on basal synaptic transmission and LTP. A). Basal field excitatory postsynaptic potentials (fEPSPs) were recorded followed by exposure to 1  $\mu$ M C13 (n=20 mice, N=23 slices) or 0.1% DMSO (n=26 mice, N=32 slices) in ACSF to check for effects of C13 on basal synaptic transmission. B) Summary graph (as percentage of fEPSP baseline) of electrically induced LTP (HFS, arrow) in presence of 1  $\mu$ M C13 (n=10 mice, N=15 slices) or 0.1% DMSO (n=11 mice, N=13 slices). Quantification of LTP magnitudes (as % of baseline) calculated 45-60 minutes post HFS (Bottom Right). All data plotted mean  $\pm$  S.E.M.

In

Figure 45A and B, there seems to be little influence of C13 (1 $\mu$ M) or DMSO (0.1%) on the fEPSPs, although statistical analysis (see Table 6 below in this chapter) evidenced a small (5%), but significant, alteration of fEPSP response after application of these compounds. This is likely due to slight perturbation of response due to the application procedure rather than a drug/vehicle specific effect. As this alteration of fEPSP response was very small, it did not prevent us from investigating the effect of GR antagonist on LTP. There was no difference in LTP response in presence of GR antagonist (Figure 45B; DMSO: 155.3  $\pm$  6.1; C13: 148  $\pm$  6.77). Hence, these findings suggested that inhibiting GRs with its antagonist C13 at 1 $\mu$ M concentration did not affect basal synaptic transmission nor LTP. We could then proceed to the use of this compound in presence of oA $\beta$ .

### **5.3.1.3 Effect of C13 on LTP impairment caused by oA $\beta$**

Strong evidence shows that different forms of A $\beta$  (dimers and oligomers both synthetically prepared and from patients) causes LTP impairment when tested on hippocampal slices (Puzzo et al., 2008, Shankar et al., 2008). We questioned if this LTP impairment occurs via the GRs.

To begin, we observed the expected oA $\beta$  effect on LTP in the control DMSO condition as seen in Figure 46A. Indeed, statistical analysis on the last 15 minutes of LTP demonstrated a significant oA $\beta$  effect (DMSO: 155.3  $\pm$  6.1; DMSO + oA $\beta$ : 130.7  $\pm$  1.5;  $p < 0.05$  unpaired t-test). Interestingly, with co-application of 1 $\mu$ M C13, this acute oA $\beta$  effect on LTP was not seen (Figure 46 C; C13: 148.0  $\pm$  6.77; C13 + oA $\beta$ : 147.9  $\pm$  2.27; unpaired t-test). Hence, upon comparison of the graphs of oA $\beta$  effect with or without inhibiting GRs (Figure 46 E and F), we could conclude blocking GRs completely occludes oA $\beta$  effects on LTP ( $p < 0.001$ , unpaired t-test).

To statistically analyse all the groups together (Figure 46 G), we performed the Approximative Kruskal-Wallis test followed by post-hoc analysis by permutation t-test with false discovery rate correction. Using this grouped comparison, it was evident that oA $\beta$  effects on LTP were prevented by blocking GRs.

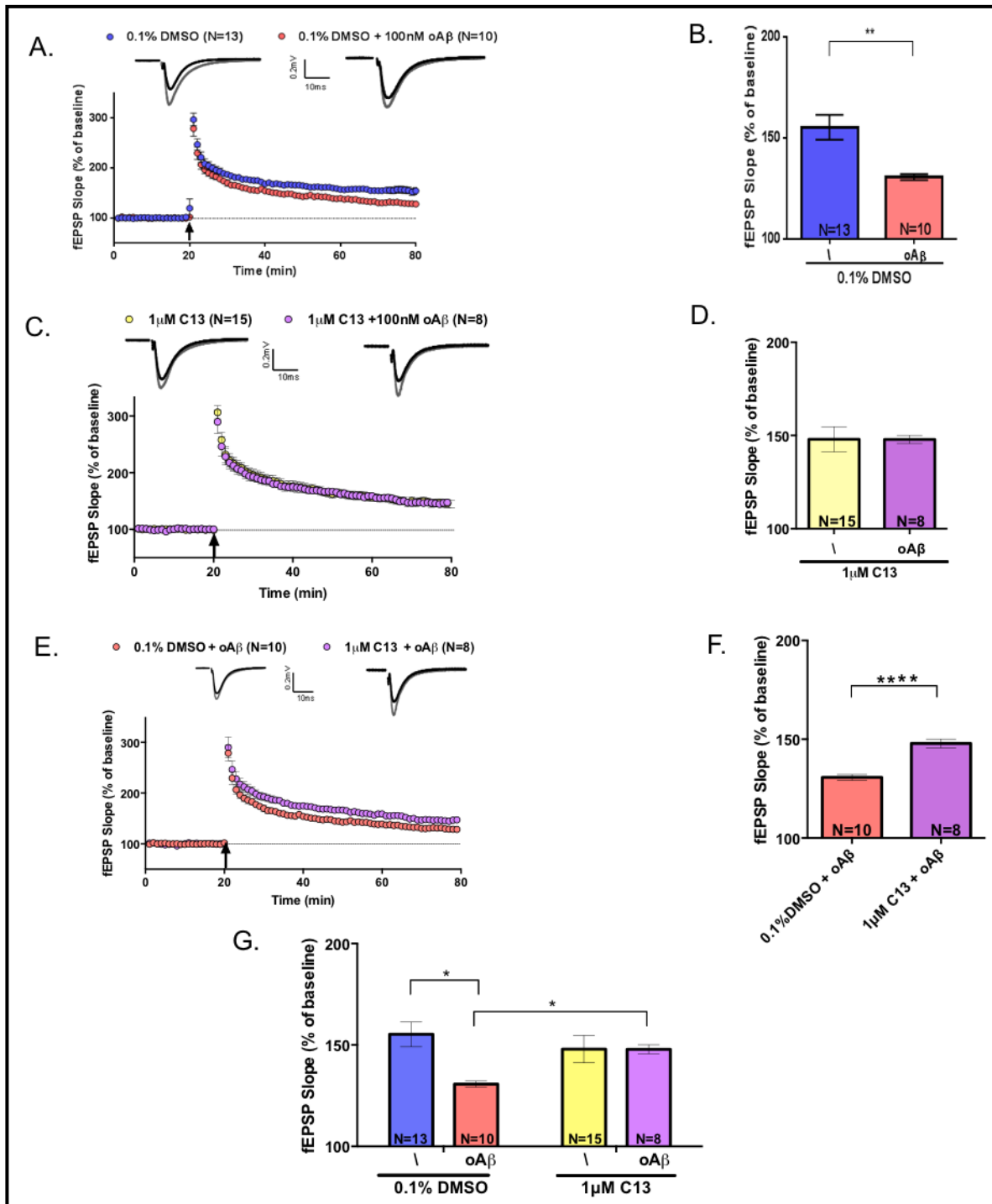


Figure 46: Effect of acute oAβ and C13 on LTP. A) Left, Summary graph (as percentage of fEPSP baseline) of electrically induced LTP (HFS, arrow) in DMSO (n=11 mice, N=13 slices) versus DMSO + 100nM oAβ (n=9, N=10). B). Left, Summary graph of HFS induced LTP in 1μM C13 (n=10, N=15) compared to 1μM C13 + 100nM oAβ (n=8, N=8). C) Left, Summary graph of HFS induced LTP in 0.1% DMSO + 100nM oAβ (n=9, N=13) compared to 1μM C13 + 100nM oAβ (n=8, N=8). (D, E, F) Average LTP magnitudes calculated from the corresponding graphs of last 15 minutes of recordings (as percentage of baseline). All data plotted mean ± S.E.M. (\*) p < 0.05; (\*\*) p < 0.01; (\*\*\*\*) p < 0.0001, by unpaired two tailed t-test. G). Global analysis of average LTP magnitudes of all groups. All data plotted mean ± S.E.M. (\*) p < 0.05, by Approximative Kruskal-Wallis test followed by post-hoc analysis by permutation t-test with false discovery rate correction.

### 5.3.1.4 Quantification of GR reduction in the CA1 of the $GR^{lox/lox} Tg^{-}$ mice upon *in vivo* Cre-GFP transduction

To confirm the data obtained by pharmacological block of GR, the Cre-Lox system was used to specifically ablate GRs in CA1 neurons *in vivo*. Two-month old  $GR^{lox/lox}$  mice were transduced either with the Cre-GFP virus or with the control eGFP virus in the CA1 region of the hippocampus by stereotaxic surgery. The Cre recombinase recognizes the Lox p sequence and cleaves the exon 3 of the GR gene hence producing a non-functional protein (see diagram in Figure 26 of material and methods chapter). These mice were left to recover for 4 weeks after surgery for complete Cre recombinase expression.

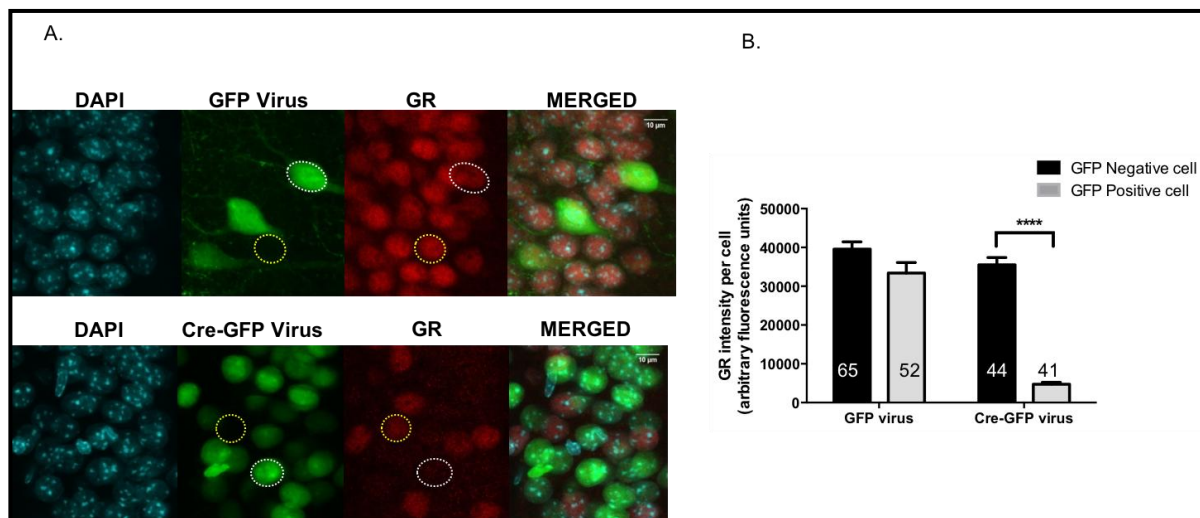


Figure 47: Expression of Cre-GFP and reduction of nuclear GR expression in CA1 of  $GR^{lox/lox}$  mice A). Confocal images of GR immunofluorescence of CA1 cells of mice injected with eGFP (upper panel) or Cre-GFP virus (lower panel). DAPI staining was used as a nuclear marker. B). Intensity of nuclear GR per cell (n=3 mice) calculated by corrected total cell fluorescence (CTCF) method using IMAGE J. Statistical analysis (\*\*\*\*)  $p < 0.0001$  two-way ANOVA and post hoc Tukey's multiple comparison test (negative and positive Cre-GFP cells). All data plotted mean  $\pm$  S.E.M.

To verify if the Cre-Lox system was functional and that the GR protein was efficiently removed after Cre recombination using our *in vivo* procedure, immunofluorescence staining was carried out on eGFP and Cre-GFP transduced hippocampal sections. Sequential images of the CA1 neurons were taken on a confocal microscope at 180x total magnification. The intensities were measured by Image J and the corrected total cell fluorescence (CTCF) technique was used to calculate GR intensity per cell as explained in materials and methods. Figure 47 A represents the images of GR immunofluorescence of the control EGFP positive and their neighbouring negative cells (upper panel) and CRE-GFP positive and neighbouring

negative cells (lower panel). As expected, we noticed a strong reduction of GR expression in the Cre-GFP positive compared to neighbour negative cells ( $P < 0.0001$ , Figure 47B), while there was no significant difference between the eGFP positive and negative cells. Quantitatively, the *in vivo* conditional ablation of the GR gene reduced the nuclear GR protein by approximately 90%. This indicates that our *in vivo* procedure worked well to decrease the GR levels in the CA1 neurons of the hippocampus.

### **5.3.1.5 Effect of GR reduction in CA1 on LTP**

After successful confirmation of reduction in GR expression upon CRE-GFP injections, the next step was to investigate the effect of GR reduction on LTP. Field recordings of high frequency stimulation (HFS) induced LTP were performed on EGFP and Cre-GFP transduced CA1 neurons (Figure 48 A). Only slices with strong EGFP expression within the CA1 pyramidal layer were selected for LTP recordings. There was no difference in the post-LTP responses between the CRE-GFP and EGFP groups (Figure 48B, eGFP:  $185.8 \pm 11.22\%$ ; Cre-GFP:  $178.8 \pm 15.46\%$ ). Hence we conclude that reducing GR in the CA1 region of the hippocampus does not affect LTP.

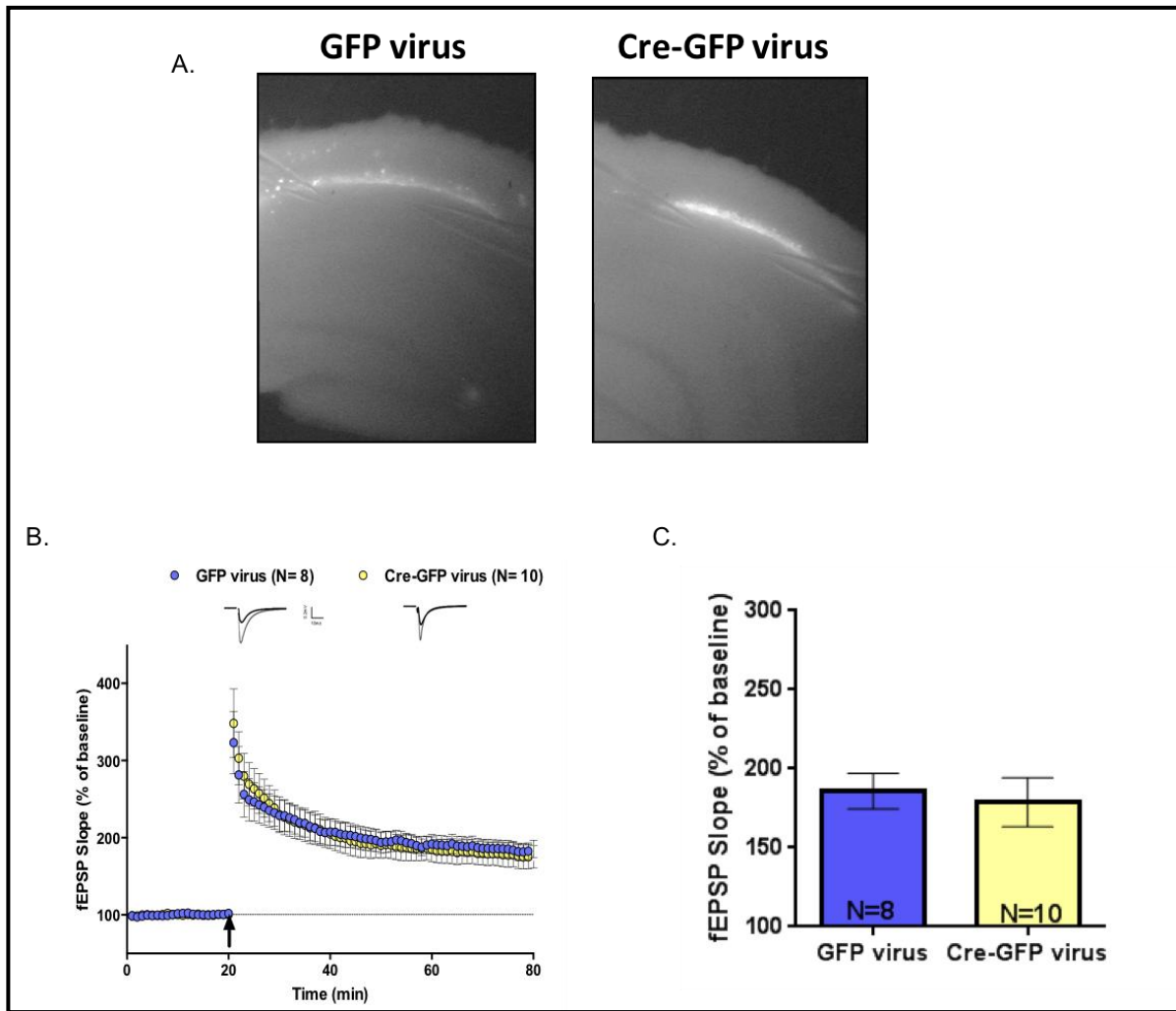


Figure 48: Effect of GR reduction on LTP. A). Representative images of eGFP and Cre-GFP transduced cells in the CA1 region under 10x. B). Summary graph (as percentage of fEPSP baseline) of HFS induced LTP in eGFP (n=8, N=8) and Cre-GFP (n=9, N=10) sections. C). Average LTP magnitude calculated from graph of last 15 minutes of recordings (as percentage of baseline). All data plotted mean  $\pm$  S.E.M.

### **5.3.1.6 Effect of GR reduction in CA1 neurons on the LTP impairment caused by oA $\beta$**

Using pharmacological approach of inhibiting GRs we demonstrated that the oA $\beta$ -mediated LTP impairment was prevented. On a similar line, we checked the acute oA $\beta$  effect on LTP after reducing GRs levels in CA1 neurons in vivo. The effect of soluble oA $\beta$  in inhibiting HFS-induced LTP has been well established and we confirmed this by adding 100nM oA $\beta$  on control eGFP sections (eGFP:  $185.8 \pm 11.22\%$ ; oA $\beta$  +eGFP:  $139.4 \pm 4.91\%$ ;  $p < 0.001$  unpaired t-test) (Figure 49A). However, this oA $\beta$  effect was not seen in GR reduced Cre-GFP sections as shown in Figure 49B (Cre-GFP:  $178.8 \pm 15.46\%$ ; oA $\beta$  + Cre-GFP:  $164.9 \pm 4.39\%$ ; unpaired t-test). To clearly see the difference of the oA $\beta$  effect with or without GR, the graphs were represented together. There was statistical significant difference between the oA $\beta$  + eGFP and oA $\beta$  + Cre-GFP groups (oA $\beta$  + eGFP:  $139.4 \pm 4.91\%$ ; oA $\beta$  +Cre-GFP:  $164.9 \pm 4.39\%$ ;  $p < 0.01$ , unpaired t-test) (Figure 8C and see table below).

For analysis of all groups together (see Figure 49 C), we performed the Approximative Kruskal-Wallis test followed by post-hoc analysis by permutation t-test with false discovery rate correction (see table below). These results indicate two key points, 1). Acute exposure to oA $\beta$  significantly impaired LTP in the control eGFP sections ( $p < 0.05$ ). 2). Upon reducing GRs in the CA1 region, this oA $\beta$ -mediated LTP impairment was not observed ( $p < 0.05$ ). These results indicate that reducing GR expression prevents acute oA $\beta$  effects on LTP.

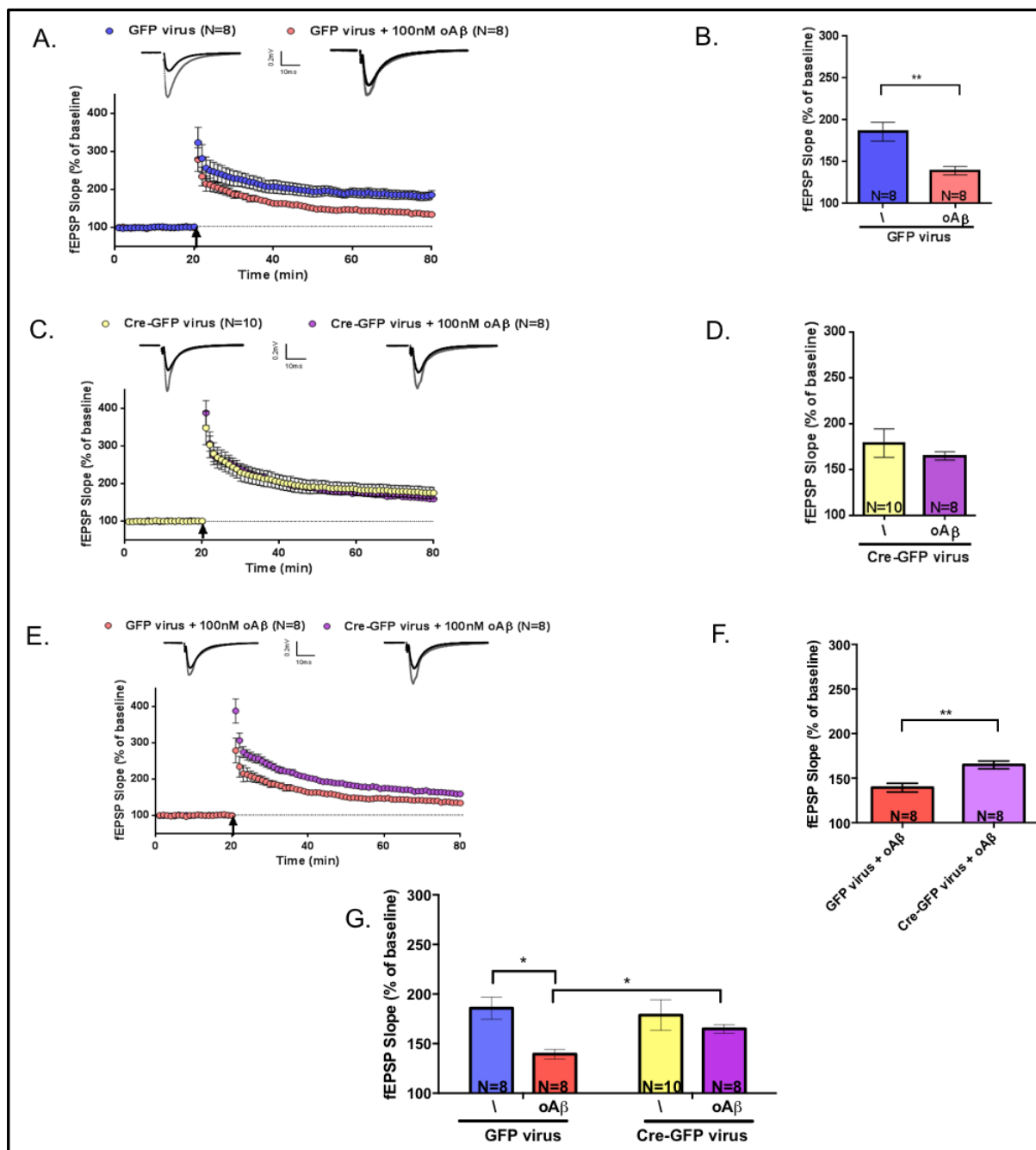


Figure 49: Effect of acute oAβ on eGFP- and Cre-GFP-transduced adult hippocampal sections. A). Left, Summary graph (as percentage of fEPSP baseline) of electrically induced LTP (HFS, arrow) in eGFP transduced slices without (eGFP; n=8, N=8) or with 100nM oAβ (eGFP + 100nM oAβ; n=8, N=8). B). Left, Summary graph of HFS induced LTP in slices transduced with Cre-GFP without (n=9, N=10) or with 100nM oAβ (Cre-GFP+100nM oAβ; n=6, N=8). C) Left, Summary graph of HFS induced LTP in eGFP + 100nM oAβ (n=8, N=8) compared to Cre-GFP + 100nM oAβ (n=6, N=8). (D, E, F) Average LTP magnitudes calculated from graphs of last 15 minutes of recordings (as percentage of baseline). All data plotted mean  $\pm$  S.E.M. (\*)  $p < 0.05$ ; (\*\*)  $p < 0.01$ ; by unpaired two tailed t-test. G). Global analysis of average LTP magnitudes of all groups. All data plotted mean  $\pm$  S.E.M. (\*)  $p < 0.05$ , by Approximative Kruskal-Wallis test followed by post-hoc analysis by permutation t-test with false discovery rate correction.

Collectively, both the pharmacological approach of GR inhibition and the genetic ablation of GR indicate that oA $\beta$  relies on GRs for its synaptic effect on LTP.

### 5.3.1.7 NOR test after oA $\beta$ local injections

After establishing the implication of GRs in the oA $\beta$  effect on LTP, we were interested to check their functional relationship at an integrative level of memory. In collaboration with Dr. Bethus, we opted to check for Novel Object Recognition Test (NOR), since this is hippocampus-dependent memory test. It is widely used for evaluating memory in AD mouse model and is based on spontaneous animal behaviour without the need of any stressor element.

It was first important to optimize a protocol with which one would observe that acute oA $\beta$  intra-hippocampal injections could cause an immediate memory deficit phenotype, as no such protocol was available in the team. This type of approach was already published, albeit with differences by other investigators. Indeed, a study by Balducci et al., 2010 showed that single icv injection of nanomolar concentration of A $\beta$  during learning in the object recognition task impaired memory consolidation within 24 hours of testing and hence we decided to use similar time points. For the concentration of the oA $\beta$ , we purposefully remained in the similar condition of electrophysiology but injected twice 100nM with a 10 minute interval.

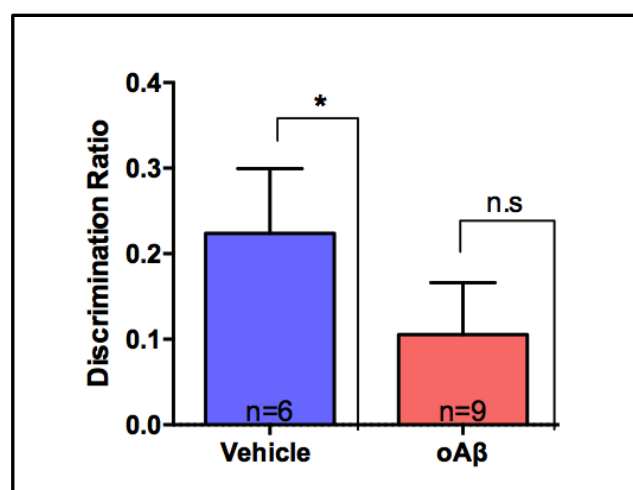


Figure 50: Discrimination ratio for oA $\beta$  versus vehicle mice. oA $\beta$  treated mice display a decreased discrimination ratio for the novel object as compared to the vehicle group using the novel object recognition test. Data plotted mean  $\pm$  S.E.M. (\*)  $p < 0.05$

We obtained a small difference in the discrimination ratio of the novel object in the oA $\beta$  treated animals as compared to the vehicle. Using one sample t-test, we proved that the discrimination ratio for the vehicle group was statistically significant from the chance level (Vehicle: 0.22; chance level: 0;  $p < 0.05$ ) while not for the oA $\beta$  group (oA $\beta$ : 0.11; chance level: 0;  $p > 0.05$ , see Figure 50). With this, we could interpret that, while the vehicle treated animals could discriminate the novel object, oA $\beta$  treated animals could not suggesting memory impairment. We need to repeat more experiments to confirm this memory deficit, after which we will test if the GR antagonist C13 could prevent this oA $\beta$ -mediated memory deficit.

Table 1: Table for unpublished data from Chapter 3

| Experiment                               | Treatment/Virus      | # Animals | # Slices | Measurement  | Average | s.e.m | Statistical test           | p value | Post-hoc                         | Figure |
|--|----------------------|-----------|----------|--------------|---------|-------|----------------------------|---------|----------------------------------|--------|
| C13 IEPSP                                | 0.1% DMSO            | 26        | 32       | last 5 mins  | 105.1   | 0.14  | unpaired two-tailed t-test | p<0.001 |                                  | 45 A   |
|  | 1µ M C13             | 20        | 23       |              | 96.87   | 0.36  |                            | p<0.001 |                                  | 45 B   |
| C13 LFS-LTP                              | 0.1% DMSO            | 11        | 13       | last 15 mins | 155.3   | 6.1   | unpaired two-tailed t-test | p>0.05  |                                  | 45 C   |
|  | 1µ M C13             | 10        | 15       |              | 148     | 6.77  |                            |         |                                  |        |
| oAβ LFS-LTP                              | 0.1% DMSO            | 11        | 13       | last 15 mins | 155.3   | 6.1   | unpaired two-tailed t-test | p<0.01  |                                  | 46 A   |
|  | 100nM oAβ            | 9         | 10       |              | 130.7   | 1.5   |                            |         |                                  |        |
| oAβ+ C13 LFS-LTP                         | 1µ M C13             | 10        | 15       | last 15 mins | 148     | 6.77  | unpaired two-tailed t-test | p>0.05  |                                  | 46 C   |
|  | 1µ M C13 + 100nM oAβ | 8         | 8        |              | 147.9   | 2.27  |                            |         |                                  |        |
| oAβ vs oAβ+ C13 LFS-LTP                  | 100nM oAβ            | 9         | 10       | last 15 mins | 130.7   | 1.5   | unpaired two-tailed t-test | p<0.001 |                                  | 46 E   |
|  | 1µ M C13 + 100nM oAβ | 8         | 8        |              | 147.9   | 2.27  |                            |         |                                  |        |
| oAβ LFS-LTP                              | 0.1% DMSO            | 11        | 13       | last 15 mins | 155.3   | 6.1   | App. Kruskal- Wallis Test  | p<0.05  | permutation t-test with FDR      | 46 G   |
|  | 100nM oAβ            | 9         | 10       |              | 130.7   | 1.5   |                            |         | 0.018                            |        |
| oAβ+ C13 LFS-LTP                         | 1µ M C13             | 10        | 15       | last 15 mins | 148     | 6.77  | App. Kruskal- Wallis Test  |         | permutation t-test with FDR      |        |
|  | 1µ M C13 + 100nM oAβ | 8         | 8        |              | 147.9   | 2.27  |                            |         | 0.966                            |        |
| oAβ vs oAβ+ C13 LFS-LTP                  | 100nM oAβ            | 9         | 10       | last 15 mins | 130.7   | 1.5   | App. Kruskal- Wallis Test  |         | permutation t-test with FDR      |        |
|  | 1µ M C13 + 100nM oAβ | 8         | 8        |              | 147.9   | 2.27  |                            |         | 0.012                            |        |
| Cre-GFP LFS-LTP                          | eGFP                 | 8         | 8        | last 15 mins | 185.8   | 11.22 | unpaired two-tailed t-test | p>0.05  |                                  | 48 B   |
|  | Cre-GFP              | 9         | 10       |              | 178.8   | 15.46 |                            |         |                                  |        |
| oAβ eGFP LFS-LTP                         | eGFP                 | 8         | 8        | last 15 mins | 185.8   | 11.22 | unpaired two-tailed t-test | p<0.01  |                                  | 49 A   |
|  | eGFP + oAβ           | 8         | 8        |              | 139.4   | 4.91  |                            |         |                                  |        |
| oAβ Cre-GFP LFS-LTP                      | Cre-GFP              | 9         | 10       | last 15 mins | 178.8   | 15.46 | unpaired two-tailed t-test | p>0.05  |                                  | 49 C   |
|  | Cre-GFP + oAβ        | 6         | 8        |              | 164.9   | 4.39  |                            |         |                                  |        |
| oAβ eGFP vs oAβ Cre-GFP LFS-LTP          | eGFP + oAβ           | 8         | 8        | last 15 mins | 139.4   | 4.91  | unpaired two-tailed t-test | p<0.01  |                                  | 49 E   |
|  | Cre-GFP + oAβ        | 6         | 8        |              | 164.9   | 4.39  |                            |         |                                  |        |
| oAβ eGFP LFS-LTP                         | eGFP                 | 8         | 8        | last 15 mins | 185.8   | 11.22 | App. Kruskal- Wallis Test  | p<0.05  | permutation t-test with FDR      | 49 G   |
|  | eGFP + oAβ           | 8         | 8        |              | 139.4   | 4.91  |                            |         | 0.012                            |        |
| oAβ Cre-GFP LFS-LTP                      | Cre-GFP              | 9         | 10       | last 15 mins | 178.8   | 15.46 | App. Kruskal- Wallis Test  |         | permutation t-test with FDR      |        |
|  | Cre-GFP + oAβ        | 6         | 8        |              | 164.9   | 4.39  |                            |         | 0.638                            |        |
| oAβ eGFP vs oAβ Cre-GFP LFS-LTP          | eGFP + oAβ           | 8         | 8        | last 15 mins | 139.4   | 4.91  | App. Kruskal- Wallis Test  |         | permutation t-test with FDR      |        |
|  | Cre-GFP + oAβ        | 6         | 8        |              | 164.9   | 4.39  |                            |         | 0.012                            |        |
| GR intensity/cell injected GFP virus     | GFP neg cell         | 3         | 65       | 4 weeks      | 39567.8 | 1883  | Two way ANOVA              | n.s.    | Tukey's multiple comparison test | 47 B   |
|  | GFP pos cell         |           | 52       |              | 33385.2 | 2728  |                            |         |                                  |        |
| GR intensity/cell injected Cre-GFP virus | GFP neg cell         | 3         | 44       | 4 weeks      | 35525.1 | 18889 | Two way ANOVA              | p<0.001 | Tukey's multiple comparison test | 47 B   |
|  | GFP pos cell         |           | 41       |              | 4708.9  | 537.6 |                            |         |                                  |        |
| Novel Object Recognition Test            | DMSO                 | 6         |          | 10 mins      | 0.22    | 0.07  | unpaired two-tailed t-test | p<0.05  |                                  | 50     |
|  | oAβ                  | 9         |          | 10 mins      | 0.11    | 0.06  |                            | p>0.05  |                                  |        |

---

## 5.4 Chapter 4

In addition to studying A $\beta$  and its relationship to GRs at synapses, I participated in a collaborative study with Dr Willem and Dr Haass, Ludwig-Maximilians University Munich, DZNE, Munich, Germany). These collaborators had discovered the existence of a new APP pathway that generates new types of peptides that they called A $\eta$ - $\alpha$  or A $\eta$ - $\beta$ . Nothing was known about how these peptides modulated brain functions (Willem et al., 2015). We therefore investigated, if these peptides (A $\eta$ - $\alpha$  or A $\eta$ - $\beta$ ) could impact basic synaptic transmission and LTP.

### 5.4.1 Discovery of $\eta$ -secretase APP processing pathway

In brief, a new physiological cleavage of the APP by the  $\eta$ -secretase at amino acid 504-505, produces a new C terminal fragment (CTF) called CTF- $\eta$  of molecular mass 30 kilodaltons. This is further processed by  $\alpha$ -secretase and  $\beta$ -secretase to release A- $\eta$  long and short peptides (termed A $\eta$ - $\alpha$  or A $\eta$ - $\beta$ ), respectively (see in Annexe supplementary fig 1 of Willem et al., 2015). Since these cleavage products were seen to be enriched in dystrophic neurites in human AD brains, we verified if they interfered with neuronal function like oA $\beta$  and hence checked their effect on synaptic transmission and LTP.

### 5.4.2 Aim 4: Effect of CHO derived A $\eta$ - $\alpha$ and A $\eta$ - $\beta$ peptides on LTP

To validate the potential effect of A $\eta$  peptides on synaptic transmission and LTP, Dr Willem produced CHO cells expressing cDNAs encoding either A $\eta$ - $\alpha$  or A $\eta$ - $\beta$  sequences. He collected the medium of these cells and purified fractions enriched in these peptides by size-exclusion chromatography (SEC) (see below in Annexe (Willem et al., 2015) for full details). After general rounds of optimization to use these types of samples on *ex vivo* hippocampal slices, we could investigate how these media enriched with either peptide would modulate synapse function. These media were applied to hippocampal slices of 3-4 week old Swiss mice. To study basic synaptic transmission, we waited for a 20 minute baseline in standard ACSF and then applied either control medium (CHO) or medium enriched in either peptide

(CHO A $\eta$ - $\alpha$ ; CHO A $\eta$ - $\beta$ ) for another 20 minutes. We did not observe significant alterations of basic synaptic transmission in presence of these media (Figure 51).

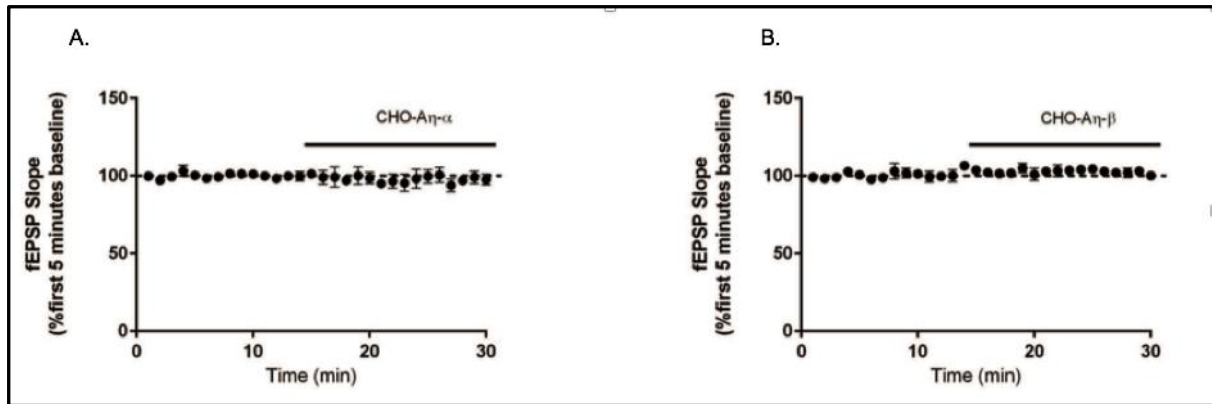


Figure 51: Effect of A $\eta$ - $\alpha$  (n=4) or A $\eta$ - $\beta$  (n=4) on baseline activity at the CA3-CA1 synapse. A) SEC fractions containing A $\eta$ - $\alpha$  were diluted (1:15) in ACSF and were perfused on mouse hippocampal slices after obtaining a 15 min baseline. Baseline recordings were carried out thereafter for the next 15 minutes. B). Similar protocol was followed for SEC fractions containing A $\eta$ - $\beta$ . These results are published in (Willem et al., 2015).

We next checked if these media could modulate LTP. We first obtained a stable fEPSP baseline and applied the medium for 20 minutes before LTP induction. We then applied an HFS protocol (2x100Hz at 20 sec inter-stimulus interval) and monitored LTP for another hour.

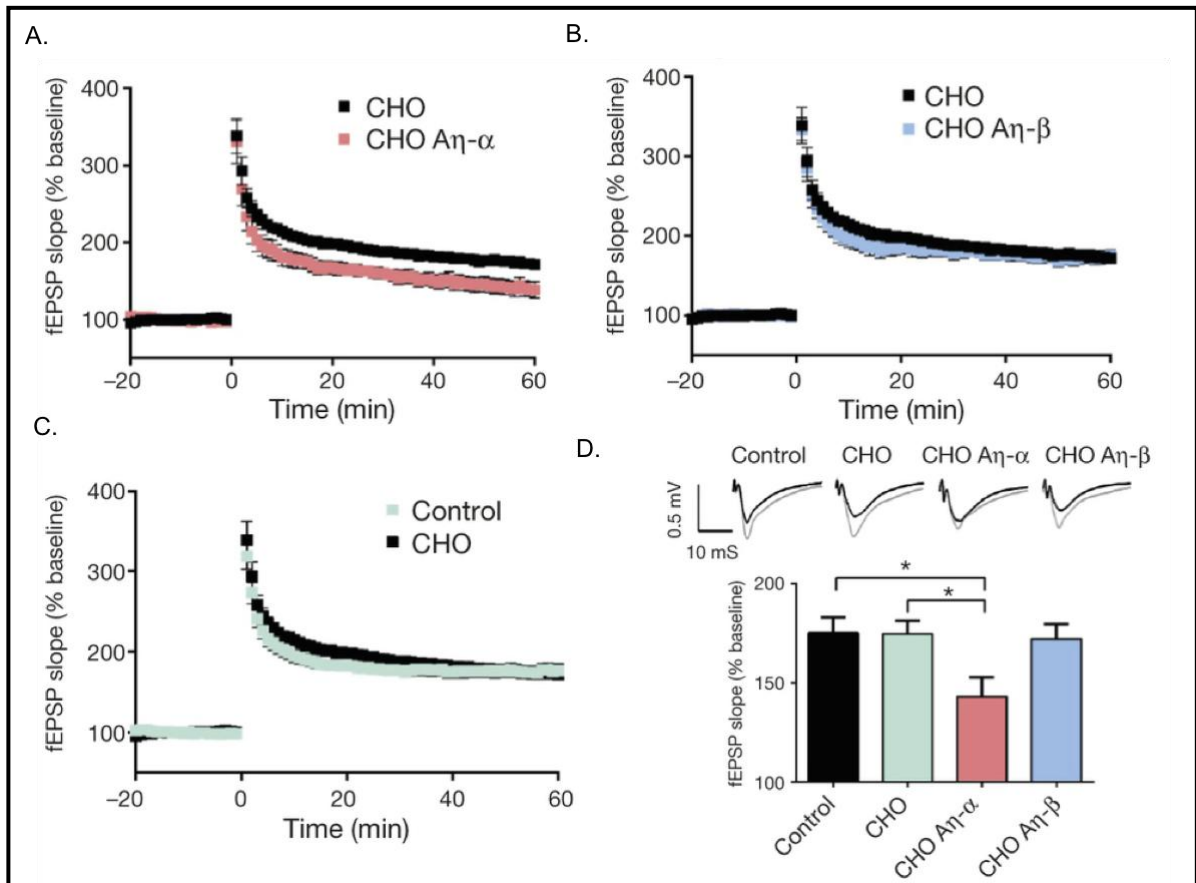


Figure 52: A $\eta$ - $\alpha$  impairs LTP. A) Summary graph (as percentage of fEPSP baseline) of electrically induced LTP in presence of A $\eta$ - $\alpha$  peptide (n=9) or B). A $\eta$ - $\beta$  peptide (n=7) or C). control ACSF (n=15) compared to conditioned media from untransfected cells (CHO; n=13). D). Average LTP magnitudes calculated from graphs of last 15 minutes of recordings (as percentage of baseline). All data plotted mean  $\pm$  S.E.M. (\*) p < 0.05; by unpaired two tailed t-test. These results are published in (Willem et al., 2015).

We observed that A $\eta$ - $\alpha$  but not A $\eta$ - $\beta$  lowered LTP magnitude. Thus, these results show that this novel  $\eta$ - secretase processing of APP produces A $\eta$ - $\alpha$  peptide, which harbours synapse modulating properties.

In this study, we also collaborated with Drs Busche and Konnerth (Technische Universität München, Munich, Germany) who demonstrated that this A $\eta$ - $\alpha$  peptide also modulates hippocampal calcium transients *in vivo* (Willem et al., 2015).

Together these data strongly suggest a neuromodulatory and possibly pathological role of this newly discovered APP peptide in the brain.

## 6 Discussion and Perspectives

### *HPA axis dysregulation in early onset of AD and its effects*

In Chapter 1, we have used the early-symptomatic AD mouse model Tg<sup>+</sup>, which chronically over-expresses APP leading to an accumulation of A $\beta$  and APP derived products in the brain. Here, we show that, at the onset of functional and behavioural symptoms (4 months), these mice show an increased production of CORT and a dysregulated feedback mechanism. It is important to note here that these mice produce high CORT levels *without any exposure to external stressors*. A similar phenotype has been evidenced in early 3xTg mice, which have an over-activated central HPA axis (Hebda-Bauer et al., 2013). The etiology of this dysfunction of the HPA axis in these models is not known and hence to address this we studied the different hormones and organs implicated in the HPA axis in the Tg<sup>+</sup> model.

4 months represents the onset of the increase in CORT levels in the AD Tg<sup>+</sup> mouse model. I contributed to show that the plasma CORT levels (during active phase) in Tg<sup>+</sup> mice, while still normal at 3 months, significantly increases at 4 months and persist even at 6 months of age. This increase in CORT suggests hyperactivity of the HPA axis in agreement with what has been seen in AD patients (Elgh et al., 2006) and in other transgenic AD mouse models (Hebda-Bauer et al., 2013). My team obtained other results regarding CORT regulation at the 4 months' time-point in this model. They also showed that the circadian plasma level variations of CORT are preserved in these mice (Figure 1 of (Lanté et al., 2015)), suggesting that aspect of HPA axis regulation is still intact. They also showed that this CORT level difference between Tg<sup>+</sup> and WT mice is remarkable only during the active phase (20:00), and not the rest phase (8:00). This suggests that basal maintenance of GC levels (levels that would activate MRs) is maintained in these mice. Finally, they observed a dysregulation in the negative feedback mechanism, as evidenced by the Dexamethasone Suppression Test. After Dexamethasone injections, CORT levels remained elevated in Tg<sup>+</sup> mice instead of returning to basal levels as observed in the WT (Lanté et al., 2015).

Report of high presence of different soluble oligomers observed in 4 month Tg<sup>+</sup> mice (Mustafiz et al., 2011) can help us predict a correlation between progressive increase of A $\beta$  oligomers evident during this early phase and onset of HPA axis dysregulation, but direct implication of A $\beta$  in this phenotype was not addressed concretely.

High CORT levels in the Tg<sup>+</sup> mice at 6 months of age decrease the weight of the thymus glands. It is well known that in chronic stress profound atrophy of the thymus is seen, hence indicating that chronic elevation of CORT in the Tg<sup>+</sup> mice mimic this metabolic phenotype of chronic stress (Scollay and Shortman, 1983).

***Decrease in ACTH levels in the Tg<sup>+</sup> mice at 6 months and the dissociation with CORT production***

Having observed this hypercortisolemia in the Tg<sup>+</sup> mice at 4 months of age, we attempted to determine whether this deregulation would be related to the ACTH. Our results show that at 4 months, during the awakening phase, the plasma concentrations of ACTH is not different from that of WT, while at 6 months ACTH levels decreased in the Tg<sup>+</sup> mice. This decrease is consistent with clinical data in patients with early AD onset, which show low ACTH levels or absence of increased ACTH drive (Umegaki et al., 2000, Näsman et al., 1995). Concurrently, reports have shown that adrenal sensitivity to ACTH enhanced in AD due to HPA axis hyperactivity (O'Brien et al., 1996). This might be one reason as to why we don't see increase in adrenal gland weight in the Tg<sup>+</sup> mice in spite of high production of CORT. In addition, low levels of ACTH in the Tg<sup>+</sup> mice or in AD patients could be associated to an increased central drive by CRH. This could be due to downregulation of the pituitary receptors or due to increased sensitivity of the adrenal gland to ACTH (as seen in the Gr<sup>NesCre</sup> mice (Tronche et al., 1999), but we have not tested these hypotheses.

On merging the CORT and ACTH data, we see that there is a divergence between the two i.e. the high levels of CORT are not due to high levels of ACTH. But this divergence is not uncommon, and has been seen in AD patients and mouse models (Bornstein et al., 2008, Tronche et al., 1999). There are numerous studies which have indicated large number of factors for example neuropeptides, neurotransmitters, growth factors, etc. capable of modulating GC release independently of pituitary ACTH (Ehrhart-Bornstein et al., 1998) (see Figure 53).

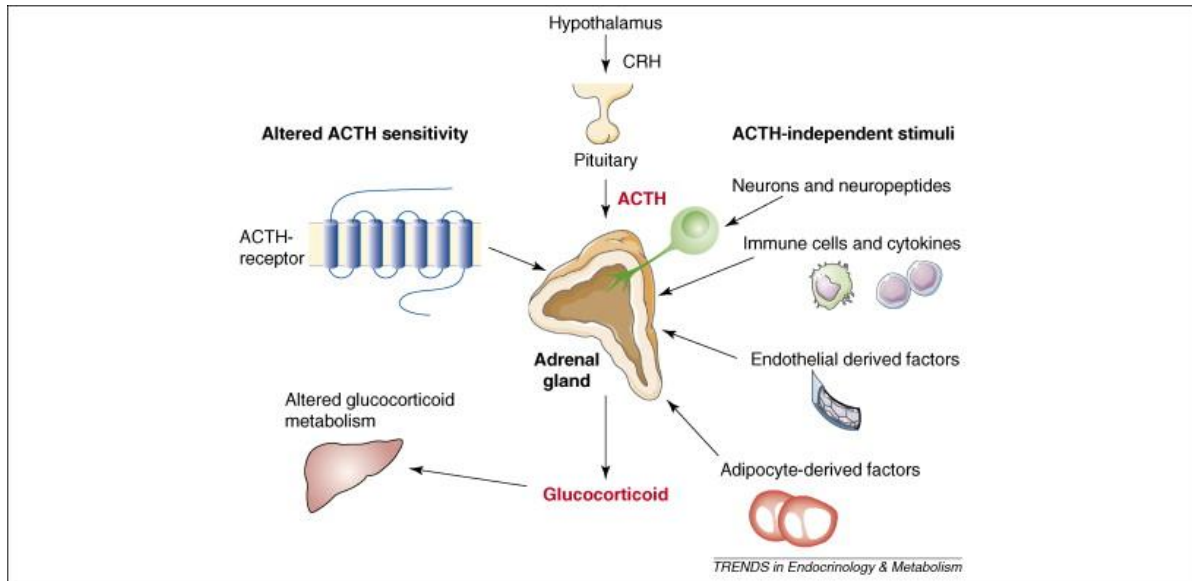


Figure 53: Possible pathways contributing to the dissociation of ACTH and GC levels. Adrenal secretion of GCs is dependent on pituitary ACTH release, which is triggered by hypothalamic CRH release. However, there are certain cases, GC production is dissociated from ACTH levels. This can be due to altered sensitivity of the adrenal cortex to ACTH, through the ACTH receptor. In addition, ACTH-independent stimuli influence the adrenal GC synthesis and release. These include innervation of the gland and neuropeptides released from neurons and adrenomedullary cells, interaction with the immune system through release of cytokines, release of paracrine factors and adipocyte derived factors. In addition, GC levels are regulated by GC metabolism in the liver (Bornstein et al., 2008).

### ***Effect of HPA axis dysregulation on GRs in the hippocampus***

Normally, when CORT levels are high, the auto-regulatory system of the steroid receptor works to decrease their numbers to bring the system back to homeostasis. This is also explained by the GC cascade hypothesis, perhaps as an adaptation to prevent GC-induced damage (Sapolsky et al., 1984).

We demonstrate that total GR levels (which include cytoplasmic, nucleic, and membrane GRs) do not change in the hippocampus of the Tg<sup>+</sup> and WT mice at 4 months of age. These results are consistent with data from AD patients which show that GR levels are maintained. This is believed to be due to the unaltered circadian rhythm of cortisol secretion, which may be a factor for maintaining the hippocampal GR numbers (Seckl et al., 1993, Wetzel et al., 1995).

Our results do not match those from the 3-4-month-old 3xTg AD mouse models, which show early activated HPA axis characterised by elevated mRNA levels of GR in the CA3 and DG sub-regions of the hippocampus (Hebda-Bauer et al., 2013). However, these results cannot be compared adequately as the AD mouse models are different and the GRs are studied in

different tissue preparations (CA3/DG vs total hippocampus) and using different protocols (mRNA vs protein).

Knowing that GRs are multifunctional receptors, they have different roles depending on their location i.e. nucleus, cytoplasm and the membrane. Hence to further understand their role at the synapses, Dr Frandemiche in the team isolated hippocampal PSDs of 4 months of Tg<sup>+</sup> mice and quantified GR levels. She observed a decrease in GR expression at the PSD of the Tg<sup>+</sup> mice (data not shown), which could be related to the lesser number of neurons/synapses present due to chronic exposure of CORT in the hippocampus.

A separate study could be conducted to isolate GRs from the nucleus and cytoplasm of the Tg<sup>+</sup> and WT mice. This would give additional information on the activity of these receptors, which could be expressed as a ratio of nuclear: cytoplasmic GRs.

#### ***Episodic memory deficit in 4 month Tg<sup>+</sup> mice and rescue by sub-chronic GR antagonist treatment***

We provide evidence of an early impairment in episodic-like memory in four-month-old Tg<sup>+</sup> mice, correlating this phenotype to early A $\beta$  oligomer aggregation but prior to plaque formation (Hsiao et al., 1996). This study is important as there are few studies which have tested episodic-like memory in AD mouse models and only at more advanced stages of AD (Baglietto –Vargas., 2013; Davis., et al. 2013; Good et al., 2007). This type of elaborated behavioral paradigm is very useful as it encompasses the “what”, “when” and “where” components of human episodic memory. Hence, it could be more readily used in pre-clinical studies to provide more adequate relevance while testing for new therapies for AD.

We also proved that a four-day treatment of sub-chronic antagonism of GR (with RU486) was sufficient to rescue memory impairment. In addition, my team obtained interesting results showing that exacerbated LTD in the Tg<sup>+</sup> mice were also rescued by RU486 but only after 4 days of sub-chronic treatment and not acutely or after 2 days (Lante et al., 2015). This suggests that *in vivo* RU486 treatment might involve the GR-dependent genomic effects which may be necessary to reset a homeostatic balance of CORT signalling in Tg<sup>+</sup> mice. This sub-chronic RU486 treatment is also serving as an advantage to avoid the side effects of prolonged GR blockage (Morgan and Laufgraben, 2013) and hence, these results are more promising than the previous study, which reports that at an advanced AD pathological state, 3 weeks of RU486 GR antagonist could reverse the memory impairment (Baglietto-Vargas et

al., 2013). It is important to point that despite the number of hippocampal GR not changing between the Tg<sup>+</sup> and the WT, the GR antagonist could rescue the early AD episodic-like memory deficits. Probably, the GR activity and sensitivity is high in the hippocampus due to either hypercortisolemia condition or its interaction with the amyloid- $\beta$  peptides. Hence, inhibition of this excess GR activity could rescue the memory deficit by RU486. Since we are aware of the unspecific binding of RU486 on progesterone receptors, it would be important to repeat with the more specific GR antagonist C13.

In conclusion, as shown in the summary Figure 54, there is a dysregulation of the HPA axis as seen with high CORT levels and the non-functional feedback mechanism. ACTH levels are decreased at 6 months of age and there is a dissociation between the ACTH and CORT levels. GR levels in the Tg<sup>+</sup> in the hippocampus were not changed despite the high levels of CORT. This excessive GR activity is involved in the episodic-like memory deficits and can be rescued with short GR antagonist treatment.

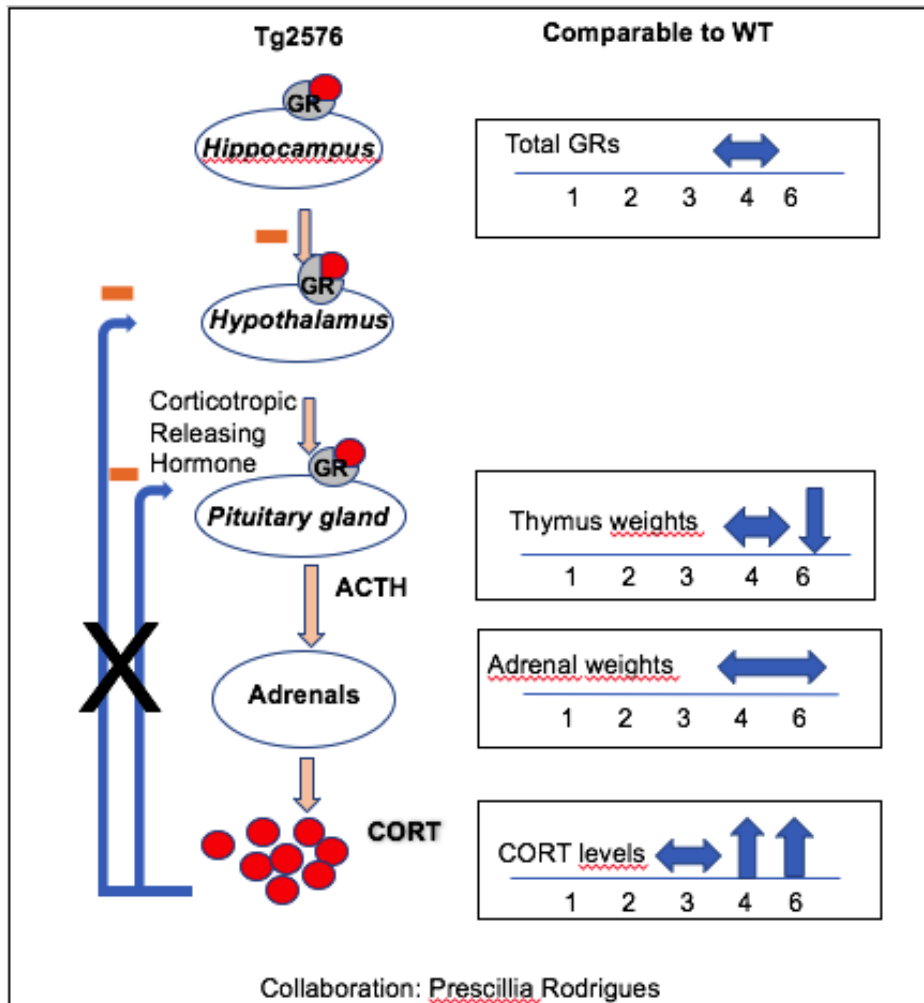


Figure 54: Summary of HPA axis alterations in Tg2576 AD mouse model. High levels of CORT are produced at 4 and 6 months. There is a dysregulation of the negative feedback mechanism using the Dexamethasone suppression test (black cross). No change in adrenal gland weight at 4 and 6 month. Decrease in thymus weight at 6 months. Total hippocampal GRs do not change at 4 months in the Tg<sup>+</sup> mice. All these are in comparison to the same aged WT mice.

### ***Severe phenotypes seen upon breeding the Tg<sup>+</sup> and GR<sup>lox/lox</sup> mice***

To have a clearer idea of the functional role of GR in AD in the hippocampus, especially the CA1, we decided to generate the conditional ablation model of GR within the AD Tg2576 model by crossing the Tg<sup>+</sup> with the GR<sup>lox/lox</sup> mice. This model was viewed as a novel AD model, which would make it easier to manipulate the GRs *in vivo* in specific regions of the brain. Hence in Chapter 2, we generated the double mutant GR<sup>lox/lox</sup> Tg<sup>+</sup> mice to understand better the role of GR specific activity in early AD onset phenotypes like episodic-like memory and synaptic deficits. These mice harboured the hAPP<sup>swe</sup> transgene along with the GR floxed gene.

We had to wait till the third generation to obtain the double mutant mice and thus the entire breeding process took around a year. This made us speculate that maybe the transgene and the GR<sup>lox/lox</sup> allele were in close proximity making their crossing over less probable. There was a difference in size and body weight between the GR<sup>lox/lox</sup> Tg<sup>+</sup> and its control, suggesting abnormal development. In addition, the double mutant mice had a low survival rate, which indicates that harbouring dual mutation leads to increased lethality. These double mutant mice exhibited exacerbated phenotypes like high CORT levels from weaning period and exacerbated LTD phenotype. Despite these drawbacks, we injected the Cre-GFP virus by stereotaxic method to reduce the GR levels *in vivo* in the hippocampus. However, the number of deaths increased after these injections making it difficult to continue using these mice.

Similarly, a review by Sigmund also highlighted the several problems faced while using transgenic mice (Sigmund, 2000). The major problem is the genetic heterogeneity among the different mice strains, because each transgenic founder mice is different from every other founder. The second issue specifically related to transgenic mice is the position effect. Due to random nature of the transgene insertion, each resultant founder contains the transgene at a different site in the genome. These can profoundly affect transgene expression and therefore the observed phenotype. This is due to presence of transcriptional regulatory elements near the site of insertion of the transgene, which could change the normal transcription of the transgene.

However, in our case, we are not sure of the exact cause for these exacerbated phenotypes and increased deaths in the double mutant mice, but speculate on the two points mentioned below:

- There could be a genetic incompatibility of the hAPP<sub>swe</sub> transgene in the hybrid background as suggested already by Carlson et al., 2007, and not due to the expression of the transgene or oligomers aggregation *per se*.
- The position of the transgene is not known and could insert into important genes disrupting some basal functions (explained as above). Also, the interaction of the GR<sup>lox/lox</sup> allele and the transgene could lead to developmental issues.

Unfortunately, due to the uncertainty of obtaining enough mice to obtain pertinent results with these double mutant mice within the time remaining of the thesis, it was decided to stop using these mice.

Development of congenic mice could be a safer idea to reach our goal of creating double mutant mice harbouring both AD phenotype and GR<sup>lox/lox</sup>. A congenic strain is one that is genetically identical to a control strain except for the single region of one chromosome i.e. the inserted transgene. Although the generation of congenic mice is simple it is time consuming. It is important to note that at least six generations of backcross breeding are required before the genetic background is statistically > 99% homogenous.

There have been additional disadvantages associated specifically with AD transgenic mouse models and Saito et al., 2014 well identifies these artifacts. There is over-production of A $\beta$  but also over-production of APP itself and other APP fragments like CTF- $\beta$  and AICD, which themselves harbour bioactivities. To address these questions in particular, Saito et al., 2014 produced 3 knock-in APP mice on C57Bl/6 background, which have humanized A $\beta$  sequence and familial AD-associated mutations into the endogenous mouse APP locus. There are advantages with these mice as they are made on pure C57Bl/6 background and not on a mixed one. In addition, one of the three KI mice is their negative control, which is very relevant as it makes the mice suitable to study only the high production of A $\beta$ <sub>42:40</sub> ratio and not the other APP processing fragments. These mice could be an alternative to the Tg<sup>+</sup> mice we used in our study, which seem to be overly sensitive due to their mixed background. Also, since the GR<sup>lox/lox</sup> are originally from the pure C57/Bl6 background, there would be less chances of genetic incompatibility when crossing with these new KI mice.

### ***Relationship between A $\beta$ oligomers and GR***

In Chapter 3, we correlate the relationship between A $\beta$  oligomers and GRs at the molecular and cellular levels. In the literature, there is very little evidence about a functional interaction of A $\beta$  and GRs at the synapses. Brureau et al., 2013 have shown that A $\beta$ <sub>(25-35)</sub> intracerebroventricular injections to the CA1 increased the concentration of GR in the nucleus. This data suggest that nuclear GR are affected by A $\beta$ , but there is a paucity of data explaining the relation of oA $\beta$  and GRs at the synapses.

In the team, Dr Frandemiche has shown that A $\beta$ <sub>1-42</sub> requires GRs to mediate some of its effects on synapses. She had previously shown that upon acute treatment of 100nM oA $\beta$  on primary cortical neurons, synaptic proteins like PSD-95, Actin and GluA1 are upregulated in the PSDs (Frandemiche et al., 2014). Similarly, using hippocampal neurons cultures, we

observed an increase in these synaptic proteins with acute treatment of 30 minutes of 100nM A $\beta$  (data not shown). In addition, she observed that inhibiting GRs with the Compound 13 or RU486 prevented some of these effects, especially A $\beta$ -dependent recruitment of PSD95 to the PSD (data not shown). Together with Dr Frandemiche, we also provide novel data that a similar preparation and concentration of oA $\beta$  treatment increases the GR levels in the PSD of cultured hippocampal neurons (Figure 44). Collectively, these data suggest a functional relationship between A $\beta$  and GR at excitatory synapses. We need to further investigate if there is a direct physical interaction between the two. However, due to the sticky nature of oA $\beta$ , it would be difficult to perform interaction studies between the A $\beta$  and GRs like analysis of GR binding using fluorescence polarisation assay or by FRET. Also, functionally, both CORT and A $\beta$  act on the glutamatergic system and hence we could check if specific action of AMPAR and/or NMDAR are involved in their interaction. There are further prospects of speculation on the involvement of ERK intracellular signalling and other secondary messenger systems in their interaction (Chen et al., 2012).

The next question is to understand the role of the elevated GRs in the PSDs. Till date, GRs are identified in the PSD as well as dendritic spines of the amygdala (Johnson et al., 2005). It is not clear if the GRs present in PSD are same as membrane GRs (mGRs). Recent findings have shown that mGRs are located in synapses and surrounding space of rapidly plastic dendritic spines and their activation leads to rapid changes in spine size and number, while mMRs are linked to receptor trafficking and regulation of synaptic transmission (Prager et al., 2010). Collectively, mMR and mGR mediate rapid regulation of synaptic structure and function is central for learning and memory. However, for the moment, we cannot conclude as to the functional role of the A $\beta$ -mediated increase of GRs within the PSD.

### ***Role of GRs on LTP***

It is well known that, in presence of high dose of CORT/ stress, there is reduction of LTP in the different regions of the hippocampus. On similar lines, using pharmacological agents like GR and MR agonists/ antagonists, it was shown that activation of MRs produce LTP enhancement, which was abolished by pre-injections of MR antagonist RU318, while activation of GRs produces a potent suppression in LTP which was prevented by pre-treatment with GR antagonist RU486 (Pavlidis et al., 1995). These studies demonstrate that GRs within the hippocampus negatively modulate hippocampal LTP.

We, however, observed that blocking GRs using the highly selective GR antagonist C13 at 1 $\mu$ M, did not modify basal synaptic transmission and LTP. In our *ex vivo* conditions, which mimics absence of stress, the CORT occupation of GR and MR should be approximately 10% and 90%, respectively (Reul and de Kloet, 1985). We could presume that in this context, if MR mediates a positive effect on LTP, then blocking of GR during non-stress conditions should be insufficient to alter hippocampal function. In contrast to this prediction, behavioural experiments on adrenalectomised rats given MR agonist aldosterone performed well on Y maze, while intact rats injected with the GR antagonist RU555 performed poorly (Conrad et al., 1999). This data shows that preventing GR activation, even in the presence of functional MRs, impair hippocampal function. To investigate further, we could increase the concentration of C13, if 1 $\mu$ M was too low to reveal the actual effect of GR on LTP *per se*. But a lack of effect of C13 *per se* at this concentration was ideal to further study its effect on A $\beta$ -mediated LTP impairment as it avoided introduction of confounding variables for linear interpretation of the results.

#### ***GR antagonist prevents A $\beta$ effects on LTP***

Frاندemiche et al., 2014 demonstrates that synaptic activation in the presence of oA $\beta$  did not lead to the expected increased levels of PSD95 or GluA1 in the PSD fraction in cultured neurons (data not shown). This prevented the long-lasting modification of synaptic strength, which is also validated with exhaustive *ex vivo* data show that oA $\beta$  acutely impairs LTP in hippocampus slices (Shankar et al., 2007, Townsend et al., 2006, Walsh et al., 2002). We report similar results, which show that 100nM oA $\beta$  impair LTP in the CA1 of the hippocampus. This preparation of oA $\beta$  mainly consists of a mixture of monomers, dimers, trimers (majorly) and some tetramers and oligomers (as prepared in Frاندemiche et al., 2014), so we cannot conclude as to exactly which species of A $\beta$  mediates this LTP impairment in this experiment. My team has, however, also observed this LTP deficit using a preparation consisting of only dimers of A $\beta$  (data not shown) (Willem et al. 2015) and others have not seen effects of monomeric A $\beta$  on LTP (Selkoe, 2008), suggesting that dimers and higher oligomers may be the main mediators of this A $\beta$ -induced synaptic modulation.

There are multiple interacting partners/receptors involved with A $\beta$  and their contribution to this synaptic impairment is not conclusive. For example, AMPAR, NMDAR, nAChR, etc are interacting partners of A $\beta$ , and are involved in LTP effects.

As we had uncovered a functional relationship between A $\beta$  and GRs at synapse in cultured hippocampal neurons (Frandsen's work), we had speculated that GRs might be involved in this A $\beta$ -mediated LTP impairment. Using C13 as a specific GR antagonist, the acute effect of A $\beta$ -dependent LTP impairment was completely prevented. These suggest that A $\beta$  relies on GRs to mediate its LTP impairment. Using this pharmacological approach, we inhibit GRs for an acute time period ranging between 20-40 minutes. It is most likely that in this time frame non-genomic actions are predominant via the membrane GRs, but could also include the genomic effect. We cannot distinguish between these two possibilities at present, but favour a non-genomic action due to the short timeline of the experiment.

In future work, we are very interested to see if GRs are involved in the A $\beta$ -mediated effect on LTD. If, by inhibiting GRs, we could also prevent the A $\beta$ -mediated LTD exacerbation, it would confirm that the two well-known A $\beta$  effects on synaptic plasticity happens via the GRs. If this were not the case, then it would suggest that different mediators are necessary for A $\beta$  to independently mediate its effects on LTP and LTD processes.

***Comparison between the pharmacological treatment of GR antagonist versus genetic ablation of GR using the GR<sup>lox/lox</sup> mice on acute A $\beta$  effect***

Using the GR floxed animals, after 4 weeks of Cre-GFP recombinase, we confirmed reduction of nuclear GRs by 90% (we are not sure about the membrane GRs as only nuclear GRs were quantified). In both the cases, that is with pharmacological inhibition of GR and with genetic ablation of GR, we can see that the acute A $\beta$  effect on LTP impairment is prevented. There is better prevention of the A $\beta$  effect in the pharmacological studies (Figure 46) as compared to the GRs ablated genetically (Figure 49). This is not surprising as this could be due to a more uniformity of action of the antagonist, leading to complete block of GRs, while with virus induced genetic ablation, the loss of GR function is not complete remaining in non-transduced neurons.

### ***Acute A $\beta$ impairs recognition memory***

Within the last months of the thesis, we were interested to provide more pertinence to our findings *ex vivo* by also studying this acute A $\beta$ -GR functional interaction at the integrative level of memory processes. We observed memory impairment in the oA $\beta$  group, as they could not discriminate between the novel and the familiar object using the NOR test. Though the A $\beta$  effect on memory impairment was very small, we got a statistical difference within the individual groups. For future experiments, we need to repeat this experiment to assure the oA $\beta$ -mediated object recognition memory impairment and to further validate the preventive effect of the GR antagonist. In addition, it would also be interesting to repeat this experiment with the Cre-lox system in the GR<sup>lox/lox</sup> mice.

### ***Novel data showing A $\eta$ - $\alpha$ impairs LTP***

In collaboration with Drs Willem and Haas, we show interesting results on the newly discovered APP fragments A $\eta$ - $\alpha$  and A $\eta$ - $\beta$  for their neuromodulatory action on synaptic transmission and LTP. These fragments were seen to be enriched in dystrophic neurites in human AD brains, indicating its potential contribution to AD pathology. We found that A $\eta$ - $\alpha$ , but not A $\eta$ - $\beta$ , negatively impairs LTP (Willem et al., 2015). In addition, in this study, work done by Drs Busche and Konnerth demonstrated that A $\eta$ - $\alpha$  also modulates calcium transients *in vivo*. Together, these results are very interesting since they demonstrate that A $\eta$ - $\alpha$  has synapse modulatory properties like the extensively studied A $\beta$ . For future experiments, it will be interesting to continue to identify exactly how A $\eta$ - $\alpha$  mediates its synaptic effects. Firstly, we could check the effect of A $\eta$ - $\alpha$  peptide on LTD by field recordings. Together with the LTP data, we would hence conclude on the effect of A $\eta$ - $\alpha$  on post-synaptic plasticity. We could also use whole cell patch clamp technique to check the effect of A $\eta$ - $\alpha$  on AMPAR and NMDAR currents, both major actors of LTP and LTD. Another interesting experiment would be to check the dose-response curve of different concentrations of A $\eta$ - $\alpha$  and its effect on synaptic plasticity. These studies on synaptic activity could eventually be extrapolated to studying the effects of this peptide on hippocampus-dependent memory processing, especially the well elaborated episodic-like memory test standardized in our lab. This would provide crucial new information on the role of A $\eta$ - $\alpha$  in the brain.

## 7 Conclusion

AD is a complex neurodegenerative disorder, which is perceived to commence with a gradual decline in synapse function leading to memory impairment before spreading through the brain to provoke global cognitive deficits. It is a multifactorial disease involving strong evidence of genetic dependence and important risk factors like stress, diet and other lifestyle conditions. There are only few therapeutics in the market for AD but none of them have been effective in controlling the progression of the disease. Hence our studies focus on the early onset of AD in mice to be able to identify the causative elements and to reverse typical AD-like phenotypes screening for potential drug treatments.

Our study is relevant as it tries to uncover the molecular mechanisms underlying stress as an important risk factor in AD. Research in this thesis extends our understanding of the role of GR in AD pathophysiology. *In vivo* studies using the Tg2576 mouse model helps us establish the relationship of early onset of AD with dysregulation of the HPA axis. Lab members and myself have produced results regarding the early-symptomatic stage of the Tg2576 mice, which help us conclude that plasma CORT levels increase early in disease progression in this model. Along with hypercortisolemia, there persisted a dysfunction in the negative feedback mechanism which prevented CORT to reach normal levels. Our results also show that this dysregulation in the HPA axis is correlated with decreasing ACTH levels at a slightly later stage of the disease. Data from peripheral tissues like thymus gland show decreased weight in the Tg<sup>+</sup> mice, while adrenal gland weight remains constant. The total hippocampal GR levels did not change despite the increased CORT levels. Finally, we also checked for episodic-like memory deficits, which is the earliest form of memory impairment in AD patients. We reported that there was a deficit in episodic-like memory in 4 month Tg<sup>+</sup> mice and this could be rescued with short GR antagonist treatment. A part of these results have been published in (Lanté et al., 2015), to which I have contributed.

To further understand the functional role of GR in AD in the hippocampus, we decided to generate the conditional ablation model of GR by crossing the Tg<sup>+</sup> with the GR<sup>lox/lox</sup> mice. Unfortunately, we could not conclude much from these mice due to genetic and background problems encountered while breeding and to the increased death toll during stereotaxic surgery. Instead, we moved on to correlate the acute functional relationship between oA $\beta$  and GRs at excitatory synapses. To address this, we shifted to an acute model of oA $\beta$  using

both hippocampal neurons in culture and *ex vivo* hippocampal sections. First, results in collaboration with Dr Frandemiche prove that oA $\beta$  modulates GRs levels within the PSD, supporting the hypothesis that there is indeed a functional relationship between A $\beta$  and GR at excitatory synapses.

We further went on to prove that GRs are necessary for oA $\beta$ -mediated impairment of LTP using two different approaches. Initially, we proved that pharmacologically blocking GRs with a specific antagonist was sufficient to prevent oA $\beta$ -induced LTP impairment. To confirm these results, we also used the genetic model of GR ablation involving the GR<sup>lox/lox</sup> mice. We successfully proved that upon reduction of GR levels using the Cre virus, we could prevent this impairment. Collectively, both the pharmacological approach of GR inhibition and the genetic ablation of GR strongly indicate that oA $\beta$  relies on GRs for its synaptic effect on LTP. These data are currently being prepared for submission of a manuscript where I will be first author.

During my thesis, I also had the opportunity to briefly collaborate with Drs Willem and Haass (LMU, Germany). Specifically, I tested if the newly discovered APP fragments A $\eta$ - $\alpha$  and A $\eta$ - $\beta$  could modulate synapse transmission and LTP using field electrophysiology. We found that A $\eta$ - $\alpha$ , but not A $\eta$ - $\beta$ , negatively impacts LTP. This contribution was rewarded by co-authorship on the Willem et al. 2015, a Nature publication that was highlighted in the press worldwide.

In conclusion, using several types of approaches, my main work provided results that provided new insights of how the stress pathway is implicated AD aetiology. I hope that these published and soon-to-be published results will prompt other scientists to fully elucidate how the HPA axis, and especially GRs, is implicated in AD. Future work on this topic could promote new therapeutic developments for this devastating disease.

## 8 Personal Accomplishments

After successfully completing my Master's degree, I got the opportunity to work as a Project Junior Research Fellow at a premier research institute in India. This was my first step into the world of scientific research and exposure to advanced equipment and technology. My hands-on experience in various techniques and my specialization in Neurobiology gave me the opportunity to do my PhD through the prestigious Labex SIGNALIFE program in France.

I specifically chose the laboratory of Dr. Hélène Marie as it specialized in my field of interest and additionally had the latest equipment to conduct high end research in electrophysiology, behavioural studies and molecular biology. Herein started my metamorphosis from a naive student to an experienced doctorate fellow. Initially, with good guidance, I started to familiarize myself to the systematic approach towards animal breeding, recording and documentation. Simultaneously, I also learnt to perform elaborated behavioural paradigms related to study AD associated episodic-like memory. Advanced training in the field of electrophysiology helped me tremendously to answer a majority of questions related to my thesis. It was the first time here that I started recording from live neurons of the hippocampus, which was very exciting. Using this technique, I was able to participate in a collaboration which carried out novel research in the field of Alzheimer's disease and was rewarded by an authorship in a Nature paper. By the end of the first year, I was familiar with most of the techniques, which I would require to complete my PhD project. Appropriate awareness on animal ethics ensured that I worked with empathy and the safety precautions taught to me for handling virus injections made me feel safe and assured.

Over a period of time I realized that I was converting my bookish knowledge to actual practical hands-on research. My exposure to stereotaxic injections slowly helped me become more patient while performing experiments. With all this training, I started organizing and managing myself better by planning the rotation of different experiments to maximize the time spent in the lab. Overall experience and knowledge that I gained using several techniques also started to improve my confidence. The opportunity to attend several conferences updated me to the latest research in AD and improved my scientific thinking. This motivated me and gave me more ideas related to my area of research. Regular lab meetings and several conferences/ meetings were grounds of opportunity to present my work and these boosted my confidence and made me open to share my ideas and experiences with others more clearly.

The downside was that we had some unforeseen issues with generating the double mutant mice. This situation was ably handled by my mentor and this helped me learn to overcome failures and take them in my stride. At the end of the 3.5 years, I feel that I have been transformed both at the scientific as well as the personal level for which I am grateful to my lab.

# **PUBLICATIONS**

# Subchronic Glucocorticoid Receptor Inhibition Rescues Early Episodic Memory and Synaptic Plasticity Deficits in a Mouse Model of Alzheimer's Disease

Fabien Lanté<sup>1,2</sup>, Magda Chafai<sup>1,3</sup>, Elisabeth Fabienne Raymond<sup>1,3</sup>, Ana Rita Salgueiro Pereira<sup>1,3</sup>, Xavier Mouska<sup>1</sup>, Scherzad Kootar<sup>1</sup>, Jacques Barik<sup>1</sup>, Ingrid Bethus<sup>1</sup> and Hélène Marie<sup>\*,1</sup>

<sup>1</sup>Institut de Pharmacologie Moléculaire et Cellulaire (IPMC), Centre National de la Recherche Scientifique (CNRS), Université de Nice Sophia Antipolis, UMR 7275, Valbonne, France

The early phase of Alzheimer's disease (AD) is characterized by hippocampus-dependent memory deficits and impaired synaptic plasticity. Increasing evidence suggests that stress and dysregulation of the hypothalamo-pituitary-adrenal (HPA) axis, marked by the elevated circulating glucocorticoids, are risk factors for AD onset. How these changes contribute to early hippocampal dysfunction remains unclear. Using an elaborated version of the object recognition task, we carefully monitored alterations in key components of episodic memory, the first type of memory altered in AD patients, in early symptomatic Tg2576 AD mice. We also combined biochemical and *ex vivo* electrophysiological analyses to reveal novel cellular and molecular dysregulations underpinning the onset of the pathology. We show that HPA axis, circadian rhythm, and feedback mechanisms, as well as episodic memory, are compromised in this early symptomatic phase, reminiscent of human AD pathology. The cognitive decline could be rescued by subchronic *in vivo* treatment with RU486, a glucocorticoid receptor antagonist. These observed phenotypes were paralleled by a specific enhancement of N-Methyl-D-aspartic acid receptor (NMDAR)-dependent LTD in CA1 pyramidal neurons, whereas LTP and metabotropic glutamate receptor-dependent LTD remain unchanged. NMDAR transmission was also enhanced. Finally, we show that, as for the behavioral deficit, RU486 treatment rescues this abnormal synaptic phenotype. These preclinical results define glucocorticoid signaling as a contributing factor to both episodic memory loss and early synaptic failure in this AD mouse model, and suggest that glucocorticoid receptor targeting strategies could be beneficial to delay AD onset.

*Neuropsychopharmacology* advance online publication, 18 February 2015; doi:10.1038/npp.2015.25

## INTRODUCTION

Alzheimer's disease (AD) is the most common cause of dementia in aging human populations, but only low-efficacy palliative treatments are currently available. The hippocampus and the type of memory it encodes (ie episodic memory) are affected very early in all forms of AD (deToledo-Morrell *et al*, 2007; Salmon and Bondi, 2009). Since the discovery of A $\beta$  as the main constituent of senile plaques observed in AD patient brains and the cloning of the amyloid precursor protein (APP), there has been an intense effort to understand how APP misprocessing and A $\beta$  affect hippocampal function.

There is now a strong evidence that A $\beta$  accumulation into soluble oligomers in this structure is most probably one of the main triggers of the pathology leading to early synaptic failure and subsequent memory loss (Palop and Mucke, 2010; Shankar *et al*, 2008). However, the exact cellular mechanism contributing to the onset of synaptic failure and memory loss in AD remains unclear.

Preclinical and clinical data suggest that stress is an important environmental risk factor leading to AD (Rothman and Mattson, 2010). Indeed, patients with a high level of distress proneness are 2.7 times more likely to develop AD, and this trait is also associated with a faster progression of the disease (Wilson *et al*, 2003, 2007). This is in line with the observations that major stressful events lower the age of onset of familial AD (Mejia *et al*, 2003). In various preclinical AD models, stress worsens deficits in hippocampus-dependent spatial learning (Catania *et al*, 2009; Cuadrado-Tejedor *et al*, 2012; Dong *et al*, 2004; Jeong *et al*, 2006; Srivareerat *et al*, 2009; Tran *et al*, 2010). These deleterious effects are in part caused by an accelerated accumulation of A $\beta$  under stressing conditions (Catania *et al*, 2009; Cuadrado-Tejedor *et al*, 2012; Dong *et al*, 2004; Green *et al*, 2006; Jeong *et al*, 2006; Srivareerat

\*Correspondence: Dr H Marie, Institut de Pharmacologie Moléculaire et Cellulaire (IPMC), Centre National de la Recherche Scientifique (CNRS), Université de Nice Sophia Antipolis, UMR 7275, 660 Route des Lucioles, 06560 Valbonne, France, Tel: +33 4 93 95 34 40, Fax: +33 4 93 95 34 08, E-mail: marie@ipmc.cnrs.fr

<sup>2</sup>Present address: Grenoble Institut des Neurosciences, INSERM U836, Université Joseph Fourier, Equipe 12 Neuropathologies et Dysfonctions Synaptiques, 38706 La Tronche Cedex, France

<sup>3</sup>These authors equally contributed to this work.

Received 16 May 2014; revised 13 January 2015; accepted 15 January 2015; accepted article preview online 27 January 2015

*et al*, 2009). Stress triggers the release of glucocorticoid hormones (CORT), the major output of the hypothalamo-pituitary-adrenal axis (HPA). CORT acts via two related receptors, the mineralocorticoid (MR) and the glucocorticoid receptors (GR). GR has a low affinity for CORT and is thus believed to be a key player under elevated CORT levels, although a role of MR cannot be excluded. Both AD patients and AD mouse models display a dysregulated HPA axis, marked by a mild hypercortisolemia that is apparent early during the pathology (Csernansky *et al*, 2006; Elgh *et al*, 2006; Hebda-Bauer *et al*, 2013; Nasman *et al*, 1995; Rasmuson *et al*, 2001; Weiner *et al*, 1997). Increased CORT levels are sufficient to exacerbate A $\beta$  deposits, and a recent study suggested that antagonism of GR could prevent this effect (Baglietto-Vargas *et al*, 2013). Albeit this increasing evidence for a synergistic relationship between dysregulated HPA function and AD pathogenesis, its cellular underpinnings remain poorly understood.

Using chronic A $\beta$  infusion in adult rat brains, the group of Alkadhi suggested a relationship between A $\beta$ , *in vivo* synaptic plasticity and chronic psychosocial stress, showing that this type of stress exacerbates A $\beta$ -induced alterations in hippocampal long-term potentiation (LTP) and long-term depression (LTD; Tran *et al*, 2011a, 2011b). These data argue for a role of stress signaling in AD-related synaptic dysfunction, but there are currently no other reports addressing this point in more detail. Importantly, there is paucity of data regarding the contribution of CORT signaling to AD-related hippocampal synapse failure ie, weakening of synaptic communication, a phenotype which is believed to drive the onset of memory loss in AD as we and others have shown previously (D'Amelio *et al*, 2011; Selkoe, 2002). Identifying how a dysregulation of CORT signaling contributes to synaptic failure in AD is of importance as CORT has a prominent role in shaping hippocampal synaptic plasticity (Chaouloff and Groc, 2011).

Here, we used the Tg2576 transgenic AD mouse model, which displays AD-like A $\beta$  accumulation as oligomers with late formation of plaques in memory-encoding areas (hippocampus and neocortex) during aging (Hsiao *et al*, 1996). We previously demonstrated that onset of cognitive deficits in this model correlated with low levels of synaptic AMPA receptors and a stronger LTD of AMPAR responses in hippocampal CA1 neurons (D'Amelio *et al*, 2011). We now further characterize these memory and synaptic deficits in the early symptomatic phase of this model and provide strong evidence for a role of dysregulated HPA activity to these deficits. Our results define enhanced CORT signaling, via GRs, as a contributing factor to both early synaptic failure and episodic memory loss in this mouse model.

## MATERIALS AND METHODS

### Mice

Hemizygous Tg2576 mice carrying the human Swedish mutation (hAPP<sup>Swe</sup> transgene: human APP695 with double mutations at KM670/671NL) are hybrids between C57BL/6 and SLJ provided by Taconic Biosciences (D'Amelio *et al*, 2011; Hsiao *et al*, 1996). Tg2576 and wild-type (WT) littermates were used for all experiments. The original transgenic mouse was developed using B6SJL/F2 zygotes

(Hsiao *et al*, 1996). The mouse is a hybrid between C57BL/6 and SLJ (Hsiao *et al*, 1996) and back-crossed to C57BL/6 mice for two generations (Carlson *et al*, 1997) before being deposited at Taconic Biosciences. Hemizygous males were back-crossed with C57BL/6NTac for derivation at Taconic Biosciences and the colony is maintained by mating hemizygous male mice with B6SJL/F1 female mice (Taconic Model 1349). These hemizygous mice are not congenic or co-isogenic mice, as they contain mixed genetic backgrounds of C57BL/6 and SJL mice. The hemizygous and WT littermates may be different in alleles near the transgene site because the original mouse and breeder mice were back-crossed to C57BL/6 mice. Thus we cannot rule out the possibility that the phenotypic difference between Tg and WT mice could be because of the allelic difference instead of the transgene (Wolfer *et al*, 2002). Four-month old Tg2576 mice were used, except for in Figures 1c and 3e where 1-month old mice were used. For behavioral, plasma corticosterone levels, dexamethasone suppression test, and RU486 experiments, only male mice were used (see Supplementary Materials and Methods for additional details on animal care).

### Plasma CORT Measurements and Dexamethasone Suppression Test

To determine plasma CORT levels, blood was collected from the submandibular vein without anesthesia (see Supplementary Materials and Methods for details). For circadian plasma CORT measurements, blood was collected at the onset of the light resting phase (0800 hours) and the dark active phase (2000 hours) in the same animal. After 15 min of centrifugation at 2000  $\times$  g, at 4  $^{\circ}$ C, plasma samples were stored at  $-80^{\circ}$ C. Plasma corticosterone concentrations were measured using an Enzyme Immunoassay (EIA) kit following the manufacturer's instructions (Enzo Life Science, France). For the dexamethasone suppression test, dexamethasone 21-phosphate disodium salt (0,05 mg/kg; Sigma-Aldrich, France) dissolved in saline (NaCl, 0.9%) or vehicle (saline) were injected intraperitoneally in WT and Tg2576 mice at 1200 hours. Blood was collected at 1800 hours and plasma corticosterone levels were assessed using the EIA kit.

### RU486 Treatment

RU486 (40 mg/kg) was dissolved in DMSO for electrophysiology experiments or in water containing a droplet of Tween-20 for behavioral experiments and injected twice daily subcutaneously in the interscapular region of mice 2 days or 4 days before they were killed. The appropriate vehicle solution (H<sub>2</sub>O/Tween-20) was administered accordingly. For *ex vivo* electrophysiological experiments, RU486 (0.5  $\mu$ M) or DMSO (vehicle) was directly applied to the slices via the bath perfusion throughout the recording.

### Object Recognition Paradigm

The episodic-like object recognition protocol was performed essentially as described previously (Dere *et al*, 2005) with minor variations in the protocol to minimize stress levels (see Supplementary Materials and Methods for

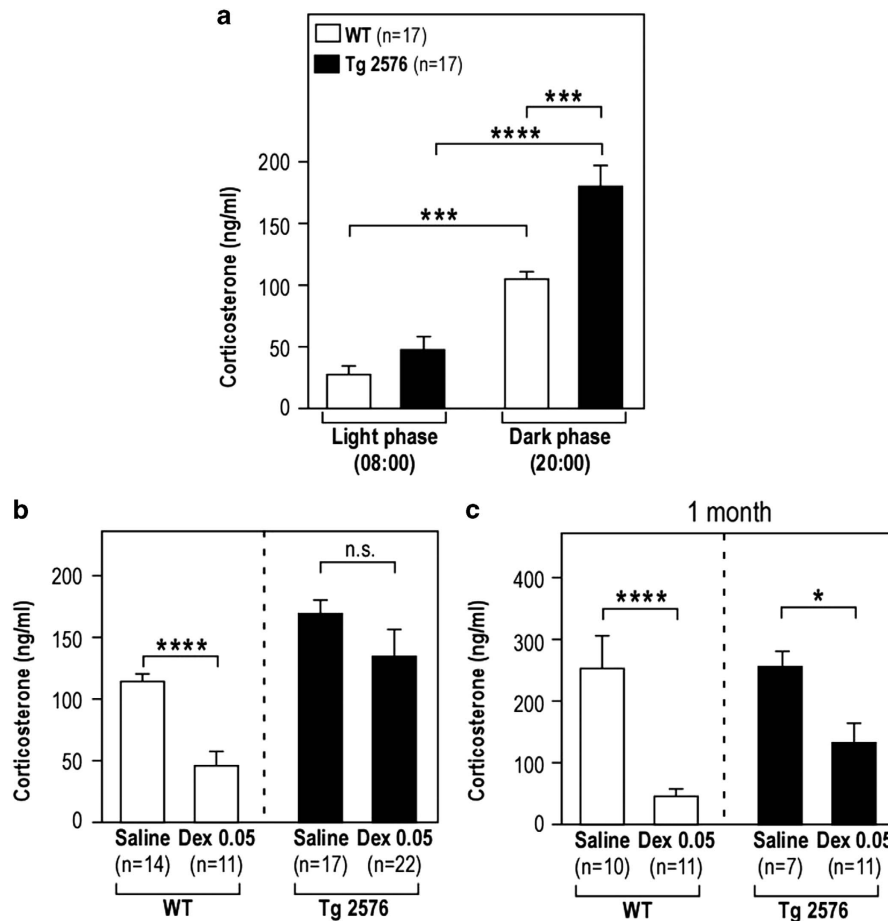


**Figure 1** Four-month old Tg2576 mice display alterations in corticosterone signaling (a) Plasma corticosterone levels (ng/ml) were measured by ELISA at the onset of the light/resting (0800 hours) and dark/awake (2000 hours) phases in 4-month old male WT (white bars) and Tg2576 (black bars) mice. Tg2576 mice display significantly elevated levels of corticosterone at the onset of the dark phase compared with WT. (b and c) Plasma corticosterone levels (ng/ml) were measured by ELISA 6 hours after *in vivo* injection of dexamethasone (Dex) at 0,05 mg/kg or saline (b) in 4-month old WT (white) and Tg2576 (black) mice; (c) in 1-month old WT (white) and Tg2576 (black) mice. One-month old WT and Tg2576 mice, and 4-month old WT mice display the expected decrease in corticosterone levels after Dex injection, whereas 4-month old Tg2576 mice do not. \* $p < 0.05$ ; \*\*\* $p < 0.001$ , \*\*\*\* $p < 0.0001$ , n.s., non-significant.  $n$  = number of mice. See Supplementary Table 1 for the statistics details.

details). This task is based on the paradigm that episodic memory is the memory of personal experiences and specific events including what happened ('What' component), location ('Where' component) and time ('When' component). A schematic description of the procedure is shown in Figure 2a. Using these test trial exploration data, we estimated three components of episodic-like memory: What = (exploration time (ET) 'olds' - ET 'recents')/(ET 'olds' + ET 'recents'); When = (ET 'old stationary' - ET 'recents')/(ET 'old stationary' + ET 'recents'); Where = (ET 'old displaced' - ET 'old stationary')/(ET 'old displaced' + ET 'old stationary'; see Supplementary Materials and Methods for details).

### Electrophysiology

Hippocampal slices were prepared as described previously (see Supplementary Materials and Methods for details). Field excitatory post-synaptic potentials (fEPSPs) were recorded in the stratum radiatum of the CA1 region and stimuli delivered to the Schaeffer Collateral Pathway by a

monopolar glass electrode filled with ACSF (see Supplementary Materials and Methods for details). LTP was induced using a TBS protocol: 10 bursts at 5 Hz repeated 10 times in 15 s intervals. Each burst consisted of four pulses of 100 Hz (see Supplementary Materials and Methods for details of analysis procedure). LTD was induced with a low frequency stimulation (LFS) protocol of 900 pulses at 1 Hz. To induce NMDAR-dependent LTD, slices were superfused with standard ACSF containing NMDA (20  $\mu$ M) for 2.5 min. To induce mGluR-dependent LTD, slices were superfused with standard ACSF containing DHPG ((S)-3,5-Dihydroxyphenylglycine; 100  $\mu$ M or 50  $\mu$ M) for 15 min in the presence of the NMDAR antagonist D,L-APV ((2R)-amino-5-phosphonovaleric acid, 100  $\mu$ M) throughout the recordings. Whole-cell voltage-clamp recordings were made from CA1 pyramidal cells (see Supplementary Materials and Methods for details). NMDA-evoked currents were recorded with an  $Mg^{2+}$ -free ACSF containing DNQX (20  $\mu$ M) and picrotoxin (50  $\mu$ M) at different holding potentials from -60 mV to +40 mV with 20 mV step increments. An average of current over ten

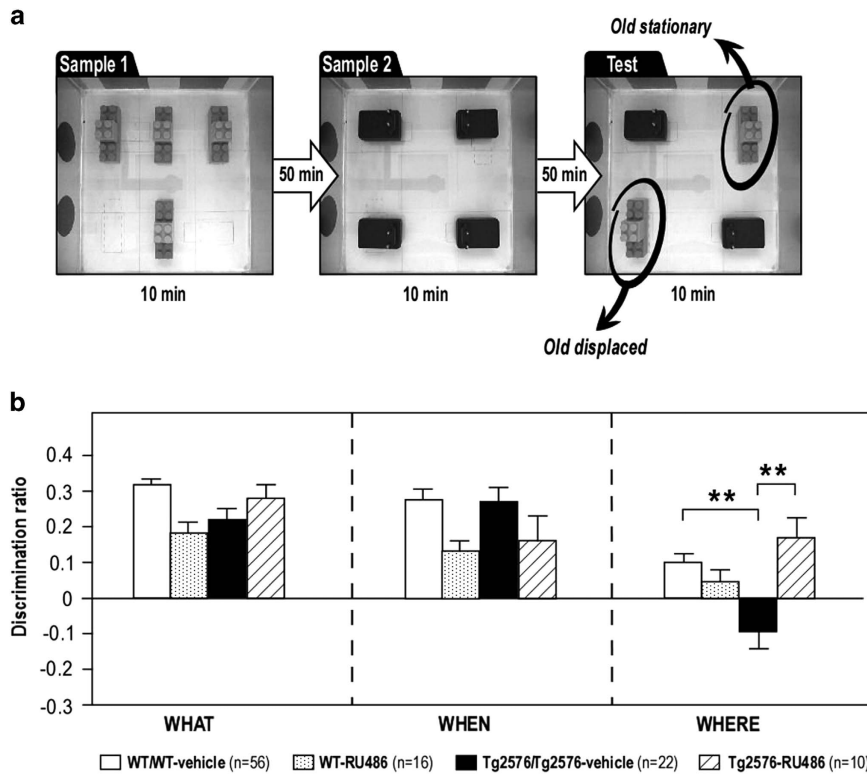


**Figure 2** Four-month old Tg2576 mice display episodic memory deficits, a behavioral phenotype which is rescued by blocking glucocorticoid receptors. (a) Schema of the What–When–Where object recognition protocol. (b) Episodic-like memory in 4-month old untreated/vehicle-treated WT (white bars), in 4-day *in vivo* RU486-treated WT (dotted bars), in untreated/vehicle-treated Tg2576 (black bars) and in 4-day *in vivo* RU486-treated Tg2576 (hashed black bars) mice. Discrimination ratios for each component of episodic-like memory are indicated. \*\* $p < 0.01$ ;  $n$  = number of mice. See Supplementary Table 1 for the statistics details.

sweeps was calculated per holding potential, which was then normalized to the value obtained at  $-60$  mV (representing  $-1$  on graphs). The data were pooled by condition and represented as mean  $\pm$  SEM. Data analysis was performed with the clampfit software (Molecular devices).

### Statistical Analysis

For Dex tests and electrophysiological recordings, statistics were performed with an unpaired two-tailed Student's *t*-test to probe for a difference between genotype (WT, Tg2576). A two-way analysis of variance (ANOVA) was used to test for an effect of treatment (vehicle, RU486) or genotype (WT, Tg2576) on behavior and electrophysiology data and repeated measures two-way ANOVAs were used to test for an effect of phase of the day (light phase, dark phase) or genotype (WT, Tg2576) on corticosterone measurements. *Post hoc* analysis was conducted with Bonferroni's comparison. All the statistical analyses were done with using Prism 6 (Graph Pad). All numerical data are presented as mean  $\pm$  SEM.  $p < 0.05$  was considered to be statistically significant. See Supplementary Data for full statistics Supplementary Tables 1, 2, and 3.

## RESULTS

### Four-Month Old Tg2576 Mice Display Alterations in HPA Axis Function

In many species, plasma CORT levels are subjected to circadian rhythmicity that is key for maintaining normal

homeostasis. Dysregulation of this pattern of secretion has been described in several disease states (Lightman and Conway-Campbell, 2010). Therefore, we first investigated the integrity of the HPA axis in 4-month old Tg2576 mice and WT littermates. We assayed nadir CORT plasma levels at the onset of the light phase (0800 hours, resting period for rodents) and peak levels at the onset of the dark phase (2000 hours, active period for rodents). Both genotypes displayed the expected circadian elevation in CORT levels at the onset of the dark phase (Figure 1a, Supplementary Table 1). We observed that, although morning CORT levels did not significantly differ between the two genotypes, Tg2576 mice displayed significantly higher levels of plasma CORT in the evening at the onset of the active phase (Figure 1a, Supplementary Table 1). These data indicate that a clear HPA axis dysregulation occurs at an early stage of AD pathogenesis in Tg2576 mouse model. To get further insights into this dysregulation, we sought to determine if there were modifications in the feedback loops that regulate CORT secretion. Thus, we submitted the 4-month old Tg2576 mice and WT littermates to the commonly employed dexamethasone (Dex) suppression test. Injection of this potent selective glucocorticoid receptor agonist triggers a negative feedback mechanism resulting in a reduction in plasma CORT levels within hours. As expected, we observed a marked reduction in plasma CORT levels in WT mice 6 hours after Dex injection when compared with the saline-injected controls (Figure 1b, Supplementary Table 1). In striking contrast, Dex did not

significantly alter CORT levels in Tg2576 mice (Figure 1b, Supplementary Table 1), suggesting pronounced disruption of the GR-dependent feedback mechanism of HPA axis regulation. We then examined the age dependency of this dysregulation in 1-month old mice. At this age, the Dex suppression test was normal in Tg2576 mice (Figure 1c, Supplementary Table 1), consistent with observations that, at this age, no cognitive deficits have been evidenced and little to no A $\beta$  accumulation is present in these mutant mice (D'Amelio *et al*, 2011; Hsiao *et al*, 1996; Mustafiz *et al*, 2011). This suggests that HPA axis deregulation is owing to chronic misprocessing of APP and accumulation of APP-derived peptides and not because of the over-expression of hAPPswe *per se*. Together, these data demonstrate that, at 4 months of age, the homeostasis of the HPA axis is compromised in these transgenic mice, leading to chronically elevated levels of circulating CORT.

#### Four-Month Old Tg2576 Mice Display Episodic Memory Deficits, which can be Reversed by Glucocorticoid Receptor Antagonism

To assess AD-related cognitive decline, we evaluated episodic memory in 4-month old WT and Tg2576 mice. Previous analyses of cognitive function in these mice at this age focused on other types of hippocampus-dependent memory tasks, such as the Morris water maze or contextual fear conditioning (D'Amelio *et al*, 2011; Stewart *et al*, 2011). These tasks, however, do not test for episodic memory, which is the first type of memory that is affected in AD patients (deToledo-Morrell *et al*, 2007; Salmon and Bondi, 2009). To specifically assess this type of memory in our mice, we used an elaborated version of the object recognition (OR) task, which can probe for the 'What', 'When', and 'Where' components of episodic memory (Dere *et al*, 2005). Exploration time for objects and discrimination ratio were evaluated during the test trial (Figure 2a). We observed that mice from both genotypes display a similar total exploration time during the 10 min test trial (WT = 63.56  $\pm$  5.73 s; Tg2576 = 59.62  $\pm$  6.11 s;  $p > 0.05$ , data not shown). These data argue against any alterations in general locomotion or anxiety-like behavior in Tg2576 mice at this age, which could have compromised the outcome of this behavioral test. We calculated the discrimination ratios for the 'What', 'When', and 'Where' components of episodic memory. For the 'What' and 'When' components, the positive discrimination ratio for the two genotypes did not differ (see Figure 2b and Supplementary Table 1). However, for the 'Where' component, although WT control animals (untreated/vehicle-treated mice) displayed a positive discrimination ratio, Tg2576 mice (untreated/vehicle-treated) displayed a marked negative discrimination ratio, significantly different from WT (Figure 2b and Supplementary Table 1). These data demonstrate that, while WT mice displayed a good episodic memory in this refined object recognition paradigm, the Tg2576 mice failed to process the 'Where' component of this task, which represents in itself the full integration of the episodic memory (object, time, and location).

In light of these data and the clear deregulation of the HPA axis, we next examined whether there was a correlation between excess CORT signaling and memory deficits. To

reach this goal, we hypothesized that blocking GRs could rescue this memory deficit, as these receptors are abundant in the hippocampus. It is indeed reasonable to speculate that, as CORT is chronically elevated, the GRs became over-active in the Tg2576 mice. WT or Tg2576 mice received twice daily subchronic (4 days) injections of the commonly employed GR antagonist, RU486, before being assessed in the episodic memory paradigm. Figure 2b reports discrimination ratios for the 'What', 'When', and 'Where' components of episodic memory in RU486-treated mice compared with the control mice (untreated/vehicle treated; see also Supplementary Table 1). Pharmacological blockade of GRs by RU486 treatment did not significantly alter episodic memory in WT, although a trend towards lower memory for the 'What' and 'When' components was apparent (Figure 2b, Supplementary Table 1). RU486, however, fully rescued the deficit in the 'Where' component of episodic memory in Tg2576 mice, as RU486-treated Tg2576 mice performed, as well as WT mice (Figure 2b, Supplementary Table 1). Together these data suggests that abnormally-elevated CORT levels trigger GRs over-activation, which in turn impairs episodic memory formation in these early symptomatic mice.

#### NMDAR-Dependent LTD is Abnormally Enhanced in 4-Month Old Tg2576 Mice, whereas mGluR-Dependent LTD and LTP Remain Intact

To further characterize the cellular underpinnings of this memory deficit, we investigated synaptic plasticity in 4-month old WT and Tg2576 mice. We performed field electrophysiology in the CA1 area of *ex vivo* hippocampal slices. Schaeffer collaterals were stimulated to evoke fEPSPs at the CA3-CA1 synapses. Using this technique, we previously reported that electrically induced LTP of the AMPAR response remained intact, whereas LTD was enhanced in the 3-month old Tg2576 mice (D'Amelio *et al*, 2011). We now confirm these phenotypes at 4 months of age (Figure 3a and b).

CA1 AMPAR LTD can be induced by activation of NMDA receptors (NMDARs) or by activation of group I metabotropic glutamate receptors (mGluRs; Luscher and Huber, 2010; Malenka and Bear, 2004). We therefore next asked which type of LTD is primarily affected in Tg2576 mice at this age, by recording NMDA-induced and DHPG-induced chemical LTD, to assess NMDARs- and mGluRs-dependent LTD, respectively. NMDA application generated an NMDAR-dependent LTD in both genotypes, but this LTD was significantly exacerbated in Tg2576 mice when compared with the WT mice (Figure 3c). In contrast, mGluR-dependent LTD, induced by the application of 100  $\mu$ M of DHPG, was similar in both genotypes (Figure 3d). This lack of difference in Tg2576 mice was not owing to saturation of the mGluR-dependent LTD as use of lower DHPG concentrations (50  $\mu$ M) resulted in similar LTD magnitudes in WT and Tg2576 mice (data not shown—WT: 59.68  $\pm$  7.3%; Tg2576: 65.34  $\pm$  3.92%,  $p < 0.05$ ).

To correlate this specific NMDAR-dependent LTD with chronic misprocessing of APP and accumulation of APP-derived peptides and not to over-expression of hAPPswe *per se*, we recorded NMDA-induced LTD in 1-month old mice. At this age, Tg2576 and WT mice exhibit comparable

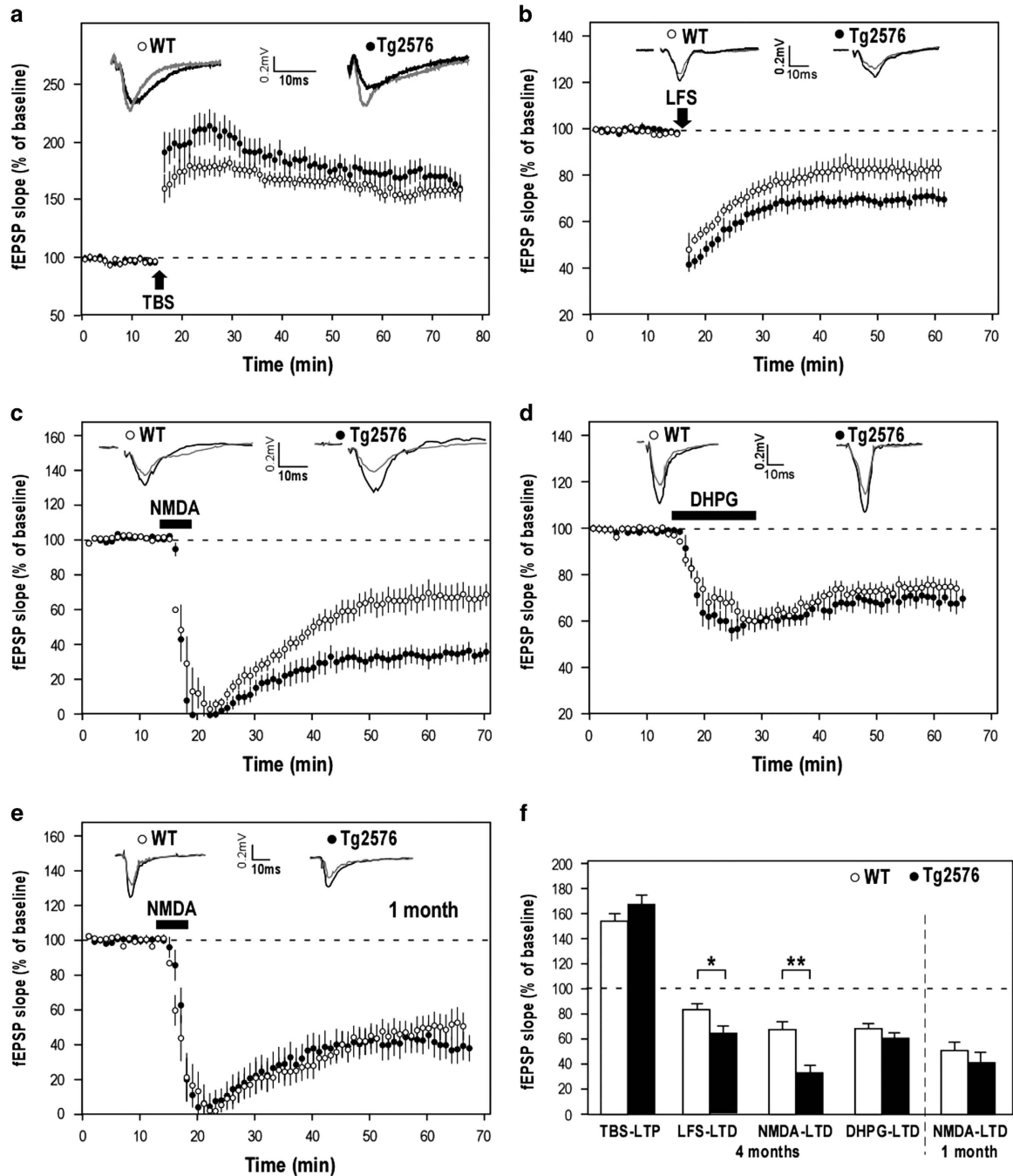


**Figure 3** NMDAR-dependent LTD is enhanced at the CA3-CA1 synapse in 4-month old Tg2576 mice compared with the 4-month old WT littermates, whereas mGluR-dependent LTD and LTP remain intact. Traces in a–e show sample fEPSPs pre- (black) and post- (gray) LTP or LTD induction. (a) Summary graphs of electrically induced LTP (theta burst stimulation (TBS), arrow) in 4-month old WT ( $n = 3$  mice,  $N = 8$  slices) and Tg2576 ( $n = 3$ ,  $N = 9$ ) mice as percentage of fEPSP baseline. (b) Summary graphs of electrically induced LTD (low frequency stimulation (LFS), arrow) displayed in 4-month old WT ( $n = 5$ ,  $N = 8$ ) and Tg2576 ( $n = 4$ ,  $N = 8$ ) mice. (c) Summary graphs of NMDAR-dependent LTD (induced by the application of NMDA  $20 \mu\text{M}/2.5$  min) displayed in 4-month old WT ( $n = 4$ ,  $N = 10$ ) and Tg2576 ( $n = 4$ ,  $N = 9$ ) mice. (d) Summary graphs of mGluR-dependent LTD (induced by the application of DHPG  $100 \mu\text{M}/15$  min) displayed in 4-month old WT ( $n = 4$ ,  $N = 10$ ) and Tg2576 ( $n = 4$ ,  $N = 12$ ) mice. (e) Summary graphs of NMDAR-dependent LTD (induced by application of NMDA  $20 \mu\text{M}/2.5$  min) displayed in 1-month old WT ( $n = 4$ ,  $N = 12$ ) and Tg2576 ( $n = 4$ ,  $N = 12$ ) mice. (f) Average LTP or LTD magnitudes calculated from graphs in a–e in last 10 min of recordings (as percentage of baseline). \* $p < 0,05$ ; \*\* $p < 0,01$ . See Supplementary Table 2 for the statistics details.

NMDA-induced LTD (Figure 3e). A summary graph of these electrophysiology data is presented in Figure 3f. Together, these results demonstrate that the episodic memory deficit

observed in the 4-month old Tg2576 mice correlates with a pathologically enhanced NMDAR-dependent LTD in CA1 pyramidal neurons.

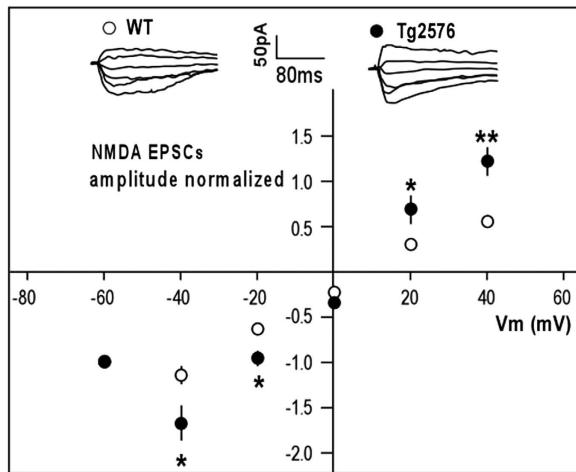


**Figure 4** NMDAR currents are higher in CA1 of 4-month old Tg2576 mice compared with the WT. Current (I, normalized to NMDA EPSC amplitude at  $-60$  mV) to Voltage (Vm) relationships of NMDA currents in CA1 pyramidal neurons in 4-month old WT ( $n=7$  mice,  $N=10/8$  cells) and Tg2576 ( $n=5$ ,  $N=8$ ) mice. Sample EPSCs are shown at Vm from  $-60$  mV to  $+40$  mV. \* $p < 0,05$ ; \*\* $p < 0,01$ . See Supplementary Table 2 for the statistics details.

#### Four-Month Old Tg2576 Mice Display Abnormally High NMDAR Currents

NMDAR-dependent LTD requires activation of synaptic NMDARs. To determine whether this transmission could be perturbed in 4-month old Tg2576 mice, we analyzed NMDAR currents of CA1 pyramidal neurons. We measured the current-voltage relationship of evoked synaptic NMDAR-mediated excitatory post-synaptic currents (EPSCs) in CA1 pyramidal neurons by whole-cell voltage clamp recordings. The amplitude of evoked NMDAR EPSCs was significantly enhanced in Tg2576 mice compared with that of WT at the various membrane potentials (Vm) tested (Figure 4).

#### Four Days of *in vivo* RU486 Treatment is Necessary to Reverse the NMDAR-dependent LTD Phenotype in 4-Month Old Tg2576 Mice

In light of the reversal of episodic memory defect observed in Tg2576 mice following subchronic RU486 treatment (Figure 2), we next tested whether this therapeutic effect resulted in the normalization of excessive NMDAR-dependent LTD, hence providing a cellular basis for this evident behavioral phenotype. Indeed, we observed that the LTD induced by NMDA application was significantly reduced in RU486-treated Tg2576 mice compared to vehicle-treated Tg2576 mice (Figure 5a), returning to WT values (see summary graph in Figure 5c and Supplementary Table 3 for statistical analysis). Vehicle- and RU486-treated WT mice exhibited identical pattern of NMDA-induced LTD (Supplementary Figure S1A). These data suggest that the dose of RU486 employed is sufficient to normalize excessive CORT signaling in CA1 neurons of Tg2576 mice, without altering the physiological LTD process as observed in WT mice.

To address the time dependency required for this cellular rescue, we tested whether direct *in vitro* application or

shorter (two days) *in vivo* administration of RU486 were effective. None of these two treatments could reverse the pathologically enhanced LTD observed in Tg2576 mice (Supplementary Figure S2; see also summary graph in Figure 5c). These data demonstrate that several days of RU486 treatment is necessary to successfully reverse this synaptic plasticity alteration.

#### Electrically Induced LTD and NMDAR Currents are Normalized by 4 Days of *in vivo* RU486 Treatment in Tg2576 Mice

We also tested the rescue potential of this 4-day *in vivo* RU486 treatment on electrically induced LTD. As for NMDA-induced LTD, the enhanced LFS-induced LTD we observed in Tg2576 mice (Figure 3b) was rescued by this treatment (Figure 5b), returning to WT levels (Figure 5c and Supplementary Table 3 for statistical analysis). Again, RU486 administration did not significantly alter LFS-induced LTD in WT mice (Supplementary Figure S1B). A summary graph of the rescue experiments attempted on the LTD phenotypes in Tg2576 mice and in WT littermates is provided in Figure 5c.

Finally, we tested if this 4-day *in vivo* RU486 treatment could normalize the excess of NMDAR current exhibited by Tg2576 mice (Figure 4). Whole-cell patch clamp recordings of CA1 pyramidal neurons from vehicle-treated and RU486-treated Tg2576 mice demonstrated that RU486 administration could significantly reduce NMDAR currents (Figure 5d), bringing them back to WT levels (Figure 5d: dashed line).

#### DISCUSSION

In recent years, numerous studies examined the relationship between CORT signaling and AD pathology, especially  $A\beta$ , with noticeable emphasis on behavioral and biochemical aspects of the disease. The major finding of this work is a precise pharmacological dissection of the changes in synaptic plasticity that occur at an early stage of the pathology with strong evidence for a central role of CORT in this process. We had previously reported normal LTP and enhanced LTD in CA1 neurons in this early symptomatic phase (D'Amelio *et al*, 2011). We now demonstrate that this enhanced synaptic depression selectively depends on NMDAR transmission, whereas mGluR contribution remains spared. Using whole-cell patch clamp recordings, we could attribute this phenotype to enhanced NMDAR EPSCs. These results are in agreement with the role played by NMDARs in this type of LTD (Malenka and Bear, 2004). Importantly, we demonstrate that the synaptic alterations are rescued by subchronic *in vivo* administration of the GR antagonist, RU486.

*In vivo* stress protocols, as well as *in vitro* and *in vivo* CORT application in rodents, mainly by recruiting GRs, which are abundant in the hippocampus, were shown to enhance both CA1 NMDAR- and mGluR-dependent LTD (Chaouloff and Groc, 2011). These protocols were also shown to either increase or decrease CA1 LTP depending on the CORT doses tested or the type of stress studied (acute or chronic; Chaouloff and Groc, 2011). Yet, only NMDAR-dependent LTD is affected in our model. It is therefore

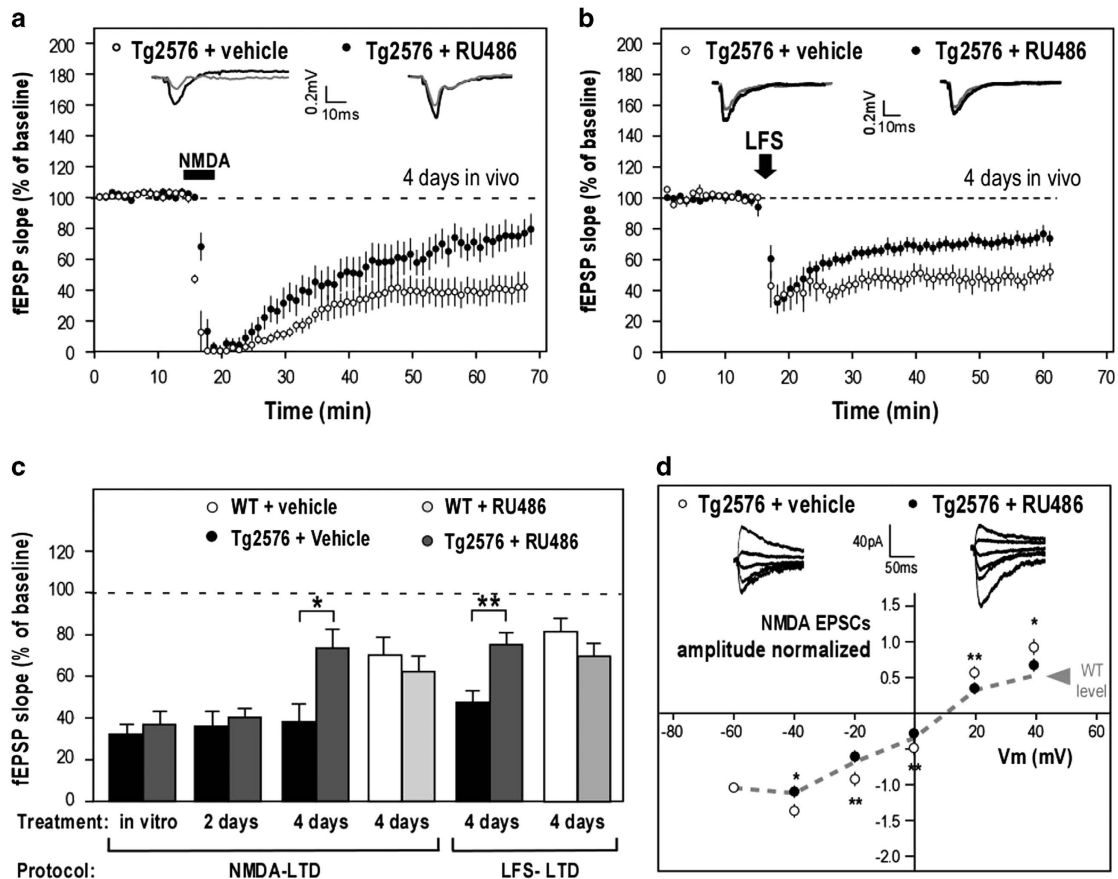


**Figure 5** Four days of *in vivo* RU486 treatment reverses the LTD and NMDAR phenotypes at the CA3-CA1 synapse in 4-month old Tg2576 mice. Summary graphs (as percentage of fEPSP baseline) of a NMDAR-dependent LTD (induced by application of NMDA 20  $\mu$ M/2.5 min) after 4 days of vehicle ( $n = 4$  mice,  $N = 8$  slices) or RU486 ( $n = 4$ ,  $N = 10$ ) treatment; (b) electrically induced LTD (low frequency stimulation (LFS), arrow) after 4 days of vehicle ( $n = 4$  mice,  $N = 7$  slices) or RU486 ( $n = 5$ ,  $N = 11$ ) treatment; Traces in a and b show sample fEPSPs pre- (black) and post- (gray) LTD induction. (c) Average LTD magnitudes calculated from graphs in 5a and 5b, and Supplementary Figures 1 and 2 in last 10 min of recordings (as percentage of baseline). (d) NMDAR currents are normalized by four days of *in vivo* RU486 treatment in Tg2576 mice. Current (I, normalized to NMDAR EPSC amplitude at  $-60$  mV) to Voltage (Vm) relationships of NMDAR currents in CA1 pyramidal neurons in 4-month old Tg2576 mice after 4 days of vehicle ( $n = 4$  mice,  $N = 9$  cells) or RU486 ( $n = 4$  mice,  $N = 11$  cells) treatment. Dashed line represents WT I/V relationship of Figure 4. Sample EPSCs are shown at Vm from  $-60$  mV to  $+40$  mV. \* $p < 0.05$ ; \*\* $p < 0.01$ . Student's *t*-test statistical results are shown with the asterisks. See Supplementary Table 3 for the statistics details and two-way ANOVAs statistics.

unlikely that the AD-related synaptic plasticity phenotype is simply because of the elevated CORT, but more probably owing to an intricate synergy between chronic APP misprocessing and increasing CORT levels, to which NMDAR-dependent LTD is particularly sensitive. The fact that we could fully reverse this aberrant synaptic phenotype with 4 days, and not 2 days, *in vivo* RU486 treatment supports the idea that GR-dependent genomic effects must be necessary to reset a homeostatic balance of CORT signaling in Tg2576 mice. In line with this idea, altering GR expression has been shown to modulate the hippocampal expression of several glutamate receptors and to trigger cognitive dysfunction (Wei *et al*, 2007), reinforcing the link between CORT/GR, glutamatergic plasticity and altered behaviors. We cannot at present exclude additional implication of the progesterone receptor in the rescue of the synaptic phenotype since this receptor is also blocked by this compound (Baulieu, 1997). This issue will in the future benefit from the generation of double GR KO/Tg2576 mice. Nevertheless, other recently published data strongly argue for a specific GR-mediated beneficial effect of RU486

on the rescue of behavioral and biochemical phenotypes in another AD mouse model with more advanced neurodegeneration (Baglietto-Vargas *et al*, 2013).

In a previous publication, we had reported a caspase- and calcineurin-dependent pathological mechanism leading to lower levels of synaptic AMPAR in the hippocampus of these early symptomatic mice (D'Amelio *et al*, 2011). As both caspase and calcineurin have been implicated in hippocampal NMDAR-dependent LTD (Li *et al*, 2010b; Mulkey *et al*, 1994), they could also contribute to the enhanced LTD we further studied here. It will be important, in future studies, to identify the interplay between this previously identified pathological mechanism and the novel CORT-dependent mechanism we report now. These two cellular pathways are certainly not mutually exclusive and could in fact be intimately linked as a study in AD and several studies in immunology research suggest (Distelhorst, 2002; Li *et al*, 2010a).

Copious information is available on the mnemonic deficits displayed by aged animal models of AD (Ashe and Zahs, 2010; Stewart *et al*, 2011). Here, we provide solid

evidence for an early impairment in episodic memory in 4-month old Tg2576 mice, correlating with early aggregation of A $\beta$  into oligomers, but before plaque formation (Hsiao *et al*, 1996; Mustafiz *et al*, 2011). To our knowledge, this is the first report of perturbation in this type of memory in the early phase of AD in AD mice, as few other studies tested this mnemonic deficit at more advanced stages of the pathology (Baglietto-Vargas *et al*, 2013; Davis *et al*, 2013; Good *et al*, 2007). In light of the impaired HPA axis feedback and the key role played by CORT in facilitating the consolidation of emotionally-charged memories (McGaugh and Roozendaal, 2002), it was crucial to monitor episodic memories in minimized stress conditions as presented here. We can therefore attribute the observed memory deficit to a prolonged dysregulation of the HPA axis accompanied by APP misprocessing and not to acute changes in CORT levels induced by the design of the behavioral paradigm. A 4 days subchronic antagonism of GR was sufficient to have fully beneficial outcomes on memory impairment, corroborating a recent study in older 3xTg mice with more advanced AD pathology, which employed a chronic infusion of GR antagonist for 3 weeks (Baglietto-Vargas *et al*, 2013). This shorter daily treatment holds the advantage of minimizing the possible side effects of prolonged GR blockade (Morgan and Laufgraben, 2013).

As described in other preclinical and clinical studies (Csernansky *et al*, 2006; Hebda-Bauer *et al*, 2013; Nasman *et al*, 1995; Rasmuson *et al*, 2001), we report an altered circadian rhythm of the HPA axis early in our mouse model. Whether this results from a dysregulation of the pulsatile ultradian pattern of CORT secretion is however yet to be demonstrated. Ultradian hormone pulsatility is inherent within the HPA axis as a result of negative feedback (Walker *et al*, 2010). The lack of responding of 4-month old Tg2576 mice to the Dex suppression test clearly argues for a strong impairment of this loop owing to the altered APP processing, hence indicating that ultradian rhythm may also be compromised. The Dex suppression test was normal in 1-month old mice, suggesting that the dysregulation occurs slowly, may be depending on A $\beta$  accumulation, before senile plaque and without tau alterations (Hsiao *et al*, 1996; Mustafiz *et al*, 2011).

Although, the presented data and the work from other labs now provide convincing behavioral, biochemical, and electrophysiological evidence that CORT and A $\beta$  are intimately linked (Rothman and Mattson, 2010), which one of CORT or A $\beta$  accumulation occurs first in our model remains to be fully elucidated. Nevertheless, our data demonstrate that RU486 treatment readily reverses episodic memory and pathologically enhanced LTD present in the early symptomatic phase in our mouse model, thus strongly arguing for a pathological synergistic interaction between chronic APP misprocessing and HPA axis dysregulation.

## FUNDING AND DISCLOSURE

This work was financed by the ATIP/AVENIR program (Centre national de la recherche scientifique—CNRS) to HM; by the French Fondation pour la Coopération Scientifique—Plan Alzheimer 2008–2012 (Senior Innovative Grant 2010) to FL, MC, EFR and HM; by the French Government (National Research Agency, ANR) through the ‘Investments

for the Future’ LABEX SIGNALIFE: program reference #ANR-11-LABX-0028-01 to HM and an Erasmus student grant to ARSP. The authors declare no conflict of interest.

## ACKNOWLEDGEMENTS

We thank Dr Beurrier (IBDML—CNRS, Marseille, France) for critical reading of the manuscript.

## REFERENCES

- Ashe KH, Zahs KR (2010). Probing the biology of Alzheimer's disease in mice. *Neuron* **66**: 631–645.
- Baglietto-Vargas D, Medeiros R, Martinez-Coria H, LaFerla FM, Green KN (2013). Mifepristone alters amyloid precursor protein processing to preclude amyloid beta and also reduces tau pathology. *Biol Psychiatry* **74**: 357–366.
- Baulieu EE (1997). RU 486 (mifepristone). A short overview of its mechanisms of action and clinical uses at the end of 1996. *Ann NY Acad Sci* **828**: 47–58.
- Carlson GA, Borchelt DR, Dake A, Turner S, Danielson V, Coffin JD *et al* (1997). Genetic modification of the phenotypes produced by amyloid precursor protein overexpression in transgenic mice. *Hum Mol Genet* **6**: 1951–1959.
- Catania C, Sotiropoulos I, Silva R, Onofri C, Breen KC, Sousa N *et al* (2009). The amyloidogenic potential and behavioral correlates of stress. *Mol Psychiatry* **14**: 95–105.
- Chaouloff F, Groc L (2011). Temporal modulation of hippocampal excitatory transmission by corticosteroids and stress. *Front Neuroendocrinol* **32**: 25–42.
- Csernansky JG, Dong H, Fagan AM, Wang L, Xiong C, Holtzman DM *et al* (2006). Plasma cortisol and progression of dementia in subjects with Alzheimer-type dementia. *Am J Psychiatry* **163**: 2164–2169.
- Cuadrado-Tejedor M, Ricobaraza A, Frechilla D, Franco R, Perez-Mediavilla A, Garcia-Osta A (2012). Chronic mild stress accelerates the onset and progression of the Alzheimer's disease phenotype in Tg2576 mice. *J Alzheimers Dis* **28**: 567–578.
- D'Amelio M, Cavallucci V, Middei S, Marchetti C, Pacioni S, Ferri A *et al* (2011). Caspase-3 triggers early synaptic dysfunction in a mouse model of Alzheimer's disease. *Nat Neurosci* **14**: 69–76.
- Davis KE, Easton A, Eacott MJ, Gigg J (2013). Episodic-like memory for what-where-which occasion is selectively impaired in the 3xTgAD mouse model of Alzheimer's disease. *J Alzheimers Dis* **33**: 681–698.
- Dere E, Huston JP, De Souza Silva MA (2005). Episodic-like memory in mice: simultaneous assessment of object, place and temporal order memory. *Brain Res Brain Res Protoc* **16**: 10–19.
- deToledo-Morrell L, Stoub TR, Wang C (2007). Hippocampal atrophy and disconnection in incipient and mild Alzheimer's disease. *Prog Brain Res* **163**: 741–753.
- Distelhorst CW (2002). Recent insights into the mechanism of glucocorticoid-induced apoptosis. *Cell Death Differ* **9**: 6–19.
- Dong H, Goico B, Martin M, Csernansky CA, Bertchume A, Csernansky JG (2004). Modulation of hippocampal cell proliferation, memory, and amyloid plaque deposition in APPsw (Tg2576) mutant mice by isolation stress. *Neuroscience* **127**: 601–609.
- Elgh E, Lindqvist AA, Fagerlund M, Eriksson S, Olsson T, Nasman B (2006). Cognitive dysfunction, hippocampal atrophy and glucocorticoid feedback in Alzheimer's disease. *Biol Psychiatry* **59**: 155–161.
- Good MA, Hale G, Staal V (2007). Impaired "episodic-like" object memory in adult APPsw transgenic mice. *Behav Neurosci* **121**: 443–448.

- Green KN, Billings LM, Roozendaal B, McGaugh JL, LaFerla FM (2006). Glucocorticoids increase amyloid-beta and tau pathology in a mouse model of Alzheimer's disease. *J Neurosci* **26**: 9047–9056.
- Hebda-Bauer EK, Simmons TA, Sugg A, Ural E, Stewart JA, Beals JL *et al* (2013). 3xTg-AD mice exhibit an activated central stress axis during early-stage pathology. *J Alzheimers Dis* **33**: 407–422.
- Hsiao K, Chapman P, Nilsen S, Eckman C, Harigaya Y, Younkin S *et al* (1996). Correlative memory deficits, A $\beta$  elevation, and amyloid plaques in transgenic mice. *Science* **274**: 99–102.
- Jeong YH, Park CH, Yoo J, Shin KY, Ahn SM, Kim HS *et al* (2006). Chronic stress accelerates learning and memory impairments and increases amyloid deposition in APPV7171-CT100 transgenic mice, an Alzheimer's disease model. *FASEB J* **20**: 729–731.
- Li WZ, Li WP, Yao YY, Zhang W, Yin YY, Wu GC *et al* (2010a). Glucocorticoids increase impairments in learning and memory due to elevated amyloid precursor protein expression and neuronal apoptosis in 12-month old mice. *Eur J Pharmacol* **628**: 108–115.
- Li Z, Jo J, Jia JM, Lo SC, Whitcomb DJ, Jiao S *et al* (2010b). Caspase-3 activation via mitochondria is required for long-term depression and AMPA receptor internalization. *Cell* **141**: 859–871.
- Lightman SL, Conway-Campbell BL (2010). The crucial role of pulsatile activity of the HPA axis for continuous dynamic equilibration. *Nat Rev Neurosci* **11**: 710–718.
- Luscher C, Huber KM (2010). Group 1 mGluR-dependent synaptic long-term depression: mechanisms and implications for circuitry and disease. *Neuron* **65**: 445–459.
- Malenka RC, Bear MF (2004). LTP and LTD: an embarrassment of riches. *Neuron* **44**: 5–21.
- McGaugh JL, Roozendaal B (2002). Role of adrenal stress hormones in forming lasting memories in the brain. *Curr Opin Neurobiol* **12**: 205–210.
- Mejia S, Giraldo M, Pineda D, Ardila A, Lopera F (2003). Nongenetic factors as modifiers of the age of onset of familial Alzheimer's disease. *Int Psychogeriatr* **15**: 337–349.
- Morgan FH, Laufgraben MJ (2013). Mifepristone for management of Cushing's syndrome. *Pharmacotherapy* **33**: 319–329.
- Mulkey RM, Endo S, Shenolikar S, Malenka RC (1994). Involvement of a calcineurin/inhibitor-1 phosphatase cascade in hippocampal long-term depression. *Nature* **369**: 486–488.
- Mustafiz T, Portelius E, Gustavsson MK, Holtta M, Zetterberg H, Blennow K *et al* (2011). Characterization of the brain beta-amyloid isoform pattern at different ages of Tg2576 mice. *Neurodegener Dis* **8**: 352–363.
- Nasman B, Olsson T, Viitanen M, Carlstrom K (1995). A subtle disturbance in the feedback regulation of the hypothalamic-pituitary-adrenal axis in the early phase of Alzheimer's disease. *Psychoneuroendocrinology* **20**: 211–220.
- Palop JJ, Mucke L (2010). Amyloid-beta-induced neuronal dysfunction in Alzheimer's disease: from synapses toward neural networks. *Nat Neurosci* **13**: 812–818.
- Rasmuson S, Andrew R, Nasman B, Seckl JR, Walker BR, Olsson T (2001). Increased glucocorticoid production and altered cortisol metabolism in women with mild to moderate Alzheimer's disease. *Biol Psychiatry* **49**: 547–552.
- Rothman SM, Mattson MP (2010). Adverse stress, hippocampal networks, and Alzheimer's disease. *Neuromolecular Med* **12**: 56–70.
- Salmon DP, Bondi MW (2009). Neuropsychological assessment of dementia. *Annu Rev Psychol* **60**: 257–282.
- Selkoe DJ (2002). Alzheimer's disease is a synaptic failure. *Science* **298**: 789–791.
- Shankar GM, Li S, Mehta TH, Garcia-Munoz A, Shepardson NE, Smith I *et al* (2008). Amyloid-beta protein dimers isolated directly from Alzheimer's brains impair synaptic plasticity and memory. *Nat Med* **14**: 837–842.
- Srivareerat M, Tran TT, Alzoubi KH, Alkadhi KA (2009). Chronic psychosocial stress exacerbates impairment of cognition and long-term potentiation in beta-amyloid rat model of Alzheimer's disease. *Biol Psychiatry* **65**: 918–926.
- Stewart S, Cacucci F, Lever C (2011). Which memory task for my mouse? A systematic review of spatial memory performance in the Tg2576 Alzheimer's mouse model. *J Alzheimers Dis* **26**: 105–126.
- Tran TT, Srivareerat M, Alhaider IA, Alkadhi KA (2011a). Chronic psychosocial stress enhances long-term depression in a subthreshold amyloid-beta rat model of Alzheimer's disease. *J Neurochem* **119**: 408–416.
- Tran TT, Srivareerat M, Alkadhi KA (2010). Chronic psychosocial stress triggers cognitive impairment in a novel at-risk model of Alzheimer's disease. *Neurobiol Dis* **37**: 756–763.
- Tran TT, Srivareerat M, Alkadhi KA (2011b). Chronic psychosocial stress accelerates impairment of long-term memory and late-phase long-term potentiation in an at-risk model of Alzheimer's disease. *Hippocampus* **21**: 724–732.
- Walker JJ, Terry JR, Tsaneva-Atanasova K, Armstrong SP, McArdle CA, Lightman SL (2010). Encoding and decoding mechanisms of pulsatile hormone secretion. *J Neuroendocrinol* **22**: 1226–1238.
- Wei Q, Hebda-Bauer EK, Pletsch A, Luo J, Hoversten MT, Osetek AJ *et al* (2007). Overexpressing the glucocorticoid receptor in forebrain causes an aging-like neuroendocrine phenotype and mild cognitive dysfunction. *J Neurosci* **27**: 8836–8844.
- Weiner MF, Vobach S, Olsson K, Svetlik D, Risser RC (1997). Cortisol secretion and Alzheimer's disease progression. *Biol Psychiatry* **42**: 1030–1038.
- Wilson RS, Evans DA, Bienias JL, Mendes de Leon CF, Schneider JA, Bennett DA (2003). Proneness to psychological distress is associated with risk of Alzheimer's disease. *Neurology* **61**: 1479–1485.
- Wilson RS, Schneider JA, Boyle PA, Arnold SE, Tang Y, Bennett DA (2007). Chronic distress and incidence of mild cognitive impairment. *Neurology* **68**: 2085–2092.
- Wolf DP, Crusio WE, Lipp HP (2002). Knockout mice: simple solutions to the problems of genetic background and flanking genes. *Trends Neurosci* **25**: 336–340.

Supplementary Information accompanies the paper on the Neuropsychopharmacology website (<http://www.nature.com/npp>)

# $\eta$ -Secretase processing of APP inhibits neuronal activity in the hippocampus

Michael Willem<sup>1</sup>, Sabina Tahirovic<sup>2</sup>, Marc Aurel Busche<sup>3,4,5</sup>, Saak V. Ovsepian<sup>2</sup>, Magda Chafai<sup>6</sup>, Scherazad Kootar<sup>6</sup>, Daniel Hornburg<sup>7</sup>, Lewis D. B. Evans<sup>8</sup>, Steven Moore<sup>8</sup>, Anna Daria<sup>1</sup>, Heike Hampel<sup>1</sup>, Veronika Müller<sup>1</sup>, Camilla Giudici<sup>1</sup>, Brigitte Nuscher<sup>1</sup>, Andrea Wenninger-Weinzierl<sup>2</sup>, Elisabeth Kremmer<sup>2,5,9</sup>, Michael T. Heneka<sup>10,11</sup>, Dietmar R. Thal<sup>12</sup>, Vilmantas Giedraitis<sup>13</sup>, Lars Lannfelt<sup>13</sup>, Ulrike Müller<sup>14</sup>, Frederick J. Livesey<sup>8</sup>, Felix Meissner<sup>7</sup>, Jochen Herms<sup>2</sup>, Arthur Konnerth<sup>4,5</sup>, H el ene Marie<sup>6</sup> & Christian Haass<sup>1,2,5</sup>

**Alzheimer disease (AD) is characterized by the accumulation of amyloid plaques, which are predominantly composed of amyloid- $\beta$  peptide<sup>1</sup>. Two principal physiological pathways either prevent or promote amyloid- $\beta$  generation from its precursor,  $\beta$ -amyloid precursor protein (APP), in a competitive manner<sup>1</sup>. Although APP processing has been studied in great detail, unknown proteolytic events seem to hinder stoichiometric analyses of APP metabolism *in vivo*<sup>2</sup>. Here we describe a new physiological APP processing pathway, which generates proteolytic fragments capable of inhibiting neuronal activity within the hippocampus. We identify higher molecular mass carboxy-terminal fragments (CTFs) of APP, termed CTF- $\eta$ , in addition to the long-known CTF- $\alpha$  and CTF- $\beta$  fragments generated by the  $\alpha$ - and  $\beta$ -secretases ADAM10 (a disintegrin and metalloproteinase 10) and BACE1 ( $\beta$ -site APP cleaving enzyme 1), respectively. CTF- $\eta$  generation is mediated in part by membrane-bound matrix metalloproteinases such as MT5-MMP, referred to as  $\eta$ -secretase activity.  $\eta$ -Secretase cleavage occurs primarily at amino acids 504–505 of APP<sub>695</sub>, releasing a truncated ectodomain. After shedding of this ectodomain, CTF- $\eta$  is further processed by ADAM10 and BACE1 to release long and short A $\eta$  peptides (termed A $\eta$ - $\alpha$  and A $\eta$ - $\beta$ ). CTFs produced by  $\eta$ -secretase are enriched in dystrophic neurites in an AD mouse model and in human AD brains. Genetic and pharmacological inhibition of BACE1 activity results in robust accumulation of CTF- $\eta$  and A $\eta$ - $\alpha$ . In mice treated with a potent BACE1 inhibitor, hippocampal long-term potentiation was reduced. Notably, when recombinant or synthetic A $\eta$ - $\alpha$  was applied on hippocampal slices *ex vivo*, long-term potentiation was lowered. Furthermore, *in vivo* single-cell two-photon calcium imaging showed that hippocampal neuronal activity was attenuated by A $\eta$ - $\alpha$ . These findings not only demonstrate a major functionally relevant APP processing pathway, but may also indicate potential translational relevance for therapeutic strategies targeting APP processing.**

To identify new proteolytic pathways of APP, we searched for CTFs other than those giving rise to P3 fragment (CTF- $\alpha$ ) or amyloid- $\beta$  (CTF- $\beta$ )<sup>3–5</sup>. A new CTF with an approximate molecular mass of 30 kilodaltons (kDa) was revealed, which was recognized by an antibody to the C terminus of APP (Y188) and was absent in the brains of APP-knockout mice<sup>6</sup> (Fig. 1a and Supplementary Table 1). The molecular mass of the novel CTF suggests an additional physiological cleavage of APP amino-terminal to the known cleavage sites of  $\beta$ - and  $\alpha$ -secretases, which we named accordingly  $\eta$ -cleavage of APP (Extended Data

Fig. 1). In the soluble fraction, we detected the N-terminal cleavage product (sAPP- $\eta$ ; Extended Data Fig. 2), with a molecular mass of approximately 80 kDa that distinguishes it from alternative N-terminal APP fragments described previously<sup>7–9</sup>. In addition, we observed lower molecular mass soluble peptides (A $\eta$ ), which presumably derived from processing of CTF- $\eta$  by BACE1 (A $\eta$ - $\beta$ ) or ADAM10 (A $\eta$ - $\alpha$ ), or alternatively from sAPP- $\alpha$ / $\beta$  cleavage (Fig. 1b). A $\eta$  was identified in the soluble fraction of mouse brains as several closely spaced peptides by antibody M3.2 (Fig. 1b), demonstrating that some of these fragments contain the N-terminal part of the amyloid- $\beta$  domain and probably end at the  $\alpha$ -secretase cleavage site. A $\eta$  fragments were further validated by antibody 9478D directed against an epitope N-terminal to the amyloid- $\beta$  domain (Fig. 1b). Consistent with  $\eta$ -secretase cleavage of APP in wild-type mice, we observed increased CTF- $\eta$  and A $\eta$  production in brain homogenates of APPPS1-21 transgenic mice<sup>10</sup> (Fig. 1c, d). Furthermore, antibody 192swe selectively identified the A $\eta$ - $\beta$  species ending at the BACE1 cleavage site (Fig. 1d). Consistent with increased BACE1 cleavage of Swedish mutant APP, only minor amounts of A $\eta$ - $\alpha$  were detected in this mouse model with antibody 2D8 (Fig. 1d). Physiological  $\eta$ -secretase processing was further confirmed in cerebrospinal fluid (CSF) from humans with and without the Swedish mutation (APP<sub>swe</sub>) (Fig. 1e). Fivefold higher A $\eta$  than amyloid- $\beta$  levels were observed in human CSF ( $5.33 \pm 1.39$  times (mean  $\pm$  s.d.) higher A $\eta$  than amyloid- $\beta$  estimated by 2D8 blot signals;  $n = 7$ ,  $P > 0.0001$ , Student's  $t$ -test). Using antibody 192swe, A $\eta$ - $\beta$  was selectively detected in the CSF of patients with the Swedish mutation, whereas antibodies 2E9 and 2D8 detected A $\eta$ - $\alpha$  in all analysed samples (Fig. 1e). Moreover, while these peptides are generated by  $\eta$ -secretase cleavage N-terminal to the amyloid- $\beta$  domain, they do not reach the  $\gamma$ -secretase site (see mass spectrometric analysis in Fig. 1f), demonstrating that they are different to the previously described N-terminally extended amyloid- $\beta$  variants<sup>11,12</sup>. Membrane-bound matrix metalloproteinases such as MT1-MMP and MT5-MMP (also known as MMP14 and MMP24, respectively) were shown to cleave APP *in vitro* at a site consistent with the molecular mass of  $\eta$ -secretase processing products<sup>13,14</sup>. We therefore produced a neo-epitope-specific antibody (10A8; Extended Data Fig. 2) to identify the  $\eta$ -secretase cleavage site. Antibody 10A8 detected a protein corresponding to sAPP- $\eta$  with an approximate molecular mass of 80 kDa in mouse brain lysates, which was absent in the APP-knockout mouse brain (Extended Data Fig. 2). Thus,  $\eta$ -secretase cleavage of APP may occur *in vivo* at least in part at amino

<sup>1</sup>Biomedical Center (BMC), Ludwig-Maximilians-University Munich, 81377 Munich, Germany. <sup>2</sup>German Center for Neurodegenerative Diseases (DZNE) Munich, 81377 Munich, Germany. <sup>3</sup>Department of Psychiatry and Psychotherapy, Technische Universit at M unchen, 81675 Munich, Germany. <sup>4</sup>Institute of Neuroscience, Technische Universit at M unchen, 80802 Munich, Germany. <sup>5</sup>Munich Cluster for Systems Neurology (SyNergy), Ludwig-Maximilians-University Munich, 81377 Munich, Germany. <sup>6</sup>Institut de Pharmacologie Mol culaire et Cellulaire (IPMC), Centre National de la Recherche Scientifique (CNRS), Universit e de Nice Sophia Antipolis, UMR 7275, 06560 Valbonne, France. <sup>7</sup>Max Planck Institute of Biochemistry, Martinsried 82152, Germany. <sup>8</sup>Gurdon Institute, Cambridge Stem Cell Institute & Department of Biochemistry, University of Cambridge, Cambridge CB2 1QN, UK. <sup>9</sup>Institute of Molecular Immunology, German Research Center for Environmental Health, 81377 Munich, Germany. <sup>10</sup>Department of Neurology, Clinical Neuroscience Unit, University of Bonn, 53127 Bonn, Germany. <sup>11</sup>German Center for Neurodegenerative Diseases (DZNE) Bonn, 53175 Bonn, Germany. <sup>12</sup>Institute of Pathology - Laboratory for Neuropathology, University of Ulm, 89081 Ulm, Germany. <sup>13</sup>Department of Public Health/Geriatrics, Uppsala University, 751 85 Uppsala, Sweden. <sup>14</sup>Institute for Pharmacy and Molecular Biotechnology IPMB, Functional Genomics, University of Heidelberg, 69120 Heidelberg, Germany.

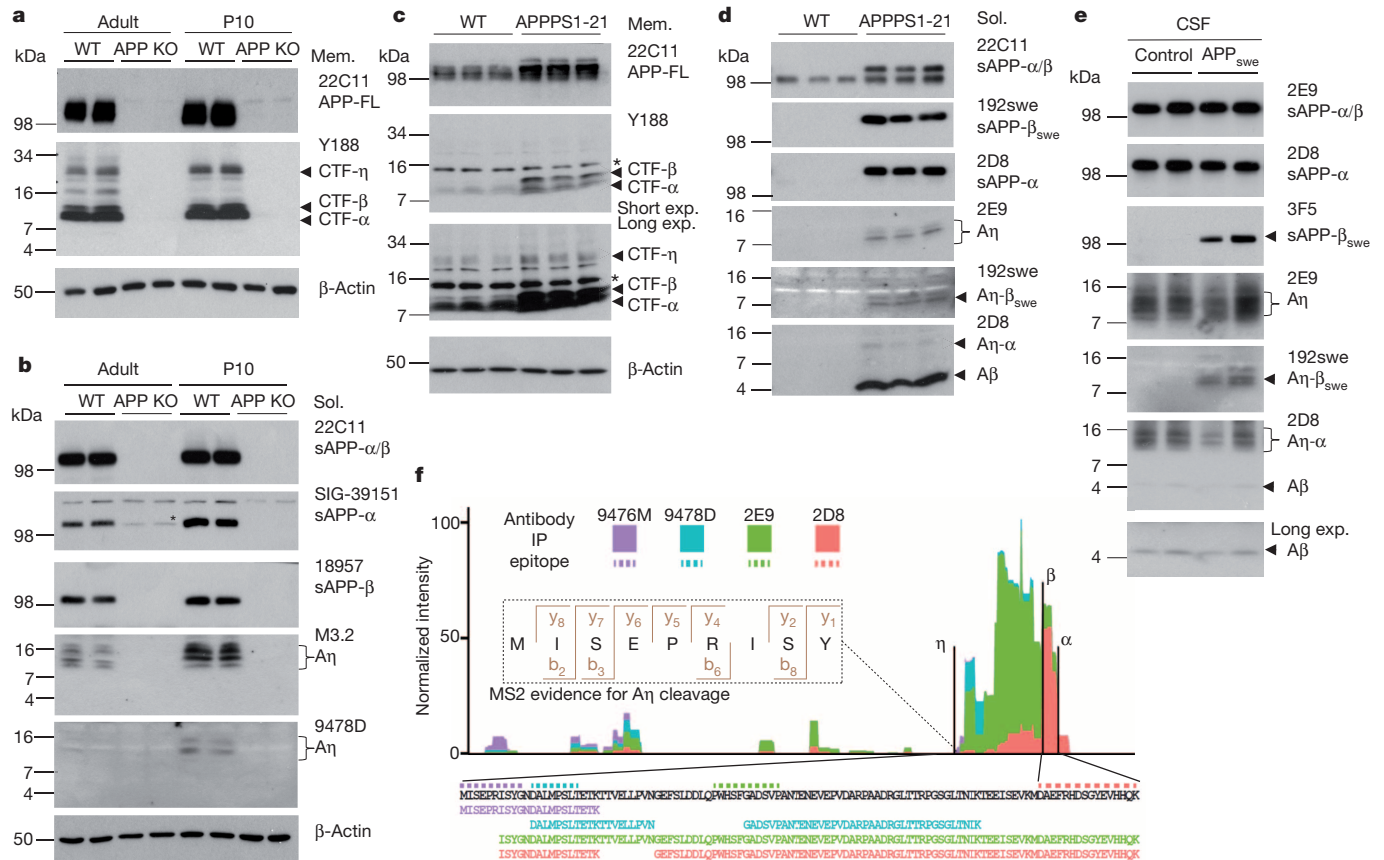


**Figure 1 | A novel APP proteolytic processing pathway.** **a**, A 30-kDa APP CTF- $\eta$  is detected in the brains of adult and postnatal mice (P10, postnatal day 10). APP-FL, full-length APP; KO, knockout; WT, wild type. **b**, A $\eta$  was detected in the soluble (sol.) fraction of adult and P10 mice by antibody M3.2 and 9478D (antibody 9478D may not be sensitive enough to detect the lower A $\eta$  levels in adult brain). **c**, Higher levels of CTF- $\eta$  are observed in APPS1-21 mouse brains as compared to wild-type in the membrane (mem.) fraction. Short and long exposures indicated. Background bands are indicated by

asterisks. **d**, Soluble extracts of APPS1-21 mouse brains contained A $\eta$  species, as detected by 2E9 antibody. A $\eta$ - $\beta_{swe}$  was selectively detected by antibody 192swe. **e**, A $\eta$  and amyloid- $\beta$  (A $\beta$ ) were readily detectable in human CSF by antibody 2D8. Antibody 2E9 allowed the detection of A $\eta$  in all samples, whereas 192swe specifically detected A $\eta$ - $\beta_{swe}$ . **f**, Mass spectrometric analysis of A $\eta$ . Peptide intensities were summed per amino acid residue and plotted in relation to each other.

acids 504–505 of APP<sub>695</sub>. To determine the N- and C-terminal cleavage sites of A $\eta$  peptides, we performed immunoprecipitation with antibodies 9476M, 9478D, 2D8 and 2E9 (Extended Data Fig. 3a, b). Isolated A $\eta$  peptides were digested with three different proteases to produce several overlapping peptides, and analysed by mass spectrometry. We identified several peptides covering the entire sequence between the cleavage site N504–M505 of APP<sub>695</sub> starting with the sequence MISEPRISY after the  $\eta$ -secretase cleavage site (Fig. 1f). Mass spectrometry also supports the C-terminal cleavages at the  $\beta$ - and  $\alpha$ -secretase sites. After immunoprecipitation with 2D8, fragments of the amyloid- $\beta$  domain were also observed in smaller amounts alongside the novel A $\eta$  peptides (Fig. 1f and Extended Data Fig. 3c). As the  $\eta$ -secretase cleavage site at amino acid 505 of APP is consistent with the previously described *in vitro* cleavage sites of APP<sub>695</sub> by MT1-MMP and MT5-MMP (refs 13, 14), we investigated brains from MT5-MMP- and MT1-MMP-knockout mice<sup>15,16</sup> (Extended Data Fig. 4). Whereas MT1-MMP knockout had no marked effect on A $\eta$ - $\alpha$  levels (Extended Data Fig. 4b), the generation of A $\eta$ - $\alpha$  was reduced in brains from MT5-MMP-knockout mice (Extended Data Fig. 4c). Furthermore, after MT5-MMP overexpression in murine N2a cells, a selective increase in A $\eta$ - $\alpha$  peptide of approximately 16 kDa was observed (data not shown). Thus, MT5-MMP displays  $\eta$ -secretase activity in intact mouse brains, although the contribution of other  $\eta$ -secretases must be considered.

While investigating protease inhibitors capable of blocking  $\eta$ -secretase, we observed that pharmacological BACE1 inhibition led

to a pronounced accumulation of the long A $\eta$ - $\alpha$  species in Chinese hamster ovary (CHO) 7PA2 cells (Fig. 2a). This indicates that after blockade of  $\beta$ -secretase activity, processing by  $\alpha$ -secretase leads to enhanced production of the long A $\eta$ - $\alpha$  species at the expense of the shorter BACE1-generated A $\eta$ - $\beta$ . Similarly, BACE1 inhibition also led to an accumulation of endogenous CTF- $\eta$  and enhanced production of endogenous A $\eta$ - $\alpha$  in primary mouse hippocampal neurons (Fig. 2b, c), as well as human neurons differentiated from embryonic pluripotent stem cells (H9 cells<sup>17</sup>; Fig. 2d–g). Furthermore, in human neurons we not only detected a 65% increase (Fig. 2g) in the slightly longer A $\eta$ - $\alpha$  species after BACE inhibition, but also a concomitant decrease in A $\eta$ - $\beta$  peptides (Fig. 2e, top). Importantly,  $\eta$ -secretase processing significantly exceeded amyloidogenic processing ( $9.5 \pm 1.87$  times A $\eta$  compared to amyloid- $\beta$  estimated for human neurons;  $n = 8$ ,  $P > 0.001$ , Student's *t*-test). Pharmacological intervention with a BACE1 inhibitor *in vivo* caused a clear and time-dependent increase in CTF- $\eta$  and A $\eta$ - $\alpha$  levels in APP<sub>V717I</sub> transgenic mice<sup>18</sup> (Fig. 2h), which was fully reversible within 24 h after administration. In agreement, increased CTF- $\eta$  and A $\eta$ - $\alpha$  levels were also observed in a BACE1-knockout mouse<sup>19</sup> *in vivo* (Fig. 2i).

To identify a potential contribution of  $\eta$ -secretase processing to AD pathology, immunohistochemical analyses were performed with brains derived from six-month-old APPS1-21 (ref. 20) mice (Extended Data Fig. 5a). This revealed co-labelling of antibody Y188 with antibody 2E9 in dystrophic neurites. No signal for A $\eta$  peptides was obtained in plaque cores in which aggregated amyloid- $\beta$  was

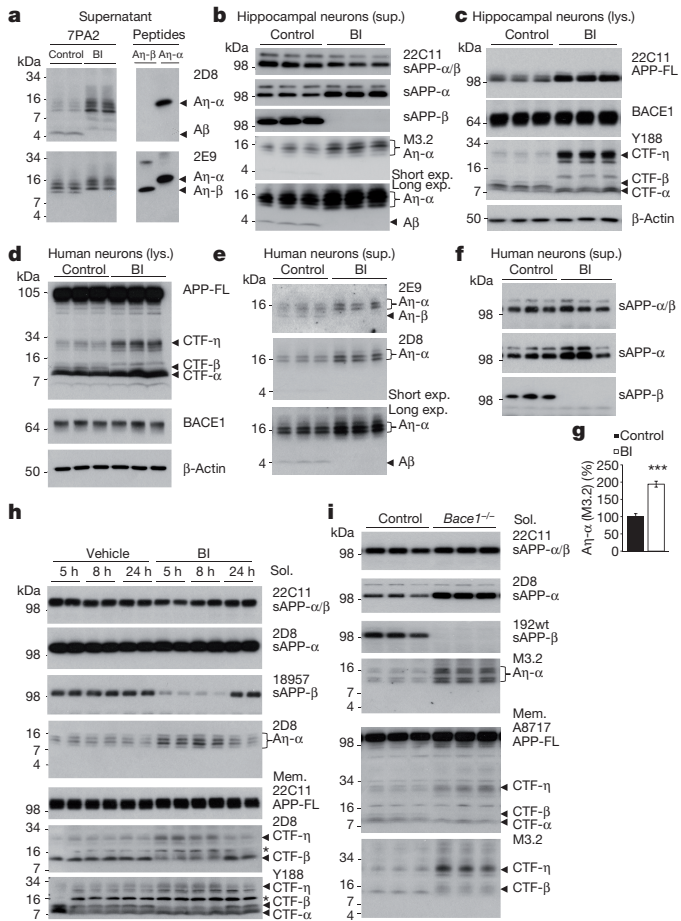


**Figure 2 | Inhibition of BACE1 results in increased levels of CTF- $\eta$  and A $\eta$ - $\alpha$ .** **a**, Conditioned media from 7PA2 cells treated with or without a BACE1 inhibitor (BI) was co-migrated with synthetic A $\eta$ - $\beta$  and A $\eta$ - $\alpha$  peptides and immunoblotted with 2D8 and 2E9 antibodies. **b–f**, After BACE inhibition in mouse hippocampal neurons and human neurons, a reduction of sAPP- $\beta$  was accompanied by a strong increase in endogenous A $\eta$ - $\alpha$  and CTF- $\eta$  levels. Lys., lysate; sup., supernatant. **g**, Quantification of intensities for 2D8 signals in **e** ( $n = 8$ ;  $***P < 0.001$ , Student's  $t$ -test). **h**, BACE1 inhibition *in vivo* resulted in enhanced production of A $\eta$ - $\alpha$  species in APP<sub>V717I</sub> mice. Background bands are indicated by asterisks. **i**, Western blot analysis of soluble extracts of P10 *Bace1*<sup>-/-</sup> mouse brains revealed a marked increase in A $\eta$ - $\alpha$  peptides as compared to controls.

detected by 6E10 staining (Extended Data Fig. 5a). Similar data were obtained in human AD brains (Extended Data Fig. 6). To verify accumulation of CTF- $\eta$  in dystrophic neurites, we used laser capture microdissection (LCM). Western blot analysis revealed not only CTF- $\beta$  and CTF- $\alpha$ , but also CTF- $\eta$  within the halo, but not within the plaque core area or regions devoid of plaques (Extended Data Fig. 5b). As expected, amyloid- $\beta$  was observed within the plaque core as well as in the surrounding halo (Extended Data Fig. 5b).

Since the cleavage products of  $\eta$ -secretase APP processing accumulate after BACE1 inhibition and are enriched in dystrophic neurites, we examined whether soluble A $\eta$  peptides interfere with neuronal function, similar to soluble amyloid- $\beta$  oligomers<sup>1</sup>. Long-term potentiation (LTP) is considered as a synaptic correlate of memory, and is widely used as a model for investigating the neurotoxic effects of amyloid- $\beta$  oligomers on synaptic function<sup>21–23</sup>. A single oral dose of the BACE1 inhibitor SCH1682496 increased the CTF- $\eta$  levels, and almost doubled the A $\eta$ - $\alpha$  level in soluble brain extracts prepared from animals 3 h after treatment (Extended Data Fig. 7). This was accompanied by a significant reduction of hippocampal LTP (Fig. 3a, b). These findings may suggest an involvement of A $\eta$ - $\alpha$  in LTP deficit

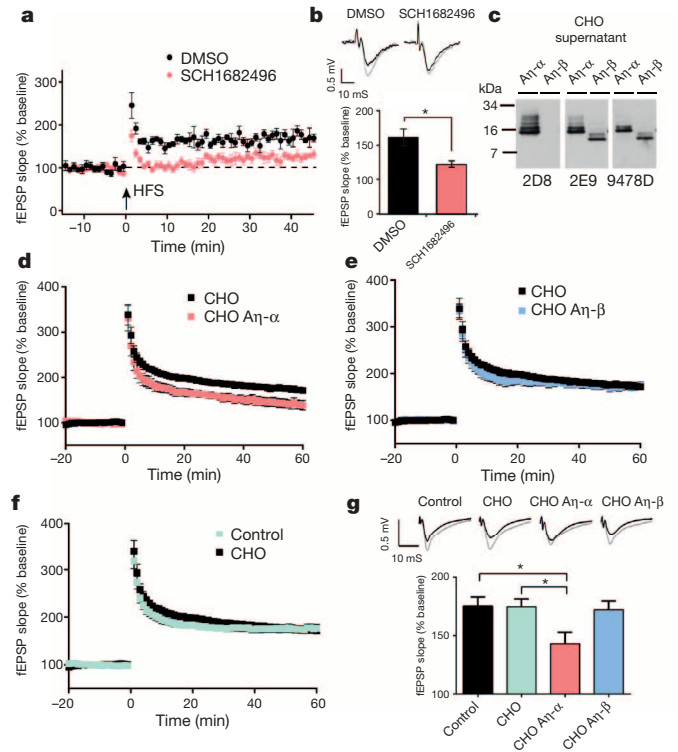


**Figure 3 | A $\eta$ - $\alpha$  impairs hippocampal LTP.** **a**, Pharmacological BACE1 inhibition with SCH1682496 lowers hippocampal LTP. DMSO, dimethylsulfoxide; fEPSP, field excitatory postsynaptic potential; HFS, high-frequency stimulation. **b**, Representative fEPSPs recorded in CA1 area before and 45 min after tetanization of Schaffer collaterals (top), with summary plot of the effects of the inhibitor (SCH1682496) and vehicle (DMSO) on fEPSP slopes in all examined groups in **a** ( $n = 9$ ). **c**, Soluble A $\eta$ - $\alpha$  and A $\eta$ - $\beta$  peptides were expressed in CHO cells and blotted with 2D8, 2E9 and 9478D antibodies. **d–f**, A $\eta$ - $\alpha$  ( $n = 9$ ) (**d**), but not A $\eta$ - $\beta$  ( $n = 7$ ) (**e**), conditioned media from untransfected cells (CHO;  $n = 13$ ) or artificial cerebrospinal fluid (ACSF) (control;  $n = 15$ ) (**f**) significantly inhibited LTP. **g**, Summary graph of LTP magnitudes calculated 45–60 min after high-frequency stimulation from graphs in **d–f** with statistical analysis ( $*P < 0.05$ ; one-way analysis of variance (ANOVA) and post hoc Bonferroni test); error bars represent s.e.m. For each condition, sample fEPSP traces pre-LTP (black) and 45–60 min post-LTP (grey) induction are shown (top).

under acute blockade of  $\beta$ -secretase activity. To validate the potential effects of A $\eta$  peptides on synaptic transmission and plasticity directly, we expressed A $\eta$ - $\beta$  and A $\eta$ - $\alpha$  in CHO cells (Fig. 3c). Concentrated conditioned media was further enriched for A $\eta$  by size-exclusion chromatography (SEC) and applied to hippocampal slices before LTP induction in CA1 pyramidal neurons. Neither A $\eta$ - $\beta$  nor A $\eta$ - $\alpha$  influenced the baseline synaptic transmission (Extended Data Fig. 8). Comparison of LTP 60 min after its induction in the presence of A $\eta$ - $\beta$  or A $\eta$ - $\alpha$  with control conditions (Fig. 3d–g) revealed that A $\eta$ - $\alpha$  lowered the LTP to a degree comparable to synthetic amyloid- $\beta$  dimers<sup>23</sup> (Extended Data Fig. 9a, b), while truncated A $\eta$ - $\beta$  had no effect (Fig. 3e, g). In support of this observation, synthetic A $\eta$ - $\alpha$  reduced LTP to a similar extent at a concentration of 100 nM (Extended Data Fig. 9c, d). To examine the direct effects of A $\eta$  peptides on neuronal activity *in vivo*, we used two-photon calcium imaging at single-cell resolution<sup>24,25</sup>. Figure 4a–d illustrates results from experiments in which the activity of neurons in the CA1 pyramidal cell layer was monitored before and after superfusion of the exposed hippocampus with A $\eta$  peptides or the respective control peptides. A $\eta$ - $\alpha$  strongly suppressed the activity of hippocampal neurons *in vivo*, an effect not observed with A $\eta$ - $\beta$  or the control peptide (Fig. 4a–d and Extended Data Fig. 10). By using local application of synthetic A $\eta$ - $\alpha$  to hippocampal neurons, we demonstrate that the inhibitory effect of A $\eta$ - $\alpha$  on neurons was readily reversible after

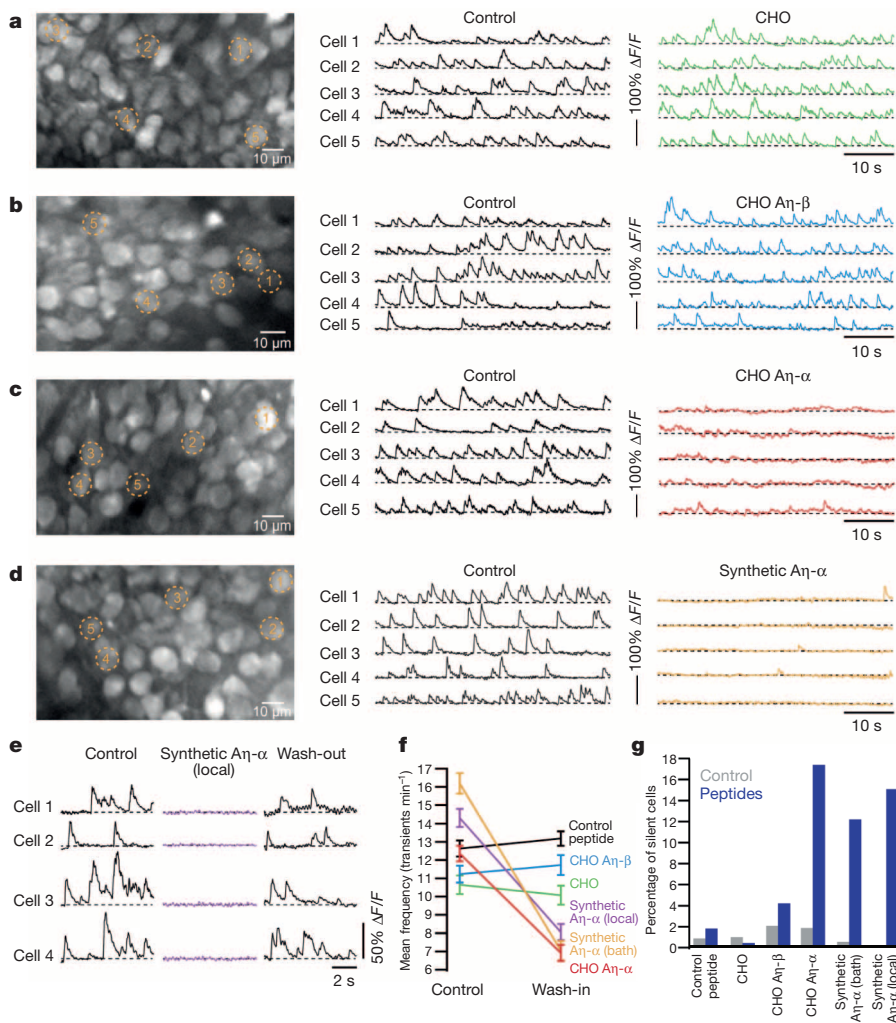


**Figure 4** | Aη-α reduces neuronal activity *in vivo*. **a–d**, Left, *in vivo* images of CA1 hippocampal neurons labelled with the fluorescent calcium indicator fluo-8AM. Middle and right, calcium transients of five representative neurons, marked in the corresponding left panels, before and during bath-application of Aη or CHO conditioned media. **e**, Calcium transients in hippocampal neurons before, during and after local application of synthetic Aη-α. **f, g**, Summary results of the changes in the average rates of calcium transients (**f**), and in the fractions of silent neurons (**g**); for statistics see Supplementary Tables 2 and 3. Error bars represent s.e.m.

washout (Fig. 4e). A summary of the results from all experiments is shown in Fig. 4f, g.

We have identified a new APP processing pathway that exceeds amyloidogenic processing. Similar to amyloid-β production<sup>26</sup>, the alternative proteolytic processing pathway occurs under physiological conditions but may be altered during AD pathogenesis. Accumulation of η-secretase<sup>27</sup> and CTF-η within dystrophic neurites in close vicinity to neuritic plaques may also support its potential contribution to AD pathology. However, all APP and presenilin-associated familial AD mutations affect amyloid-β production and aggregation (reviewed in ref. 26), whereas the Icelandic mutation APP<sub>A673T</sub> prevents AD and dementia by moderately reducing amyloid-β production<sup>28</sup>. Indeed, the Swedish mutation decreased Aη-α by strongly enhancing BACE1-mediated APP processing. However, η-secretase accumulation<sup>27</sup> and its activity near amyloid plaques may suggest that η-secretase stimulation by amyloid-β could be a downstream effector within the amyloid cascade. Although Aη may be involved in the modulation of neuronal activity and synaptic plasticity, the differential bioactivity of recombinant Aη-α and Aη-β is currently unclear. One may speculate that the longer Aη-α peptide is more stable owing to unknown post-translational modifications. This would be consistent with our observation that, in contrast to cell-produced Aη-β, 100 nM of synthetic Aη-β inhibits LTP (data not shown). Finally, it is important to note that low-*n* amyloid-β oligomer preparations from 7PA2 supernatants contain considerable amounts of Aη (data not shown). Thus, the previously observed inhibition of LTP with such fractions may also be attributed to the presence of Aη. Our findings may also be considered in the context of continuing clinical trials with BACE1 inhibitors. Together with the identification of numerous

brain-specific BACE1 substrates<sup>29,30</sup>, our data indicate that therapeutic inhibition of BACE1 activity requires careful titration to prevent unwanted adverse effects at several levels.

**Online Content** Methods, along with any additional Extended Data display items and Source Data, are available in the online version of the paper; references unique to these sections appear only in the online paper.

Received 27 March; accepted 25 June 2015.

Published online 31 August 2015.

- Haass, C. & Selkoe, D. J. Soluble protein oligomers in neurodegeneration: lessons from the Alzheimer's amyloid β-peptide. *Nature Rev. Mol. Cell Biol.* **8**, 101–112 (2007).
- Dobrowolska, J. A. *et al.* CNS amyloid-β, soluble APP-α and -β kinetics during BACE1 inhibition. *J. Neurosci.* **34**, 8336–8346 (2014).
- Haass, C., Koo, E. H., Mellon, A., Hung, A. Y. & Selkoe, D. J. Targeting of cell-surface β-amyloid precursor protein to lysosomes: alternative processing into amyloid-bearing fragments. *Nature* **357**, 500–503 (1992).
- Estus, S. *et al.* Potentially amyloidogenic, carboxyl-terminal derivatives of the amyloid protein precursor. *Science* **255**, 726–728 (1992).
- Haass, C. *et al.* β-Amyloid peptide and a 3-kDa fragment are derived by distinct cellular mechanisms. *J. Biol. Chem.* **268**, 3021–3024 (1993).
- Müller, U. *et al.* Behavioral and anatomical deficits in mice homozygous for a modified β-amyloid precursor protein gene. *Cell* **79**, 755–765 (1994).
- Nikolaev, A., McLaughlin, T., O'Leary, D. D. & Tessier-Lavigne, M. APP binds DR6 to trigger axon pruning and neuron death via distinct caspases. *Nature* **457**, 981–989 (2009).
- Jefferson, T. *et al.* Metalloprotease meprin β generates nontoxic N-terminal amyloid precursor protein fragments *in vivo*. *J. Biol. Chem.* **286**, 27741–27750 (2011).
- Vella, L. J. & Cappai, R. Identification of a novel amyloid precursor protein processing pathway that generates secreted N-terminal fragments. *FASEB J.* **26**, 2930–2940 (2012).
- Radde, R. *et al.* β42-driven cerebral amyloidosis in transgenic mice reveals early and robust pathology. *EMBO Rep.* **7**, 940–946 (2006).

11. Portelius, E. *et al.* Mass spectrometric characterization of amyloid- $\beta$  species in the 7PA2 cell model of Alzheimer's disease. *J. Alzheimers Dis.* **33**, 85–93 (2013).
12. Welzel, A. T. *et al.* Secreted amyloid  $\beta$ -proteins in a cell culture model include N-terminally extended peptides that impair synaptic plasticity. *Biochemistry* **53**, 3908–3921 (2014).
13. Higashi, S. & Miyazaki, K. Novel processing of  $\beta$ -amyloid precursor protein catalyzed by membrane type 1 matrix metalloproteinase releases a fragment lacking the inhibitor domain against gelatinase A. *Biochemistry* **42**, 6514–6526 (2003).
14. Ahmad, M. *et al.* Cleavage of amyloid- $\beta$  precursor protein (APP) by membrane-type matrix metalloproteinases. *J. Biochem.* **139**, 517–526 (2006).
15. Folgueras, A. R. *et al.* Metalloproteinase MT5-MMP is an essential modulator of neuro-immune interactions in thermal pain stimulation. *Proc. Natl Acad. Sci. USA* **106**, 16451–16456 (2009).
16. Zhou, Z. *et al.* Impaired endochondral ossification and angiogenesis in mice deficient in membrane-type matrix metalloproteinase 1. *Proc. Natl Acad. Sci. USA* **97**, 4052–4057 (2000).
17. Shi, Y., Kirwan, P. & Livesey, F. J. Directed differentiation of human pluripotent stem cells to cerebral cortex neurons and neural networks. *Nature Protocols* **7**, 1836–1846 (2012).
18. Moechars, D. *et al.* Early phenotypic changes in transgenic mice that overexpress different mutants of amyloid precursor protein in brain. *J. Biol. Chem.* **274**, 6483–6492 (1999).
19. Cai, H. *et al.* BACE1 is the major  $\beta$ -secretase for generation of A $\beta$  peptides by neurons. *Nature Neurosci.* **4**, 233–234 (2001).
20. Radde, R. *et al.* A $\beta$ 42-driven cerebral amyloidosis in transgenic mice reveals early and robust pathology. *EMBO Rep.* **7**, 940–946 (2006).
21. Walsh, D. M. *et al.* Naturally secreted oligomers of amyloid  $\beta$  protein potently inhibit hippocampal long-term potentiation *in vivo*. *Nature* **416**, 535–539 (2002).
22. Shankar, G. M. *et al.* Natural oligomers of the Alzheimer amyloid- $\beta$  protein induce reversible synapse loss by modulating an NMDA-type glutamate receptor-dependent signaling pathway. *J. Neurosci.* **27**, 2866–2875 (2007).
23. Shankar, G. M. *et al.* Amyloid- $\beta$  protein dimers isolated directly from Alzheimer's brains impair synaptic plasticity and memory. *Nature Med.* **14**, 837–842 (2008).
24. Busche, M. A. *et al.* Clusters of hyperactive neurons near amyloid plaques in a mouse model of Alzheimer's disease. *Science* **321**, 1686–1689 (2008).
25. Busche, M. A. *et al.* Critical role of soluble amyloid- $\beta$  for early hippocampal hyperactivity in a mouse model of Alzheimer's disease. *Proc. Natl Acad. Sci. USA* **109**, 8740–8745 (2012).
26. Haass, C. Take five—BACE and the  $\gamma$ -secretase quartet conduct Alzheimer's amyloid  $\beta$ -peptide generation. *EMBO J.* **23**, 483–488 (2004).
27. Sekine-Aizawa, Y. *et al.* Matrix metalloproteinase (MMP) system in brain: identification and characterization of brain-specific MMP highly expressed in cerebellum. *Eur. J. Neurosci.* **13**, 935–948 (2001).
28. Jonsson, T. *et al.* A mutation in APP protects against Alzheimer's disease and age-related cognitive decline. *Nature* **488**, 96–99 (2012).
29. Kuhn, P. H. *et al.* Secretome protein enrichment identifies physiological BACE1 protease substrates in neurons. *EMBO J.* **31**, 3157–3168 (2012).
30. Zhou, L. *et al.* The neural cell adhesion molecules L1 and CHL1 are cleaved by BACE1 protease *in vivo*. *J. Biol. Chem.* **287**, 25927–25940 (2012).

Supplementary Information is available in the online version of the paper.

**Acknowledgements** The authors thank S. Lammich, N. Exner and H. Steiner for critical comments. We thank A. Sülzen, N. Astola, S. Diederich, E. Grieflinger and J. Gobbert for technical help. The APPPS1-21 colony was established from a breeding pair provided by M. Jucker. *MT1-MMP*<sup>-/-</sup> mouse brains were obtained from Z. Zhou. *MT5-MMP*<sup>-/-</sup> mouse brains were obtained from I. Farinas. We thank H. Jacobsen for the BACE1 inhibitor RO5508887. This work was supported by the European Research Council under the European Union's Seventh Framework Program (FP7/2007–2013)/ERC grant agreement no. 321366-Amyloid (advanced grant to C.H.). The work of D.R.T. was supported by AFI (grant 13803). The research leading to these results has received funding (F.M. and D.H.) from the European Research Council under the European Union's Seventh Framework Programme (FP7/2007-2013)/ERC grant agreement no. 318987 [TOPAG]. We thank J. Cox and M. Mann for critical discussions and the mass spectrometry infrastructure. We also acknowledge support by grants from Deutsche Forschungsgemeinschaft (MU 1457/9-1, 9-2 to U.M.) and the ERA-Net Neuron (O1EW1305A to U.M.). Further support came from the ATIP/AVENIR program (Centre national de la recherche scientifique, CNRS) to H.M.; the French Fondation pour la Coopération Scientifique – Plan Alzheimer (Senior Innovative Grant 2010) to M.C. and H.M., and the French Government (National Research Agency, ANR) through the “Investments for the Future” LABEX SIGNALIFE: program reference ANR-11-LABX-0028-01 to S.K. M.A.B. was supported by the Langmatz Stiftung. F.J.L. is a Wellcome Trust Investigator. *In vivo* BACE1 inhibition experiments with APP transgenic mice were performed together with reMYND (Bio-Incubator, 3001 Leuven-Heverlee, Belgium).

**Author Contributions** M.W. and C.H. designed the study and interpreted the results. M.W. generated all biochemical data together with H.H., V.M., B.N. and C.G. S.T., supported by A.W.-W., provided primary neuronal cultures, performed and analysed immunohistological stainings, and together with A.D. performed LCM. D.R.T. provided and analysed human brain sections. M.T.H. provided CSF samples. U.M. provided APP-knockout mice. E.K. produced new monoclonal antibodies. D.H. and F.M. designed and conducted mass spectrometry and data analysis. L.D.B.E., S.M. and F.J.L. carried out BACE1 inhibition of human neurons. H.M. together with M.C. and S.K. performed all electrophysiological recordings (LTP) *in vitro* and analysis in relation to application of peptides. S.V.O. and J.H. performed all electrophysiological recordings (LTP) *in vitro* in relation to the BACE1 inhibitor tests. M.A.B. and A.K. performed all Ca<sup>2+</sup>-imaging experiments *in vivo* and analysis. M.W. and C.H. wrote the manuscript with input from the other authors. Correspondence and requests for materials should be addressed to M.W. and C.H.

**Author Information** Reprints and permissions information is available at [www.nature.com/reprints](http://www.nature.com/reprints). The authors declare competing financial interests: details are available in the online version of the paper. Readers are welcome to comment on the online version of the paper. Correspondence and requests for materials should be addressed to M.W. ([michael.willem@mail03.med.uni-muenchen.de](mailto:michael.willem@mail03.med.uni-muenchen.de)) or C.H. ([christian.haass@mail03.med.uni-muenchen.de](mailto:christian.haass@mail03.med.uni-muenchen.de)).

## METHODS

**Cell culture.** Mycoplasma-free CHO and 7PA2 (ref. 31) cells (gift from E. Koo) were grown in DMEM/F12 (Thermo Scientific) supplemented with 10% FCS (Thermo Scientific) plus penicillin/streptomycin and non-essential amino acids (PAA) in a humid incubator with 5% CO<sub>2</sub> at a temperature of 37 °C. For inhibitor treatment, cell culture medium was replaced with fresh, pre-warmed serum free medium (OPTIMEM; Thermo Scientific) supplemented with inhibitors or DMSO as vehicle control. Treatment was initiated when cells reached 90–100% confluency and conditioned media were collected after 20–24 h. Supernatants were cleared by centrifugation (10 min, 5,500g at 4 °C). To obtain cell lysates, cell monolayers were washed once with ice-cold PBS and detached in 1 ml PBS using a cell scraper. The cell suspension was pelleted by centrifugation (5 min, 1,000g at 4 °C) and lysed with RIPA buffer (20 mM sodium citrate, pH 6.4, 1 mM EDTA, 1% Triton X-100 in ddH<sub>2</sub>O) supplemented with Protease Inhibitor Cocktail (Sigma-Aldrich). The protein concentration of lysates was determined using the Uptima BC Assay Protein Quantitation kit (Interchim).

**Primary cell culture.** Hippocampal neurons were isolated from embryonic day 18 CD rats (Charles River) as described previously<sup>32</sup>. Dissociated neurons were plated at 17,700 cells cm<sup>-2</sup> onto 6-cm dishes coated with poly-L-lysine (1 mg ml<sup>-1</sup>; Sigma) and cultured in Neurobasal medium supplemented with 2% B27 and 0.5 mM L-glutamine (all from Invitrogen). Hippocampal cultures were maintained in a humidified 5% CO<sub>2</sub> incubator at 37 °C. For inhibitor treatment, DIV16 culture medium was replaced with fresh, pre-equilibrated N2 medium (supplemented with 20% of 4 days conditioned N2 medium from pure primary cultured astrocytes) to which inhibitors or DMSO as vehicle control were added.

**Generation and BACE1 inhibition of cerebral cortex neurons induced from human embryonic stem cells.** Cell lines in this study were H9 ES (WiCell Research Institute)<sup>33</sup>. Pluripotent cells were cultured on mouse embryonic fibroblasts (GlobalStem) in DMEM/F12 containing 20% (v/v) KSR, 100 μM non-essential amino acids, 100 μM 2-mercaptoethanol, 50 U ml<sup>-1</sup> penicillin and 50 mg ml<sup>-1</sup> streptomycin (Life Technologies) and 10 ng ml<sup>-1</sup> FGF2. Directed differentiation of human embryonic stem cells to cerebral cortex neurons was carried out as described<sup>17,34</sup>. Human neurons (75 days after induction) were treated with 1 μM β-secretase inhibitor LY2886721 (Selleck) dissolved in DMSO (20 mM stock). Vehicle-only control assays were performed using DMSO. The compound was applied twice at 48-h intervals. Extracellular media was collected before drug addition and at subsequent 48-h intervals. Neurons were collected after 4 days of treatment using 0.5 mM EDTA in PBS.

**Transgenic mice, animal care and animal handling.** *Bace1*<sup>-/-</sup> and APPS1-21 mice were described before<sup>10,19</sup> and were bred for this study in a Bl6C57/J background. All treatments were approved by the local committee for animal use and were performed in accordance to state and federal regulations (license number KVR-I/221-TA116/09). Mice had access to pre-filtered sterile water and standard mouse chow (Ssniff Ms-H, Ssniff Spezialdiäten GmbH, Soest, Germany) *ad libitum* and were housed under a reversed day–night rhythm in IVC System Type II L-cages (528 cm<sup>2</sup>) equipped with solid floors and a layer of bedding, in accordance to local legislation on animal welfare.

**BACE1 inhibitor treatment.** Randomized APP<sub>V7171</sub> (ref. 18) mice were treated with vehicle or with the inhibitor RO5508887 provided by Hoffmann-La Roche<sup>35</sup>. The groups of treated mice were blinded to the examiner and uncoded at the end of the experiments. Three-month-old heterozygous female transgenic mice in mixed FVB/N × C57Bl/6J background expressing human APP<sub>V7171</sub> (ref. 18) were used for BACE1 inhibition studies. Gavage mediated administration of BACE1 inhibitor (90 mg kg<sup>-1</sup>, 14.06 ml kg<sup>-1</sup>) or vehicle (14.06 ml kg<sup>-1</sup>) was performed once<sup>35</sup>. The BACE1 inhibitor was diluted in 5% ethanol (Merck) and 10% solutol (Sigma-Aldrich) in sterile water (Baxter). Animals were sacrificed after 5, 8 and 24 h. Mice were anaesthetized with 3.5 μl per gram body weight of a mixture of ketamine (115 mg ml<sup>-1</sup> ketamine hydrochloride, Eurovet), xylazine 2% (23.32 mg ml<sup>-1</sup> xylazine hydrochloride, VMD Arendonk), atropine (0.50 mg ml<sup>-1</sup> atropine sulphate, Sterop) and saline (8.5:2.5, v/v/v/v). For brain preparation, mice were flushed *trans-cardially* with ice-cold saline (3.5 ml min<sup>-1</sup>, 3 min). The brain was removed from the cranium and dissected into left and right hemiforebrain, brainstem, cerebellum and olfactory bulb. The brain structures were promptly immersed in liquid nitrogen and stored at -80 °C. Different tissues (kidneys, spleen, liver, stomach, gut, lungs and heart) were examined and checked for gross abnormalities. No obvious abnormalities were observed in any of the treatment groups.

**Preparation of protein extracts from brain.** Brains were removed from the cranium and dissected into left and right hemispheres. Brain tissue was snap-frozen in liquid nitrogen and stored at -80 °C. Soluble proteins were extracted with DEA buffer (50 mM NaCl, 0.2% diethylamine, pH 10, plus protease inhibitor (P8340, Sigma-Aldrich))<sup>36</sup>, membrane proteins were extracted with RIPA buffer (20 mM Tris-HCl, pH 7.5, 150 mM NaCl, 1 mM EDTA, 1 mM EGTA, 1% NP-40, 1% sodium deoxycholate, 2.5 mM sodium pyrophosphate

plus protease inhibitor) or applying a membrane preparation protocol as described before<sup>37</sup>.

**Protein analysis.** Proteins were separated under denaturing conditions using discontinuous SDS-PAGE. Equal amounts of proteins denatured in Laemmli buffer were loaded onto the gel and 10 μl of the SeeBlue Plus2 Prestained Standard (Invitrogen) served as molecular mass marker. Electrophoresis was performed in Tris-glycine buffer (25 mM Tris, 190 mM glycine in ddH<sub>2</sub>O) using the Mini-PROTEAN system (BIORAD) on activated PVDF membranes. Low molecular mass proteins (<16 kDa) were separated using precast gradient Tricine Protein Gels (10–20%, 1 mm, Novex) in Tris-tricine buffer using the XCell SureLock Mini-Cell system (Novex). After separation by SDS-PAGE, proteins were transferred onto membranes using the tank/wet Mini Trans-Blot cell system (BIORAD). CTFs, A $\eta$  and amyloid- $\beta$  were detected after transfer on Nitrocellulose membranes (Protran BA85; GE Healthcare), while other proteins were blotted on PVDF (Immobilon-P, Merck Millipore). As size markers for A $\eta$  synthetic peptides A $\eta$ - $\beta$  (92 amino acids; 1-MISEPRISYGNDALMPSLTETKT TVELLVPVNGEFLSDDLQPVHSGADSV PANTENEVEVPDARPAADRGLTT RPSGLTNIKTEEISEVKM-92) and the slightly longer A $\eta$ - $\alpha$  (108 amino acids; 1-MISEPRISYGNDALMPSLTETKTTVELLPVNGEFLSDDLQPVHSGADSV PANTENEVEVPDARPAADRGLTTRPSGLTNIKTEEISEVKMDAEFRHDSG YEVHHQK-108) were obtained from Peptide Speciality Laboratories. After completion of the transfer and before blocking, proteins transferred to nitrocellulose membranes were additionally denatured by boiling the membrane in PBS (140 mM NaCl, 10 mM Na<sub>2</sub>HPO<sub>4</sub>, 1.75 mM KH<sub>2</sub>PO<sub>4</sub>, 2.7 mM KCl in ddH<sub>2</sub>O, pH 7.4) for 5 min. After cooling to room temperature, nitrocellulose membranes as well as the PVDF membranes were blocked in I-Block solution (0.2% Tropix I-Block (Applied Biosystems), 0.1% Tween20 in PBS) for 1 h at room temperature or overnight at 4 °C (with agitation). Transferred proteins were detected using immunodetection and enhanced chemiluminescence (ECL). First, blocked membranes were incubated with primary antibodies diluted in I-Block solution overnight at 4 °C (with agitation). After removal of the antibody, membranes were washed three times in TBS-T buffer (10 min each, at room temperature, with agitation; 140 mM NaCl, 2.68 mM KCl, 24.76 mM Tris, 0.3% Triton X-100 in ddH<sub>2</sub>O, pH 7.6) and subsequently incubated with a horseradish-peroxidase-coupled secondary antibody (obtained from Promega or Santa Cruz). Secondary antibodies were diluted in I-Block solution and membranes were incubated for 1 h at room temperature (with agitation) followed by three washes in TBS-T. For ECL detection, membranes were incubated with horseradish peroxidase substrate (ECL, GE Healthcare or ECL Plus, Thermo Scientific) for 1 min at room temperature and signals were captured with X-ray films (Super RX Medical X-Ray, Fujifilm), which were subsequently developed using an automated film developer (CAWOMAT 2000 IR, CAWO). Quantitation of protein was conducted using ImageJ software. Ratios were obtained from signals on the same film for A $\eta$  over amyloid- $\beta$ . Quantitative data were analysed statistically by using a two-tailed Student's *t*-test.

**Molecular cloning and transfection.** For the expression of A $\eta$ - $\alpha$  and A $\eta$ - $\beta$  in CHO cells, the complementary DNAs of the respective fragments were amplified by PCR and subcloned into the pSecTag2A (Invitrogen) vector that features an N-terminal secretion signal. CHO cells were cultured in DMEM with 10% FCS and non-essential amino acids. Transfections were carried out using Lipofectamine 2000 (Invitrogen) according to the manufacturer's instructions.

**Mass spectrometry analysis of samples.** Beads with immunoprecipitated peptides were resuspended in ddH<sub>2</sub>O and reduced with 10 mM dithiothreitol followed by alkylation with 55 mM 2-chloroacetamide. Samples were divided into three parts and digested with either 1 μg of trypsin (1.2 M urea, 0.4 M thiourea and 50 mM ammonium bicarbonate), LysC (5 M urea, 1.7 M thiourea and 50 mM ammonium bicarbonate) or chymotrypsin (0.3 M urea, 0.1 M thiourea and 50 mM ammonium bicarbonate). To increase the sequence coverage further, partially cleaved peptides were generated by digesting for 5, 10, 20, 40, 60, 120, 180 and 720 min. Samples from all time points of a respective protease were pooled and desalted on stage tips<sup>38</sup>.

For liquid chromatography–tandem mass spectrometry (LC–MS/MS), peptides were separated on a Thermo Scientific EASY-nLC 1000 HPLC system (Thermo Fisher Scientific) and in-house packed columns (75 μm inner diameter, 20 cm length, 1.9 μm C18 particles (Dr. Maisch GmbH). The peptide mixture was loaded in buffer A (0.5% formic acid) and separated with a gradient from 10% to 60% buffer B (80% acetonitrile, 0.5% formic acid) within 40 min at 250 nl min<sup>-1</sup> at a column temperature of 50 °C. A Quadrupole Orbitrap mass spectrometer<sup>39</sup> (Q Exactive, Thermo Fisher Scientific) was coupled to the HPLC system via a nano electrospray source. We used data-dependent acquisition with a survey scan range of 300 to 1,650 *m/z*, at a resolution of 60,000 *m/z* and selected up to five most abundant features with a charge state  $\geq 2$  for HCD fragmentation<sup>40</sup> at a normalized collision energy of 27 and a resolution of 15,000 at *m/z* 200. To limit repeated

sequencing, dynamic exclusion of sequenced peptides was set to 20 s. Thresholds for ion injection time and ion target values were set to 20 ms and  $3 \times 10^6$  for the survey scans, and 120 ms and  $1 \times 10^5$  for the MS/MS scans. Data were acquired using the Xcalibur software (Thermo Scientific).

**Data analysis.** To process mass spectrometry raw files, we used the MaxQuant software (v1.5.2.16)<sup>41</sup>. We used the Andromeda search engine<sup>42</sup>, which is integrated into MaxQuant, to search MS/MS spectra against the APP<sub>695</sub> and 247 common contaminating proteins<sup>42</sup>. We set enzyme specificity to unspecific to detect novel cleavage sites and set a peptide search length from 7 to 40 amino acids. A false discovery rate cutoff of 1% was applied at the peptide level. For data visualization we used R<sup>43</sup>. Identified peptides were mapped to APP<sub>695</sub>. To display quantitative evidence for overlapping peptides, intensities of identified peptides were summed and plotted per amino acid residue. The data of the individual immunoprecipitation and mass spectrometry analyses are depicted in Extended Data Fig. 3.

**Human CSF samples.** Human CSF samples collected at the Department of Neurology Outpatient unit for neurodegenerative disease (KBFZ) of the University of Bonn were obtained by lumbar puncture at position L3, centrifuged and divided in small aliquots. For further analysis, samples were stored at  $-80^\circ\text{C}$ . Turbid or blood-contaminated samples were excluded from analysis. Use of these samples for research purposes has been consented by all patients according to the ethical committee requirements of the University of Bonn Ethical committee and approval number 279/10. For the analysis of APP<sub>swe</sub> carriers with antibodies 192swe (ref. 44) lumbar CSF was obtained from family members. Tubes with CSF were stored at  $-70^\circ\text{C}$  until analysis. The clinical diagnosis of probable AD was based on NINCDS-ADRDA criteria<sup>45</sup>. The diagnosis of AD was confirmed by neuropathological examination of the brain of one deceased mutation-carrier<sup>46,47</sup>. This study was approved by research ethics committee at the Uppsala University Hospital (Dnr 048-2005).

**Neuropathology and immunohistochemistry.** Use of brain samples for research purposes has been consented by all patients according to the ethical committee requirements of the University of Ulm Ethical committee and approval number 54/08. Braak-NFT stages<sup>48</sup>, and CERAD<sup>49</sup> scores for neuritic plaques were used to determine the degree of AD pathology according to the NIA-AA guidelines<sup>50</sup>. Consecutive paraffin sections from the human medial lobe were stained with 22C11, 9476M and 9478D. Primary antibodies were detected with biotinylated anti-mouse and anti-rabbit IgG secondary antibodies and visualized with avidin-biotin-complex (ABC-Kit, Vector Laboratories) and diaminobenzidine-HCl (DAB). The sections were counterstained with haematoxylin. Positive and negative controls were performed. 9476M and 9478D stainings were assessed in 10 control and 10 AD patient cases.

For double immunofluorescence analysis of APPS1-21 brain sections, 6-month-old mice were killed by CO<sub>2</sub> inhalation according to animal handling laws. Brains were dissected and fixed with 4% paraformaldehyde in 0.1 M PBS, pH 7.4 for 48 h. For immunohistochemistry, 25- $\mu\text{m}$ -thick sagittal mouse brain cryosections were treated with 10 mM sodium citrate, pH 6 at  $95^\circ\text{C}$  for 20 min, washed with 0.5% Triton X-100 in PBS, blocked with 5% goat serum (Invitrogen) and 0.5% Triton X-100 in PBS for 1 h and subsequently incubated overnight with primary antibodies diluted in blocking solution. Primary antibodies were used as listed in Supplementary Table 1. DAPI was used to counterstain nuclei. Signals were visualized using fluorescently labelled secondary antibodies. Confocal images were acquired using a Plan-Apochromat 25 $\times$ /0.8 oil differential interference contrast objective on a LSM 710 confocal microscope (Zeiss) in sequential scanning mode using ZEN 2011 software package (black edition, Zeiss).

**LCM of plaque enriched brain material.** For laser capture microdissection of plaque cores and halos, 10-, 11-, 14-, 16- and 24-month-old transgenic APPS1-21 mice were used according to a previously published protocol<sup>51</sup> with slight modifications. Mice brains were dissected and immediately frozen on crushed dry ice. Ten-micrometre-thick sagittal sections were cut using a Microm HM 560 cryostat (Thermo Scientific), mounted on frame slides containing a 1.4  $\mu\text{m}$  polyethylene terephthalate membrane (Leica Microsystems) and subsequently stained or stored at  $-80^\circ\text{C}$  for later usage. Staining was performed as follows: brain sections were thawed briefly at room temperature, fixed with 75% ethanol for 1 min, stained with 0.05% Thioflavin-S for 5 min, washed with 75% ethanol and dried at room temperature. LCM was performed on the same day using a laser dissection microscope (Leica, LMD 7000) with the following settings: excitation wavelength 495 nm, laser power 30, aperture 5, speed 6 and pulse frequency 119. From each animal, at least 800 plaque cores and halos, dissected from 12 brain sections were cut using a 63 $\times$  magnification objective, collected in 0.5 ml caps (Leica Microsystem) and subsequently pooled for protein analysis. Areas containing no plaques were cut using a 10 $\times$  magnification objective and were used as controls. Protein lysates were done essentially as described above using RIPA with 0.1% SDS.

**Slice preparation and electrophysiological recordings applying A $\eta$  peptides *in vitro*.** Transverse hippocampal slices (350  $\mu\text{m}$ ) were prepared from P20–30 Swiss mice following standard procedures<sup>52</sup>. Slices were cut in ice-cold oxygenated (95% O<sub>2</sub>, 5% CO<sub>2</sub>) solution containing 206 mM sucrose, 2.8 mM KCl, 1.25 mM NaH<sub>2</sub>PO<sub>4</sub>, 2 mM MgSO<sub>4</sub>, 1 mM MgCl<sub>2</sub>, 1 mM CaCl<sub>2</sub>, 26 mM NaHCO<sub>3</sub>, 0.4 mM sodium ascorbate and 10 mM glucose, pH 7.4. For recovery (1 h), slices were incubated at  $27^\circ\text{C}$  in oxygenated standard ACSF containing: 124 mM NaCl, 2.8 mM KCl, 1.25 mM NaH<sub>2</sub>PO<sub>4</sub>, 2 mM MgSO<sub>4</sub>, 3.6 mM CaCl<sub>2</sub>, 26 mM NaHCO<sub>3</sub>, 0.4 mM sodium ascorbate, 10 mM glucose (pH 7.4)<sup>53</sup>. Slices were inspected in a chamber on an upright microscope (Slicescope, Scientifica Ltd) with infrared differential interference contrast illumination, and were perfused with the oxygenated ACSF at  $27 \pm 1^\circ\text{C}$ . fEPSPs were recorded in the stratum radiatum of the CA1 region using a glass electrode (filled with 1 M NaCl, 10 mM HEPES, pH 7.4) and the stimuli (30% of maximal fEPSP) were delivered to the Schaeffer Collateral pathway by a monopolar glass electrode (filled with ACSF). Electrodes were specifically placed just below the surface of the slice to maximize the exposure to circulating peptides. A minimum of 15–20 min stable baseline was first obtained in standard ACSF followed by another 15–20 min of bath application of ACSF containing SEC fractions (CHO, A $\eta$ - $\alpha$  or A $\eta$ - $\beta$ ; 1/15 dilution, interleaved recordings) using re-circulation with a peristaltic pump at  $2.5\text{--}3\text{ ml min}^{-1}$  while being continuously aerated with 95% oxygen. No alterations in fEPSP baseline responses were observed after incubation with the SEC fractions (Extended Data Fig. 8). In the continuous presence of ACSF/SEC solution, LTP was induced using a high-frequency stimulation protocol with two pulses of 100 Hz for 1 s with a 20 s interval between pulses, and recorded for 1 h. Control recordings (no application of SEC fractions) were obtained in an interleaved fashion in which ACSF was re-circulated using an identical procedure. For LTP analysis, the first third of the fEPSP slope was calculated in baseline condition (15–20 min before induction of LTP) and compared to that after LTP induction (60 min after tetanization of Schaffer collaterals). The average baseline value was normalized to 100% and all values of the experiment were normalized to this baseline average (1-min bins). Experimental data were pooled per condition and presented as mean  $\pm$  s.e.m. Data analysis was performed with the Clampfit software (Molecular Devices). The test samples were blinded to the investigator and uncoded at the end of the experiments. Statistical analysis was performed using GraphPad (Prism 6) with the last 15 min of the recordings compared to measurements of 15–20 min of baseline, using a two-tailed Student's *t*-test for statistical analysis on two samples or one-way ANOVA and post hoc Bonferroni test for statistical analysis on three and more samples, with  $P < 0.05$  taken as statistically significant. No power analysis was done to estimate sample size, and there was no randomization.

**Electrophysiological recordings of the effects of BACE1 inhibitor *in vitro*.** BACE1 inhibitor (100 mg kg<sup>-1</sup>, single gavage) or vehicle-treated mice (12 weeks old) were deeply anaesthetized with isoflurane (1% in O<sub>2</sub>) and decapitated with brains rapidly extracted and placed for 5–6 min in ice-cold bubbled (95% O<sub>2</sub>, 5% CO<sub>2</sub>) slicing solution (in mM): 75 sucrose, 85 NaCl, 2.5 KCl, 1.25 NaH<sub>2</sub>PO<sub>4</sub>, 25 NaHCO<sub>3</sub>, 0.5 CaCl<sub>2</sub>, 4 MgCl<sub>2</sub>, 25 glucose, pH 7.4. Coronal slices (400  $\mu\text{m}$ ) containing the hippocampus were cut (VT1200S; Leica) and transferred into a warming chamber ( $35^\circ\text{C}$ ) filled with bubbled solution of the same composition, except sucrose was omitted and NaCl increased to 125 mM (30 min). This was followed by the transfer of slices into recording ACSF (in mM): 125 NaCl, 2.5 KCl, 1.25 NaH<sub>2</sub>PO<sub>4</sub>, 25 NaHCO<sub>3</sub>, 2 CaCl<sub>2</sub>, 2 MgCl<sub>2</sub>, 25 glucose. Recordings of fEPSP were made from the hippocampal CA1 area. A glass bipolar stimulating electrode was placed in the stratum radiatum of CA2–CA3 subfields to stimulate Schaffer collaterals with 0.2 ms current pulses at 0.033 Hz (A-360, WPI), with evoked responses recorded in the stratum radiatum of CA1 area. Incrementing current pulses (0.2 mA) were used for obtaining stimulus-response relationship graphs. Stable baseline and LTP recordings were made using one-half of the maximal stimulus intensities; LTP was induced by high-frequency stimulation of Schaffer collaterals with 10 trains of 10 pulses at 100 Hz applied, with 2-s inter-train intervals. Signals were filtered at 5 kHz, digitally sampled at 10 kHz and stored for offline analysis. The relative slope and peak amplitude of evoked fEPSPs were measured using FitMaster (HEKA Electronics). The groups of treated mice were blinded to the investigator and uncoded at the end of the experiments. A one-way ANOVA and post hoc Bonferroni test have been used for statistical analysis, with  $P < 0.05$  taken as statistically significant.

***In vivo* two-photon Ca<sup>2+</sup> imaging.** All experimental procedures were in compliance with institutional animal welfare guidelines and were approved by the state government of Bavaria, Germany. The animal preparation procedure was similar to that described previously<sup>25</sup>. In brief, C57Bl/6 mice (male or female, ~P40) were anaesthetized with isoflurane (1–1.5%) and placed onto a warming plate ( $37\text{--}38^\circ\text{C}$ ). The skin was removed and a custom-made recording chamber was glued to the exposed skull. A craniotomy (~1 mm) was made over the

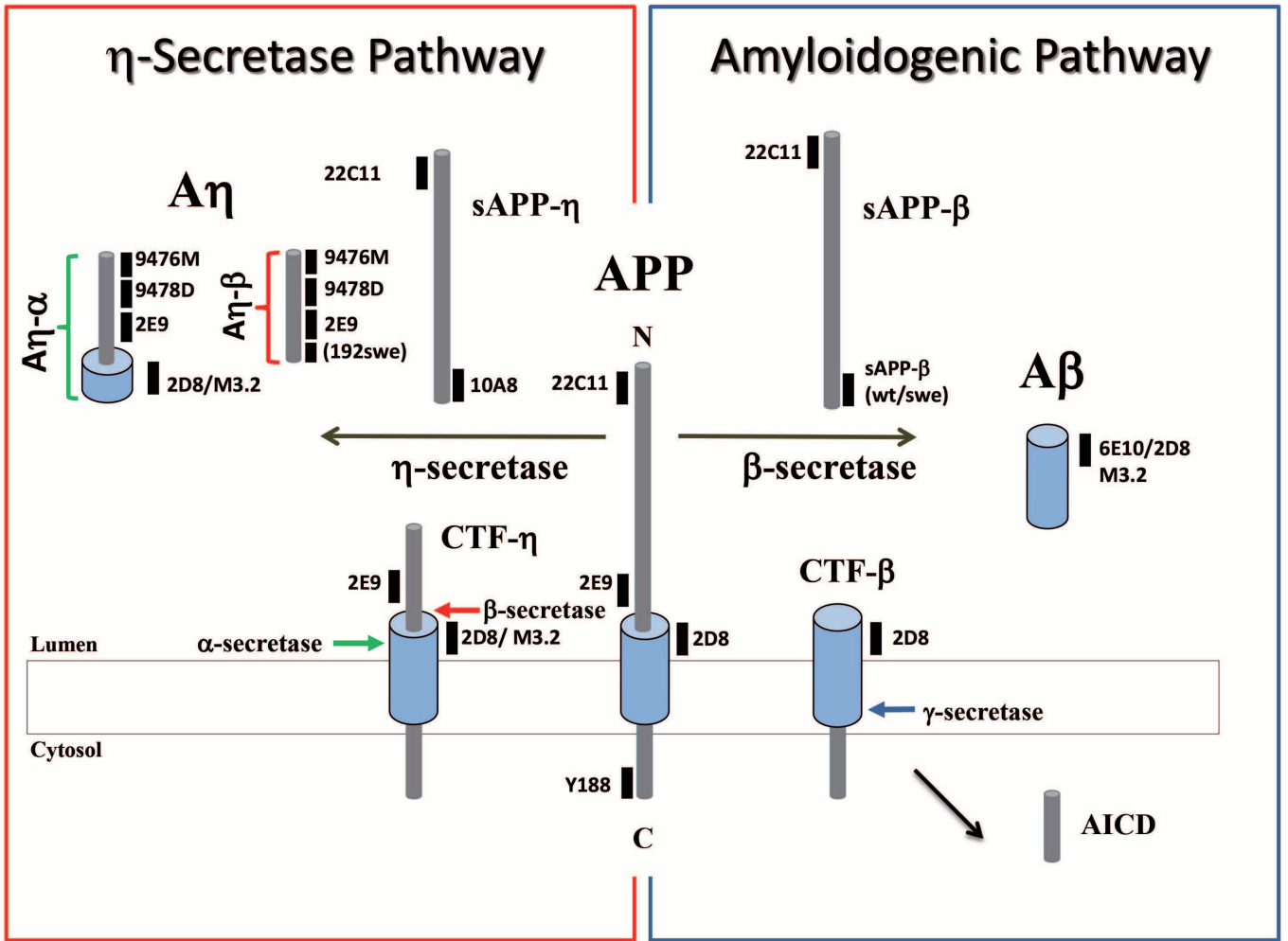
hippocampus (2.5 mm posterior to bregma, 2.2 mm lateral to the midline) and a small portion of the overlying cortical tissue was carefully removed by aspiration. The animal was placed under a microscope on a warm heating plate (37–38 °C) and kept anaesthetized with low-levels of isoflurane (~0.8%). Respiratory and pulse rates were continuously monitored. The recording chamber was perfused with warm normal Ringer's solution containing 125 mM NaCl, 4.5 mM KCl, 26 mM NaHCO<sub>3</sub>, 1.25 mM NaH<sub>2</sub>PO<sub>4</sub>, 2 mM CaCl<sub>2</sub>, 1 mM MgCl<sub>2</sub> and 20 mM glucose (pH 7.4 when bubbled with 95% O<sub>2</sub> and 5% CO<sub>2</sub>). The exposed CA1 region of the hippocampus was then stained with fluo-8AM (AAT Bioquest; 0.6 mM) using the multi-cell bolus loading technique<sup>54</sup>.

*In vivo* imaging was performed with a custom-built two-photon microscope equipped with a Ti:sapphire laser system (Coherent; laser wavelength 925 nm), a resonant scanner and a Pockel's cell for laser intensity modulation. Full-frame images were acquired at 30 Hz using a water-immersion objective (Nikon; 40×, 0.8 numerical aperture). Data acquisition was controlled using custom-written software based on LabVIEW (National Instruments). Image analysis was performed off-line by using custom routines in LabVIEW and Igor Pro (Wavemetrics). Cellular regions of interest were drawn around individual somata, and then relative fluorescence change ( $\Delta F/F$ ) versus time traces were generated for each region of interest. Ca<sup>2+</sup> transients were identified as changes in  $\Delta F/F$  that were three times larger than the s.d. of the noise band.

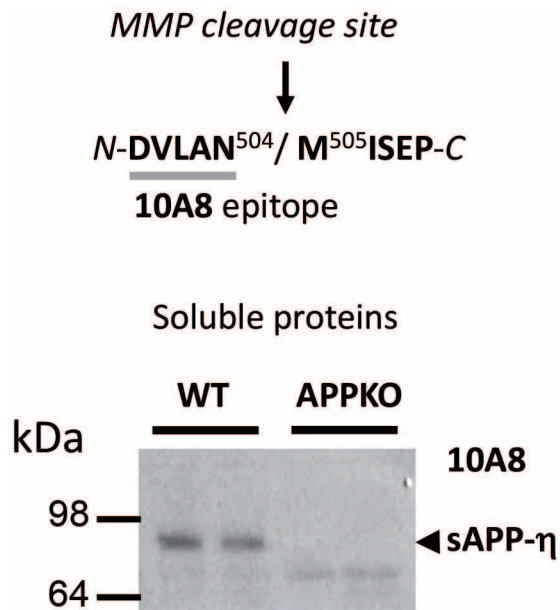
To assess the effects of A $\eta$  peptides on neuronal activity *in vivo*, the peptides or the respective controls (SEC fractions obtained from untransfected CHO cells or a synthetic peptide (46 amino acids; 1-ADSVPANTENEVEPVDARPAADRGLTTRPGSGLTNIKTEEISEVKM-46) of a middle part of A $\eta$  were added to the normal Ringer's solution used for perfusion of the recording chamber (bath-application technique; 45–60 min each wash-in). In a subset of experiments, synthetic A $\eta$ - $\alpha$  (92 amino acids; 1-MISEPRISYGNDALMPSLTETKTTVELLPVNGEFLDDLQPWHSFGADSVANTENEVEPVDARPAADRGLTTRPGSGLTNIKTEEISEVKM-92) was applied locally by gentle pressure injection through a glass pipette that was placed close to the neurons of interest (local application technique; 40 s each pressure injection).

The samples were blinded to the investigator and uncoded at the end of the experiments. Statistical analysis was performed using SPSS. The statistical methods used were the Student's *t*-test and the Fisher's exact test. *P* < 0.05 was considered statistically significant.

31. Podlisy, M. B. *et al.* Aggregation of secreted amyloid  $\beta$ -protein into sodium dodecyl sulfate-stable oligomers in cell-culture. *J. Biol. Chem.* **270**, 9564–9570 (1995).
32. Kaech, S. & Banker, G. Culturing hippocampal neurons. *Nature Protocols* **1**, 2406–2415 (2006).
33. Israel, M. A. *et al.* Probing sporadic and familial Alzheimer's disease using induced pluripotent stem cells. *Nature* **482**, 216–220 (2012).
34. Shi, Y., Kirwan, P., Smith, J., Robinson, H. P. & Livesey, F. J. Human cerebral cortex development from pluripotent stem cells to functional excitatory synapses. *Nature Neurosci.* **15**, 477–486 (2012).
35. Jacobsen, H. *et al.* Combined treatment with a BACE inhibitor and anti-Ab antibody gantenerumab enhances amyloid reduction in APPLondon mice. *J. Neurosci.* **34**, 11621–11630 (2014).
36. Nolan, R. L. & Teller, J. K. Diethylamine extraction of proteins and peptides isolated with a mono-phasic solution of phenol and guanidine isothiocyanate. *J. Biochem. Biophys. Methods* **68**, 127–131 (2006).
37. Westmeyer, G. G. *et al.* Dimerization of  $\beta$ -site  $\beta$ -amyloid precursor protein-cleaving enzyme. *J. Biol. Chem.* **279**, 53205–53212 (2004).
38. Rappsilber, J., Mann, M. & Ishihama, Y. Protocol for micro-purification, enrichment, pre-fractionation and storage of peptides for proteomics using StageTips. *Nature Protocols* **2**, 1896–1906 (2007).
39. Scheltema, R. A. *et al.* The Q Exactive HF, a Benchtop mass spectrometer with a pre-filter, high-performance quadrupole and an ultra-high-field Orbitrap analyzer. *Mol. Cell. Proteomics* **13**, 3698–3708 (2014).
40. Olsen, J. V. *et al.* Higher-energy C-trap dissociation for peptide modification analysis. *Nature Methods* **4**, 709–712 (2007).
41. Cox, J. & Mann, M. MaxQuant enables high peptide identification rates, individualized p.p.b.-range mass accuracies and proteome-wide protein quantification. *Nature Biotechnol.* **26**, 1367–1372 (2008).
42. Cox, J. *et al.* Andromeda: a peptide search engine integrated into the MaxQuant environment. *J. Proteome Res.* **10**, 1794–1805 (2011).
43. R Development Core Team. *R: A Language and Environment for Statistical Computing* (R Foundation for Statistical Computing, <http://www.R-project.org/> (2014)).
44. Haass, C. *et al.* The Swedish mutation causes early-onset Alzheimer's-disease by  $\beta$ -secretase cleavage within the secretory pathway. *Nature Med.* **1**, 1291–1296 (1995).
45. McKhann, G. *et al.* Clinical diagnosis of Alzheimer's disease: report of the NINCDS-ADRDA Work Group under the auspices of Department of Health and Human Services Task Force on Alzheimer's Disease. *Neurology* **34**, 939–944 (1984).
46. Lannfelt, L. *et al.* Amyloid precursor protein mutation causes Alzheimer's disease in a Swedish family. *Neurosci. Lett.* **168**, 254–256 (1994).
47. Lannfelt, L. *et al.* Amyloid  $\beta$ -peptide in cerebrospinal fluid in individuals with the Swedish Alzheimer amyloid precursor protein mutation. *Neurosci. Lett.* **199**, 203–206 (1995).
48. Braak, H. & Braak, E. Neuropathological staging of Alzheimer-related changes. *Acta Neuropathol.* **82**, 239–259 (1991).
49. Mirra, S. S. *et al.* The Consortium to Establish a Registry for Alzheimer's Disease (CERAD). Part II. Standardization of the neuropathologic assessment of Alzheimer's disease. *Neurology* **41**, 479–486 (1991).
50. Hyman, B. T. *et al.* National Institute on Aging-Alzheimer's Association guidelines for the neuropathologic assessment of Alzheimer's disease. *Alzheimers Dement.* **8**, 1–13 (2012).
51. Liao, L. *et al.* Proteomic characterization of postmortem amyloid plaques isolated by laser capture microdissection. *J. Biol. Chem.* **279**, 37061–37068 (2004).
52. Houeland, G. *et al.* Transgenic mice with chronic NGF deprivation and Alzheimer's disease-like pathology display hippocampal region-specific impairments in short- and long-term plasticities. *J. Neurosci.* **30**, 13089–13094 (2010).
53. Townsend, M., Shankar, G. M., Mehta, T., Walsh, D. M. & Selkoe, D. J. Effects of secreted oligomers of amyloid beta-protein on hippocampal synaptic plasticity: a potent role for trimers. *J. Physiol. (Lond.)* **572**, 477–492 (2006).
54. Stosiek, C., Garaschuk, O., Holthoff, K. & Konnerth, A. *In vivo* two-photon calcium imaging of neuronal networks. *Proc. Natl Acad. Sci. USA* **100**, 7319–7324 (2003).

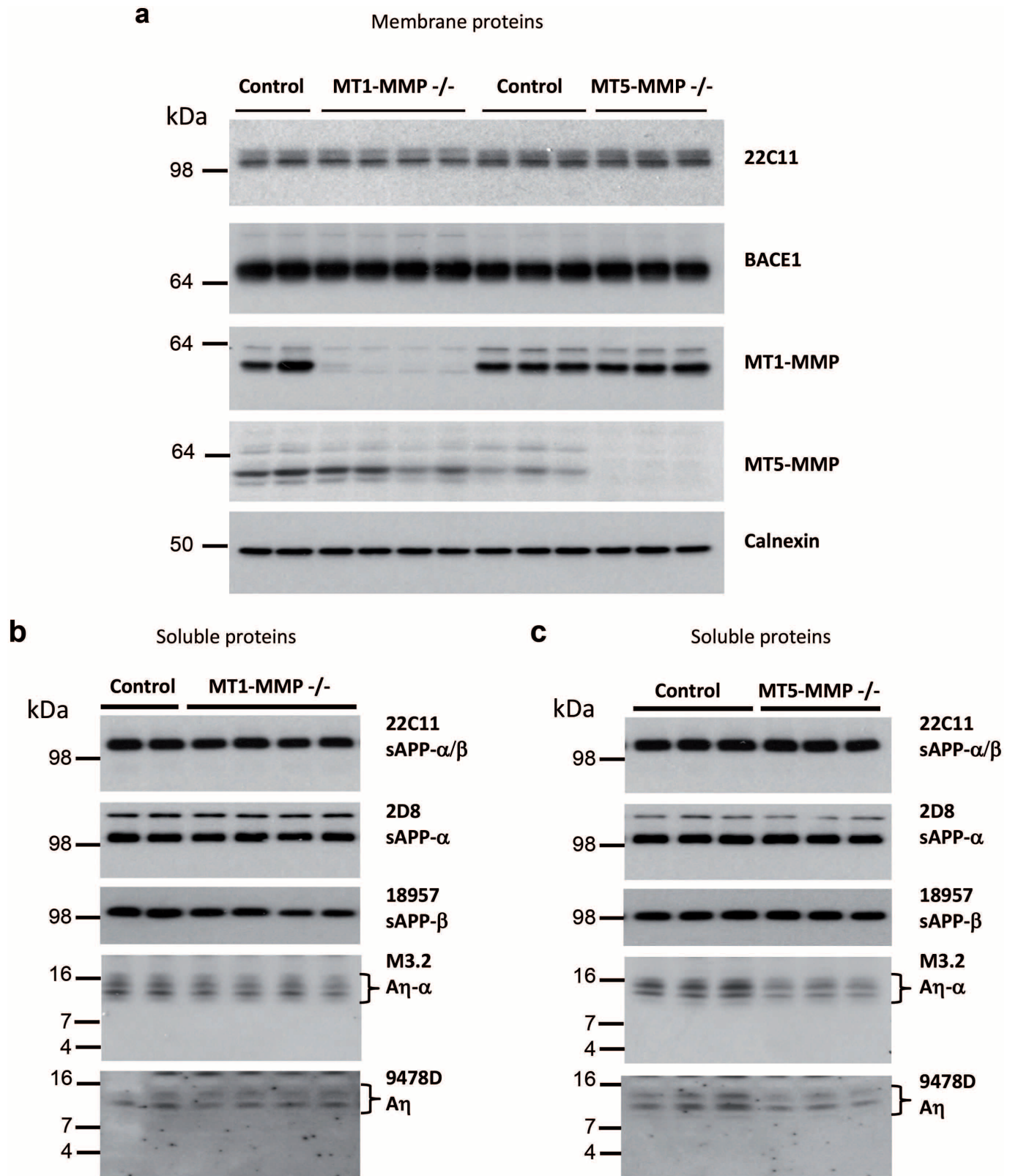


Extended Data Figure 1 | Schematic presentation of the η-secretase processing pathway. Schematic representation of the η-secretase pathway (left) as compared to the amyloidogenic pathway (right). Antibodies used in this study are indicated.



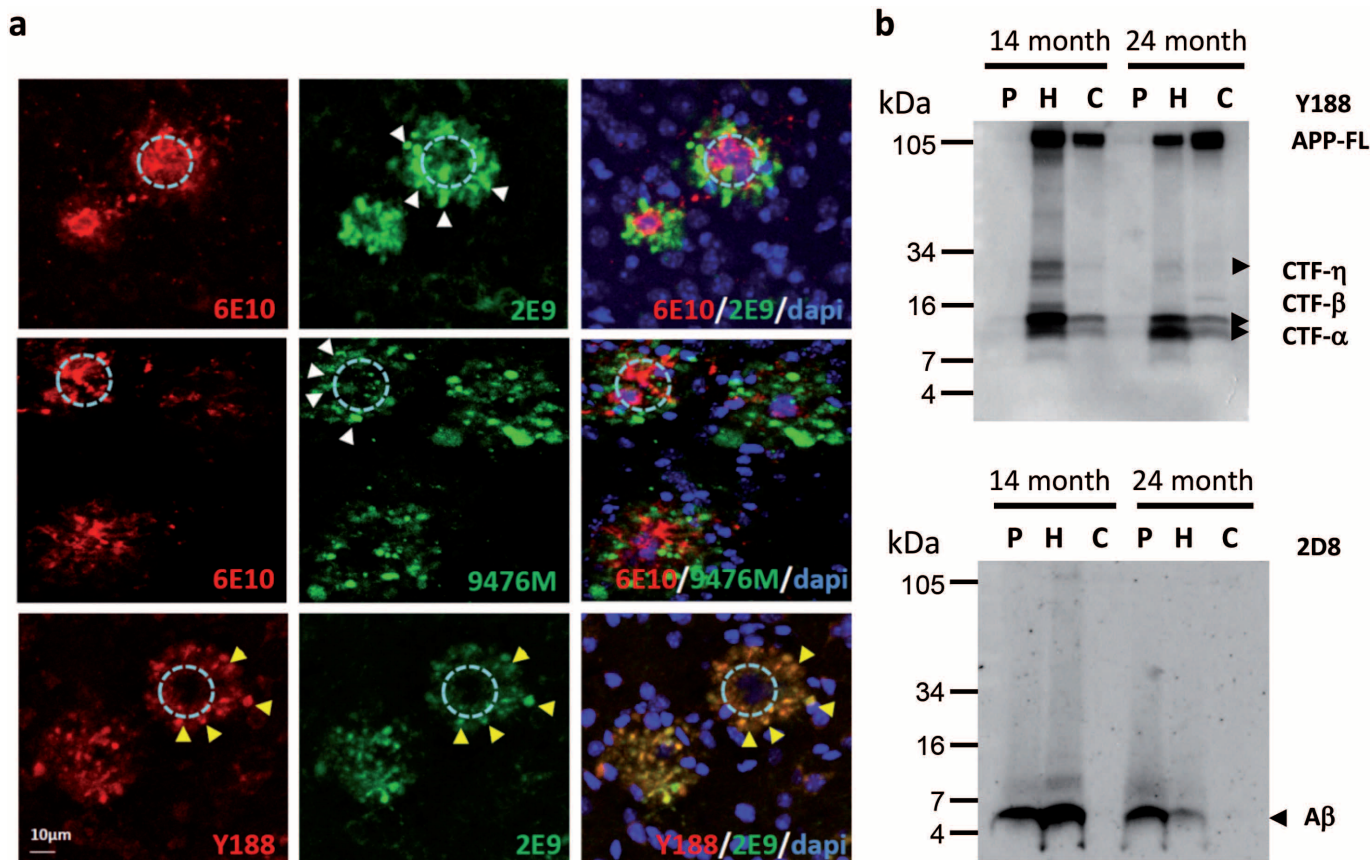
**Extended Data Figure 2 |  $\eta$ -Secretase cleavage at Met505 of APP<sub>695</sub>.** MMP proteins can cleave human APP<sub>695</sub> at the indicated position (arrow) between amino acids N504 and M505 in the N-terminal domain. The epitope for the neo-epitope-specific antibody 10A8 is indicated (grey line). sAPP- $\eta$  was specifically detected in diethylamine (DEA; 0.2% diethylamine in 50 mM NaCl, pH 10) extracts of P10 wild-type mouse brain using antibody 10A8, but was absent in APP-knockout brains. Of note, antibody 10A8 failed to detect sAPP- $\alpha/\beta$ , confirming its selectivity for the  $\eta$ -cleavage site.

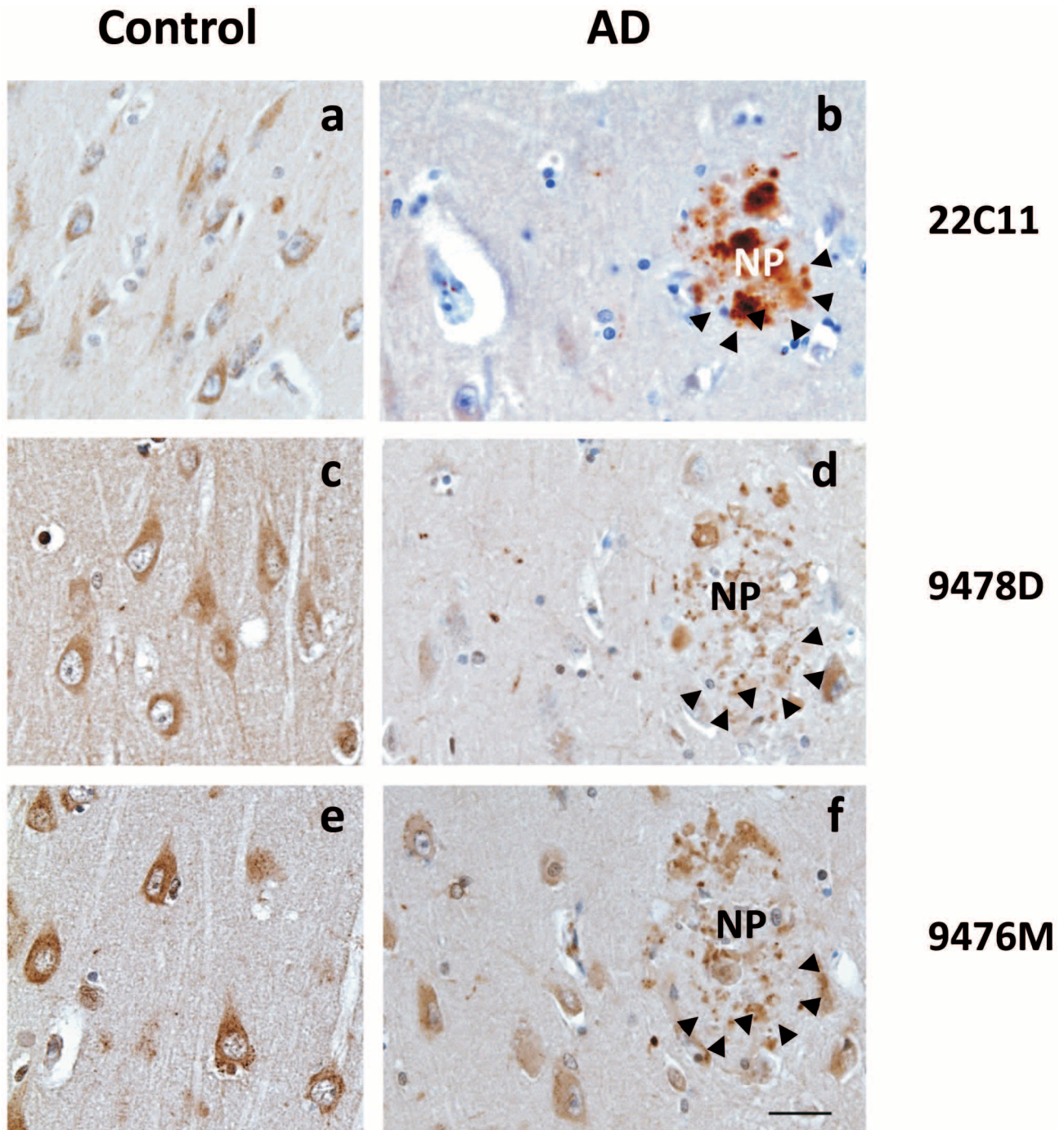




**Extended Data Figure 4 | MT5-MMP displays  $\eta$ -secretase activity in brain.** **a–c**, *MT1-MMP* $^{-/-}$  and *MT5-MMP* $^{-/-}$  (also known as *Mmp14* $^{-/-}$  and *Mmp24* $^{-/-}$ , respectively) mice were analysed for changes in  $\eta$ -secretase activity. Membrane and soluble proteins from P10 mouse brains were analysed. **a**, In RIPA lysates, no changes in APP and BACE1 levels were detected in knockout brains. MT1- and MT5-MMP were selectively knocked out as shown

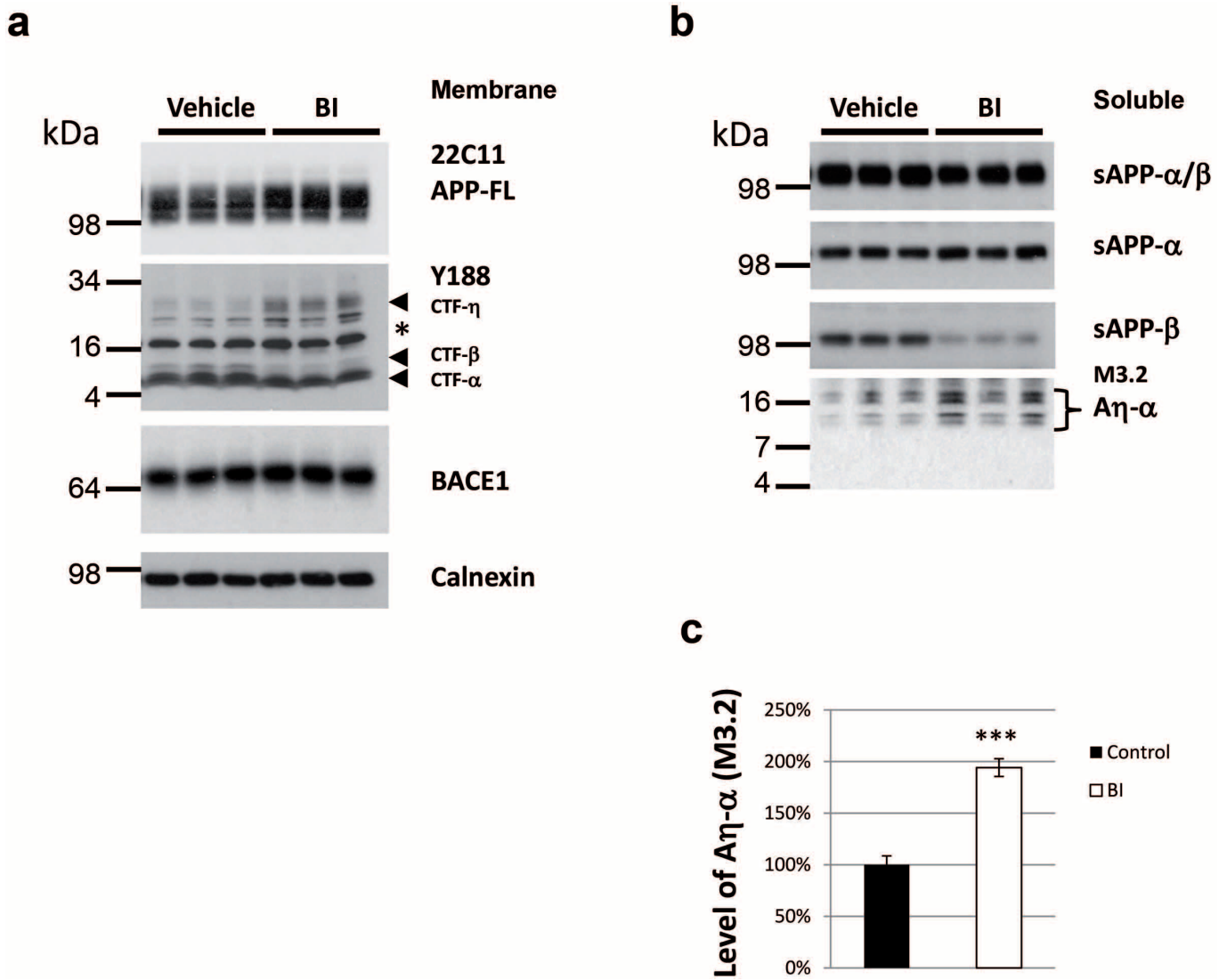
by the lack of signals in western blots. Calnexin served as a loading control. Soluble A $\eta$  levels, detected by antibodies 9478D and M3.2 (A $\eta$ - $\alpha$ ) were unchanged in *MT1-MMP* $^{-/-}$  mouse brains (**b**), but reduced in *MT5-MMP* $^{-/-}$  mouse brains (**c**). Total levels of secreted APP (22C11), sAPP- $\alpha$  or sAPP- $\beta$  were unchanged (**b**, **c**).





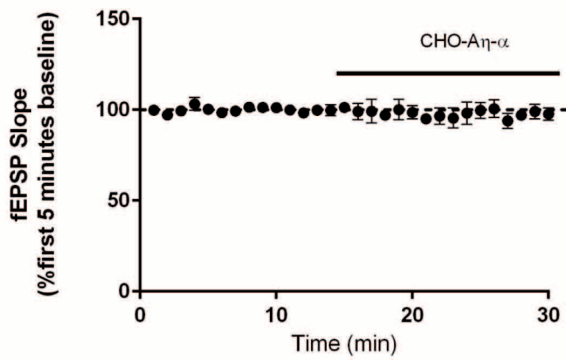
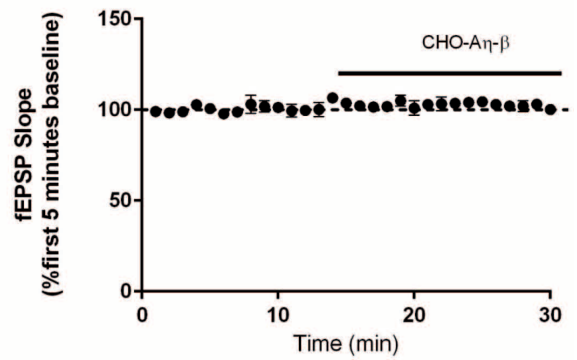
**Extended Data Figure 6 | Dystrophic neurites in AD brains are positive for A $\eta$ -epitope antibodies.** a–f, Immunohistochemistry with 22C11 (a, b), 9478D (c, d) and 9476M (e, f) antibodies in the human hippocampus (CA1-subiculum region) of a control case (a, c, e) and an AD case (b, d, f).

Immuno-positive signals were observed with 22C11 (a), 9478D (c) and 9476M (e) antibodies in the somata and neuropils of a normal and AD brain. In AD brains, these antibodies decorate dystrophic neurites (b, d, f, denoted by arrowheads). Scale bar, 30  $\mu$ m. NP, neuritic plaque.



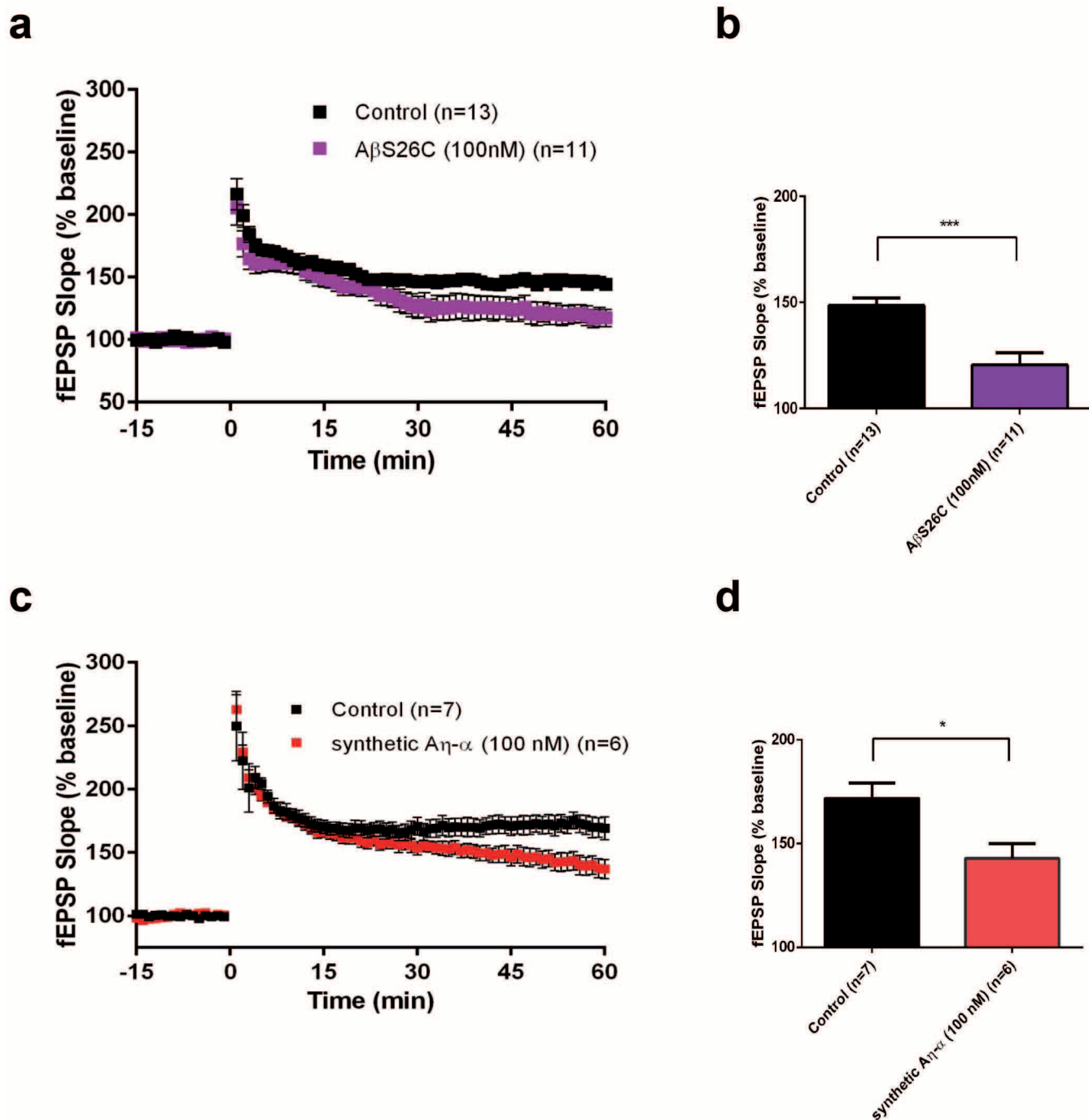
**Extended Data Figure 7 | Increased Aη levels after acute treatment with a BACE1 inhibitor.** **a**, In membrane lysates of brains obtained from animals treated with BACE1 inhibitor (BI, 100 mg kg<sup>-1</sup> SCH1682496), an increase in CTF-η was observed, which was paralleled by a strong reduction of CTF-β, while CTF-α was unchanged. APP-FL and BACE1 signals remained

unchanged (asterisk indicates background band). Calnexin served as a loading control. **b**, In the soluble fraction, BACE1 inhibition resulted in enhanced Aη-α levels and reduced sAPP-β levels, indicating efficient BACE1 inhibition. **c**, Production of Aη-α species, which was detected by antibody M3.2, revealed a 95.4% increase after BACE1 inhibition.  $n = 3$ ;  $P < 0.01$ , Student's *t*-test.

**a****b**

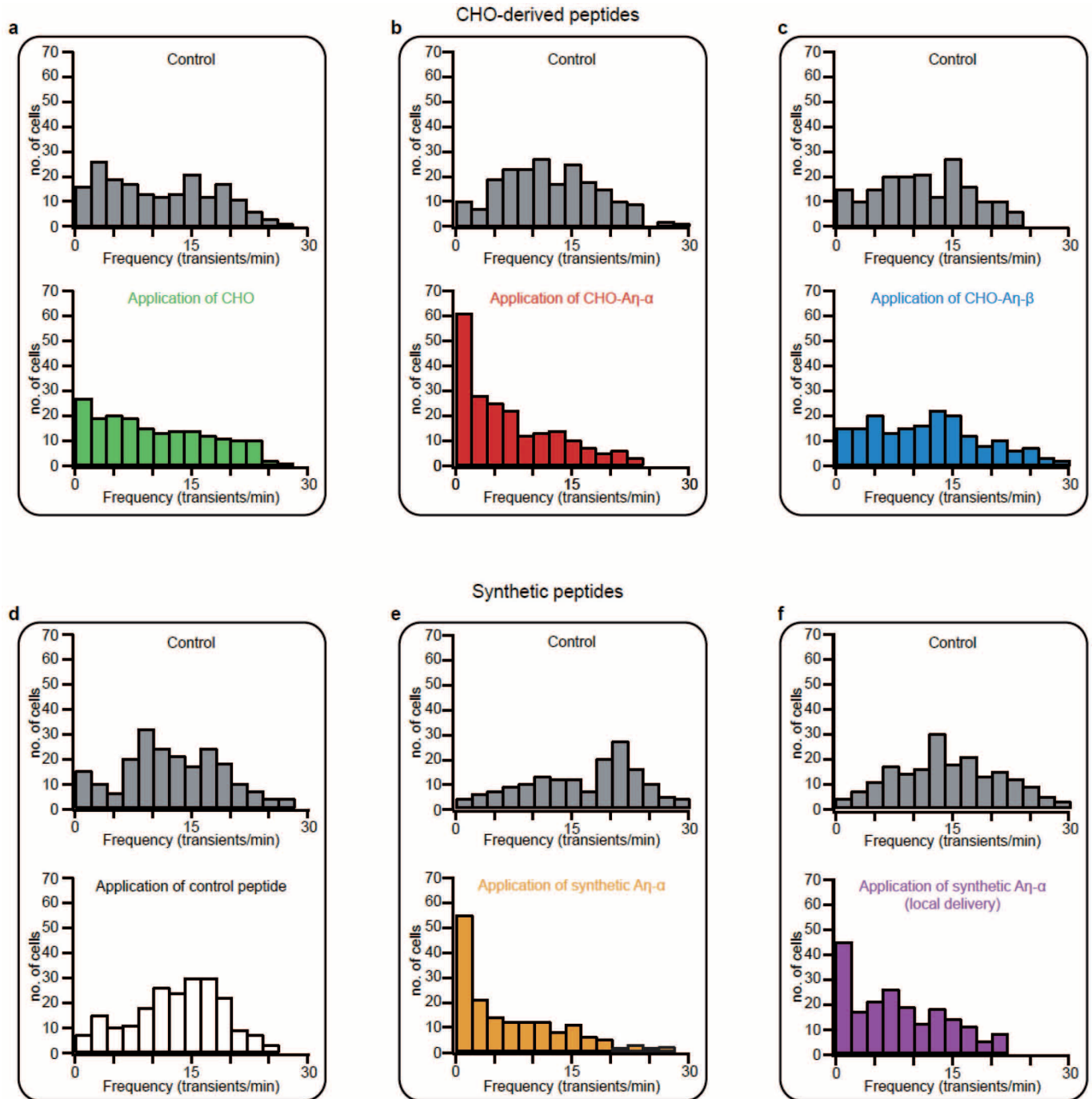
**Extended Data Figure 8 | Aη-α and Aη-β derived from CHO cells did not influence baseline activity at the hippocampal CA3–CA1 synapse.** Soluble Aη-α and Aη-β peptides were expressed in CHO cells and collected in OPTIMEM medium. **a**, **b**, SEC fractions containing Aη were diluted (1:15) in ACSF for the treatment of hippocampal slices and LTP measurements. Aη-α or

Aη-β SEC fractions were perfused over mouse hippocampal slices after obtaining a 15-min stable baseline of a fEPSP at the CA3–CA1 synapse. The baseline remained unchanged for another 15 min when slices were incubated with CHO-cell-derived recombinant Aη-α (**a**) or Aη-β (**b**).



**Extended Data Figure 9 | A $\beta$ <sub>S26C</sub> dimers and synthetic A $\eta$ - $\alpha$  impair hippocampal LTP.** **a**, In line with previous findings<sup>23</sup>, A $\beta$ <sub>S26C</sub> cross-linked dimers (containing cysteine instead of serine at residue 26; 100 nM final; JPT Peptide Technologies; diluted in 25 ml re-circulating ACSF) reduced LTP as compared to interleaved control LTP recordings in 25 ml re-circulating ACSF. **b**, Illustrated is the average LTP magnitude (at 45–60 min after LTP induction) normalized to pre-LTP baseline values (100%) in untreated and

treated conditions (\*\**P* < 0.001; Student's *t*-test). **c**, Treatment with synthetic A $\eta$ - $\alpha$  (100 nM final; Peptide Speciality Laboratories; diluted in 25 ml re-circulating ACSF) reduced LTP as compared to interleaved control LTP recordings in 25 ml re-circulating ACSF. **d**, Illustrated is the average LTP magnitude (at 45–60 min post-LTP induction) normalized to pre-LTP baseline values (100%) in treated and untreated conditions (\**P* < 0.05; Student's *t*-test).



**Extended Data Figure 10 | A $\eta$ - $\alpha$  decreases the frequencies of neuronal calcium transients *in vivo*.** a–f, Histograms showing in each panel the corresponding distributions of calcium transients before (control) and during subsequent exposure of A $\eta$  peptides (b, c, e, f) and controls (a, d).

## 10 References

- Alberini, C. M., Ghirardi, M., Huang, Y. Y., Nguyen, P. V. and Kandel, E. R. (1995) 'A molecular switch for the consolidation of long-term memory: cAMP-inducible gene expression', *Ann N Y Acad Sci*, 758, pp. 261-86.
- Almeida, C. G., Tampellini, D., Takahashi, R. H., Greengard, P., Lin, M. T., Snyder, E. M. and Gouras, G. K. (2005) 'Beta-amyloid accumulation in APP mutant neurons reduces PSD-95 and GluR1 in synapses', *Neurobiol Dis*, 20(2), pp. 187-98.
- Ambroggi, F., Turiault, M., Milet, A., Deroche-Gamonet, V., Parnaudeau, S., Balado, E., Barik, J., van der Veen, R., Maroteaux, G., Lemberger, T., Schütz, G., Lazar, M., Marinelli, M., Piazza, P. V. and Tronche, F. (2009) 'Stress and addiction: glucocorticoid receptor in dopaminergic neurons facilitates cocaine seeking', *Nat Neurosci*, 12(3), pp. 247-9.
- Amsterdam, J. D., Maislin, G., Berwisch, N., Phillips, J. and Winokur, A. (1989) 'Enhanced adrenocortical sensitivity to submaximal doses of cosyntropin (alpha1-24-corticotropin) in depressed patients', *Arch Gen Psychiatry*, 46(6), pp. 550-4.
- Arendash, G. W., Gordon, M. N., Diamond, D. M., Austin, L. A., Hatcher, J. M., Jantzen, P., DiCarlo, G., Wilcock, D. and Morgan, D. (2001) 'Behavioral assessment of Alzheimer's transgenic mice following long-term Abeta vaccination: task specificity and correlations between Abeta deposition and spatial memory', *DNA Cell Biol*, 20(11), pp. 737-44.
- Arnold, K. M. and McDermott, K. B. (2013) 'Free recall enhances subsequent learning', *Psychon Bull Rev*, 20(3), pp. 507-13.
- Arriagada, P. V., Marzloff, K. and Hyman, B. T. (1992) 'Distribution of Alzheimer-type pathologic changes in nondemented elderly individuals matches the pattern in Alzheimer's disease', *Neurology*, 42(9), pp. 1681-8.
- Aschauer, D. F., Kreuz, S. and Rumpel, S. (2013) 'Analysis of transduction efficiency, tropism and axonal transport of AAV serotypes 1, 2, 5, 6, 8 and 9 in the mouse brain', *PLoS One*, 8(9), pp. e76310.
- Ashe, K. H. and Zahs, K. R. (2010) 'Probing the biology of Alzheimer's disease in mice', *Neuron*, 66(5), pp. 631-45.
- Baglietto-Vargas, D., Medeiros, R., Martinez-Coria, H., LaFerla, F. M. and Green, K. N. (2013) 'Mifepristone alters amyloid precursor protein processing to preclude amyloid beta and also reduces tau pathology', *Biol Psychiatry*, 74(5), pp. 357-66.
- Balducci, C., Beeg, M., Stravalaci, M., Bastone, A., Scip, A., Biasini, E., Tapella, L., Colombo, L., Manzoni, C., Borsello, T., Chiesa, R., Gobbi, M., Salmona, M. and Forloni, G. (2010) 'Synthetic amyloid-beta oligomers impair long-term memory independently of cellular prion protein', *Proc Natl Acad Sci U S A*, 107(5), pp. 2295-300.
- Balducci, C. and Forloni, G. (2014) 'In vivo application of beta amyloid oligomers: a simple tool to evaluate mechanisms of action and new therapeutic approaches', *Curr Pharm Des*, 20(15), pp. 2491-505.
- Barik, J., Marti, F., Morel, C., Fernandez, S. P., Lanteri, C., Godeheu, G., Tassin, J. P., Mombereau, C., Faure, P. and Tronche, F. (2013) 'Chronic stress triggers social aversion via glucocorticoid receptor in dopaminergic neurons', *Science*, 339(6117), pp. 332-5.

- Barnes, J., Lewis, E. B., Scahill, R. I., Bartlett, J. W., Frost, C., Schott, J. M., Rossor, M. N. and Fox, N. C. (2007) 'Automated measurement of hippocampal atrophy using fluid-registered serial MRI in AD and controls', *J Comput Assist Tomogr*, 31(4), pp. 581-7.
- Baulieu, E. E. (1997) 'RU 486 (mifepristone). A short overview of its mechanisms of action and clinical uses at the end of 1996', *Ann N Y Acad Sci*, 828, pp. 47-58.
- Bellone, C., Luscher, C. and Mamei, M. (2008) 'Mechanisms of synaptic depression triggered by metabotropic glutamate receptors', *Cell Mol Life Sci*, 65(18), pp. 2913-23.
- Benilova, I., Karran, E. and De Strooper, B. (2012) 'The toxic Abeta oligomer and Alzheimer's disease: an emperor in need of clothes', *Nat Neurosci*, 15(3), pp. 349-57.
- Bertram, L., Lill, C. M. and Tanzi, R. E. (2010) 'The genetics of Alzheimer disease: back to the future', *Neuron*, 68(2), pp. 270-81.
- Bliss, T. V. and Lomo, T. (1973) 'Long-lasting potentiation of synaptic transmission in the dentate area of the anaesthetized rabbit following stimulation of the perforant path', *J Physiol*, 232(2), pp. 331-56.
- Bornstein, S. R., Engeland, W. C., Ehrhart-Bornstein, M. and Herman, J. P. (2008) 'Dissociation of ACTH and glucocorticoids', *Trends Endocrinol Metab*, 19(5), pp. 175-80.
- Braak, H. and Braak, E. (1991) 'Neuropathological staging of Alzheimer-related changes', *Acta Neuropathol*, 82(4), pp. 239-59.
- Bramblett, G. T., Goedert, M., Jakes, R., Merrick, S. E., Trojanowski, J. Q. and Lee, V. M. (1993) 'Abnormal tau phosphorylation at Ser396 in Alzheimer's disease recapitulates development and contributes to reduced microtubule binding', *Neuron*, 10(6), pp. 1089-99.
- Brureau, A., Zussy, C., Delair, B., Ogier, C., Ixart, G., Maurice, T. and Givalois, L. (2013) 'Deregulation of hypothalamic-pituitary-adrenal axis functions in an Alzheimer's disease rat model', *Neurobiol Aging*, 34(5), pp. 1426-39.
- Buee, L., Bussiere, T., Buee-Scherrer, V., Delacourte, A. and Hof, P. R. (2000) 'Tau protein isoforms, phosphorylation and role in neurodegenerative disorders', *Brain Res Brain Res Rev*, 33(1), pp. 95-130.
- Buxbaum, J. D., Liu, K. N., Luo, Y., Slack, J. L., Stocking, K. L., Peschon, J. J., Johnson, R. S., Castner, B. J., Cerretti, D. P. and Black, R. A. (1998) 'Evidence that tumor necrosis factor alpha converting enzyme is involved in regulated alpha-secretase cleavage of the Alzheimer amyloid protein precursor', *J Biol Chem*, 273(43), pp. 27765-7.
- Cai, X. D., Golde, T. E. and Younkin, S. G. (1993) 'Release of excess amyloid beta protein from a mutant amyloid beta protein precursor', *Science*, 259(5094), pp. 514-6.
- Capone, R., Quiroz, F. G., Prangkio, P., Saluja, I., Sauer, A. M., Bautista, M. R., Turner, R. S., Yang, J. and Mayer, M. (2009) 'Amyloid-beta-induced ion flux in artificial lipid bilayers and neuronal cells: resolving a controversy', *Neurotox Res*, 16(1), pp. 1-13.
- Caraci, F., Copani, A., Nicoletti, F. and Drago, F. (2010) 'Depression and Alzheimer's disease: neurobiological links and common pharmacological targets', *Eur J Pharmacol*, 626(1), pp. 64-71.
- Carlin, R. K., Grab, D. J., Cohen, R. S. and Siekevitz, P. (1980) 'Isolation and characterization of postsynaptic densities from various brain regions: enrichment of different types of postsynaptic densities', *J Cell Biol*, 86(3), pp. 831-45.

- Carlson, G. A., Borchelt, D. R., Dake, A., Turner, S., Danielson, V., Coffin, J. D., Eckman, C., Meiners, J., Nilsen, S. P., Younkin, S. G. and Hsiao, K. K. (1997) 'Genetic modification of the phenotypes produced by amyloid precursor protein overexpression in transgenic mice', *Hum Mol Genet*, 6(11), pp. 1951-9.
- Carroll, J. C., Iba, M., Bangasser, D. A., Valentino, R. J., James, M. J., Brunden, K. R., Lee, V. M. and Trojanowski, J. Q. (2011) 'Chronic stress exacerbates tau pathology, neurodegeneration, and cognitive performance through a corticotropin-releasing factor receptor-dependent mechanism in a transgenic mouse model of tauopathy', *J Neurosci*, 31(40), pp. 14436-49.
- Catania, C., Sotiropoulos, I., Silva, R., Onofri, C., Breen, K. C., Sousa, N. and Almeida, O. F. (2009) 'The amyloidogenic potential and behavioral correlates of stress', *Mol Psychiatry*, 14(1), pp. 95-105.
- Chen, D. Y., Bambah-Mukku, D., Pollonini, G. and Alberini, C. M. (2012) 'Glucocorticoid receptors recruit the CaMKIIalpha-BDNF-CREB pathways to mediate memory consolidation', *Nat Neurosci*, 15(12), pp. 1707-14.
- Chen, L., Chetkovich, D. M., Petralia, R. S., Sweeney, N. T., Kawasaki, Y., Wenthold, R. J., Brecht, D. S. and Nicoll, R. A. (2000) 'Stargazin regulates synaptic targeting of AMPA receptors by two distinct mechanisms', *Nature*, 408(6815), pp. 936-43.
- Chourbaji, S., Vogt, M. A. and Gass, P. (2008) 'Mice that under- or overexpress glucocorticoid receptors as models for depression or posttraumatic stress disorder', *Prog Brain Res*, 167, pp. 65-77.
- Citron, M. (2010) 'Alzheimer's disease: strategies for disease modification', *Nat Rev Drug Discov*, 9(5), pp. 387-98.
- Clayton, N. S. and Dickinson, A. (1998) 'Episodic-like memory during cache recovery by scrub jays', *Nature*, 395(6699), pp. 272-4.
- Cole, M. A., Kim, P. J., Kalman, B. A. and Spencer, R. L. (2000) 'Dexamethasone suppression of corticosteroid secretion: evaluation of the site of action by receptor measures and functional studies', *Psychoneuroendocrinology*, 25(2), pp. 151-67.
- Cole, T. J. (2006) 'Glucocorticoid action and the development of selective glucocorticoid receptor ligands', *Biotechnol Annu Rev*, 12, pp. 269-300.
- Cole, T. J., Blendy, J. A., Monaghan, A. P., Kriegstein, K., Schmid, W., Aguzzi, A., Fantuzzi, G., Hummler, E., Unsicker, K. and Schutz, G. (1995) 'Targeted disruption of the glucocorticoid receptor gene blocks adrenergic chromaffin cell development and severely retards lung maturation', *Genes Dev*, 9(13), pp. 1608-21.
- Conboy, L. and Sandi, C. (2010) 'Stress at learning facilitates memory formation by regulating AMPA receptor trafficking through a glucocorticoid action', *Neuropsychopharmacology*, 35(3), pp. 674-85.
- Conrad, C. D., Lupien, S. J. and McEwen, B. S. (1999) 'Support for a bimodal role for type II adrenal steroid receptors in spatial memory', *Neurobiol Learn Mem*, 72(1), pp. 39-46.
- Cortes-Mendoza, J., Diaz de Leon-Guerrero, S., Pedraza-Alva, G. and Perez-Martinez, L. (2013) 'Shaping synaptic plasticity: the role of activity-mediated epigenetic regulation on gene transcription', *Int J Dev Neurosci*, 31(6), pp. 359-69.
- Coussens, C. M., Kerr, D. S. and Abraham, W. C. (1997) 'Glucocorticoid receptor activation lowers the threshold for NMDA-receptor-dependent homosynaptic long-term

- depression in the hippocampus through activation of voltage-dependent calcium channels', *J Neurophysiol*, 78(1), pp. 1-9.
- Cowan, N. (2008) 'What are the differences between long-term, short-term, and working memory?', *Prog Brain Res*, 169, pp. 323-38.
- Csernansky, J. G., Dong, H., Fagan, A. M., Wang, L., Xiong, C., Holtzman, D. M. and Morris, J. C. (2006) 'Plasma cortisol and progression of dementia in subjects with Alzheimer-type dementia', *Am J Psychiatry*, 163(12), pp. 2164-9.
- Cupers, P., Orlans, I., Craessaerts, K., Annaert, W. and De Strooper, B. (2001) 'The amyloid precursor protein (APP)-cytoplasmic fragment generated by gamma-secretase is rapidly degraded but distributes partially in a nuclear fraction of neurones in culture', *J Neurochem*, 78(5), pp. 1168-78.
- D'Amelio, M., Cavallucci, V., Middei, S., Marchetti, C., Pacioni, S., Ferri, A., Diamantini, A., De Zio, D., Carrara, P., Battistini, L., Moreno, S., Bacci, A., Ammassari-Teule, M., Marie, H. and Cecconi, F. (2011) 'Caspase-3 triggers early synaptic dysfunction in a mouse model of Alzheimer's disease', *Nat Neurosci*, 14(1), pp. 69-76.
- Dauvilliers, Y. (2007) 'Insomnia in patients with neurodegenerative conditions', *Sleep Med*, 8 Suppl 4, pp. S27-34.
- Davies, C. A., Mann, D. M., Sumpter, P. Q. and Yates, P. O. (1987) 'A quantitative morphometric analysis of the neuronal and synaptic content of the frontal and temporal cortex in patients with Alzheimer's disease', *J Neurol Sci*, 78(2), pp. 151-64.
- Dawson, G. R., Seabrook, G. R., Zheng, H., Smith, D. W., Graham, S., O'Dowd, G., Bowery, B. J., Boyce, S., Trumbauer, M. E., Chen, H. Y., Van der Ploeg, L. H. and Sirinathsinghji, D. J. (1999) 'Age-related cognitive deficits, impaired long-term potentiation and reduction in synaptic marker density in mice lacking the beta-amyloid precursor protein', *Neuroscience*, 90(1), pp. 1-13.
- de Kloet, E. R., Joels, M. and Holsboer, F. (2005) 'Stress and the brain: from adaptation to disease', *Nat Rev Neurosci*, 6(6), pp. 463-75.
- de Kloet, E. R., Karst, H. and Joels, M. (2008) 'Corticosteroid hormones in the central stress response: quick-and-slow', *Front Neuroendocrinol*, 29(2), pp. 268-72.
- de Quervain, D. J., Poirier, R., Wollmer, M. A., Grimaldi, L. M., Tzolaki, M., Streffer, J. R., Hock, C., Nitsch, R. M., Mohajeri, M. H. and Papassotiropoulos, A. (2004) 'Glucocorticoid-related genetic susceptibility for Alzheimer's disease', *Hum Mol Genet*, 13(1), pp. 47-52.
- de Quervain, D. J., Roozendaal, B. and McGaugh, J. L. (1998) 'Stress and glucocorticoids impair retrieval of long-term spatial memory', *Nature*, 394(6695), pp. 787-90.
- De Strooper, B., Annaert, W., Cupers, P., Saftig, P., Craessaerts, K., Mumm, J. S., Schroeter, E. H., Schrijvers, V., Wolfe, M. S., Ray, W. J., Goate, A. and Kopan, R. (1999) 'A presenilin-1-dependent gamma-secretase-like protease mediates release of Notch intracellular domain', *Nature*, 398(6727), pp. 518-22.
- De Strooper, B. and Karran, E. (2016) 'The Cellular Phase of Alzheimer's Disease', *Cell*, 164(4), pp. 603-15.
- Deane, R., Du Yan, S., Subramanian, R. K., LaRue, B., Jovanovic, S., Hogg, E., Welch, D., Manness, L., Lin, C., Yu, J., Zhu, H., Ghiso, J., Frangione, B., Stern, A., Schmidt, A. M., Armstrong, D. L., Arnold, B., Liliensiek, B., Nawroth, P., Hofman, F., Kindy, M., Stern,

- D. and Zlokovic, B. (2003) 'RAGE mediates amyloid-beta peptide transport across the blood-brain barrier and accumulation in brain', *Nat Med*, 9(7), pp. 907-13.
- DeKosky, S. T. and Scheff, S. W. (1990) 'Synapse loss in frontal cortex biopsies in Alzheimer's disease: correlation with cognitive severity', *Ann Neurol*, 27(5), pp. 457-64.
- Deng, W., Aimone, J. B. and Gage, F. H. (2010) 'New neurons and new memories: how does adult hippocampal neurogenesis affect learning and memory?', *Nat Rev Neurosci*, 11(5), pp. 339-50.
- Dere, E., Huston, J. P. and De Souza Silva, M. A. (2005) 'Episodic-like memory in mice: simultaneous assessment of object, place and temporal order memory', *Brain Res Brain Res Protoc*, 16(1-3), pp. 10-9.
- deToledo-Morrell, L., Stoub, T. R. and Wang, C. (2007) 'Hippocampal atrophy and disconnection in incipient and mild Alzheimer's disease', *Prog Brain Res*, 163, pp. 741-53.
- Diamond, D. M., Bennett, M. C., Fleshner, M. and Rose, G. M. (1992) 'Inverted-U relationship between the level of peripheral corticosterone and the magnitude of hippocampal primed burst potentiation', *Hippocampus*, 2(4), pp. 421-30.
- Dickerson, B. C. and Wolk, D. A. (2012) 'MRI cortical thickness biomarker predicts AD-like CSF and cognitive decline in normal adults', *Neurology*, 78(2), pp. 84-90.
- Dineley, K. T., Kaye, R., Neugebauer, V., Fu, Y., Zhang, W., Reese, L. C. and Tagliavola, G. (2010) 'Amyloid-beta oligomers impair fear conditioned memory in a calcineurin-dependent fashion in mice', *J Neurosci Res*, 88(13), pp. 2923-32.
- Dineley, K. T., Westerman, M., Bui, D., Bell, K., Ashe, K. H. and Sweatt, J. D. (2001) 'Beta-amyloid activates the mitogen-activated protein kinase cascade via hippocampal alpha7 nicotinic acetylcholine receptors: In vitro and in vivo mechanisms related to Alzheimer's disease', *J Neurosci*, 21(12), pp. 4125-33.
- Dingledine, R., Borges, K., Bowie, D. and Traynelis, S. F. (1999) 'The glutamate receptor ion channels', *Pharmacol Rev*, 51(1), pp. 7-61.
- Diorio, D., Viau, V. and Meaney, M. J. (1993) 'The role of the medial prefrontal cortex (cingulate gyrus) in the regulation of hypothalamic-pituitary-adrenal responses to stress', *J Neurosci*, 13(9), pp. 3839-47.
- Dong, H., Yuede, C. M., Yoo, H. S., Martin, M. V., Deal, C., Mace, A. G. and Csernansky, J. G. (2008) 'Corticosterone and related receptor expression are associated with increased beta-amyloid plaques in isolated Tg2576 mice', *Neuroscience*, 155(1), pp. 154-63.
- Donley, M. P., Schulkin, J. and Rosen, J. B. (2005) 'Glucocorticoid receptor antagonism in the basolateral amygdala and ventral hippocampus interferes with long-term memory of contextual fear', *Behav Brain Res*, 164(2), pp. 197-205.
- Ehrhart-Bornstein, M., Hinson, J. P., Bornstein, S. R., Scherbaum, W. A. and Vinson, G. P. (1998) 'Intraadrenal interactions in the regulation of adrenocortical steroidogenesis', *Endocr Rev*, 19(2), pp. 101-43.
- Elgh, E., Lindqvist Astot, A., Fagerlund, M., Eriksson, S., Olsson, T. and Näsman, B. (2006) 'Cognitive dysfunction, hippocampal atrophy and glucocorticoid feedback in Alzheimer's disease', *Biol Psychiatry*, 59(2), pp. 155-61.
- Esler, W. P. and Wolfe, M. S. (2001) 'A portrait of Alzheimer secretases--new features and familiar faces', *Science*, 293(5534), pp. 1449-54.

- Evanson, N. K., Tasker, J. G., Hill, M. N., Hillard, C. J. and Herman, J. P. (2010) 'Fast feedback inhibition of the HPA axis by glucocorticoids is mediated by endocannabinoid signaling', *Endocrinology*, 151(10), pp. 4811-9.
- Fendler, K., Karmos, G. and Telegdy, G. (1961) 'The effect of hippocampal lesion on pituitary-adrenal function', *Acta Physiol Acad Sci Hung*, 20, pp. 293-7.
- French-Mullen, J. M. (1995) 'Cortisol inhibition of calcium currents in guinea pig hippocampal CA1 neurons via G-protein-coupled activation of protein kinase C', *J Neurosci*, 15(1 Pt 2), pp. 903-11.
- Finsterwald, C. and Alberini, C. M. (2014) 'Stress and glucocorticoid receptor-dependent mechanisms in long-term memory: from adaptive responses to psychopathologies', *Neurobiol Learn Mem*, 112, pp. 17-29.
- Frändemich, M. L., De Seranno, S., Rush, T., Borel, E., Elie, A., Arnal, I., Lanté, F. and Buisson, A. (2014) 'Activity-dependent tau protein translocation to excitatory synapse is disrupted by exposure to amyloid-beta oligomers', *J Neurosci*, 34(17), pp. 6084-97.
- Frankland, P. W. and Bontempi, B. (2005) 'The organization of recent and remote memories', *Nat Rev Neurosci*, 6(2), pp. 119-30.
- Frick, K. M. and Gresack, J. E. (2003) 'Sex differences in the behavioral response to spatial and object novelty in adult C57BL/6 mice', *Behav Neurosci*, 117(6), pp. 1283-91.
- Friedman, D., Nessler, D. and Johnson, R., Jr. (2007) 'Memory encoding and retrieval in the aging brain', *Clin EEG Neurosci*, 38(1), pp. 2-7.
- Funder, J. W. (1990) 'Corticosteroid receptors and renal 11 beta-hydroxysteroid dehydrogenase activity', *Semin Nephrol*, 10(4), pp. 311-9.
- Genin, E., Hannequin, D., Wallon, D., Sleegers, K., Hiltunen, M., Combarros, O., Bullido, M. J., Engelborghs, S., De Deyn, P., Berr, C., Pasquier, F., Dubois, B., Tognoni, G., Fiévet, N., Brouwers, N., Bettens, K., Arosio, B., Coto, E., Del Zompo, M., Mateo, I., Epelbaum, J., Frank-Garcia, A., Helisalmi, S., Porcellini, E., Pilotto, A., Forti, P., Ferri, R., Scarpini, E., Siciliano, G., Solfrizzi, V., Sorbi, S., Spalletta, G., Valdivieso, F., Vepsäläinen, S., Alvarez, V., Bosco, P., Mancuso, M., Panza, F., Nacmias, B., Bossù, P., Hanon, O., Piccardi, P., Annoni, G., Seripa, D., Galimberti, D., Licastro, F., Soininen, H., Dartigues, J. F., Kamboh, M. I., Van Broeckhoven, C., Lambert, J. C., Amouyel, P. and Campion, D. (2011) 'APOE and Alzheimer disease: a major gene with semi-dominant inheritance', *Mol Psychiatry*, 16(9), pp. 903-7.
- Giedraitis, V., Sundelöf, J., Irizarry, M. C., Gårevik, N., Hyman, B. T., Wahlund, L. O., Ingelsson, M. and Lannfelt, L. (2007) 'The normal equilibrium between CSF and plasma amyloid beta levels is disrupted in Alzheimer's disease', *Neurosci Lett*, 427(3), pp. 127-31.
- Gilman, S., Koller, M., Black, R. S., Jenkins, L., Griffith, S. G., Fox, N. C., Eisner, L., Kirby, L., Rovira, M. B., Forette, F. and Orgogozo, J. M. (2005) 'Clinical effects of Aβ immunization (AN1792) in patients with AD in an interrupted trial', *Neurology*, 64(9), pp. 1553-62.
- Giubilei, F., Patacchioli, F. R., Antonini, G., Sepe Monti, M., Tisei, P., Bastianello, S., Monnazzi, P. and Angelucci, L. (2001) 'Altered circadian cortisol secretion in Alzheimer's disease: clinical and neuroradiological aspects', *J Neurosci Res*, 66(2), pp. 262-5.

- Goedert, M., Sisodia, S. S. and Price, D. L. (1991) 'Neurofibrillary tangles and beta-amyloid deposits in Alzheimer's disease', *Curr Opin Neurobiol*, 1(3), pp. 441-7.
- Gold, C. A. and Budson, A. E. (2008) 'Memory loss in Alzheimer's disease: implications for development of therapeutics', *Expert Rev Neurother*, 8(12), pp. 1879-91.
- Goulart, B. K., de Lima, M. N., de Farias, C. B., Reolon, G. K., Almeida, V. R., Quevedo, J., Kapczinski, F., Schroder, N. and Roesler, R. (2010) 'Ketamine impairs recognition memory consolidation and prevents learning-induced increase in hippocampal brain-derived neurotrophic factor levels', *Neuroscience*, 167(4), pp. 969-73.
- Gould, E. and Tanapat, P. (1999) 'Stress and hippocampal neurogenesis', *Biol Psychiatry*, 46(11), pp. 1472-9.
- Green, K. N., Billings, L. M., Roozendaal, B., McGaugh, J. L. and LaFerla, F. M. (2006) 'Glucocorticoids increase amyloid-beta and tau pathology in a mouse model of Alzheimer's disease', *J Neurosci*, 26(35), pp. 9047-56.
- Greenfield, J. P., Tsai, J., Gouras, G. K., Hai, B., Thinakaran, G., Checler, F., Sisodia, S. S., Greengard, P. and Xu, H. (1999) 'Endoplasmic reticulum and trans-Golgi network generate distinct populations of Alzheimer beta-amyloid peptides', *Proc Natl Acad Sci U S A*, 96(2), pp. 742-7.
- Groc, L., Choquet, D. and Chaouloff, F. (2008) 'The stress hormone corticosterone conditions AMPAR surface trafficking and synaptic potentiation', *Nat Neurosci*, 11(8), pp. 868-70.
- Guillozet, A. L., Weintraub, S., Mash, D. C. and Mesulam, M. M. (2003) 'Neurofibrillary tangles, amyloid, and memory in aging and mild cognitive impairment', *Arch Neurol*, 60(5), pp. 729-36.
- Götz, J., Xia, D., Leinenga, G., Chew, Y. L. and Nicholas, H. (2013) 'What Renders TAU Toxic', *Front Neurol*, 4, pp. 72.
- Habib, A., Sawmiller, D. and Tan, J. (2016) 'Restoring Soluble Amyloid Precursor Protein  $\alpha$  Functions as a Potential Treatment for Alzheimer's Disease', *J Neurosci Res*.
- Hansson, O., Zetterberg, H., Buchhave, P., Andreasson, U., Londos, E., Minthon, L. and Blennow, K. (2007) 'Prediction of Alzheimer's disease using the CSF A $\beta$ 42/A $\beta$ 40 ratio in patients with mild cognitive impairment', *Dement Geriatr Cogn Disord*, 23(5), pp. 316-20.
- Hardy, J. and Allsop, D. (1991) 'Amyloid deposition as the central event in the aetiology of Alzheimer's disease', *Trends Pharmacol Sci*, 12(10), pp. 383-8.
- Hardy, J. A. and Higgins, G. A. (1992) 'Alzheimer's disease: the amyloid cascade hypothesis', *Science*, 256(5054), pp. 184-5.
- Hartmann, A., Krumrey, K., Vogl, L., Dirlich, G., Holsboer, F. and Heuser-Link, M. (1996) 'Changes in late auditory evoked potentials induced by corticotropin-releasing hormone and corticotropin fragment 4-9 in male controls', *Neuropsychobiology*, 33(2), pp. 90-6.
- Hebda-Bauer, E. K., Simmons, T. A., Sugg, A., Ural, E., Stewart, J. A., Beals, J. L., Wei, Q., Watson, S. J. and Akil, H. (2013) '3xTg-AD mice exhibit an activated central stress axis during early-stage pathology', *J Alzheimers Dis*, 33(2), pp. 407-22.
- Heber, S., Herms, J., Gajic, V., Hainfellner, J., Aguzzi, A., Rüllicke, T., von Kretschmar, H., von Koch, C., Sisodia, S., Tremml, P., Lipp, H. P., Wolfer, D. P. and Müller, U. (2000) 'Mice

- with combined gene knock-outs reveal essential and partially redundant functions of amyloid precursor protein family members', *J Neurosci*, 20(21), pp. 7951-63.
- Herman, J. P. and Cullinan, W. E. (1997) 'Neurocircuitry of stress: central control of the hypothalamo-pituitary-adrenocortical axis', *Trends Neurosci*, 20(2), pp. 78-84.
- Herman, J. P., Ostrander, M. M., Mueller, N. K. and Figueiredo, H. (2005) 'Limbic system mechanisms of stress regulation: hypothalamo-pituitary-adrenocortical axis', *Prog Neuropsychopharmacol Biol Psychiatry*, 29(8), pp. 1201-13.
- Herman, J. P. and Seroogy, K. (2006) 'Hypothalamic-pituitary-adrenal axis, glucocorticoids, and neurologic disease', *Neurol Clin*, 24(3), pp. 461-81, vi.
- Herrup, K. (2015) 'The case for rejecting the amyloid cascade hypothesis', *Nat Neurosci*, 18(6), pp. 794-9.
- Higgins, L. S., Holtzman, D. M., Rabin, J., Mobley, W. C. and Cordell, B. (1994) 'Transgenic mouse brain histopathology resembles early Alzheimer's disease', *Ann Neurol*, 35(5), pp. 598-607.
- Hill, M. N., Hillard, C. J. and McEwen, B. S. (2011) 'Alterations in corticolimbic dendritic morphology and emotional behavior in cannabinoid CB1 receptor-deficient mice parallel the effects of chronic stress', *Cereb Cortex*, 21(9), pp. 2056-64.
- Howland, J. G. and Cazakoff, B. N. (2010) 'Effects of acute stress and GluN2B-containing NMDA receptor antagonism on object and object-place recognition memory', *Neurobiol Learn Mem*, 93(2), pp. 261-7.
- Hsiao, K., Chapman, P., Nilsen, S., Eckman, C., Harigaya, Y., Younkin, S., Yang, F. and Cole, G. (1996) 'Correlative memory deficits, A $\beta$  elevation, and amyloid plaques in transgenic mice', *Science*, 274(5284), pp. 99-102.
- Hsieh, H., Boehm, J., Sato, C., Iwatsubo, T., Tomita, T., Sisodia, S. and Malinow, R. (2006) 'AMPA removal underlies A $\beta$ -induced synaptic depression and dendritic spine loss', *Neuron*, 52(5), pp. 831-43.
- Huang, Y. A., Zhou, B., Wernig, M. and Südhof, T. C. (2017) 'ApoE2, ApoE3, and ApoE4 Differentially Stimulate APP Transcription and A $\beta$  Secretion', *Cell*, 168(3), pp. 427-441.e21.
- Hung, A. Y. and Selkoe, D. J. (1994) 'Selective ectodomain phosphorylation and regulated cleavage of beta-amyloid precursor protein', *EMBO J*, 13(3), pp. 534-42.
- Hunt, H. J., Belanoff, J. K., Golding, E., Gourdet, B., Phillips, T., Swift, D., Thomas, J., Unitt, J. F. and Walters, I. (2015) '1H-Pyrazolo[3,4-g]hexahydro-isoquinolines as potent GR antagonists with reduced hERG inhibition and an improved pharmacokinetic profile', *Bioorg Med Chem Lett*, 25(24), pp. 5720-5.
- Hussain, I., Powell, D., Howlett, D. R., Tew, D. G., Meek, T. D., Chapman, C., Gloger, I. S., Murphy, K. E., Southan, C. D., Ryan, D. M., Smith, T. S., Simmons, D. L., Walsh, F. S., Dingwall, C. and Christie, G. (1999) 'Identification of a novel aspartic protease (Asp 2) as beta-secretase', *Mol Cell Neurosci*, 14(6), pp. 419-27.
- Hyman, B. T. and Van Hoesen, G. W. (1987) 'Neuron numbers in Alzheimer's disease: cell-specific pathology', *Neurobiol Aging*, 8(6), pp. 555-6.
- Jacobson, L. and Sapolsky, R. (1991) 'The role of the hippocampus in feedback regulation of the hypothalamic-pituitary-adrenocortical axis', *Endocr Rev*, 12(2), pp. 118-34.

- Jaferi, A., Nowak, N. and Bhatnagar, S. (2003) 'Negative feedback functions in chronically stressed rats: role of the posterior paraventricular thalamus', *Physiol Behav*, 78(3), pp. 365-73.
- Jarrett, J. T., Berger, E. P. and Lansbury, P. T., Jr. (1993) 'The C-terminus of the beta protein is critical in amyloidogenesis', *Ann N Y Acad Sci*, 695, pp. 144-8.
- Jeong, Y. H., Park, C. H., Yoo, J., Shin, K. Y., Ahn, S. M., Kim, H. S., Lee, S. H., Emson, P. C. and Suh, Y. H. (2006) 'Chronic stress accelerates learning and memory impairments and increases amyloid deposition in APPV717I-CT100 transgenic mice, an Alzheimer's disease model', *Faseb j*, 20(6), pp. 729-31.
- Johnson, L. R., Farb, C., Morrison, J. H., McEwen, B. S. and LeDoux, J. E. (2005) 'Localization of glucocorticoid receptors at postsynaptic membranes in the lateral amygdala', *Neuroscience*, 136(1), pp. 289-99.
- Jonsson, T., Atwal, J. K., Steinberg, S., Snaedal, J., Jonsson, P. V., Bjornsson, S., Stefansson, H., Sulem, P., Gudbjartsson, D., Maloney, J., Hoyte, K., Gustafson, A., Liu, Y., Lu, Y., Bhangale, T., Graham, R. R., Huttenlocher, J., Bjornsdottir, G., Andreassen, O. A., Jönsson, E. G., Palotie, A., Behrens, T. W., Magnusson, O. T., Kong, A., Thorsteinsdottir, U., Watts, R. J. and Stefansson, K. (2012) 'A mutation in APP protects against Alzheimer's disease and age-related cognitive decline', *Nature*, 488(7409), pp. 96-9.
- Joëls, M. and Karst, H. (2012) 'Corticosteroid effects on calcium signaling in limbic neurons', *Cell Calcium*, 51(3-4), pp. 277-83.
- Ju, Y. E., Lucey, B. P. and Holtzman, D. M. (2014) 'Sleep and Alzheimer disease pathology--a bidirectional relationship', *Nat Rev Neurol*, 10(2), pp. 115-9.
- Kamboh, M. I., Demirci, F. Y., Wang, X., Minster, R. L., Carrasquillo, M. M., Pankratz, V. S., Younkin, S. G., Saykin, A. J., Jun, G., Baldwin, C., Logue, M. W., Buross, J., Farrer, L., Pericak-Vance, M. A., Haines, J. L., Sweet, R. A., Ganguli, M., Feingold, E., Dekosky, S. T., Lopez, O. L., Barmada, M. M. and Initiative, A. s. D. N. (2012) 'Genome-wide association study of Alzheimer's disease', *Transl Psychiatry*, 2, pp. e117.
- Kamenetz, F., Tomita, T., Hsieh, H., Seabrook, G., Borchelt, D., Iwatsubo, T., Sisodia, S. and Malinow, R. (2003) 'APP processing and synaptic function', *Neuron*, 37(6), pp. 925-37.
- Kawarabayashi, T., Shoji, M., Younkin, L. H., Wen-Lang, L., Dickson, D. W., Murakami, T., Matsubara, E., Abe, K., Ashe, K. H. and Younkin, S. G. (2004) 'Dimeric amyloid beta protein rapidly accumulates in lipid rafts followed by apolipoprotein E and phosphorylated tau accumulation in the Tg2576 mouse model of Alzheimer's disease', *J Neurosci*, 24(15), pp. 3801-9.
- Kehoe, P. G. (2003) 'The renin-angiotensin-aldosterone system and Alzheimer's disease?', *J Renin Angiotensin Aldosterone Syst*, 4(2), pp. 80-93.
- Kessels, H. W. and Malinow, R. (2009) 'Synaptic AMPA receptor plasticity and behavior', *Neuron*, 61(3), pp. 340-50.
- Kessels, R. P. and Kopelman, M. D. (2012) 'Context memory in Korsakoff's syndrome', *Neuropsychol Rev*, 22(2), pp. 117-31.
- Killiany, R. J., Hyman, B. T., Gomez-Isla, T., Moss, M. B., Kikinis, R., Jolesz, F., Tanzi, R., Jones, K. and Albert, M. S. (2002) 'MRI measures of entorhinal cortex vs hippocampus in preclinical AD', *Neurology*, 58(8), pp. 1188-96.

- King, D. L., Arendash, G. W., Crawford, F., Sterk, T., Menendez, J. and Mullan, M. J. (1999) 'Progressive and gender-dependent cognitive impairment in the APP(SW) transgenic mouse model for Alzheimer's disease', *Behav Brain Res*, 103(2), pp. 145-62.
- King, M. E., Kan, H. M., Baas, P. W., Erisir, A., Glabe, C. G. and Bloom, G. S. (2006) 'Tau-dependent microtubule disassembly initiated by prefibrillar beta-amyloid', *J Cell Biol*, 175(4), pp. 541-6.
- Kino, T., Kozasa, T. and Chrousos, G. P. (2005) 'Statin-induced blockade of prenylation alters nucleocytoplasmic shuttling of GTP-binding proteins gamma2 and beta2 and enhances their suppressive effect on glucocorticoid receptor transcriptional activity', *Eur J Clin Invest*, 35(8), pp. 508-13.
- Koffie, R. M., Meyer-Luehmann, M., Hashimoto, T., Adams, K. W., Mielke, M. L., Garcia-Alloza, M., Micheva, K. D., Smith, S. J., Kim, M. L., Lee, V. M., Hyman, B. T. and Spire-Jones, T. L. (2009) 'Oligomeric amyloid beta associates with postsynaptic densities and correlates with excitatory synapse loss near senile plaques', *Proc Natl Acad Sci U S A*, 106(10), pp. 4012-7.
- Krugers, H. J., Hoogenraad, C. C. and Groc, L. (2010) 'Stress hormones and AMPA receptor trafficking in synaptic plasticity and memory', *Nat Rev Neurosci*, 11(10), pp. 675-81.
- Lacor, P. N., Buniel, M. C., Furlow, P. W., Clemente, A. S., Velasco, P. T., Wood, M., Viola, K. L. and Klein, W. L. (2007) 'Abeta oligomer-induced aberrations in synapse composition, shape, and density provide a molecular basis for loss of connectivity in Alzheimer's disease', *J Neurosci*, 27(4), pp. 796-807.
- Lambert, M. P., Barlow, A. K., Chromy, B. A., Edwards, C., Freed, R., Liosatos, M., Morgan, T. E., Rozovsky, I., Trommer, B., Viola, K. L., Wals, P., Zhang, C., Finch, C. E., Krafft, G. A. and Klein, W. L. (1998) 'Diffusible, nonfibrillar ligands derived from Abeta1-42 are potent central nervous system neurotoxins', *Proc Natl Acad Sci U S A*, 95(11), pp. 6448-53.
- Lammich, S., Kojro, E., Postina, R., Gilbert, S., Pfeiffer, R., Jasionowski, M., Haass, C. and Fahrenholz, F. (1999) 'Constitutive and regulated alpha-secretase cleavage of Alzheimer's amyloid precursor protein by a disintegrin metalloprotease', *Proc Natl Acad Sci U S A*, 96(7), pp. 3922-7.
- Lanté, F., Chafai, M., Raymond, E. F., Pereira, A. R., Mouska, X., Kootar, S., Barik, J., Bethus, I. and Marie, H. (2015) 'Subchronic glucocorticoid receptor inhibition rescues early episodic memory and synaptic plasticity deficits in a mouse model of Alzheimer's disease', *Neuropsychopharmacology*, 40(7), pp. 1772-81.
- Laurén, J., Gimbel, D. A., Nygaard, H. B., Gilbert, J. W. and Strittmatter, S. M. (2009) 'Cellular prion protein mediates impairment of synaptic plasticity by amyloid-beta oligomers', *Nature*, 457(7233), pp. 1128-32.
- Laxton, A. W., Tang-Wai, D. F., McAndrews, M. P., Zumsteg, D., Wennberg, R., Keren, R., Wherrett, J., Naglie, G., Hamani, C., Smith, G. S. and Lozano, A. M. (2010) 'A phase I trial of deep brain stimulation of memory circuits in Alzheimer's disease', *Ann Neurol*, 68(4), pp. 521-34.
- Lee, K. W., Kim, J. B., Seo, J. S., Kim, T. K., Im, J. Y., Baek, I. S., Kim, K. S., Lee, J. K. and Han, P. L. (2009) 'Behavioral stress accelerates plaque pathogenesis in the brain of Tg2576 mice via generation of metabolic oxidative stress', *J Neurochem*, 108(1), pp. 165-75.

- Lesne, S., Koh, M. T., Kotilinek, L., Kaye, R., Glabe, C. G., Yang, A., Gallagher, M. and Ashe, K. H. (2006) 'A specific amyloid-beta protein assembly in the brain impairs memory', *Nature*, 440(7082), pp. 352-7.
- Li, S., Hong, S., Shepardson, N. E., Walsh, D. M., Shankar, G. M. and Selkoe, D. (2009) 'Soluble oligomers of amyloid Beta protein facilitate hippocampal long-term depression by disrupting neuronal glutamate uptake', *Neuron*, 62(6), pp. 788-801.
- Li, T., Ma, G., Cai, H., Price, D. L. and Wong, P. C. (2003) 'Nicastrin is required for assembly of presenilin/gamma-secretase complexes to mediate Notch signaling and for processing and trafficking of beta-amyloid precursor protein in mammals', *J Neurosci*, 23(8), pp. 3272-7.
- Lightman, S. L. and Conway-Campbell, B. L. (2010) 'The crucial role of pulsatile activity of the HPA axis for continuous dynamic equilibration', *Nat Rev Neurosci*, 11(10), pp. 710-8.
- Lisman, J., Yasuda, R. and Raghavachari, S. (2012) 'Mechanisms of CaMKII action in long-term potentiation', *Nat Rev Neurosci*, 13(3), pp. 169-82.
- Liston, C., Cichon, J. M., Jeanneteau, F., Jia, Z., Chao, M. V. and Gan, W. B. (2013) 'Circadian glucocorticoid oscillations promote learning-dependent synapse formation and maintenance', *Nat Neurosci*, 16(6), pp. 698-705.
- Liu, Q., Lee, H. G., Honda, K., Siedlak, S. L., Harris, P. L., Cash, A. D., Zhu, X., Avila, J., Nunomura, A., Takeda, A., Smith, M. A. and Perry, G. (2005) 'Tau modifiers as therapeutic targets for Alzheimer's disease', *Biochim Biophys Acta*, 1739(2-3), pp. 211-5.
- Lowy, M. T., Gault, L. and Yamamoto, B. K. (1993) 'Adrenalectomy attenuates stress-induced elevations in extracellular glutamate concentrations in the hippocampus', *J Neurochem*, 61(5), pp. 1957-60.
- Lue, L. F., Kuo, Y. M., Roher, A. E., Brachova, L., Shen, Y., Sue, L., Beach, T., Kurth, J. H., Rydel, R. E. and Rogers, J. (1999) 'Soluble amyloid beta peptide concentration as a predictor of synaptic change in Alzheimer's disease', *Am J Pathol*, 155(3), pp. 853-62.
- Lynch, G., Larson, J., Kelso, S., Barrionuevo, G. and Schottler, F. (1983) 'Intracellular injections of EGTA block induction of hippocampal long-term potentiation', *Nature*, 305(5936), pp. 719-21.
- Marchetti, C., Tafi, E., Middei, S., Rubinacci, M. A., Restivo, L., Ammassari-Teule, M. and Marie, H. (2010) 'Synaptic adaptations of CA1 pyramidal neurons induced by a highly effective combinational antidepressant therapy', *Biol Psychiatry*, 67(2), pp. 146-54.
- Martin, S., Henley, J. M., Holman, D., Zhou, M., Wiegert, O., van Spronsen, M., Joels, M., Hoogenraad, C. C. and Krugers, H. J. (2009) 'Corticosterone alters AMPAR mobility and facilitates bidirectional synaptic plasticity', *PLoS One*, 4(3), pp. e4714.
- Mattson, M. P., Cheng, B., Culwell, A. R., Esch, F. S., Lieberburg, I. and Rydel, R. E. (1993) 'Evidence for excitoprotective and intraneuronal calcium-regulating roles for secreted forms of the beta-amyloid precursor protein', *Neuron*, 10(2), pp. 243-54.
- Matus, A., Ackermann, M., Pehling, G., Byers, H. R. and Fujiwara, K. (1982) 'High actin concentrations in brain dendritic spines and postsynaptic densities', *Proc Natl Acad Sci U S A*, 79(23), pp. 7590-4.
- Maurer, K., Volk, S. and Gerbaldo, H. (1997) 'Auguste D and Alzheimer's disease', *Lancet*, 349(9064), pp. 1546-9.

- McCloy, R. A., Rogers, S., Caldon, C. E., Lorca, T., Castro, A. and Burgess, A. (2014) 'Partial inhibition of Cdk1 in G 2 phase overrides the SAC and decouples mitotic events', *Cell Cycle*, 13(9), pp. 1400-12.
- McCurry, S. M., Logsdon, R. G., Teri, L., Gibbons, L. E., Kukull, W. A., Bowen, J. D., McCormick, W. C. and Larson, E. B. (1999) 'Characteristics of sleep disturbance in community-dwelling Alzheimer's disease patients', *J Geriatr Psychiatry Neurol*, 12(2), pp. 53-9.
- McEwen, B. S. and Sapolsky, R. M. (1995) 'Stress and cognitive function', *Curr Opin Neurobiol*, 5(2), pp. 205-16.
- McIntyre, C. K., McGaugh, J. L. and Williams, C. L. (2012) 'Interacting brain systems modulate memory consolidation', *Neurosci Biobehav Rev*, 36(7), pp. 1750-62.
- Mejia, S., Giraldo, M., Pineda, D., Ardila, A. and Lopera, F. (2003) 'Nongenetic factors as modifiers of the age of onset of familial Alzheimer's disease', *Int Psychogeriatr*, 15(4), pp. 337-49.
- Morgan, F. H. and Laufgraben, M. J. (2013) 'Mifepristone for management of Cushing's syndrome', *Pharmacotherapy*, 33(3), pp. 319-29.
- Morley, J. E., Farr, S. A., Banks, W. A., Johnson, S. N., Yamada, K. A. and Xu, L. (2010) 'A physiological role for amyloid-beta protein: enhancement of learning and memory', *J Alzheimers Dis*, 19(2), pp. 441-9.
- Morris, M., Maeda, S., Vossel, K. and Mucke, L. (2011) 'The many faces of tau', *Neuron*, 70(3), pp. 410-26.
- Morris, R. G., Anderson, E., Lynch, G. S. and Baudry, M. (1986) 'Selective impairment of learning and blockade of long-term potentiation by an N-methyl-D-aspartate receptor antagonist, AP5', *Nature*, 319(6056), pp. 774-6.
- Musiek, E. S. and Holtzman, D. M. (2015) 'Three dimensions of the amyloid hypothesis: time, space and 'wingmen'', *Nat Neurosci*, 18(6), pp. 800-6.
- Mustafiz, T., Portelius, E., Gustavsson, M. K., Hölttä, M., Zetterberg, H., Blennow, K., Nordberg, A. and Lithner, C. U. (2011) 'Characterization of the brain  $\beta$ -amyloid isoform pattern at different ages of Tg2576 mice', *Neurodegener Dis*, 8(5), pp. 352-63.
- Nabavi, S., Kessels, H. W., Alfonso, S., Aow, J., Fox, R. and Malinow, R. (2013) 'Metabotropic NMDA receptor function is required for NMDA receptor-dependent long-term depression', *Proc Natl Acad Sci U S A*, 110(10), pp. 4027-32.
- Nadel, L., Campbell, J. and Ryan, L. (2007) 'Autobiographical memory retrieval and hippocampal activation as a function of repetition and the passage of time', *Neural Plast*, 2007, pp. 90472.
- Nelson, P. T., Braak, H. and Markesbery, W. R. (2009) 'Neuropathology and cognitive impairment in Alzheimer disease: a complex but coherent relationship', *J Neuropathol Exp Neurol*, 68(1), pp. 1-14.
- Neves, G., Cooke, S. F. and Bliss, T. V. (2008) 'Synaptic plasticity, memory and the hippocampus: a neural network approach to causality', *Nat Rev Neurosci*, 9(1), pp. 65-75.
- Nishiyama, M., Hong, K., Mikoshiba, K., Poo, M. M. and Kato, K. (2000) 'Calcium stores regulate the polarity and input specificity of synaptic modification', *Nature*, 408(6812), pp. 584-8.

- Notarianni, E. (2013) 'Hypercortisolemia and glucocorticoid receptor-signaling insufficiency in Alzheimer's disease initiation and development', *Curr Alzheimer Res*, 10(7), pp. 714-31.
- Nowak, L., Bregestovski, P., Ascher, P., Herbet, A. and Prochiantz, A. (1984) 'Magnesium gates glutamate-activated channels in mouse central neurones', *Nature*, 307(5950), pp. 462-5.
- Nyberg, L., McIntosh, A. R., Cabeza, R., Habib, R., Houle, S. and Tulving, E. (1996) 'General and specific brain regions involved in encoding and retrieval of events: what, where, and when', *Proc Natl Acad Sci U S A*, 93(20), pp. 11280-5.
- Näsman, B., Olsson, T., Viitanen, M. and Carlström, K. (1995) 'A subtle disturbance in the feedback regulation of the hypothalamic-pituitary-adrenal axis in the early phase of Alzheimer's disease', *Psychoneuroendocrinology*, 20(2), pp. 211-20.
- O'Brien, J. T., Ames, D., Schweitzer, I., Mastwyk, M. and Colman, P. (1996) 'Enhanced adrenal sensitivity to adrenocorticotrophic hormone (ACTH) is evidence of HPA axis hyperactivity in Alzheimer's disease', *Psychol Med*, 26(1), pp. 7-14.
- Oddo, S., Caccamo, A., Shepherd, J. D., Murphy, M. P., Golde, T. E., Kaye, R., Metherate, R., Mattson, M. P., Akbari, Y. and LaFerla, F. M. (2003) 'Triple-transgenic model of Alzheimer's disease with plaques and tangles: intracellular Abeta and synaptic dysfunction', *Neuron*, 39(3), pp. 409-21.
- Oltersdorf, T., Ward, P. J., Henriksson, T., Beattie, E. C., Neve, R., Lieberburg, I. and Fritz, L. C. (1990) 'The Alzheimer amyloid precursor protein. Identification of a stable intermediate in the biosynthetic/degradative pathway', *J Biol Chem*, 265(8), pp. 4492-7.
- Palmer, M. J., Irving, A. J., Seabrook, G. R., Jane, D. E. and Collingridge, G. L. (1997) 'The group I mGlu receptor agonist DHPG induces a novel form of LTD in the CA1 region of the hippocampus', *Neuropharmacology*, 36(11-12), pp. 1517-32.
- Palop, J. J. and Mucke, L. (2010) 'Amyloid-beta-induced neuronal dysfunction in Alzheimer's disease: from synapses toward neural networks', *Nat Neurosci*, 13(7), pp. 812-8.
- Paoletti, P. and Neyton, J. (2007) 'NMDA receptor subunits: function and pharmacology', *Curr Opin Pharmacol*, 7(1), pp. 39-47.
- Papoutsis, A., Sidiropoulou, K., Cutsuridis, V. and Poirazi, P. (2013) 'Induction and modulation of persistent activity in a layer V PFC microcircuit model', *Front Neural Circuits*, 7, pp. 161.
- Pavlidis, C., Watanabe, Y., Magariños, A. M. and McEwen, B. S. (1995) 'Opposing roles of type I and type II adrenal steroid receptors in hippocampal long-term potentiation', *Neuroscience*, 68(2), pp. 387-94.
- Pedersen, J. T. and Sigurdsson, E. M. (2015) 'Tau immunotherapy for Alzheimer's disease', *Trends Mol Med*, 21(6), pp. 394-402.
- Peineau, S., Taghibiglou, C., Bradley, C., Wong, T. P., Liu, L., Lu, J., Lo, E., Wu, D., Saule, E., Bouschet, T., Matthews, P., Isaac, J. T., Bortolotto, Z. A., Wang, Y. T. and Collingridge, G. L. (2007) 'LTP inhibits LTD in the hippocampus via regulation of GSK3beta', *Neuron*, 53(5), pp. 703-17.
- Pena-Casanova, J., Sanchez-Benavides, G., de Sola, S., Manero-Borras, R. M. and Casals-Coll, M. (2012) 'Neuropsychology of Alzheimer's disease', *Arch Med Res*, 43(8), pp. 686-93.

- Pepin, M. C., Pothier, F. and Barden, N. (1992) 'Impaired type II glucocorticoid-receptor function in mice bearing antisense RNA transgene', *Nature*, 355(6362), pp. 725-8.
- Perlmutter, L. S., Scott, S. A., Barrón, E. and Chui, H. C. (1992) 'MHC class II-positive microglia in human brain: association with Alzheimer lesions', *J Neurosci Res*, 33(4), pp. 549-58.
- Petersen, R. C. (2003) 'Mild cognitive impairment clinical trials', *Nat Rev Drug Discov*, 2(8), pp. 646-53.
- Phinney, A. L., Deller, T., Stalder, M., Calhoun, M. E., Frotscher, M., Sommer, B., Staufenbiel, M. and Jucker, M. (1999) 'Cerebral amyloid induces aberrant axonal sprouting and ectopic terminal formation in amyloid precursor protein transgenic mice', *J Neurosci*, 19(19), pp. 8552-9.
- Pineau, F., Canet, G., Desrumaux, C., Hunt, H., Chevallier, N., Ollivier, M., Belanoff, J. K. and Givalois, L. (2016) 'New selective glucocorticoid receptor modulators reverse amyloid- $\beta$  peptide-induced hippocampus toxicity', *Neurobiol Aging*, 45, pp. 109-22.
- Pooler, A. M., Noble, W. and Hanger, D. P. (2014) 'A role for tau at the synapse in Alzheimer's disease pathogenesis', *Neuropharmacology*, 76 Pt A, pp. 1-8.
- Popoli, M., Yan, Z., McEwen, B. S. and Sanacora, G. (2011) 'The stressed synapse: the impact of stress and glucocorticoids on glutamate transmission', *Nat Rev Neurosci*, 13(1), pp. 22-37.
- Prox, J., Rittger, A. and Saftig, P. (2012) 'Physiological functions of the amyloid precursor protein secretases ADAM10, BACE1, and presenilin', *Exp Brain Res*, 217(3-4), pp. 331-41.
- Puzzo, D., Lee, L., Palmeri, A., Calabrese, G. and Arancio, O. (2014) 'Behavioral assays with mouse models of Alzheimer's disease: practical considerations and guidelines', *Biochem Pharmacol*, 88(4), pp. 450-67.
- Puzzo, D., Privitera, L., Leznik, E., Fà, M., Staniszewski, A., Palmeri, A. and Arancio, O. (2008) 'Picomolar amyloid-beta positively modulates synaptic plasticity and memory in hippocampus', *J Neurosci*, 28(53), pp. 14537-45.
- Raff, H., Sharma, S. T. and Nieman, L. K. (2014) 'Physiological basis for the etiology, diagnosis, and treatment of adrenal disorders: Cushing's syndrome, adrenal insufficiency, and congenital adrenal hyperplasia', *Compr Physiol*, 4(2), pp. 739-69.
- Rasmuson, S., Andrew, R., Nasman, B., Seckl, J. R., Walker, B. R. and Olsson, T. (2001) 'Increased glucocorticoid production and altered cortisol metabolism in women with mild to moderate Alzheimer's disease', *Biol Psychiatry*, 49(6), pp. 547-52.
- Raz, N., Rodrigue, K. M., Head, D., Kennedy, K. M. and Acker, J. D. (2004) 'Differential aging of the medial temporal lobe: a study of a five-year change', *Neurology*, 62(3), pp. 433-8.
- Redgate, E. S. and Fahringer, E. E. (1973) 'A comparison of the pituitary adrenal activity elicited by electrical stimulation of preoptic, amygdaloid and hypothalamic sites in the rat brain', *Neuroendocrinology*, 12(6), pp. 334-43.
- Reed, J. M. and Squire, L. R. (1997) 'Impaired recognition memory in patients with lesions limited to the hippocampal formation', *Behav Neurosci*, 111(4), pp. 667-75.
- Reichardt, H. M., Umland, T., Bauer, A., Kretz, O. and Schutz, G. (2000) 'Mice with an increased glucocorticoid receptor gene dosage show enhanced resistance to stress and endotoxic shock', *Mol Cell Biol*, 20(23), pp. 9009-17.

- Restivo, L., Tafi, E., Ammassari-Teule, M. and Marie, H. (2009) 'Viral-mediated expression of a constitutively active form of CREB in hippocampal neurons increases memory', *Hippocampus*, 19(3), pp. 228-34.
- Reul, J. M. and de Kloet, E. R. (1985) 'Two receptor systems for corticosterone in rat brain: microdistribution and differential occupation', *Endocrinology*, 117(6), pp. 2505-11.
- Rissman, R. A. (2009) 'Stress-induced tau phosphorylation: functional neuroplasticity or neuronal vulnerability?', *J Alzheimers Dis*, 18(2), pp. 453-7.
- Roosendaal, B. (2000) '1999 Curt P. Richter award. Glucocorticoids and the regulation of memory consolidation', *Psychoneuroendocrinology*, 25(3), pp. 213-38.
- Rothman, S. M. and Mattson, M. P. (2010) 'Adverse stress, hippocampal networks, and Alzheimer's disease', *Neuromolecular Med*, 12(1), pp. 56-70.
- Rugg, M. D. and Vilberg, K. L. (2013) 'Brain networks underlying episodic memory retrieval', *Curr Opin Neurobiol*, 23(2), pp. 255-60.
- Russo, M. F., Ah Loy, S. R., Battle, A. R. and Johnson, L. R. (2016) 'Membrane Associated Synaptic Mineralocorticoid and Glucocorticoid Receptors Are Rapid Regulators of Dendritic Spines', *Front Cell Neurosci*, 10, pp. 161.
- Salmon, D. P. and Bondi, M. W. (2009) 'Neuropsychological assessment of dementia', *Annu Rev Psychol*, 60, pp. 257-82.
- Sandhu, F. A., Salim, M. and Zain, S. B. (1991) 'Expression of the human beta-amyloid protein of Alzheimer's disease specifically in the brains of transgenic mice', *J Biol Chem*, 266(32), pp. 21331-4.
- Sandi, C. (2011) 'Glucocorticoids act on glutamatergic pathways to affect memory processes', *Trends Neurosci*, 34(4), pp. 165-76.
- Sapolsky, R. M. (1985) 'Glucocorticoid toxicity in the hippocampus: temporal aspects of neuronal vulnerability', *Brain Res*, 359(1-2), pp. 300-5.
- Sapolsky, R. M. (1992) 'Do glucocorticoid concentrations rise with age in the rat?', *Neurobiol Aging*, 13(1), pp. 171-4.
- Sapolsky, R. M., Krey, L. C. and McEwen, B. S. (1984) 'Glucocorticoid-sensitive hippocampal neurons are involved in terminating the adrenocortical stress response', *Proc Natl Acad Sci U S A*, 81(19), pp. 6174-7.
- Sapolsky, R. M., Romero, L. M. and Munck, A. U. (2000) 'How do glucocorticoids influence stress responses? Integrating permissive, suppressive, stimulatory, and preparative actions', *Endocr Rev*, 21(1), pp. 55-89.
- Saura, C. A., Choi, S. Y., Beglopoulos, V., Malkani, S., Zhang, D., Shankaranarayana Rao, B. S., Chattarji, S., Kelleher, R. J., 3rd, Kandel, E. R., Duff, K., Kirkwood, A. and Shen, J. (2004) 'Loss of presenilin function causes impairments of memory and synaptic plasticity followed by age-dependent neurodegeneration', *Neuron*, 42(1), pp. 23-36.
- Scher, A. I., Xu, Y., Korf, E. S., White, L. R., Scheltens, P., Toga, A. W., Thompson, P. M., Hartley, S. W., Witter, M. P., Valentino, D. J. and Launer, L. J. (2007) 'Hippocampal shape analysis in Alzheimer's disease: a population-based study', *Neuroimage*, 36(1), pp. 8-18.
- Schibler, U. and Sassone-Corsi, P. (2002) 'A web of circadian pacemakers', *Cell*, 111(7), pp. 919-22.
- Schmidt, S. D., Nixon, R. A. and Mathews, P. M. (2005) 'ELISA method for measurement of amyloid-beta levels', *Methods Mol Biol*, 299, pp. 279-97.

- Schor, N. F. (2011) 'What the halted phase III gamma-secretase inhibitor trial may (or may not) be telling us', *Ann Neurol*, 69(2), pp. 237-9.
- Scollay, R. and Shortman, K. (1983) 'Thymocyte subpopulations: an experimental review, including flow cytometric cross-correlations between the major murine thymocyte markers', *Thymus*, 5(5-6), pp. 245-95.
- Seabrook, G. R., Smith, D. W., Bowery, B. J., Easter, A., Reynolds, T., Fitzjohn, S. M., Morton, R. A., Zheng, H., Dawson, G. R., Sirinathsinghji, D. J., Davies, C. H., Collingridge, G. L. and Hill, R. G. (1999) 'Mechanisms contributing to the deficits in hippocampal synaptic plasticity in mice lacking amyloid precursor protein', *Neuropharmacology*, 38(3), pp. 349-59.
- Seckl, J. R., French, K. L., O'Donnell, D., Meaney, M. J., Nair, N. P., Yates, C. M. and Fink, G. (1993) 'Glucocorticoid receptor gene expression is unaltered in hippocampal neurons in Alzheimer's disease', *Brain Res Mol Brain Res*, 18(3), pp. 239-45.
- Sehgal, M., Song, C., Ehlers, V. L. and Moyer, J. R., Jr. (2013) 'Learning to learn - intrinsic plasticity as a metaplasticity mechanism for memory formation', *Neurobiol Learn Mem*, 105, pp. 186-99.
- Selkoe, D. J. (2001) 'Presenilin, Notch, and the genesis and treatment of Alzheimer's disease', *Proc Natl Acad Sci U S A*, 98(20), pp. 11039-41.
- Selkoe, D. J. (2002) 'Alzheimer's disease is a synaptic failure', *Science*, 298(5594), pp. 789-91.
- Selkoe, D. J. (2008) 'Soluble oligomers of the amyloid beta-protein impair synaptic plasticity and behavior', *Behav Brain Res*, 192(1), pp. 106-13.
- Sevigny, J., Chiao, P., Bussière, T., Weinreb, P. H., Williams, L., Maier, M., Dunstan, R., Salloway, S., Chen, T., Ling, Y., O'Gorman, J., Qian, F., Arastu, M., Li, M., Chollate, S., Brennan, M. S., Quintero-Monzon, O., Scannevin, R. H., Arnold, H. M., Engber, T., Rhodes, K., Ferrero, J., Hang, Y., Mikulskis, A., Grimm, J., Hock, C., Nitsch, R. M. and Sandrock, A. (2016) 'The antibody aducanumab reduces A $\beta$  plaques in Alzheimer's disease', *Nature*, 537(7618), pp. 50-6.
- Shankar, G. M., Bloodgood, B. L., Townsend, M., Walsh, D. M., Selkoe, D. J. and Sabatini, B. L. (2007) 'Natural oligomers of the Alzheimer amyloid-beta protein induce reversible synapse loss by modulating an NMDA-type glutamate receptor-dependent signaling pathway', *J Neurosci*, 27(11), pp. 2866-75.
- Shankar, G. M., Li, S., Mehta, T. H., Garcia-Munoz, A., Shepardson, N. E., Smith, I., Brett, F. M., Farrell, M. A., Rowan, M. J., Lemere, C. A., Regan, C. M., Walsh, D. M., Sabatini, B. L. and Selkoe, D. J. (2008) 'Amyloid-beta protein dimers isolated directly from Alzheimer's brains impair synaptic plasticity and memory', *Nat Med*, 14(8), pp. 837-42.
- Sigmund, C. D. (2000) 'Viewpoint: are studies in genetically altered mice out of control?', *Arterioscler Thromb Vasc Biol*, 20(6), pp. 1425-9.
- Sinha, S., Anderson, J. P., Barbour, R., Basi, G. S., Caccavello, R., Davis, D., Doan, M., Dovey, H. F., Frigon, N., Hong, J., Jacobson-Croak, K., Jewett, N., Keim, P., Knops, J., Lieberburg, I., Power, M., Tan, H., Tatsuno, G., Tung, J., Schenk, D., Seubert, P., Suomensaari, S. M., Wang, S., Walker, D., Zhao, J., McConlogue, L. and John, V. (1999) 'Purification and cloning of amyloid precursor protein beta-secretase from human brain', *Nature*, 402(6761), pp. 537-40.

- Slegers, K., Roks, G., Theuns, J., Aulchenko, Y. S., Rademakers, R., Cruts, M., van Gool, W. A., Van Broeckhoven, C., Heutink, P., Oostra, B. A., van Swieten, J. C. and van Duijn, C. M. (2004) 'Familial clustering and genetic risk for dementia in a genetically isolated Dutch population', *Brain*, 127(Pt 7), pp. 1641-9.
- Snyder, E. M., Nong, Y., Almeida, C. G., Paul, S., Moran, T., Choi, E. Y., Nairn, A. C., Salter, M. W., Lombroso, P. J., Gouras, G. K. and Greengard, P. (2005) 'Regulation of NMDA receptor trafficking by amyloid-beta', *Nat Neurosci*, 8(8), pp. 1051-8.
- Snyder, S. W., Lador, U. S., Wade, W. S., Wang, G. T., Barrett, L. W., Matayoshi, E. D., Huffaker, H. J., Krafft, G. A. and Holzman, T. F. (1994) 'Amyloid-beta aggregation: selective inhibition of aggregation in mixtures of amyloid with different chain lengths', *Biophys J*, 67(3), pp. 1216-28.
- Sotiropoulos, I., Catania, C., Pinto, L. G., Silva, R., Pollerberg, G. E., Takashima, A., Sousa, N. and Almeida, O. F. (2011) 'Stress acts cumulatively to precipitate Alzheimer's disease-like tau pathology and cognitive deficits', *J Neurosci*, 31(21), pp. 7840-7.
- Sotiropoulos, I., Silva, J., Kimura, T., Rodrigues, A. J., Costa, P., Almeida, O. F., Sousa, N. and Takashima, A. (2015) 'Female hippocampus vulnerability to environmental stress, a precipitating factor in Tau aggregation pathology', *J Alzheimers Dis*, 43(3), pp. 763-74.
- Sousa, N., Cerqueira, J. J. and Almeida, O. F. (2008) 'Corticosteroid receptors and neuroplasticity', *Brain Res Rev*, 57(2), pp. 561-70.
- Sousa, N., Lukoyanov, N. V., Madeira, M. D., Almeida, O. F. and Paula-Barbosa, M. M. (2000) 'Reorganization of the morphology of hippocampal neurites and synapses after stress-induced damage correlates with behavioral improvement', *Neuroscience*, 97(2), pp. 253-66.
- Squire, L. R., Shimamura, A. P. and Graf, P. (1987) 'Strength and duration of priming effects in normal subjects and amnesic patients', *Neuropsychologia*, 25(1b), pp. 195-210.
- Squire, L. R. and Zola-Morgan, J. (2011) 'The cognitive neuroscience of human memory since H.M.', *Annu Rev Neurosci*, 34, pp. 259-88.
- Steinbach, J. P., Muller, U., Leist, M., Li, Z. W., Nicotera, P. and Aguzzi, A. (1998) 'Hypersensitivity to seizures in beta-amyloid precursor protein deficient mice', *Cell Death Differ*, 5(10), pp. 858-66.
- Steiner, H., Winkler, E., Edbauer, D., Prokop, S., Basset, G., Yamasaki, A., Kostka, M. and Haass, C. (2002) 'PEN-2 is an integral component of the gamma-secretase complex required for coordinated expression of presenilin and nicastrin', *J Biol Chem*, 277(42), pp. 39062-5.
- Stewart, S., Cacucci, F. and Lever, C. (2011) 'Which memory task for my mouse? A systematic review of spatial memory performance in the Tg2576 Alzheimer's mouse model', *J Alzheimers Dis*, 26(1), pp. 105-26.
- Stine, W. B., Dahlgren, K. N., Krafft, G. A. and LaDu, M. J. (2003) 'In vitro characterization of conditions for amyloid-beta peptide oligomerization and fibrillogenesis', *J Biol Chem*, 278(13), pp. 11612-22.
- Stranahan, A. M. and Mattson, M. P. (2010) 'Selective vulnerability of neurons in layer II of the entorhinal cortex during aging and Alzheimer's disease', *Neural Plast*, 2010, pp. 108190.

- Straube, B. (2012) 'An overview of the neuro-cognitive processes involved in the encoding, consolidation, and retrieval of true and false memories', *Behav Brain Funct*, 8, pp. 35.
- Swanwick, G. R., Kirby, M., Bruce, I., Buggy, F., Coen, R. F., Coakley, D. and Lawlor, B. A. (1998) 'Hypothalamic-pituitary-adrenal axis dysfunction in Alzheimer's disease: lack of association between longitudinal and cross-sectional findings', *Am J Psychiatry*, 155(2), pp. 286-9.
- Takahashi, T., Kimoto, T., Tanabe, N., Hattori, T. A., Yasumatsu, N. and Kawato, S. (2002) 'Corticosterone acutely prolonged N-methyl-d-aspartate receptor-mediated Ca<sup>2+</sup> elevation in cultured rat hippocampal neurons', *J Neurochem*, 83(6), pp. 1441-51.
- Tan, M. S., Yu, J. T. and Tan, L. (2013) 'Bridging integrator 1 (BIN1): form, function, and Alzheimer's disease', *Trends Mol Med*, 19(10), pp. 594-603.
- Tasker, J. G., Di, S. and Malcher-Lopes, R. (2006) 'Minireview: rapid glucocorticoid signaling via membrane-associated receptors', *Endocrinology*, 147(12), pp. 5549-56.
- Ter Horst, J. P., Carobrez, A. P., van der Mark, M. H., de Kloet, E. R. and Oitzl, M. S. (2012) 'Sex differences in fear memory and extinction of mice with forebrain-specific disruption of the mineralocorticoid receptor', *Eur J Neurosci*, 36(8), pp. 3096-102.
- Terry, R. D., Masliah, E., Salmon, D. P., Butters, N., DeTeresa, R., Hill, R., Hansen, L. A. and Katzman, R. (1991) 'Physical basis of cognitive alterations in Alzheimer's disease: synapse loss is the major correlate of cognitive impairment', *Ann Neurol*, 30(4), pp. 572-80.
- Thal, D. R., Arendt, T., Waldmann, G., Holzer, M., Zedlick, D., Rub, U. and Schober, R. (1998) 'Progression of neurofibrillary changes and PHF-tau in end-stage Alzheimer's disease is different from plaque and cortical microglial pathology', *Neurobiol Aging*, 19(6), pp. 517-25.
- Thal, D. R., Rub, U., Orantes, M. and Braak, H. (2002a) 'Phases of A beta-deposition in the human brain and its relevance for the development of AD', *Neurology*, 58(12), pp. 1791-800.
- Thal, D. R., Rüb, U., Orantes, M. and Braak, H. (2002b) 'Phases of A beta-deposition in the human brain and its relevance for the development of AD', *Neurology*, 58(12), pp. 1791-800.
- Townsend, M., Shankar, G. M., Mehta, T., Walsh, D. M. and Selkoe, D. J. (2006) 'Effects of secreted oligomers of amyloid beta-protein on hippocampal synaptic plasticity: a potent role for trimers', *J Physiol*, 572(Pt 2), pp. 477-92.
- Trapp, T., Rupprecht, R., Castren, M., Reul, J. M. and Holsboer, F. (1994) 'Heterodimerization between mineralocorticoid and glucocorticoid receptor: a new principle of glucocorticoid action in the CNS', *Neuron*, 13(6), pp. 1457-62.
- Trojanowski, J. Q., Schuck, T., Schmidt, M. L. and Lee, V. M. (1989) 'Distribution of tau proteins in the normal human central and peripheral nervous system', *J Histochem Cytochem*, 37(2), pp. 209-15.
- Tromp, D., Dufour, A., Lithfous, S., Pebayle, T. and Després, O. (2015) 'Episodic memory in normal aging and Alzheimer disease: Insights from imaging and behavioral studies', *Ageing Res Rev*, 24(Pt B), pp. 232-62.

- Tronche, F., Kellendonk, C., Kretz, O., Gass, P., Anlag, K., Orban, P. C., Bock, R., Klein, R. and Schütz, G. (1999) 'Disruption of the glucocorticoid receptor gene in the nervous system results in reduced anxiety', *Nat Genet*, 23(1), pp. 99-103.
- Tulving, E. and Markowitsch, H. J. (1998) 'Episodic and declarative memory: role of the hippocampus', *Hippocampus*, 8(3), pp. 198-204.
- Turner, P. R., O'Connor, K., Tate, W. P. and Abraham, W. C. (2003) 'Roles of amyloid precursor protein and its fragments in regulating neural activity, plasticity and memory', *Prog Neurobiol*, 70(1), pp. 1-32.
- Ulrich-Lai, Y. M., Figueiredo, H. F., Ostrander, M. M., Choi, D. C., Engeland, W. C. and Herman, J. P. (2006) 'Chronic stress induces adrenal hyperplasia and hypertrophy in a subregion-specific manner', *Am J Physiol Endocrinol Metab*, 291(5), pp. E965-73.
- Ulrich-Lai, Y. M. and Herman, J. P. (2009) 'Neural regulation of endocrine and autonomic stress responses', *Nat Rev Neurosci*, 10(6), pp. 397-409.
- Um, J. W. and Strittmatter, S. M. (2013) 'Amyloid-beta induced signaling by cellular prion protein and Fyn kinase in Alzheimer disease', *Prion*, 7(1), pp. 37-41.
- Umegaki, H., Ikari, H., Nakahata, H., Endo, H., Suzuki, Y., Ogawa, O., Nakamura, A., Yamamoto, T. and Iguchi, A. (2000) 'Plasma cortisol levels in elderly female subjects with Alzheimer's disease: a cross-sectional and longitudinal study', *Brain Res*, 881(2), pp. 241-3.
- Valtschanoff, J. G. and Weinberg, R. J. (2001) 'Laminar organization of the NMDA receptor complex within the postsynaptic density', *J Neurosci*, 21(4), pp. 1211-7.
- van der Lely, A. J., Foeken, K., van der Mast, R. C. and Lamberts, S. W. (1991) 'Rapid reversal of acute psychosis in the Cushing syndrome with the cortisol-receptor antagonist mifepristone (RU 486)', *Ann Intern Med*, 114(2), pp. 143-4.
- van Rossum, E. F., de Jong, F. J., Koper, J. W., Uitterlinden, A. G., Prins, N. D., van Dijk, E. J., Koudstaal, P. J., Hofman, A., de Jong, F. H., Lamberts, S. W. and Breteler, M. M. (2008) 'Glucocorticoid receptor variant and risk of dementia and white matter lesions', *Neurobiol Aging*, 29(5), pp. 716-23.
- Walsh, D. M., Klyubin, I., Fadeeva, J. V., Cullen, W. K., Anwyl, R., Wolfe, M. S., Rowan, M. J. and Selkoe, D. J. (2002) 'Naturally secreted oligomers of amyloid beta protein potently inhibit hippocampal long-term potentiation in vivo', *Nature*, 416(6880), pp. 535-9.
- Wang, H., Megill, A., He, K., Kirkwood, A. and Lee, H. K. (2012) 'Consequences of inhibiting amyloid precursor protein processing enzymes on synaptic function and plasticity', *Neural Plast*, 2012, pp. 272374.
- Wang, Q., Walsh, D. M., Rowan, M. J., Selkoe, D. J. and Anwyl, R. (2004) 'Block of long-term potentiation by naturally secreted and synthetic amyloid beta-peptide in hippocampal slices is mediated via activation of the kinases c-Jun N-terminal kinase, cyclin-dependent kinase 5, and p38 mitogen-activated protein kinase as well as metabotropic glutamate receptor type 5', *J Neurosci*, 24(13), pp. 3370-8.
- Wetzel, D. M., Bohn, M. C., Kazee, A. M. and Hamill, R. W. (1995) 'Glucocorticoid receptor mRNA in Alzheimer's diseased hippocampus', *Brain Res*, 679(1), pp. 72-81.
- Whitehouse, P. J., Price, D. L., Clark, A. W., Coyle, J. T. and DeLong, M. R. (1981) 'Alzheimer disease: evidence for selective loss of cholinergic neurons in the nucleus basalis', *Ann Neurol*, 10(2), pp. 122-6.

- Willem, M., Tahirovic, S., Busche, M. A., Ovsepian, S. V., Chafai, M., Kootar, S., Hornburg, D., Evans, L. D., Moore, S., Daria, A., Hampel, H., Müller, V., Giudici, C., Nuscher, B., Wenninger-Weinzierl, A., Kremmer, E., Heneka, M. T., Thal, D. R., Giedraitis, V., Lannfelt, L., Müller, U., Livesey, F. J., Meissner, F., Herms, J., Konnerth, A., Marie, H. and Haass, C. (2015) ' $\eta$ -Secretase processing of APP inhibits neuronal activity in the hippocampus', *Nature*, 526(7573), pp. 443-7.
- Wilson, R. S., Evans, D. A., Bienias, J. L., Mendes de Leon, C. F., Schneider, J. A. and Bennett, D. A. (2003) 'Proneness to psychological distress is associated with risk of Alzheimer's disease', *Neurology*, 61(11), pp. 1479-85.
- Wilson, R. S., Schneider, J. A., Boyle, P. A., Arnold, S. E., Tang, Y. and Bennett, D. A. (2007) 'Chronic distress and incidence of mild cognitive impairment', *Neurology*, 68(24), pp. 2085-92.
- Wolfe, M. S. and Guénette, S. Y. (2007) 'APP at a glance', *J Cell Sci*, 120(Pt 18), pp. 3157-61.
- Wulsin, A. C., Herman, J. P. and Solomon, M. B. (2010) 'Mifepristone decreases depression-like behavior and modulates neuroendocrine and central hypothalamic-pituitary-adrenocortical axis responsiveness to stress', *Psychoneuroendocrinology*, 35(7), pp. 1100-12.
- Xu, H., Sweeney, D., Wang, R., Thinakaran, G., Lo, A. C., Sisodia, S. S., Greengard, P. and Gandy, S. (1997) 'Generation of Alzheimer beta-amyloid protein in the trans-Golgi network in the apparent absence of vesicle formation', *Proc Natl Acad Sci U S A*, 94(8), pp. 3748-52.
- Yamin, G. (2009) 'NMDA receptor-dependent signaling pathways that underlie amyloid beta-protein disruption of LTP in the hippocampus', *J Neurosci Res*, 87(8), pp. 1729-36.
- Yang, C. H., Huang, C. C. and Hsu, K. S. (2005) 'Behavioral stress enhances hippocampal CA1 long-term depression through the blockade of the glutamate uptake', *J Neurosci*, 25(17), pp. 4288-93.
- Young, E. A., Abelson, J. and Lightman, S. L. (2004) 'Cortisol pulsatility and its role in stress regulation and health', *Front Neuroendocrinol*, 25(2), pp. 69-76.
- Yuen, E. Y., Liu, W., Karatsoreos, I. N., Ren, Y., Feng, J., McEwen, B. S. and Yan, Z. (2011) 'Mechanisms for acute stress-induced enhancement of glutamatergic transmission and working memory', *Mol Psychiatry*, 16(2), pp. 156-70.
- Yuen, E. Y. and Yan, Z. (2009) 'Dopamine D4 receptors regulate AMPA receptor trafficking and glutamatergic transmission in GABAergic interneurons of prefrontal cortex', *J Neurosci*, 29(2), pp. 550-62.
- Zalachoras, I., Houtman, R., Atucha, E., Devos, R., Tijssen, A. M., Hu, P., Lockey, P. M., Datson, N. A., Belanoff, J. K., Lucassen, P. J., Joëls, M., de Kloet, E. R., Roozendaal, B., Hunt, H. and Meijer, O. C. (2013) 'Differential targeting of brain stress circuits with a selective glucocorticoid receptor modulator', *Proc Natl Acad Sci U S A*, 110(19), pp. 7910-5.
- Zemek, F., Drtinova, L., Nepovimova, E., Sepsova, V., Korabecny, J., Klimes, J. and Kuca, K. (2014) 'Outcomes of Alzheimer's disease therapy with acetylcholinesterase inhibitors and memantine', *Expert Opin Drug Saf*, 13(6), pp. 759-74.
- Zempel, H., Thies, E., Mandelkow, E. and Mandelkow, E. M. (2010) ' $\beta$  oligomers cause localized  $Ca^{2+}$  elevation, missorting of endogenous Tau into dendrites, Tau

- phosphorylation, and destruction of microtubules and spines', *J Neurosci*, 30(36), pp. 11938-50.
- Zennaro, M. C., Keightley, M. C., Kotelevtsev, Y., Conway, G. S., Soubrier, F. and Fuller, P. J. (1995) 'Human mineralocorticoid receptor genomic structure and identification of expressed isoforms', *J Biol Chem*, 270(36), pp. 21016-20.
- Zhu, C. W., Livote, E. E., Scarneas, N., Albert, M., Brandt, J., Blacker, D., Sano, M. and Stern, Y. (2013) 'Long-term associations between cholinesterase inhibitors and memantine use and health outcomes among patients with Alzheimer's disease', *Alzheimers Dement*, 9(6), pp. 733-40.





## RESUME

La maladie d'Alzheimer (MA) est une maladie neurodégénérative caractérisée par une perte irréversible des fonctions cognitives. En début de maladie, il a été mis en évidence que la perte de fonction des synapses de l'hippocampe engendre la perte de mémoires de type épisodique. Les données actuelles suggèrent fortement que les formes oligomériques du peptide  $\beta$ -amyloïde ( $\text{oA}\beta$ ), qui s'accumulent dans le cerveau des patients, sont toxiques pour la fonction de ces synapses. La MA est aussi associée à une dérégulation de l'axe du stress, l'axe hypothalamo-pituitaire-surrénal (HPA), comme observée chez les patients et les modèles animaux de la MA. Cette dérégulation engendre une augmentation de la production des glucocorticoïdes (GCs) qui activent les récepteurs associés (GRs). Nous avons récemment mis en évidence que l'inhibition de ces GRs dans un modèle murin de la maladie, les souris Tg2576 ( $\text{Tg}^+$ ), prévient les déficits de mémoire épisodique et de plasticité synaptique (Lanté et al. Neuropsychopharmacology. 2015).

Dans ce contexte, nous avons étudié l'étendue de la contribution des GRs dans la physiopathologie de la MA. D'abord, nous avons étudié la relation entre la dérégulation de l'axe HPA et le début de la pathologie dans les souris  $\text{Tg}^+$ . Nous montrons que cette dérégulation était caractérisée par des niveaux élevés de GCs à 4 et 6 mois d'âge ainsi que par la perte de la boucle de rétroaction négative. Ensuite, nous avons croisé les souris  $\text{Tg}^+$  avec des souris GR floxées pour générer des double mutants  $\text{GR}^{\text{lox/lox}} \text{Tg}^+$ , dont nous avons fait la caractérisation phénotypique. Alors même que les GRs étaient encore présents, ces double mutants exhibaient des niveaux élevés de GCs dès le sevrage, une exacerbation des déficits synaptiques, un poids faible et un taux de survie faible lors de chirurgies. Nous concluons, qu'ensemble, la présence du transgène et de l'allèle GR floxé sont trop nuisibles pour permettre un développement adéquat des souris double mutantes. Nous avons donc décidé de mettre fin à cette lignée de souris. A la place, pour identifier la relation fonctionnelle entre les GRs et  $\text{oA}\beta$  à la synapse, nous avons utilisé des cultures de neurones et des tranches d'hippocampes soumises à un traitement aigu d' $\text{oA}\beta$ . Dans les cultures, ce traitement a favorisé une augmentation des niveaux de GRs à la synapse. Dans les tranches, ce traitement a provoqué une diminution de la potentialisation à long-terme (LTP), un effet totalement bloqué en présence d'un inhibiteur spécifique des GRs. Confirmant ce résultat, nous n'avons pas vu d'effet d' $\text{oA}\beta$  sur la LTP sur des tranches de souris  $\text{GR}^{\text{lox/lox}}$  où l'expression génique des GRs dans les neurones CA1 de l'hippocampe avait été supprimée par transduction virale Cre-GFP *in vivo*. La réduction de la fonction des GRs prévient donc l'action aiguë d' $\text{oA}\beta$  sur la LTP.

En conclusion, nos résultats avec les souris  $\text{Tg}^+$  suggèrent qu'une dérégulation neuroendocrine est présente en début de maladie. Aussi, nous mettons en évidence une relation fonctionnelle entre  $\text{oA}\beta$  et les GRs à la synapse, les GRs jouant un rôle clé dans la synaptotoxicité induite par  $\text{oA}\beta$ .